A conceptual study of a natural circulation cooling loop for a PWR containment

L.E. Jacobs (B.Eng)

Mini-dissertation submitted as partial fulfilment of the requirements for the degree Master in Engineering at the Potchefstroom Campus of the North-West University

Supervisor:
Prof. C.G. du Toit
North-West University (Potchefstroom Campus)

November 2011

Acknowledgements and foreword

This investigation was the result of a discussion between the author and his employer. A question was raised on the possibility of using a natural circulation loop for the cooling of a nuclear reactor containment building during upset or accident conditions. This provided the inspiration for this investigation.

Many thanks to Prof. C.G. du Toit for being willing to be my supervisor and for always making time for my work.

Also thanks to my colleagues for giving me space and for supporting me through tough times.

I would like to express appreciation to my family for their endless support and love.

Yolandi, for believing in me and supporting me during the execution of this investigation.

Finally, all praise to the Lord for blessing me with so much, while I deserve so little.

Abstract

The removal of heat from the containment building is an important consideration in the design of a nuclear power plant. In this investigation a simple rectangular natural circulation loop was simulated to determine whether it could possibly be used to remove usable quantities of heat from a containment building. The loop had a vertical pipe on the inside and outside of the containment building. These pipes acted as heat exchangers. Single phase and two phase cases were simulated by imposing a temperature on the respective vertical leg pipe walls and determining the heat absorption from the containment building. The heat was conveyed from the inside of the building to the outside via the natural circulation phenomenon.

A literature study was done to cover topics relevant to this investigation. A theoretical model using conservation equations and control volumes was derived. This model was based largely on knowledge gleaned from the literature study. The theoretical model was a simple homogenous model, which was sufficiently detailed for a conceptual investigation. The theoretical model was then manipulated into a form suitable for use in a computer simulation program. Simplifications were made to the simulation model and underlying theory due to the nature of the investigation. The simulation model was validated against published experimental results.

During the simulation phase a number of cases were investigated. These cases were divided into base cases and parametric studies. During the base case simulations the change of key fluid variables along the loop was examined. During the parametric studies the hot and cold leg inside wall temperatures, loop geometry and pipe diameter were varied. The effect of these parameters on the heat absorption from the containment was determined.

The simulations showed that with the current assumptions about 75 to 120 of the natural circulation loops are needed depending on their geometry and containment conditions. The heat removal rates that were calculated varied from 50 kW to 600 kW for a single loop. As explained in the final chapter, there are many factors that influence the results obtained. The natural circulation concept was deemed to be able to remove usable quantities of heat from the containment building.

Keywords: Natural circulation loop, simulation, containment building cooling, single phase, two phase.

Table of contents

Acknowledgements and foreword ii

Abstract iii

Table of contents iv

List of figures viii

List of tables x

Nomenclature xi

Chapter 1 - Introduction 1

1.1 Project purpose 1
1.2 Introductory information 1
1.2.1 Pressurised water reactors 1
1.2.2 Containment buildings 4
1.3 Introduction to concepts used 6
1.3.1 Containment cooling systems on PWRs 6
1.4 Project definition 9
1.4.1 Problem statement 9
1.4.2 Scope of investigation 10
1.4.2.1 General scoping 10
1.4.2.2 Overall licensing of the NCL concept 10
1.4.2.3 Parameters that were varied 11
1.4.2.4 Parameters that were kept constant 11
1.4.3 Deliverables 13
1.5 Main project matters that were addressed 13
1.5.1 Literature study 13
1.5.2 Setting up the model 14
1.5.3 Verification and validation of the model 14
1.5.3.1 Verification 14
1.5.3.2 Validation 14
1.5.4 Evaluating results 15
1.6 Project execution 15
1.6.1 Literature study 15
1.6.2 Building a theoretical model 15

1.6.3 Programming model 16
1.6.4 Verification and validation of the model 16
1.6.5 Simulation 16
1.6.6 Analysing and evaluating results 17
1.7 Conclusion of introduction 17

Chapter 2 - Literature study 18

2.1 Passive containment cooling at nuclear power stations 18
2.2 Other applications of NCLs 24
2.3 Single phase NCLs and related experiments and correlations 25
2.4 Two phase NCLs and related experiments and correlations 31
2.5 Stability of NCLs 40
2.5.1 Types of instabilities 41
2.5.1.1 Static instabilities 41
2.5.1.2 Dynamic instabilities 42
2.5.1.3 Start-up transients 43
2.5.1.4 Stability maps 43
2.6 Conclusion of the literature study 44

Chapter 3 - Theoretical background 45

3.1 Introduction 45
3.1.1 Natural circulation systems 45
3.1.2 Stability considerations 46
3.1.3 Advective heat transfer 47
3.1.4 Convection heat transfer 48
3.1.5 Fluid properties and other flow related quantities 52
3.2 Introduction to conservation equations 56
3.3 Conservation equations for the pipe loop 56
3.3.1 Mass conservation for the pipe loop 57
3.3.2 Momentum conservation for the pipe loop 58
3.3.3 Energy conservation for the pipe loop 60
3.3.4 Boundary conditions for the pipe loop 61
3.4 Conservation equations of the reservoir 62
3.4.1 Mass conservation in the reservoir 62
3.4.2 Momentum conservation in the reservoir 63
3.4.3 Energy conservation in the reservoir 65
3.4.4 Boundary conditions for the reservoir 67
3.5 Stability and convergence 67

3.6 Constitutive equations 67
3.6.1 Convection heat transfer 67
3.6.1.1 Single phase heat transfer 67
3.6.1.2 Two phase saturated and subcooled boiling heat transfer 70
3.6.2 Pressure drop 72
3.7 Conclusion of the theoretical background 77

Chapter 4 - Simulation 78

4.1 Software 78
4.2 Simulation model philosophy 78
4.3 Assumptions used in the simulation program 80
4.4 Structure of the simulation program 82
4.4.1 Simulation method 82
4.4.2 Simulation program structure 83
4.4.3 Simulation discretisation 84
4.5 Component-specific conservation equations discretisation – Pipe loop 86
4.5.1 Naming convention 86
4.5.2 Discretised conservation of mass – Pipe loop 87
4.5.3 Discretised conservation of momentum – Pipe loop 87
4.5.4 Discretised conservation of energy – Pipe loop 88
4.6 Component-specific model – Reservoir 88
4.6.1 Naming convention 88
4.6.2 Discretised conservation of mass – Reservoir 89
4.6.3 Discretised conservation of energy – Reservoir 89
4.7 Program code, heat transfer and other functions 90
4.7.1 Function used for fluid quality calculations 90
4.7.2 Functions used for the calculation of dimensionless numbers and two phase quantities 91
4.7.3 Functions used for fluid property calculations 92
4.7.4 Functions used for reservoir-related quantities 93
4.7.5 Functions used for frictional pressure drop calculations 93
4.7.6 Functions used in the calculation of heat transfer 95
4.7.7 Calculated parameters used to calculate overall loop performance 97
4.7.8 Simulation program input parameters and boundary values 97
4.7.9 Loop pipes simulation code 99
4.8 Conclusion of simulation program description 101

Chapter 5 - Simulation model validation and verification 102

5.1 Grid-size independence check 102

5.2 Kyung and Lee study – Experimental facility 103
5.3 Validation program preparation and adaption 106
5.4 Comparison between Kyung and Lee results and adapted simulation program results 108
5.5 Heat transfer and frictional pressure drop function verification 112
5.6 Conclusion of the simulation model validation and verification 113

Chapter 6 - Results and analysis 114

6.1 Base case simulations 114
6.1.1 Whole-loop results from the base case simulations 114
6.1.2 Examination of base case results – Enthalpy and temperatures 117
6.1.3 Examination of base case results – Heat transfer, quality, densities and velocities 118
6.2 Results from the parametric simulations 124
6.2.1 Variation of pipe diameter 124
6.2.2 Variation of loop height and width 125
6.2.3 Variation of pipe wall temperatures 127
6.3 Analysis of results 128
6.4 Closing comments and conclusion of results 130

Chapter 7 - Conclusion and recommendations 134

7.1 Summary of the investigation 134
7.2 Recommendations 135
7.3 Concluding remarks 136
7.4 Conclusion 136

References 137

Appendix A – EES program code 143

List of figures

Figure 1-1. Overview of PWR power plant thermal cycles. 2
Figure 1-2. PWR heat removal circuits. 3
Figure 1-3. Different containment designs. 5
Figure 1-4. Containment cooling designs....6
Figure 1-5. Containment cooling via a natural circulation loop. 7
Figure 1-6. Natural circulation loop for containment cooling....8
Figure 1-7. Physical parameters to be varied....12
Figure 2-1. Containment passive cooling concepts (Adapted from Gavrilas *et al*., 1998:649). 19
Figure 2-2. Energy removal during a LOCA (Adapted from Gavrilas *et al.,* 1998:654). 20
Figure 2-3. Passive containment cooling designs (Adapted from Lee *et al.,* 1997:469-471). 21
Figure 2-4. Containment cooling with open NCL and water tank (Adapted from Byun *et al.*, 2000:230). 22
Figure 2-5. Experimental investigation on a simplified NCL (Adapted from Liu *et al.,* 2000:246). 23
Figure 2-6. NCLs showing different heating and cooling section orientations....25
Figure 2-7. Various oscillation modes of an NCL (Adapted from Vijayan *et al.,* 2007:941). 26
Figure 2-8 Friction factor determination (Adapted from Ambrosini *et al.*, 2004:1841). 30
Figure 2-9. Comparison graphs between homogenous and drift-flux models (Rao *et al.,* 2006:1050)....32
Figure 2-10. Rectangular and annular NCLs for gas reactor cavity cooling (Adapted from Oosthuizen, 2003:57-58). 34
Figure 2-11. Friction factor determination (Oosthuizen, 2003:64). 35
Figure 2-12. NCL with expansion tank connected by length of pipe (Adapted from Kim and Lee, 2000:361). 36
Figure 2-13. Schematic representation of subcooled flow boiling (Adapted from Kandlikar, 1998)....39
Figure 2-14. Example of an NCL stability map (Nayak *et al.*, 1995:85). 44
Figure 3-1. Fluid velocity profiles for laminar and turbulent flow through a tube (Adapted from Incropera *et al.*, 2006:486). 47
Figure 3-2 Boiling in a vertical pipe *(*Bejan & Kraus, 2003:671). 48
Figure 3-3. Convection heat transfer to a fluid flowing inside a pipe. 49
Figure 3-4. Natural circulation loop reservoir and pipes. 50
Figure 3-5. Fluid property interpolation function. 55
Figure 3-6. Naming convention for pipe loop conservation equation derivation....57
Figure 3-7. Pressure interfaces for the reservoir. 64
Figure 3-8. Comparison of different friction factor correlations and transition zone switching....76
Figure 4-1. Natural circulation loop subcomponent breakdown. 79
Figure 4-2. Steady state simulation program execution flow. 82
Figure 4-3. Single and two control volume stringing in the simulation program. 85

Figure 4-4. Control volume stringing in the NCL. 85
Figure 4-5. Naming convention for pipe control volumes in the simulation program. 86
Figure 4-6. Reservoir naming convention for simulation program. 89
Figure 5-1. Experimental setup of Kyung and Lee. 105
Figure 5-2. Representation of the adapted simulation model. 108
Figure 5-3. Graph of the change of heater inlet velocity as a result of the variation in heating flux (The first set of results from the current study overlaid on the graph of Kyung and Lee (1996)). 109
Figure 5-4. Graph of the change of heater inlet velocity as a result of the variation in heating flux (The second set of results from the current study overlaid on the graph of Kyung and Lee (1996)). 110
Figure 5-5. Graph of the change of heater inlet velocity as a result of the variation in heating flux (The third set of results from the current study overlaid on the graph of Kyung and Lee (1996)). 111
Figure 6-1. The variation of enthalpy, pipe wall temperature and fluid temperature along the length of the base single phase simulation case. 120
Figure 6-2. The variation of enthalpy, pipe wall temperature and fluid temperature along the length of the base two phase loop. 121
Figure 6-3. The variation of heat transfer per metre and fluid quality along the length of the single and two phase base loops. 122
Figure 6-4. The variation of density and velocity along the length of the single and two phase loops. 123
Figure 6-5. The variation of heat absorbed from the containment building by the hot leg as a result of change in the loop pipe diameter. 131
Figure 6-6. The variation of heat absorbed from the containment building by the hot leg as a result of a change in the loop pipe height and width. 132
Figure 6-7. The variation of heat absorbed from the containment building by the hot leg as a result of a change in the imposed pipe wall temperatures. 133

List of tables

Table 1. Conservation equations of various one-dimensional models (Adapted from Reyes, 2005:167). 31
Table 2. Form loss coefficients for piping.....73
Table 3. Subcomponent classification groups.....81
Table 4. Description of the fixed variables used in the simulation program code. 98
Table 5. Description of the variables used in the simulation program code that will be varied parametrically. 99
Table 6. Grid independence: Range of tested control volume counts, choice and deviations from the smallest control volume size that was tested. 103
Table 7. Experimental setup and other input parameters to the validation model. 107
Table 8. Input parameters set for the single and two phase base case simulations. 115
Table 9. Global results for the single and two phase simulation cases of the NCL.....115
Table 10. Pipe loop diameter variation simulations and cases.....124
Table 11. Pipe loop height and width variation simulations and cases.....126
Table 12. Pipe loop hot and cold leg wall temperature variation simulations and cases.....127
Table 13. Analysis of the NCL as a suitable containment cooling device.....129

Nomenclature

Abbreviations

CFD	Computational Fluid Dynamics
CV	Control Volume
EES	Engineering Equation Solver
FDB	Fully Developed Boiling
HEM	Homogenous Equation Model
HHHC	Horizontal Heater Horizontal Cooler
LOCA	Loss of Coolant Accident
M-C	Multiple Modes of Circulation
NCL	Natural Circulation Loop
NVG	Net Vapour Generation
ONB	Onset of Nucleate Boiling
PWR	Pressurised Water Reactor
TEDFM	Two Equation Drift-Flux Model
VHVC	Vertical Heater Vertical Cooler

Symbols

A	Area	m^2
C_p	Fluid specific heat	$J.kg^{-1}K^{-1}$
D_H	Hydraulic diameter	m
e	Fluid energy content	$J.kg^{-1}$
F	Force or two phase and liquid Reynolds numbers ratio	$kg.m.s^{-2}$
f	Friction factor	
Gr_m	Modified Grasshoff number	
g	Gravitational acceleration	$m.s^{-2}$
h	Fluid enthalpy or heat transfer coefficient	$J.kg^{-1}$
K	Flow loss coefficients	
k	Fluid conductivity	$W.m^{-1}K^{-1}$
L	Length	m

$\dot{m}_{mix}$	Mass flow	$kg.s^{-1}$
Nu_D	Nusselt number	
$\bar{n}$	Normal vector	
Pr	Prandtl number	
p	Fluid pressure	$kg.m^{-1}s^{-2}$
q	Heat	$J.s^{-1}$
Re	Reynolds number	
S	Boiling suppression factor	
St_m	Modified Stanton number	
s	Distance	m
T	Fluid temperature	K
t	Time	s
u	Fluid internal energy	$J.kg^{-1}$
V	Volume	m^3
v	Fluid velocity	$m.s^{-1}$
W	Rate of work	$J.s^{-1}$
X_{tt}	Martenelli factor	
x	Fluid quality	
z	Elevation of various positions in the reservoir	m

Greek symbols

Δ	Change in a parameter through a control volume	
ε	Pipe wall roughness	m
θ	Angle from the horizontal	
μ	Fluid dynamic viscosity	$kg.m^{-1}s^{-1}$
π	Value of Pi	
ρ	Fluid density	$kg.m^{-3}$
σ	Fluid surface tension	$kg.s^{-2}$
τ_w	Shear force per unit area on fluid due to friction	$kg.m^{-1}s^{-2}$
ϕ	Arbitrary value or fluid property	

Subscripts

$\phi_1, \phi_2, \phi_3, \phi_4$	Number of control volume or reservoir interface
ϕ_{acc}	Accelerational
ϕ_{avg}	Average value variable
ϕ_{atm}	Variable related to atmospheric conditions
ϕ_{coef}	Heat transfer coefficient
ϕ_{CS}	Control surface
ϕ_{CV}	Control volume
ϕ_{DW}	Darcy-Weisbach friction factor
ϕ_{ex}	Value of variable at outlet of control volume
ϕ_{fan}	Fanning friction factor
ϕ_{fg}	Heat of vaporisation
ϕ_{flow}	Value of variable related to physical dimensions where flow is present
ϕ_{fluid}	Value of fluid related variable
$\phi_{friction}$	Value of fluid friction related variable
ϕ_{heat}	Value of heat transfer related variable
ϕ_{lam}	Laminar flow
ϕ_{liq}	Value of variable in liquid phase of fluid
ϕ_{loss}	Loss values or secondary losses
ϕ_i	Value of counter i
ϕ_{in}	Value of variable at inlet of control volume
ϕ_{mac}	Macro boiling
ϕ_{mic}	Micro boiling
ϕ_{mix}	Value of variable in fluid mixture, single phase or two phase
ϕ_{net}	Net value variable
ϕ_{ONB}	Value of variable regarding to the onset of nucleate boiling
ϕ_{orf}	Orifice

ϕ_{rel}	Relative value
ϕ_{res}	Resultant or net force
ϕ_{RV}	Reservoir related quantity
ϕ_{sat}	Value of variable at saturated conditions of fluid
$\phi_{\sup}$	Value of variable regarding wall superheat temperature
ϕ_{sp}	Value of variable at single phase fluid conditions
ϕ_{sub}	Value of variable regarding fluid subcooling
ϕ_{tp}	Value of variable at two phase fluid conditions
ϕ_{trans}	Transition regime between laminar and turbulent flow or heat transfer
ϕ_{turb}	Turbulent flow
ϕ_{vap}	Value of variable in vapour phase of fluid
ϕ_{wall}	Value of variable at the pipe wall

Superscripts

ϕ''	Rate of heat transfer per unit area
ϕ'''	Rate of heat generation per unit volume
$\bar{\phi}$	Vector quantity

Chapter 1 - Introduction

In this chapter the topic of this investigation is introduced. Some background is provided while the purpose, scope and deliverables of the investigation are discussed.

1.1 Project purpose

The following question posed to the author provided inspiration and a purpose to this investigation:

“What value can a natural circulation loop, running along the height of a pressurised water reactor (PWR) containment building, have in terms of removing heat from the building?”

This investigation was initiated in order to answer this question. Using this question as a starting point, the rest of the investigation was developed.

To introduce the reader to the basic concepts and terminology used in this report, the basic concepts of a PWR, containment buildings and a natural circulation loop (NCL) are presented in this chapter. This chapter also includes the project definition, scope and deliverables.

1.2 Introductory information

In this section, some background to the investigation is provided. The aim is to provide a good understanding of the topic at hand. The main primary loop components are listed and containment designs are introduced.

1.2.1 Pressurised water reactors

PWRs are one of the most common nuclear reactor designs used for electricity production in the energy industry today. The design of these reactors have been updated and improved with time as safety and other factors are taken into consideration. Regardless of new designs, the basic concept of a PWR power plant remains evident.

The main thermal cycles of a PWR power plant are shown in Figure 1-1. The illustrated power plant consists of three main loops. These are the primary (Figure 1-1, a), secondary (Figure 1-1, b) and tertiary (Figure 1-1, c) cycles (or loops). Each thermal cycle has a heat source and sink. The primary loop is heated by the fission process in the reactor and is cooled by the secondary loop through the primary heat exchanger (the steam generators). The secondary loop is therefore heated in this way. It therefore follows logically that the main heat sink for the secondary loop is the tertiary loop. The tertiary loop is heated and thus provides cooling capability to the secondary system. In many cases the ultimate heat sink for the tertiary loop and the power plant is the sea or a cooling tower.

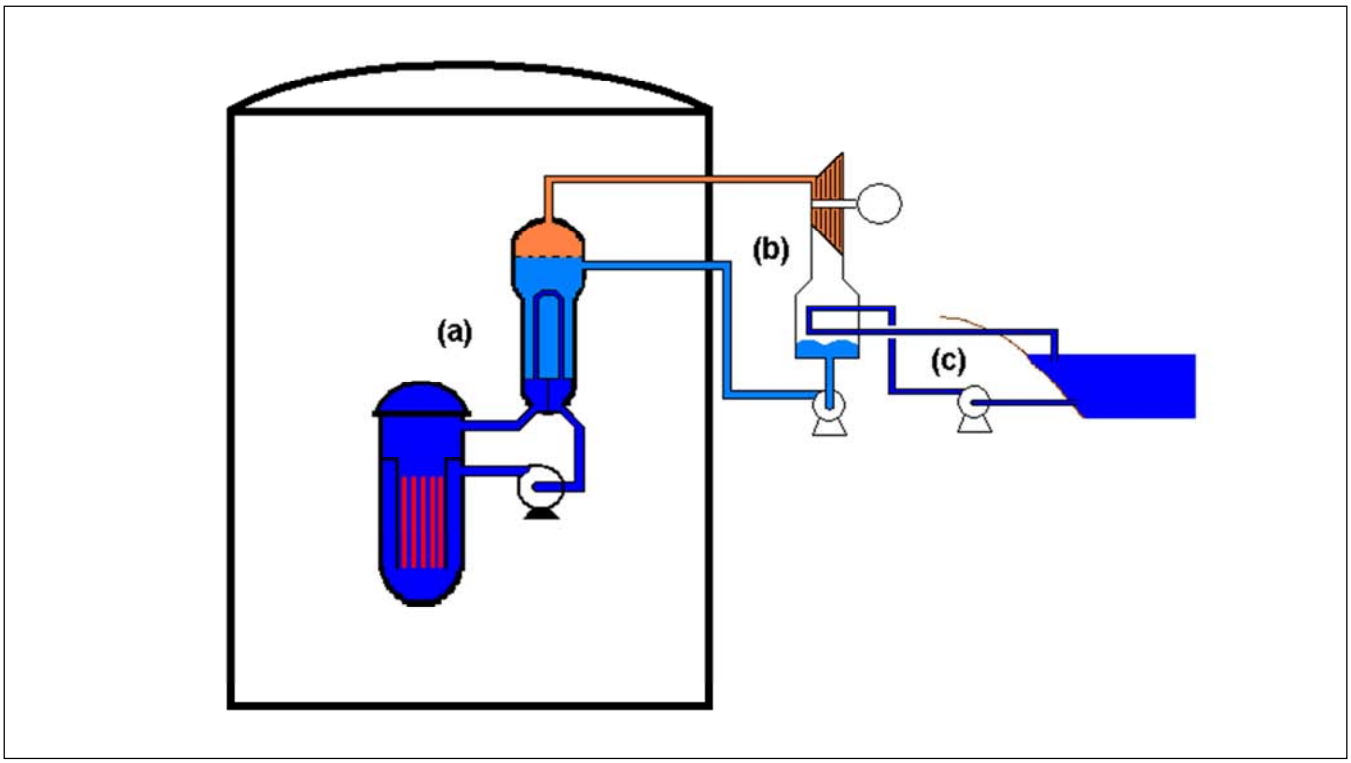


Figure 1-1. Overview of PWR power plant thermal cycles.

A more detailed view of the primary loop and some of the typical systems in the thermal cycle are shown in Figure 1-2.

The main components of the primary side are the following:

a. Reactor (Figure 1-2, a), which produces the heat through the fission process used in making steam for power generation.
b. Steam generators (Figure 1-2, b), which are the heat exchangers between the primary and secondary loops. The steam generators cool the primary loop and generate the steam for use in driving the turbine-generator set.

c. Primary pumps (Figure 1-2, c), used to circulate cooling water through the primary loop.
d. Primary piping (Figure 1-2, d), which connects all the components.
e. Pressuriser (Figure 1-2, e), used to control the primary system pressure.
f. Containment building, the barrier between the environment and the primary loop.

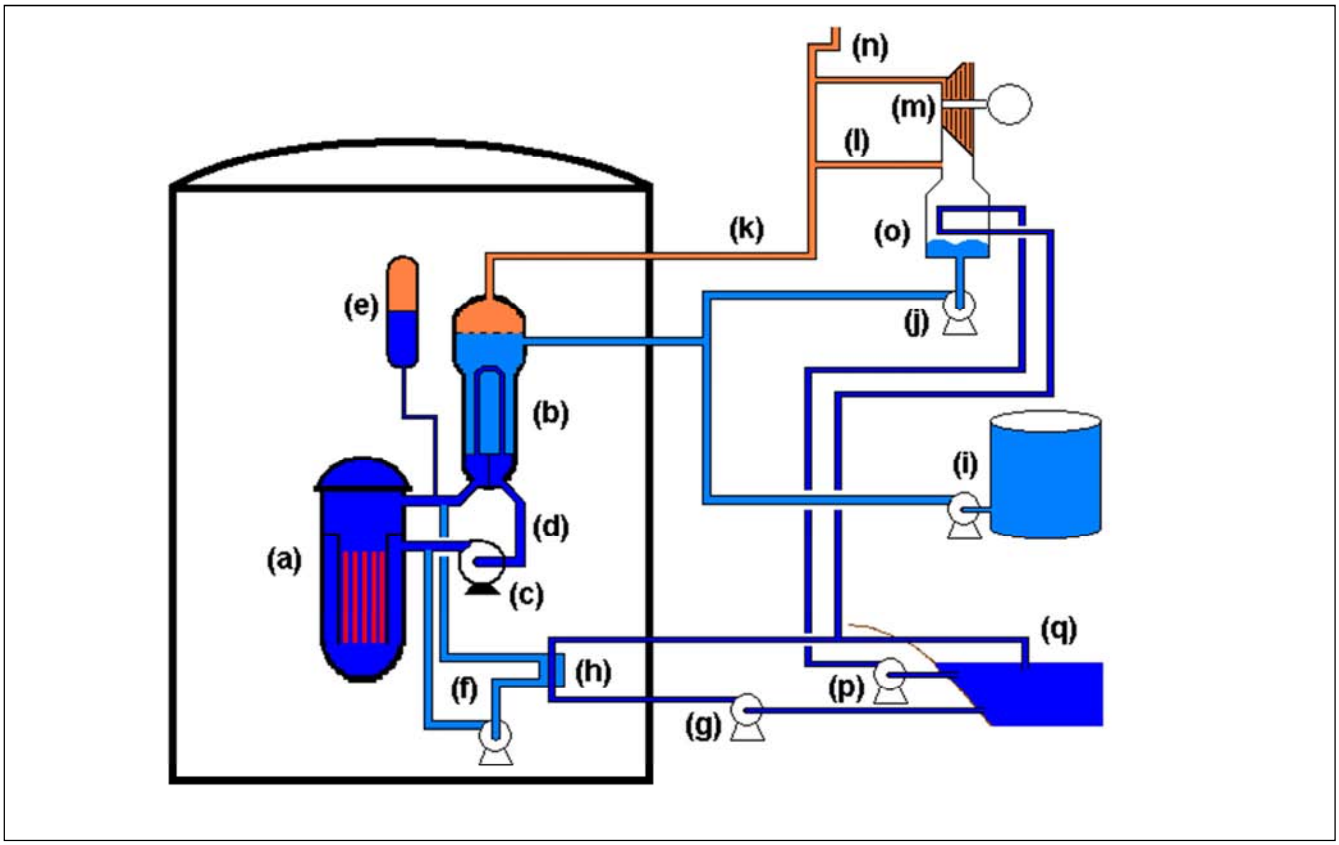


Figure 1-2. PWR heat removal circuits.

The primary circuit's main heat sink during operation is the steam generator. Water is supplied to the steam generator (Figure 1-2, j) and absorbs the heat from the primary circuit by boiling. The steam is then piped from the steam generator (Figure 1-2, k) and expanded through a turbine generator (Figure 1-2, m). The turbine generator produces electrical power. The turbine exhaust is then cooled down in the condenser (Figure 1-2, o), which is cooled by water pumped (Figure 1-2, p) from the ultimate heat sink. The heated water is then returned to the source (Figure 1-2, q). During shutdown or emergencies heat can be removed from the primary circuit using the following methods:

a. A backup feedwater system with sufficient capacity to remove decay heat from the building through the steam generators (Figure 1-2, i).
b. If the turbine generator is unavailable, steam from the steam generators can be vented directly to the condenser (Figure 1-2, l). Alternatively, it can be vented to the atmosphere (Figure 1-2, n).

c. An alternative heat sink to the steam generators can also be used. Water is pumped (Figure 1-2, f) from the primary circuit to a heat exchanger (Figure 1-2, h), which is cooled by water from the ultimate heat sink (Figure 1-2, g).
d. An alternative heat removal method to the decay heat removal systems listed above.

There are many more systems that can be used for heat removal other than those mentioned above. For the purpose of this investigation the overly simplified versions of the power plant cycle and primary loop are sufficient to explain the basic operation of primary side heat removal.

For emergency conditions when the plant integrity is at stake and a breach of the primary system is imminent the containment building, which houses the primary circuit, must be cooled. This will lessen the chances of a primary system breach or, in case of a primary system breach, reduce the impact on the containment building of the substantial quantity of heat that may be released.

1.2.2 Containment buildings

One of the most recognisable features of a PWR power plant is the containment building that surrounds the reactor and primary circuit. The building is constructed from reinforced concrete and steel linings or shells and acts as a barrier between radioactive material and the environment (IAEA, 1994:10–12).

The containment barrier may be challenged by external or internal events. Therefore, the containment design must take into consideration the possibility of these events happening and their subsequent consequences. Plane crashes, meteorological conditions and others are classified as external events. Internal events are events that originate from within the building which may lead to the release of radioactive substances into the environment. A typical example of this is a primary system breach with the subsequent release of primary circuit water.

The containment building on a PWR plant typically consists of a thick reinforced concrete shell (Figure 1-3, a). Other than the traditional design, containment designs may also be of a double shell type. An example of this is a concrete outer shell surrounding another concrete inner shell (Figure 1-3, b) or alternatively an inner steel shell (Figure 1-3, c). There are other containment types as well which will not be discussed here. To prevent the release of radioactive material into the environment from a breached primary circuit the containment building must be virtually leak proof.

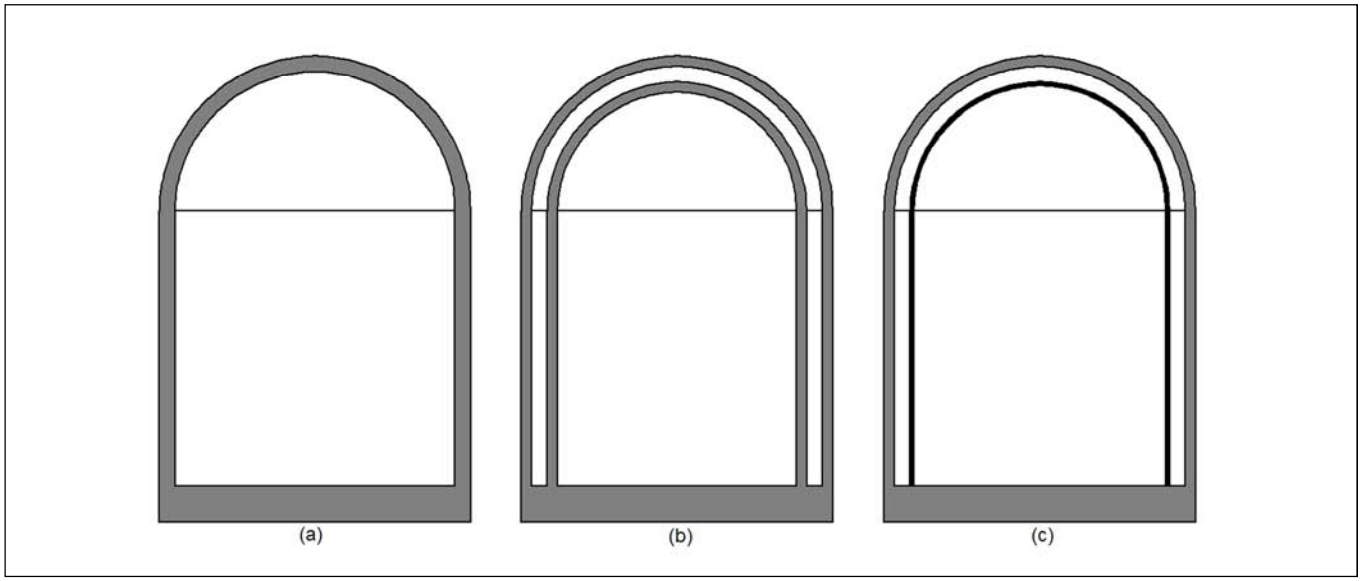


Figure 1-3. Different containment designs.

The containment building of a nuclear reactor houses many components that are critical to the operation and safety of the power plant. The primary cooling circuit, steam generators and reactor core housed inside the containment all contribute to the heat load of the interior during normal operations. This heat may be removed using a cooling system of some design.

In the event of an accident, for example a loss of coolant accident (LOCA), more heat is released into the building. The heat produced may be removed by using a variety of systems depending on the design of the reactor and containment. Since the handling of these accidents play an important role in the safety of a reactor design, these types of accidents are the subjects of many studies.

What is apparent is that some of the newer designs for cooling the primary circuit, steam generator or containment building are of a passive nature (IAEA, 2002:2–3). These passive cooling systems come into action without any operator or automatic system action. These systems, when correctly designed, can be more reliable than an active system. Of these emergency systems many use the natural circulation phenomenon as a means of circulating cooling fluid. Several of these passive containment cooling designs have been proposed or are in use. Some details of these cooling designs will be discussed in the next section.

1.3 Introduction to concepts used

In this section several containment cooling concepts will be introduced and discussed to ensure that the relevant background to this investigation is provided. The cooling loop and other matters relevant to this investigation are discussed. The stability of passive cooling loops is also discussed.

1.3.1 Containment cooling systems on PWRs

Cooling the inside of the containment building during an accident will assist in reducing the severity of the accident or even in preventing it. Several containment cooling systems are in use and have been proposed. These include, but are not limited to the following (IAEA, 2002:12–14):

a. A spray-water system inside the containment that sprays water into the containment airspace in the case of elevated temperatures or pressures (Figure 1-4, a).
b. A system that uses heat exchangers on the inside and outside of the containment building. In some designs the outside heat exchangers are immersed in water. In others a simple tank and vent system provides a heat sink. There are a number of variations to this concept (Figure 1-4, b).
c. A double shell containment building with water sprays on the outside of the inner steel liner and/or natural air circulation through the annular space between the concrete and steel shells (Figure 1-4, c).

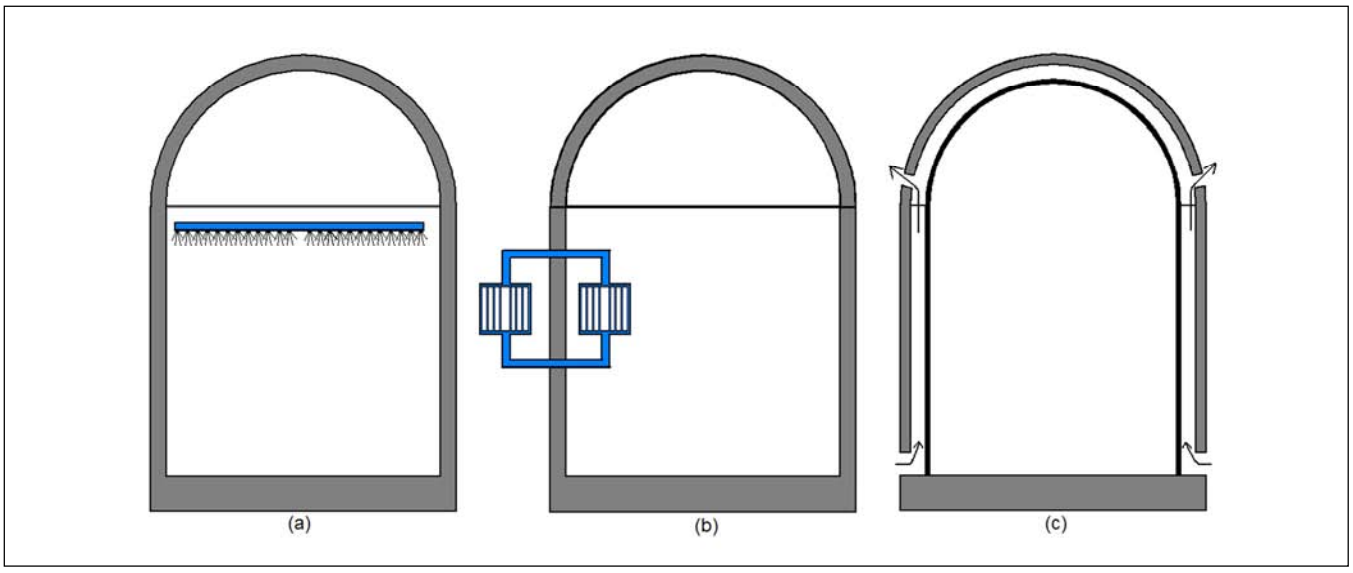


Figure 1-4. Containment cooling designs.

During the course of this investigation a simple rectangular cooling loop with a reservoir will be investigated (Figure 1-5). The difference in densities between the fluid in the hot and the cold leg of the cooling loop, which are acted upon by gravity, will produce a force that will drive the circulation of the fluid in the loop. The fluid flow will enable heat transfer from the containment building. This phenomenon of fluid circulation, driven by the gravity-induced buoyancy forces, is called natural circulation.

The design that will be investigated during the course of this project will be based on a cooling system with single heat exchanger pipes. Instead of using heat exchangers, like the example shown above (Figure 1-4, b), the cooling loop will utilise vertical pipes on the inside and outside of the containment building. The motive force for the circulation of coolant through the loop will come from a density difference between the two vertical pipe legs caused by heat transfer to and from the fluid inside the loop. Natural circulation will take place and thus the system will not need any pumps or other active components.

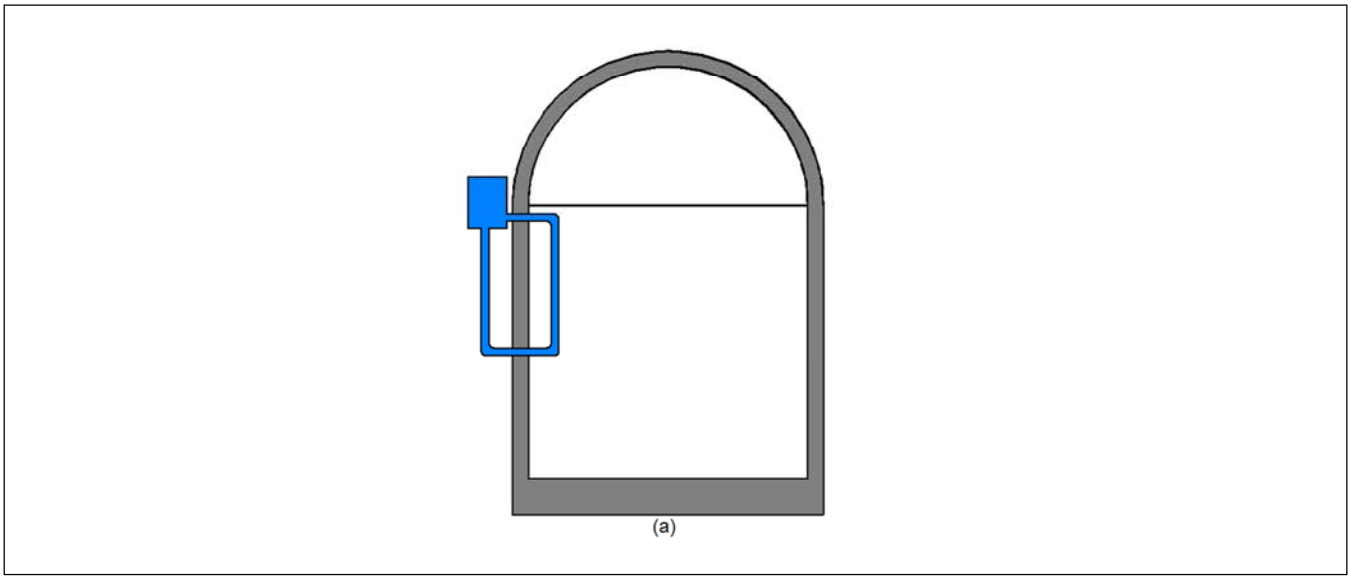


Figure 1-5. Containment cooling via a natural circulation loop.

The cooling loop will have four pipe sections and a reservoir. The vertical pipe sections will be used as heat transfer sections and the horizontal sections will be used to connect the vertical pipes. A reservoir is provided to compensate for any fluid expansions and the release of water vapour should any boiling occur.

The operation of the system where the containment airspace is hotter than the surrounding environment will be as follows:

a. Heat is transferred from the containment airspace to the inner vertical pipe, also called the hot leg (Figure 1-6, a).
b. The fluid inside the pipe is heated and may boil to a vapour-liquid mixture (Figure 1-6, b).
c. The warmer, lighter fluid circulates through the connecting horizontal pipe to the reservoir outside the containment (Figure 1-6, c).
d. If present, vapour is vented into the atmosphere (Figure 1-6, d).
e. The mass of water that has been released into the atmosphere is replaced by water fed into the reservoir (Figure 1-6, e).
f. The intake of the downward vertical pipe takes water from the bottom of the reservoir (Figure 1-6, f).
g. The water, which is still warm, moves downward in the outer vertical pipe, also called the cold leg and is cooled by heat transfer to the environment (Figure 1-6, g).
h. The cooled water then circulates via the bottom horizontal pipe to the inside of the containment building (Figure 1-6, h).

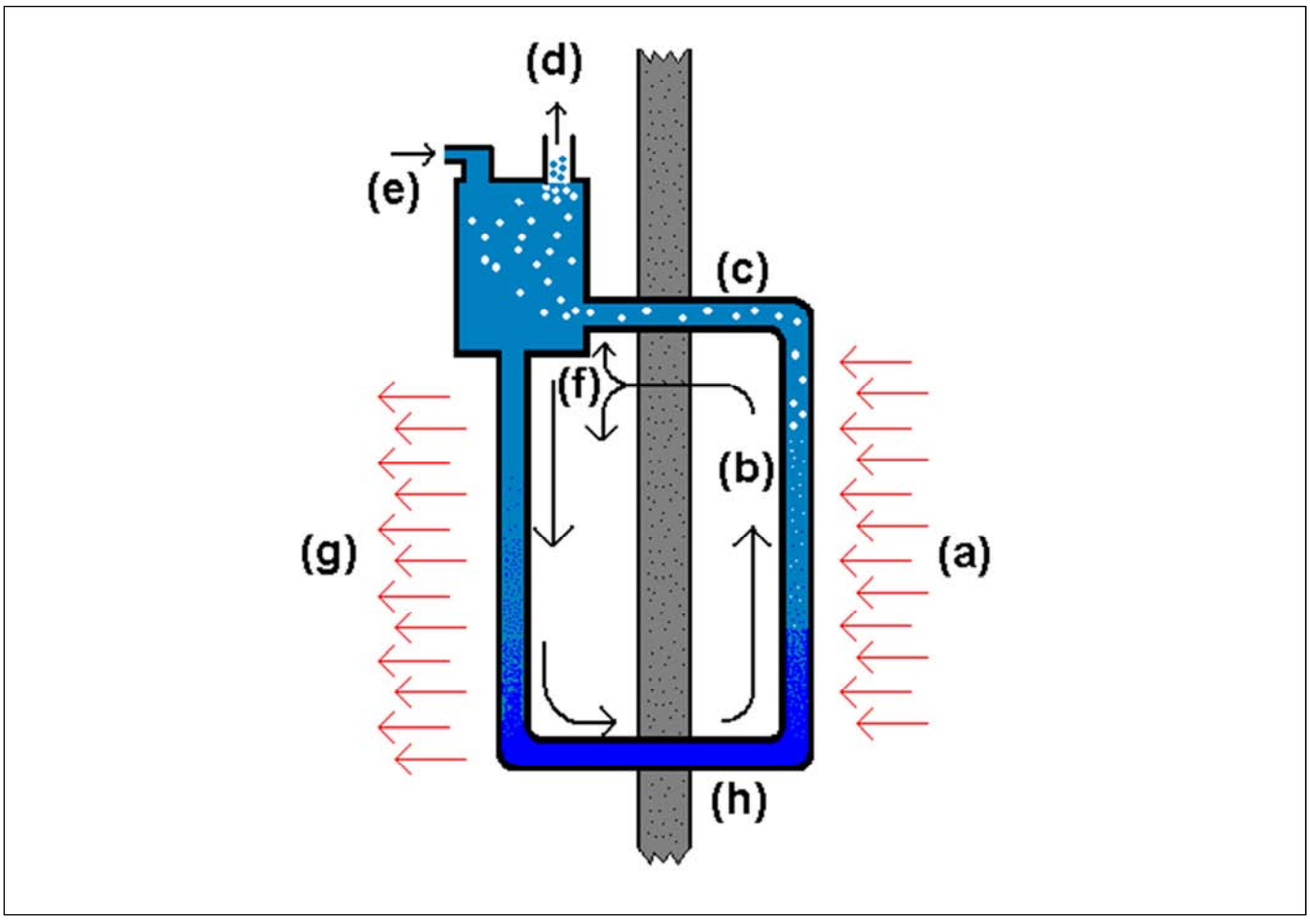


Figure 1-6. Natural circulation loop for containment cooling.

An NCL can be either of the open or closed type. In the case of a closed NCL the flow around the loop is not discontinuous anywhere although the loop may contain an expansion tank. An open loop has the inlet to the loop connected to a large source and thus the outlet conditions of the fluid does not affect the fluid conditions at the inlet to the loop. The NCL that is the subject of this study can be classified as a closed loop.

1.4 Project definition

This section will be used to define the investigation, as well as to set limits, deliverables and other detail that will aid in the execution of this investigation.

1.4.1 Problem statement

For the natural circulation loop (NCL) to be a viable concept for a containment cooling system, it must be able to remove sufficient heat from the interior airspace of the containment building and transfer it to the outside environment. To determine the effectiveness of the loop in this application it will be modelled using a simulation program specifically written for this investigation. Since this is a conceptual investigation a one-dimensional approach will be used.

Modelling any system has many advantages over experimentation or directly constructing it from a theoretical design. Conceptual models aim to provide a better understanding of the characteristics and orders of magnitude that are involved in the actual system. It may serve to highlight any fundamental flaws that were overlooked. Experimental setups are necessary in some cases where theoretical modelling may be lacking. Thus, each approach has its advantages and disadvantages. The modelling approach was selected so as to verify a conceptual design. A theoretical model is easily scaled and the input parameters of simulation runs can easily be adjusted.

Different simulations were conducted to reproduce the expected performance of the loop in certain situations. The data obtained, especially that related to the predicted heat transfer, was used to evaluate the suitability of the loop for this application and to determine if it is worth pursuing this concept in a containment cooling design.

This investigation covered the following:

a. A relevant literature study was conducted to obtain the background as well as the theoretical and empirical information that was required on the topic.
b. A suitable simulation model was used to determine the loop's behaviour in a steady state.
c. The simulation model was used to perform a parametric study on the loop with different temperature values on the heating and cooling sections of the loop.
d. In addition to the varying temperatures, the effect of pipe diameter, length and width of the loop was determined.
e. Based on the results an evaluation was done to determine whether the loop is a viable concept for removing heat from the containment building.

1.4.2 Scope of investigation

1.4.2.1 General scoping

This investigation aimed to produce a set of results that could be used to evaluate the natural circulation loop, based on the heat transfer it achieves. The approach used was to model the loop with simple models and approximations, where appropriate, to produce the required results. By keeping the simulation model simple, the time duration of simulation runs were kept short and a larger volume of results was obtained within a reasonable timeframe. The transient behaviour of the loop was not considered.

The simulated containment loop was open to atmosphere and thus at atmospheric pressure. Due to the higher than boiling point temperatures, which could be experienced inside the containment, two phase flow had to be considered, in addition to single phase flow.

A number of steady state simulations were performed with different wall temperatures and other loop parameters. This produced a large volume of results. These results were used to determine the viability of the concept.

1.4.2.2 Overall licensing of the NCL concept

As with all commercial nuclear reactor designs, safety is of the utmost importance. A regulation authority will review a reactor, containment, core cooling and other designs to ensure adherence to the required high standards of safety. A concept for cooling the containment, such as the NCL of this investigation, may or may not be licensable. This ultimately depends on how safe the regulation authority finds the final design of the NCL in conjunction with the rest of the plant.

Debating the suitability of licensing the NCL at this conceptual stage is not the aim of this investigation. This should only be done after careful consideration of all the advantages and disadvantages of such as system, coupled with its effect on overall plant safety.

The main disadvantage of a concept such as the NCL is arguably the intrusion of pipes through the containment wall. How the regulation authority views this depends on how many mitigation measures are put in place and the final design of the nuclear island in its entirety.

The focus of this investigation was the thermal performance of the loop and its potential for removing heat from the containment space. Licensing the NCL will not be discussed in this study.

1.4.2.3 Parameters that were varied

As input parameters to the simulation model the following parameters were varied during the simulation of the loop to obtain the results that would be used in the evaluation of the NCL:

a. Wall temperatures on the vertical legs

A fixed temperature value was specified for the vertical pipe walls (Figure 1-7, a and b). The heat transfer was then calculated. The values and increments of temperatures used were planned according to the maximum and minimum temperatures that could reasonably be expected inside a containment building and within an environmental temperature range that was deemed as being reasonable.

b. Pipe lengths and diameters

The simulations considered a series of vertical pipe lengths (Figure 1-7, c) and diameters (Figure 1-7, e). All the pipe lengths were varied in such a way that the loop remained rectangular. The entire loop was specified to be of the same diameter pipe. The length of the horizontal pipes, which connect the vertical sections, was also varied (Figure 1-7, d).

1.4.2.4 Parameters that were kept constant

As input parameters to the simulation model, the following parameters were kept constant during the simulation of the NCL.

a. Working fluid

The working fluid was water, since it is readily available at a nuclear power plant and is used as a coolant in many applications.

b. Design of the pipe simulation model

The design of the NCL simulation model remained fixed with a rectangular shape and an open reservoir. This excluded the vertical pipe lengths, widths and diameters that were varied, as was explained in the previous section.

c. Loop pressure

The loop was not pressurised since it was open to atmosphere. Local pressure increases due to elevation changes, as well as primary and secondary pressure losses, were taken into account.

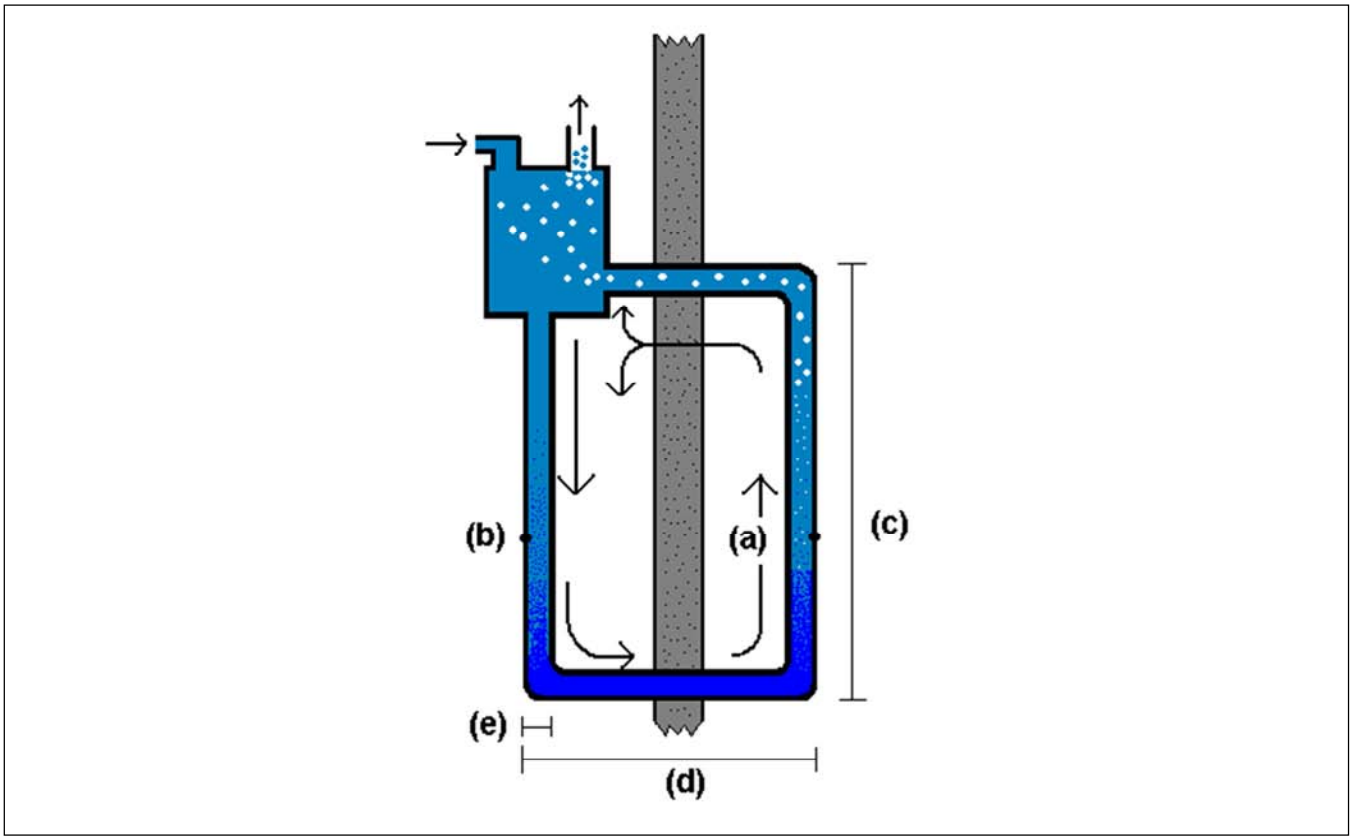


Figure 1-7. Physical parameters to be varied.

1.4.3 Deliverables

The investigation was considered to have been completed successfully when the following deliverables were produced with reasonable quality and accuracy in a technical report:

a) A summary of relevant published work on the subject.
b) A description of the underlying theory used in the simulation program.
c) A set of key results for the behaviour of the loop with different wall temperatures inside and outside the containment. These results can be used as a future reference for follow-up projects.
d) A description of the most important results with graphs and other information to assist with the interpretation of the investigation results.
e) An evaluation of the concept based on the results obtained with the model.
f) Recommendations for further studies on the subject.

This concludes the project definition section. The investigation scope was discussed and topics such a general scoping statement, as well as more specific details on scoping parameters, were mentioned. The following section will deal with matters that needed to be addressed to successfully complete the investigation.

1.5 Main project matters that were addressed

During the course of this investigation several challenges had to be addressed. This section summarises these matters and how each was dealt with.

1.5.1 Literature study

A number of areas had to be covered in the literature survey to ensure that the investigation was based on a sound foundation of knowledge. Items that were covered include the following:

a. Two phase and single phase heat and mass transfer theory.
b. Steady state models and simulations.
c. Natural circulation theory, experiments, studies and correlations applicable to this study.
d. Heat rejection load imposed on typical containment cooling concepts during normal and accident conditions so that approximate figures could be used in the evaluation of the results.
e. Temperatures in containment buildings during normal and accident conditions.
f. Validation data for the numerical model from other experiments.

Each of these items had to be researched in the article databases available in the literature. Some of the items listed above only described the need for a value, formula or quantity. In these cases the research strategy was focused on obtaining experimental results or correlations.

1.5.2 Setting up the model

The numerical model of the loop had to be programmed into a suitable software package. The preferred program that was used was Engineering Equation Solver (EES) as it comes with a number of thermodynamic functions and was easily accessible to the author. The model that was used had to be based on sound theoretical principles obtained in the literature study.

1.5.3 Verification and validation of the model

Upon completion of the programming of the numerical model it had to be verified. It then had to be validated using published test data.

1.5.3.1 Verification

Verification of a simulation model can be done using two methods (Babuska & Oden, 2004:4065). The first is code verification. Code verification ensures that the computer code used in the simulation program is written correctly and that it does not contain errors. The second verification process that can be used is solution verification. Solution verification is the process of determining how accurately the mathematical (or theoretical) model is approximated by the computational method (or model).

For this investigation only code verification was used.

1.5.3.2 Validation

Validation can loosely be thought of as how well the model is able to produce results that accurately reflect the physical phenomena being modelled (Babuska & Oden, 2004:4064). The simulation model was validated by using test data as inputs to the simulation model and comparing the results to published results obtained during the literature study. The validation process ensured that the results were of a reasonable quality and reflected reality with some degree of accuracy.

1.5.4 Evaluating results

The raw data obtained from the simulation program results had to be processed so that the NCL could be evaluated. The suitability of the NCL for the removal of heat from containment buildings was based on the collective heat removal capacity of a number of NCLs. For the parametric simulations the NCLs were also compared based on the heat absorbed from the containment building. To aid in the understanding of the NCL some fluid parameters along the length of the NCL were compared between different loop conditions."

1.6 Project execution

The execution of the investigation is discussed in this section.

1.6.1 Literature study

The first phase in the investigation involved undertaking a literature study that addressed all the relevant subject matter, as was stated in the previous section. The literature study aided an understanding of the fundamentals of simulating an NCL. This included underlying theory, experimental results, correlations and assumptions that were made.

The aim was to obtain a base of knowledge from which to launch the next phase of the project. As the project progressed the literature study was extended to cover additional information that was required during the project execution. Both articles and textbooks were used as sources of information.

1.6.2 Building a theoretical model

After the completion of the literature study a theoretical model was built based on the knowledge obtained. It incorporated the chosen correlations, equations and other relevant theory into the model. This theoretical model was implemented in the simulation program.

1.6.3 Programming model

The theoretical model was manipulated into a form suitable for programming into the EES model. The simulation model equations had a slightly different form to that of the theoretical model. Differences stemmed from the naming conventions used in the equations which allowed the simulation model to be used for a set of control volumes (CVs). However, the derived equations remained unchanged.

A numerical model was programmed into EES based on the simulation model that had been drawn up. The setting up of the numerical model in EES was done in two steps: Programming the model in manageable routines and integrating these building blocks into a complete simulation model. The process of building the model using small building blocks helped ensure that the implementation of the model in EES was done systematically to minimise the time needed for debugging.

A peculiar trait of a computer simulation program is that it may take a large amount of time to complete, especially if it proves to be troublesome. Although systematic programming methods improved the quality of the programming code, some time-consuming problems appeared during the course of the model programming.

1.6.4 Verification and validation of the model

As stated in the previous section, the model was built using small building blocks. Code verification was done by comparing the implemented code to the theory used to compile it.

Validation of the model was done, after the model programming had been completed, using data obtained during the literature study.

1.6.5 Simulation

After completing the model verification and validation the input sets for the model were compiled and simulated using the full model. Results were then stored and analysed. The generated set of results was large, so input datasets had to be carefully chosen.

1.6.6 Analysing and evaluating results

The modelling results were analysed to evaluate the effectiveness of the NCL in removing heat from the containment building. Based on the evaluation further recommendations were made for future research.

1.7 Conclusion of introduction

In this chapter the elements of the investigation that were performed to investigate the NCL concept, which can be used to cool PWR containment buildings, were discussed. The following project information was discussed: Purpose, scope, deliverables and execution. Some of the heat transfer phenomena that had an important influence on the results were also discussed in more detail.

The chapters of this report each detail a part of the investigation. To provide a basic overview of this report, a short summary of each chapter is given below:

Chapter 1: The conceptual investigation is introduced, basic principles are discussed, the purpose and scope of the investigation are given and other information is stated.

Chapter 2: The information obtained through the literature study is presented.

Chapter 3: The theory on which the simulation program, which forms part of the current investigation, is based, is derived and explained.

Chapter 4: The theory of the previous chapter is manipulated into a form suitable for use in the simulation program. Various other details of the simulation program are explained.

Chapter 5: The simulation program is validated against experimental results and certain functions in the program are verified. The results obtained from the simulation program are proven to be trustworthy.

Chapter 6: The simulation program input parameters and results are discussed.

Chapter 7: Based on the results in the previous chapter the pipe loop that was the object of this investigation is evaluated. The investigation is concluded and various recommendations are made for further related studies.

Chapter 2 - Literature study

The transport of heat using natural phenomena holds many promises. In the specific case of an NCL, gravity or buoyancy driven flow eliminates the need for pumps. A system design that uses passive heat removal mechanisms has many possible advantages. Examples are reduced plant power usage, reduced capital cost and reliability. Disadvantages include stability issues, potentially lower heat transfer capabilities and others. In this section literature relevant to the NCL that was investigated will be discussed. Since this is a conceptual study the focus was on laying down the basics so that a simulation model could be built. This includes possible models that could be used, correlations and other related information. Detail phenomena, for example, stability and flow regimes were not considered in the simulation program.

Topics that were covered during the course of this investigation are:

a. Studies related to the cooling of containment buildings using passive systems and related studies. This was used to prove that this investigation had merit.
b. Other applications to demonstrate that an NCL has applications other than containment cooling. This proved that even if the NCL which was the subject of this investigation was not suitable for its intended purpose, other options exist for its use.
c. Relevant theory and correlations to support the derivation of the theoretical model. This was done to support the simulation model used for the modelling of the NCL.

IAEA (1994), IAEA (2001), IAEA (2002) and IAEA (2005) provide good information on almost all aspects of natural circulation. These references are invaluable as a general guide and source of knowledge.

2.1 Passive containment cooling at nuclear power stations

This section of the literature study discusses various methods of passive containment heat removal.

Gavrilas *et al.* (1998) investigated a passive containment cooling design for a high-power rating reactor. It was found that other cooling designs have only been proposed in conjunction with a low-rating reactor. The authors examined several methods of implementing passive cooling so that the design limits of the plant would not be exceeded during accidents. Various configurations of containment cooling features were analysed (Figure 2-1).

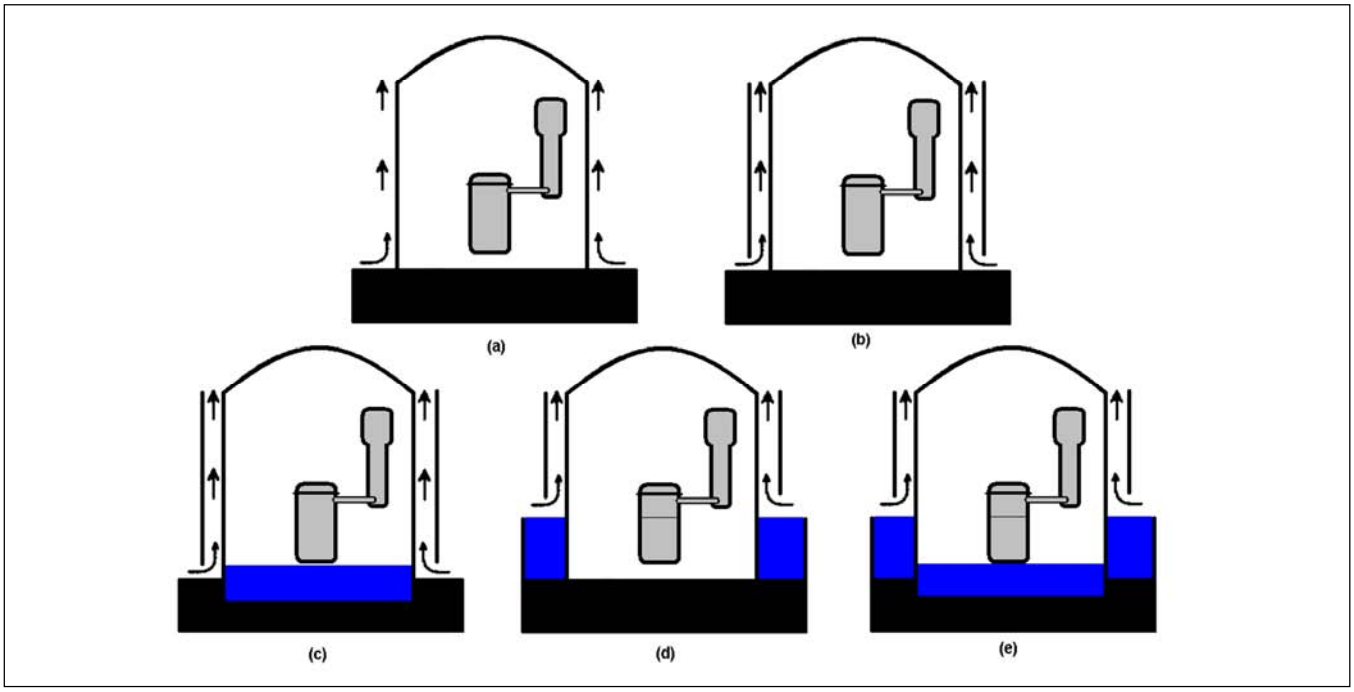


Figure 2-1. Containment passive cooling concepts (Adapted from Gavrilas *et al*., 1998:649).

It was found that heat can successfully be removed from the containment space if a number of design characteristics are incorporated. These characteristics are the following:

a. Bare steel shell (Figure 2-1, a);
b. Annular convection path (Figure 2-1, b);
c. Annular convection path and an internal pool (Figure 2-1, c);
d. Annular convection path and an external pool (Figure 2-1, d); or
e. Annular convection path in combination with an internal and external storage pool (Figure 2-1, e).

A double containment wall with an inner steel shell and outer concrete shell was proposed. By combining it with water storage pools it was found to remove sufficient heat from the containment space. Steel was used on the inside of the containment building to promote heat transfer, while the outer concrete shell protects the steel shell from external threats.

In the case of a primary circuit breach the energy released into the containment building is initially absorbed by the atmosphere (or airspace). Heat is removed from the containment airspace by conduction through the steel shell to the annular airspace. Natural convection of the air through the space between the two containment shells ensures that heat is continually removed from the steel shell and thus also the containment. Together with energy storage in the main structures inside the containment volume, an external subcooled moat around the containment and an internal water pool, sufficient heat is expected to be removed passively to ensure the integrity of the containment system. It

was suggested that since the heat transfer coefficient is easily affected by surface treatment special attention should be paid to enhancing heat transfer on the steel shell. This would most likely result in even larger heat removal rates or would enable a reduction in the large storage pools. It was also mentioned that although a passive system can reliably remove energy from a containment building, this can be done even faster if the passive cooling system is augmented by an active system.

The authors also showed how much energy can be released and absorbed during a loss of coolant accident (LOCA) in a pressurised water reactor. As can be seen in Figure 2-2, a considerable quantity of heat is released and absorbed.

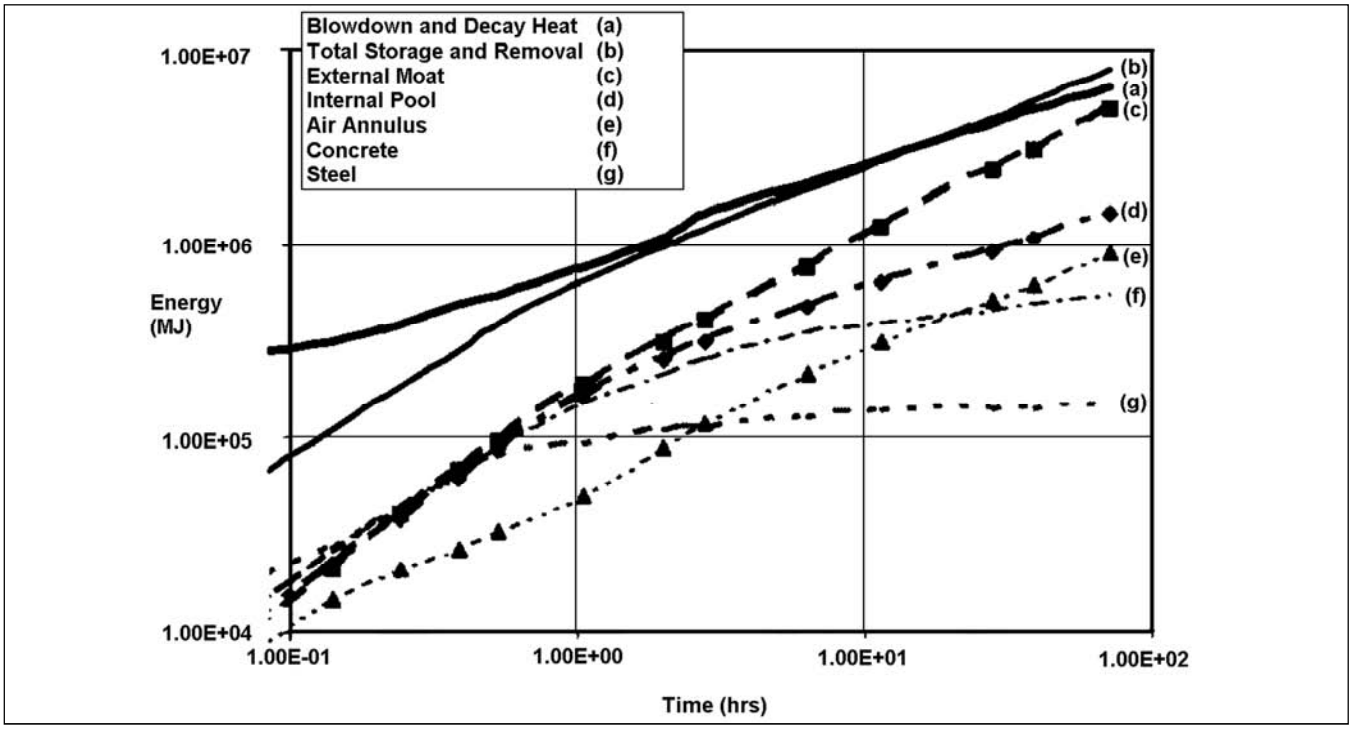


Figure 2-2. Energy removal during a LOCA (Adapted from Gavrilas *et al.,* 1998:654).

A nuclear power plant uses the containment system as an ultimate barrier to prevent the release of radioactive material into the environment. It is thus very important to ensure that it maintains its integrity. Lee *et al.* (1997) compared a variety of passive containment cooling designs. The following concepts were investigated:

a. Water spray on the inner steel containment shell from water tanks on the top of the containment building (Figure 2-3, a).
b. A storage pool around the steel containment shell (not shown).
c. A storage pool for concrete containment with convection air cooling over an inner steel shell (Figure 2-3, b).

d. A combination of internal water sprays and external or internal condensers with a closed NCL (Figure 2-3, c).
e. An NCL open to atmospheric cooling by a closed circuit of internal water sprays (Figure 2-3, d).
f. Combinations or derivatives of the abovementioned concepts.

The heat transfer area needed for a closed NCL system is reasonable, provided that a good flow path is provided for the fluids to the heat transfer surfaces and non-condensable gas effects are minimised. The non-condensable gases affect heat transfer negatively since these gases tend to reduce the fluid contact with heat transfer surfaces. Lee *et al.* (1997) concluded that steel containment shells provide a general advantage in terms of passive heat removal with minimal containment penetrations. However, the increase in cost with an increase in reactor power may pose a problem.

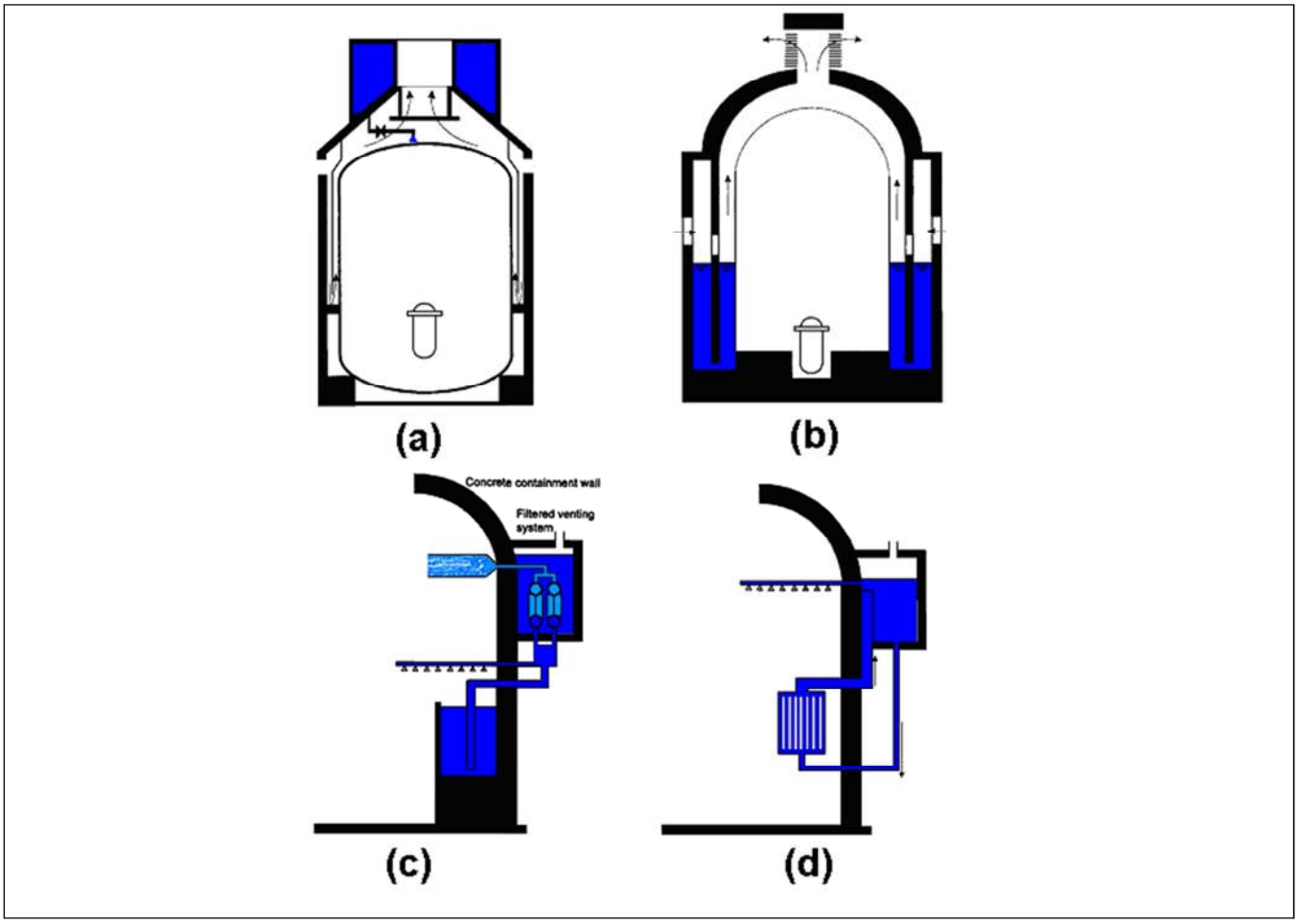


Figure 2-3. Passive containment cooling designs (Adapted from Lee *et al.,* 1997:469-471).

Passive heat removal systems, together with concrete containment structures, may have significant advantages. According to Lee *et al.* (1997) concrete containment buildings have a large experience base, are easily scalable and have a lower cost. It must be noted that the heat removal systems can become rather complex, which may offset the advantages of a passive system as a whole.

Byun *et al.* (2000) investigated a containment cooling concept which was very similar to the loop being investigated in this study (Figure 2-4). It was made up of an open NCL with an evaporator inside the containment space. A number of stainless steel tubes inside the containment absorbed heat from the airspace (Figure 2-4, a). Heated fluid collected in a single pipe and flowed through the containment to a level-controlled pool outside (Figure 2-4, b and c). Fluid from the bottom of the pool was fed back through the containment wall to the tube bundle (Figure 2-4, d). Fins were also proposed to enhance heat transfer. The open loop concept was found to perform better than a closed NCL simply because of reduced thermal resistance.

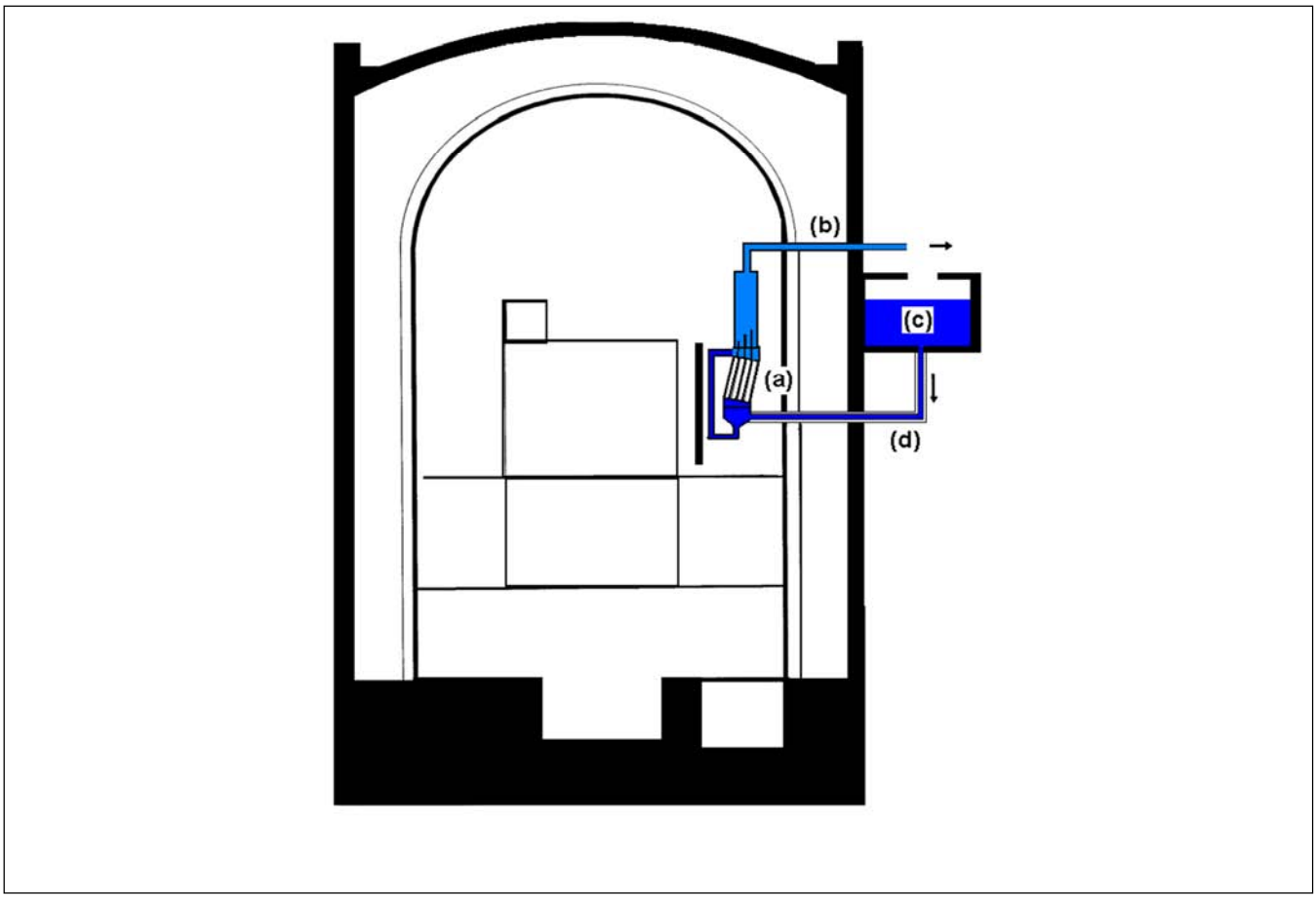


Figure 2-4. Containment cooling with open NCL and water tank (Adapted from Byun *et al.*, 2000:230).

According to the authors containment temperatures can be as high as 130℃. Loop performance was investigated at tube wall temperatures of 125℃ and simulations were done to see how the pressure inside the containment would react to the cooling concept. The cooling concept was found to be able to meet severe accident requirements, but the long-term reduction of pressure was not met due to the lower temperature differences available for driving heat removal. In conclusion, it was stated that further studies should focus on enhancing heat transfer to meet all the requirements.

An experimental study on a simplified version of the above concept (Figure 2-4) was performed by Liu *et al.* (2000). Heat removal from the concept (Figure 2-5) took place by boiling the fluid and replenishing the lost vapour from a water source.

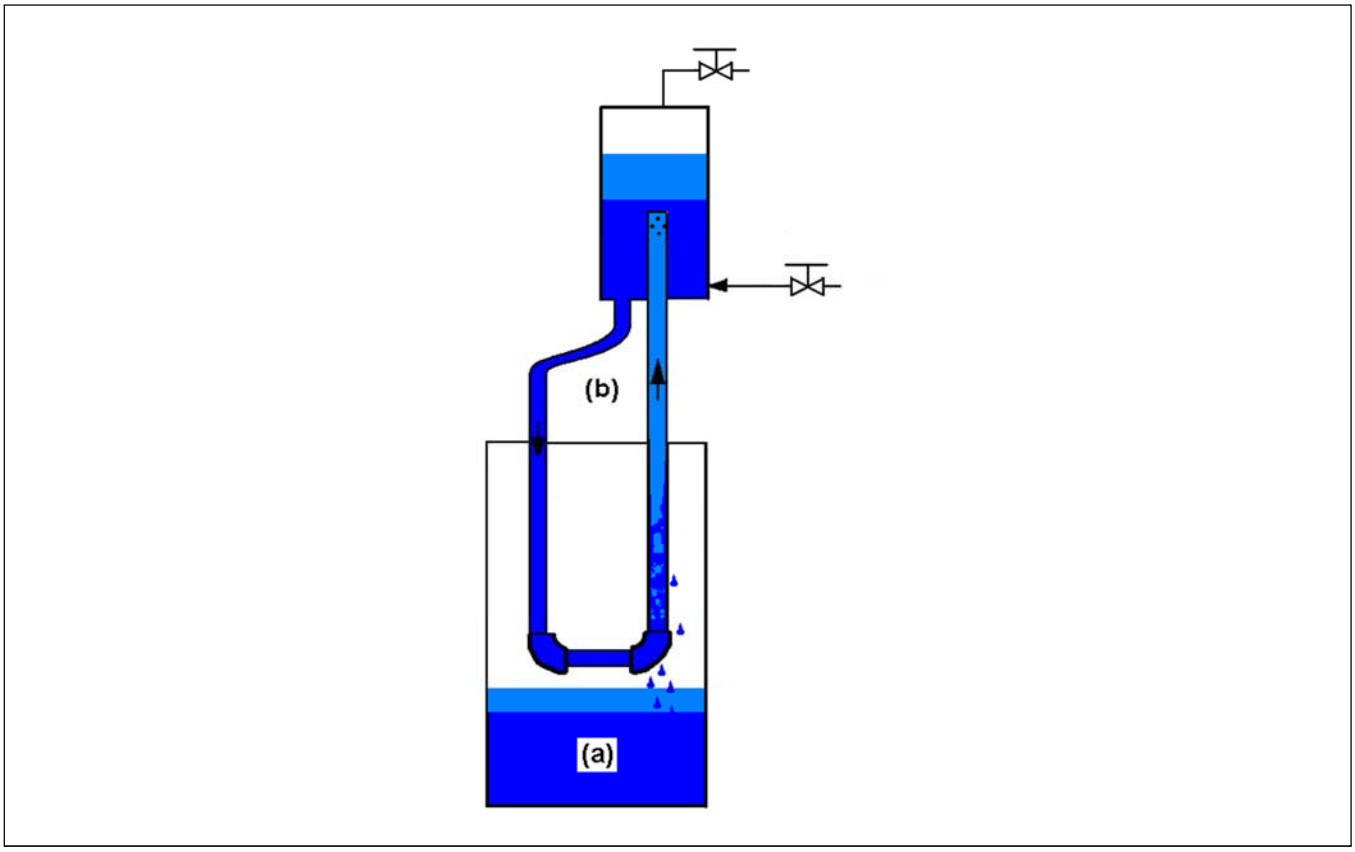


Figure 2-5. Experimental investigation on a simplified NCL **(**Adapted from Liu *et al.,* 2000:246).

The paper investigated a specific phenomenon associated with the open NCL concept. Steam was generated (Figure 2-5, a) and condensed on the surface of a single phase NCL cooling loop pipe (Figure 2-5, b). The fluid was supplied from a top mounted reservoir with its liquid level held at a constant height. Heat transfer coefficients on the outside of the heated sections were experimentally obtained and compared with other correlations. The presence of non-condensable gases was determined to negatively affect the heat transfer coefficient. A correlation was developed for correlating the heat transfer coefficient with a number of other factors.

Forsberg and Conklin (1994) investigated a passive cooling loop that only provided cooling above a certain design temperature. Although not specifically designed for containment cooling, it is one of the proposed applications of this type of loop. This concept was designed so that the loop could act as a thermal diode. Heat could only be transferred in one direction from one particular side to the other. This is in contrast with a normal NCL, where the heat transfer would reverse if the temperature gradient across the loop was reversed. Below a certain temperature, the fluid circulation in the loop would cease

due to a vapour lock in the loop. The use of this device was evaluated for the cooling of the reactor cavity of a modular high temperature gas-cooled nuclear reactor. Significant potential for performance and economic advantages were identified.

In this section of the literature study the following findings were made:

a. Passive containment cooling designs are feasible.
b. Sufficient heat can be removed from the containment airspace with passive containment cooling devices.
c. Heat transfer limitations are the most limiting factors for an NCL-type heat removal system.
d. Containment airspace temperatures can be as high as 130 ℃, but heat transfer resistance may limit the NCL tube wall temperatures attained.

2.2 Other applications of NCLs

There are various other areas, many of which are not related to nuclear containment cooling, that also use NCLs as a means of transporting heat. If the NCL investigated in this study was found to be unsuitable, the model or data developed could still be used elsewhere as a starting point for other application designs. This section of the literature study discusses some other examples of the different applications of NCLs.

Another application of NCLs in the nuclear energy field is for the removal of heat directly from the primary circuit. Chung *et al.* (2006) investigated the removal of decay heat for a small reactor by means of a natural circulation principle at nuclear plants. A test facility for the testing of this concept was modelled using thermal hydraulic codes. Their initial results looked promising.

Another nuclear energy-related application is the production of hydrogen (Sabharwall & Gunnerson, 2009). The transport of heat energy from a high temperature gas-cooled reactor to a hydrogen plant poses some technical difficulty. Converting heat to electricity and back again is very inefficient and pumping a high temperature fluid places very high demands on equipment. Many advantages can be realised by considering the use of an NCL to transfer heat from the reactor to the hydrogen plant. Through the appropriate choice of working fluid, heat exchanger parameters and good design practices the use of an NCL to transport high temperature heat can be successful.

Other possible non-nuclear energy related applications for the use of natural circulation include use in reboilers (Kumar *et al.,* 2003, Kamil *et al.,* 1995a and Kamil *et al.,* 1995b), as waste heat recovery

devices (Akyurt *et al.,* 1995, Abu-Mulaweh, 2006 and Liu *et al.,* 2006) and domestic water heating applications (Belessiotis & Mathioulakis, 2002, Joudi & Al-Tabbakh, 1999, Esen & Esen, 2005 and Hussein, 2002). Another use, especially relevant today, is in the cooling of electronic components (Khodabandeh, 2004).

From this literature study section, it is clear that heat transport using natural circulation has a variety of applications. Given the simplicity of the NCL design proposed in this investigation, it may contribute to applications beyond the originally intended containment concept.

2.3 Single phase NCLs and related experiments and correlations

This section summarises literature relevant to single phase natural circulation.

Vijayan *et al.* (2007) experimented with a rectangular loop to investigate the effect that the orientation of the heating and cooling sections had on the stability of an NCL. The NCL was tested with a combination of heater and cooler section orientations with either sections being vertical or horizontal (Figure 2-6). An expansion tank located on the uppermost part of the loop took care of any fluid expansions due to heating.

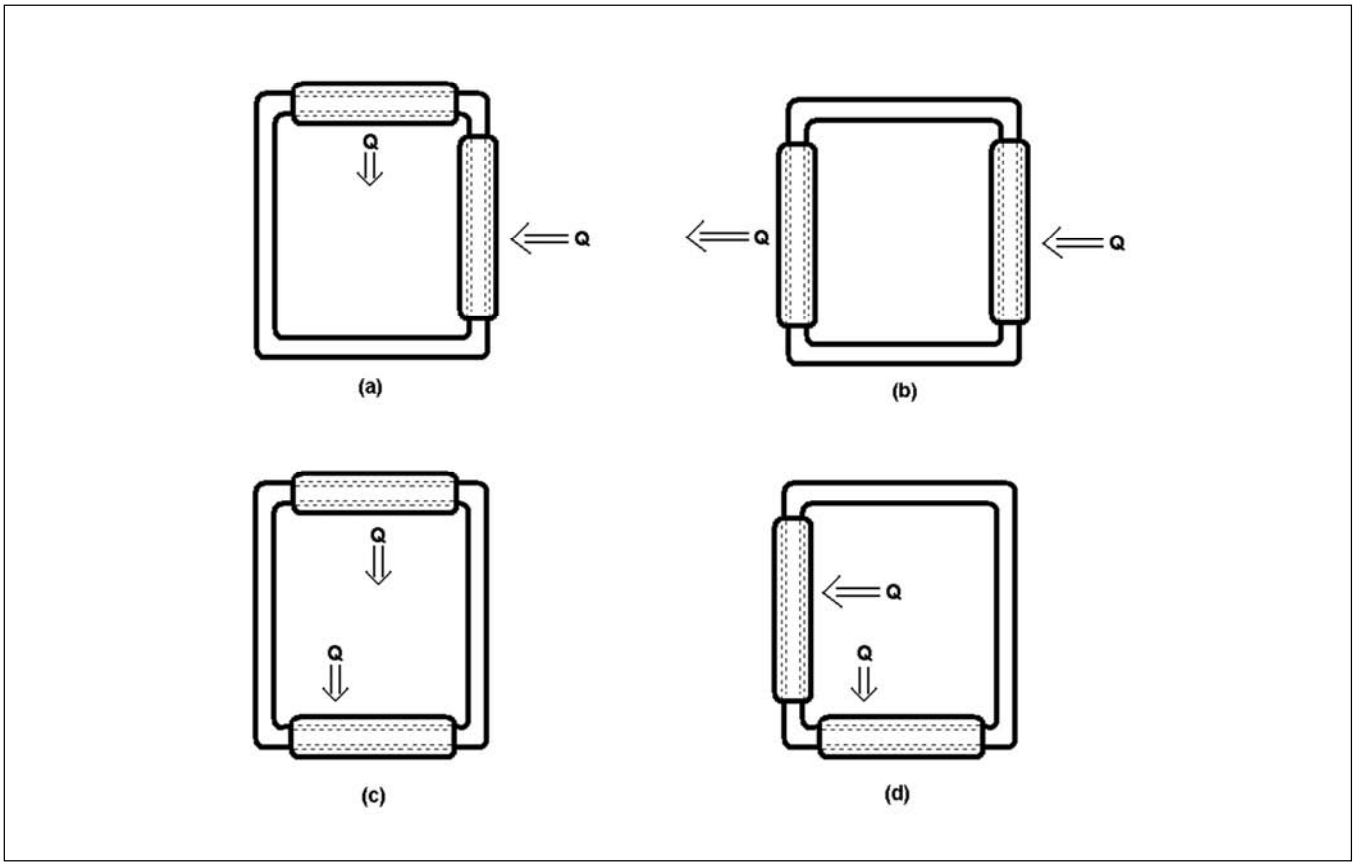


Figure 2-6. NCLs showing different heating and cooling section orientations.

The authors found that an individual loop may have one of three flow oscillation modes if it was unstable. By means of illustration, the experimental graphs are reproduced to provide a visual indication of the behaviour of unstable single phase flow. These were taken at different heating powers.

a. Near periodic uni-directional pulsing (Figure 2-7, a): The flow rate drops very low and may even reverse slightly before rapidly accelerating again in the original direction.
b. Near periodic bi-directional pulsing (Figure 2-7, b): The flow rate drops to zero, reverses and accelerates rapidly in the reverse direction before dropping to zero and reversing again. Flow rates in both directions are the same.
c. Chaotic switching (Figure 2-7, c): The flow rate chaotically switches between forward and reverse flow.

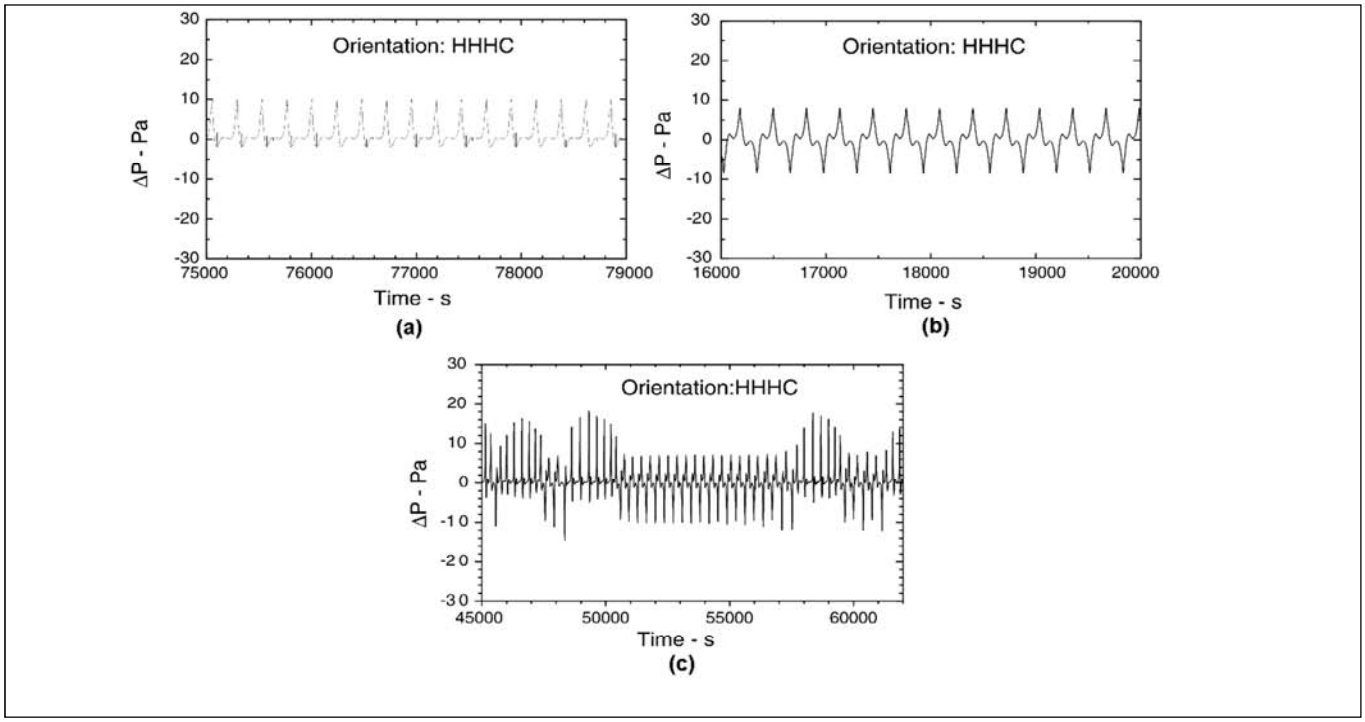


Figure 2-7. Various oscillation modes of an NCL (Adapted from Vijayan *et al.,* 2007:941).

In the vertical heater, vertical cooler (VHVC) setup it was found that flow was almost immediately initiated following the heating of the NCL. It was also found that the VHVC setup was the most stable of the possible heater and cooler orientations. The experimental results were compared with the results obtained from a one-dimensional model. Significant deviation was observed between the predicted power levels of the onset of instability and the experimentally determined power levels. This was the case even after the effects of pipe wall damping, local pressure losses and heat losses had been considered in the model. It was attributed to the limitations of the one-dimensional modelling approach, which could not capture the multidimensional causes of oscillations.

Misale and Frogheri (2001) used an NCL with a horizontal heater, horizontal cooler (HHHC) configured loop with orifices in the vertical legs. The aim was to determine the effect of the added frictional resistance from different sizes of orifices on the stability characteristics of the NCL. The result was that the smaller orifices had a larger stabilising effect. Although the loop with installed orifices took longer to achieve steady state operation, it was much more stable. Some of the larger orifices did not have a stabilising effect on the loop. It was concluded that appropriate pressure drops in an NCL can stabilise or at least add to the stability of an NCL.

Mousavian *et al.* (2004) used a finite difference one-dimensional model to simulate an experimental HHHC loop and analyse its transient behaviour and stability. Assumptions made included neglecting axial conduction, viscous dissipation effects and variation of density, except in the buoyancy force term. The finite difference technique was used to solve the conservation equations. A further comparison was made between the numerical results, results from a commonly used systems code and experimental results. It was concluded that the systems code and finite difference method (or non-linear analysis) showed good agreement with the experimental results. The final conclusion was that although the study was done on an NCL with HHHC configuration, the methods used seem to be applicable to VHVC configured loops as well.

Vijayan (2002) stated that to understand the steady state and stability behaviour of NCLs, non-dimensional groups (or scaling parameters) may be used. These dimensionless groups, which are not loop specific, enable the comparison of different NCLs, as well as upscaling from small-scale experiments. During the derivation of such non-dimensional groups, two different boundary conditions are normally used for the heating and cooling sections:

a. An isothermal (or constant temperature source and sink); or
b. The imposition of a uniform heat flux.

For each specified boundary condition a different set of non-dimensional groups have to be derived. These non-dimensional groups of variables were derived by considering the case of an HHHC configured NCL with imposed heat flux on their heat transfer sections. Of interest to the present study were the limits on the Reynolds numbers for laminar and turbulent flow. The range of Reynolds numbers where the loop was neither fully laminar nor fully turbulent was determined to be between 1000 and 4000:

Using non-dimensional flow parameters and certain assumptions for the pressure drop, good agreement was found between the experimental and predicted results. It was suggested that these parameters could be used for the validation of single phase NCL system simulation codes.

Pilkhwal *et al.* (2007) compared the simulation results obtained from an experimental setup, computational fluid dynamics (CFD) simulation code and a one-dimensional systems code. The following assumptions were noted to be common in systems codes:

a. The use of friction and heat transfer laws derived from forced convection experiments;
b. Ignoring boundary layer conditions in heating and cooling sections;
c. Ignoring axial conduction;
d. The use of first-order numerical schemes; and
e. One-dimensional conservation equations and cross-section averaged variables.

However, the model used in the study of Pilkhwal *et al.* (2007) differed from the abovementioned assumptions in the following ways:

a. Axial conduction in the fluid and heat structures was taken into account.
b. The Churchill and Chu correlation for natural convection flow heat transfer was introduced instead of the forced flow Colburn correlation.
c. A slight improvement was realised by taking thermal entry lengths into account in the cooling section.

Different heater and cooler orientations were simulated and the VHVC configuration (the same configuration type investigated in the current study) was found to be the most stable of the different configurations that were simulated. The vertical orientation of a heating or cooling section has a stabilising effect on an NCL system. The article concluded that one-dimensional tools provide relatively accurate results of steady state NCLs. However, even at a simplified level discrepancies appear due to different correlations for different phenomena and the inability to simulate multidimensional effects. The use of CFD models provides improved modelling capabilities, especially where the loop is not in a steady state condition.

Ambrosini and Ferreri (2000) performed stability analyses on three NCLs using a finite difference scheme. An HHHC rectangular loop with finite length heaters and coolers was investigated. A circular loop with an imposed heat flux and a rectangular loop with point sources and sinks were also included in the study. Several differencing schemes were used and compared. The importance of connecting (non-heat transferring) pipes was also noted in determining the reaction of the NCL to oscillation disturbances. It was concluded that the truncation error during the finite differencing process may have an adverse effect on the calculated results if a coarse discretisation is used. In general, stability is more likely to be predicted when coarse grids are used with single-order methods. Second-order models were found to be much better at predicting stability boundaries on a theoretical stability map.

Ambrosini and Ferreri (2003) started by stating that the transient analysis of fluid dynamic systems is very sensitive to the discretisation of the governing partial differential equations when finite difference methods are used. The main culprit was identified as being the truncation error. Other sources of discrepancies are the heat transfer and friction correlations, which were intended for forced flow. Again it was determined that second-order methods behaved much better than first-order methods. Numerical diffusion caused problems when system codes were used with first-order numerical schemes. A low diffusion scheme was proposed, which seemed suitable for the analysis of the thermal hydraulic behaviour of water-cooled nuclear reactors. The advantages of the low-diffusion scheme were found to be the following:

a. Providing reliable predictions of stability, even with coarse nodalisation.
b. The rapid improvement of the level of convergence when the number of nodes is increased.
c. The time-dependant behaviour of variables was much less sensitive to time-step size.

Ambrosini *et al.* (2004) investigated the effect of wall friction in the transition zone (between turbulent and laminar flow) on the stability of natural circulation. Of particular interest to this study was the calculation of the friction factor in the transition zone (Figure 2-8). Figure 2-8 shows two correlations (Figure 2-8, a and b) used by Ambrosini *et al.* (2004) for the prediction of friction values. The figure shows that the two correlations produce identical friction factor results in the region with Reynolds numbers less than 1 000 and also in the turbulent region for Reynolds numbers roughly more than 3 000.

The predicted friction factors from the two correlations are only different in the transition zone where Reynolds numbers are between 1 000 and 3 000. One correlation (Figure 2-8, a) predicted lower friction factors compared to the other. The correlation also had negative and positive slopes in the transition Reynolds number range. The other correlation (Figure 2-8, b) used the maximum value of the friction factor calculated by the turbulent and laminar region formulas in the transition zone. This produced a smoother calculated friction factor curve.

Ambrosini *et al.* (2004) concluded that:

a. A stability band appeared when the flow was in the transition zone between laminar and turbulent flow. This was due to the practice of taking the maximum friction factor predicted by laminar and turbulent friction factor correlations.
b. When localised pressure drops (for example, in pipe bends) were accounted for by using pressure drop coefficients, classic laminar and turbulent friction correlations gave reasonable results.

c. No fixed solution exists yet for the friction factor in the transition zone. Making use of a non-monotonous branch, which connects the lower predicted laminar friction factor to a higher turbulent friction factor using a relatively straight line with a positive gradient, predicted stability in the transition zone where experimental results showed unstable behaviour.

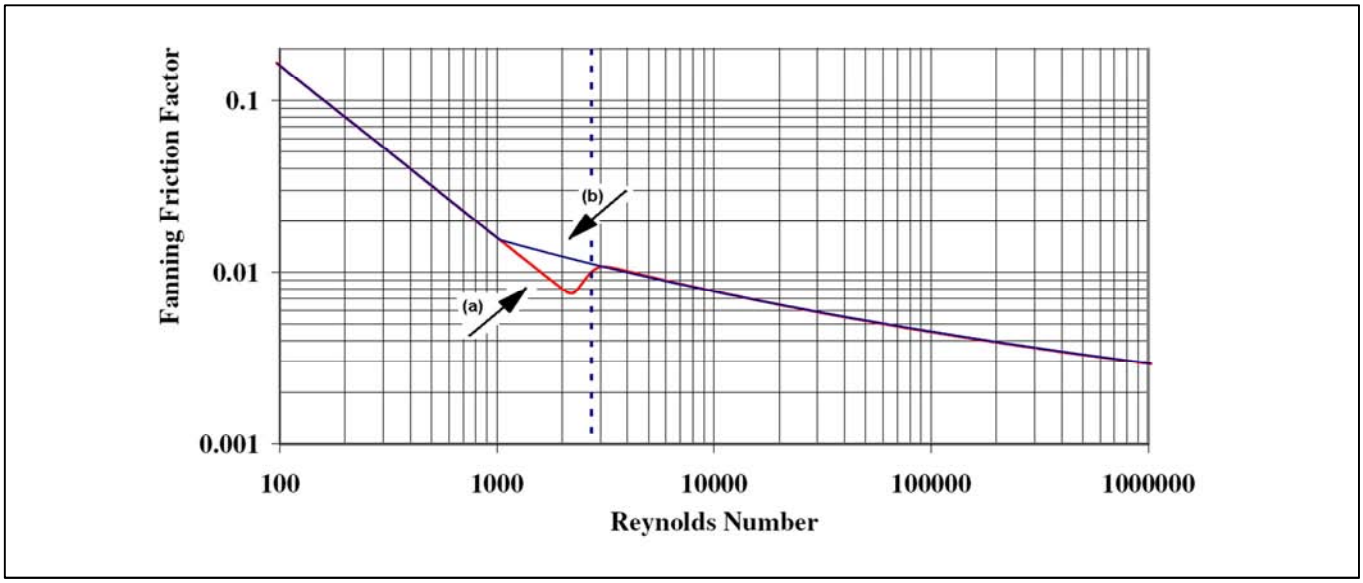


Figure 2-8 Friction factor determination (Adapted from Ambrosini *et al.*, 2004:1841).

Vijayan *et al.* (1995) examined the characteristics of the oscillatory behaviour that was observed when certain NCL experimental setups were simulated with a systems code. It was noted that the thermal capacitance of pipe walls provided a certain measure of damping of the flow oscillations. During simulations of flow instability friction factor correlations were switched whenever the flow was in the laminar or turbulent region. The transition zone's friction factors were determined by taking the maximum friction factor value calculated by the laminar and turbulent correlations. This led to the switchover from laminar to turbulent at a Reynolds number of about 1 100. For heat transfer calculations the familiar Dittus-Boelter equation was used.

During experiments significant thermal stratification was found, leading to the conclusion that better predictions were expected from two- or three-dimensional codes. However predicted stability characteristics using the system code were found to be similar to those obtained in the experiments, although some discrepancies existed.

This section provided a summary of literature relevant to single phase NCLs. The following was determined:

a. Single phase NCLs in the VHVC configuration are the most stable of all configurations.

b. The Reynolds number limits of the transition zone in an NCL could be determined.
c. NCLs with high or low aspect ratios are more stable than square shaped ones.
d. The single dimensional approach is satisfactory for a conceptual simulation of an NCL.
e. The forced flow correlations for friction factors and heat transfer can be used with some success.
f. The friction correlations for single phase flow could be determined.

2.4 Two phase NCLs and related experiments and correlations

This section discusses and summarises literature that may be relevant to two phase natural circulation modelling.

Table 1, adapted from the paper of Reyes (2005), compares the different one-dimensional modelling approaches for single phase natural circulation flows by showing the difference between two 3-equation models and a 6-equation two-fluid model used for the modelling of two phase flow.

Table 1. Conservation equations of various one-dimensional models (Adapted from Reyes, 2005:167).

Conservation equations	**Constitutive laws**
6-equation model – Two-fluid non-equilibrium model	
2 x mass phase balance	2 x phase wall friction
2 x momentum phase balance	2 x phase heat flux friction
2 x energy phase balance	1 x interfacial mass
	1 x interfacial momentum
	1 x interfacial energy
3-equation model – Slip or drift equilibrium model	
1 x mixture mass balance	1 x mixture wall friction
1 x mixture momentum balance	1 x mixture wall heat flux
1 x mixture energy balance	
3-equation model – Homogeneous equilibrium model	
1 x mixture mass balance	1 x mixture wall friction
1 x mixture momentum balance	1 x mixture wall heat flux
1 x mixture energy balance	
Notes: 1. Restrictions are imposed on fluid phase velocities or temperatures (or enthalpies as a function of temperature). 2. The minimum number of constitutive laws is stated here. If there is a number N flow phases, then N heat flux and N wall friction correlations may be required.	

As can be seen from Table 1, the complexity and number of equations increase as a model takes more detail into account. Methods of simulation that use the homogenous equilibrium models are the simplest to use for the modelling of two phase flows. On the other end of the scale of one-dimensional two phase simulation are the two-fluid non-equilibrium methods or six-equation models. These models use a set of conservation equations for each phase and two equations for each phase to describe heat and friction. In addition, there are also equations for the exchange of mass between the phases. These models will have improved accuracy, but will be complex to implement and more time consuming to solve using a simulation program.

According to Reyes (2005:8) the drift-flux method provides a reasonably accurate, yet simple to implement method of providing the capability to simulate the different phase velocities.

The most significant difference between the conservation equations of the two 3-equation models in Table 1 is the incorporation of the drift-flux parameter in the drift-flux model. This enables the specification of the vapour velocity relative to the liquid phase velocity as well as the modelling of situations where the vapour phase moves faster than the liquid phase or even when it moves in opposite directions.

Rao *et al.* (2006) studied a two phase NCL using one-dimensional models. A homogeneous equilibrium model and the thermal equilibrium drift-flux model were used to simulate an NCL in VHVC configuration. Single phase friction factors were determined from the Blasius equation. Two phase pressure drop was accounted for by using a two phase friction multiplier. The drift-flux correlation was simple and did not consider flow regimes. Three cases were investigated, one case used the homogenous modelling approach, while the other two cases used a drift-flux model. The latter two cases used two different methods to obtain the two phase friction multiplier. For all three cases a constant heat flux boundary was used. The predicted flow rates and exit qualities for certain imposed heat fluxes were illustrated in graph form (Figure 2-9).

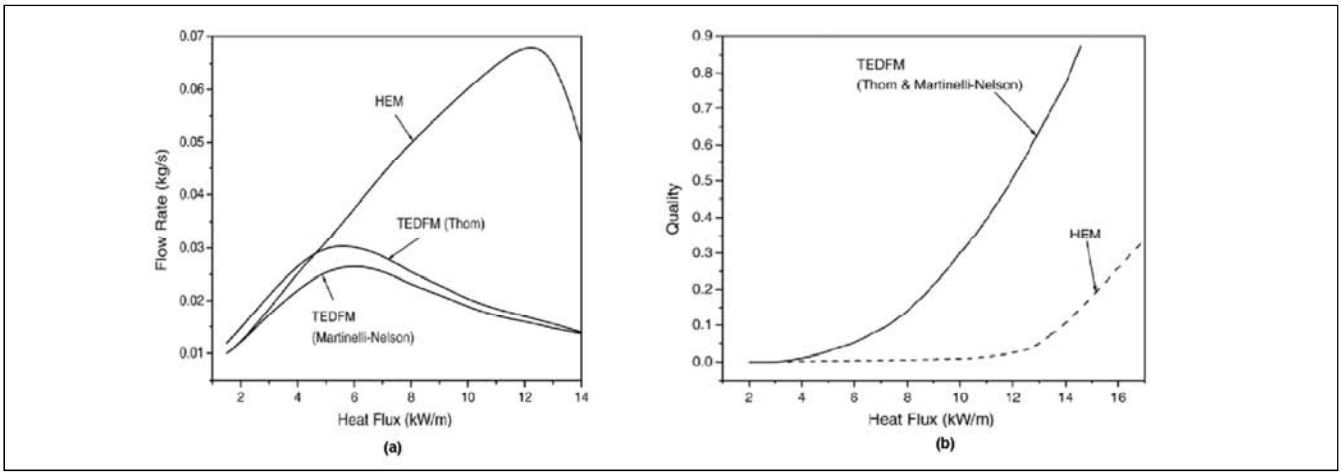


Figure 2-9. Comparison graphs between homogenous and drift-flux models (Rao *et al.,* 2006:1050).

From Figure 2-9 it can be seen that the two equation drift-flux models (TEDFM (Thom) and TEDFM (Martinelli-Nelson)) that use different friction multipliers are in close agreement with each other while the homogeneous equation model (HEM) was not. From the obtained graphs it can be seen that the drift-flux model which predicts a decrease in flow rate with an increase in heat flux due to wall friction playing a greater role. The results obtained using the homogenous model predicted a decrease in the flow rate at much higher heat fluxes compared to the drift-flux models. An interesting observation from the figure is that both graphs show that the homogenous model starts to deviate from the drift-flux models at approximately 4000 $W.m^{-1}$ (Watt per metre length). The following conclusions were made from this study:

a. Two phase pressure drop consumes a large fraction of the driving head of the NCL.
b. A two phase NCL of certain dimensions has an optimal heat flux where the flow and heat transfer rates reach a maximum.
c. To achieve maximum heat transfer the water inlet temperature and the heating and cooling section lengths must be optimised.
d. Although the drift-flux based model is expected to be the more accurate model, further investigation is necessary.
e. The results obtained from the homogeneous model deviate significantly from the results obtained from the drift-flux model at higher constant, imposed heat fluxes at the heating section of the NCL.
f. Flow rates increase with an increase in loop height.

A notable quantity of work has been done in studying the various drift-flux parameters and using the drift-flux model for two phase flow. Hibiki and Ishii (2002) chose the drift-flux model over a two-fluid model on the basis that the introduction of two momentum equations leads to many difficulties. The drift-flux model is especially appropriate when the coupling between the two phases in terms of movement is strong.

Hibiki and Ishii (2003a) continued in the same fashion and derived the drift velocity and distribution parameters for the drift-flux model based on flow regimes. Satisfactory agreement was found with experimental data. This study was extended to large diameter pipes (Hibiki & Ishii, 2003b) and it was found that low flow conditions in a large pipe may differ considerably from those in a small diameter pipe. The inlet conditions of the fluid also played a much larger role. A new set of drift-flux correlations was developed, which gave reasonably good results. Experimental data was not extensive and it was recommended that boiling flow in a large pipe should be evaluated more extensively.

A study using the drift-flux model was also conducted by Jeng and Pan (1999). A vertical heated pipe section was modelled using the two phase drift-flux theory. The following is highlighted from this study:

a. The single phase pressure drop was different from that obtained for fully developed forced flows.
b. The Dittus-Boelter equation was used to calculate single phase heat transfer.
c. The Chen correlation was used for heat transfer coefficients in boiling flow.
d. Pressure drop was calculated using a very complex equation with many dimensionless groups.
e. The complexity of pressure drop calculations alone indicates how many factors influence the performance of an NCL.
f. When there is a high degree of heater inlet subcooling, multiple steady state solutions can exist which lead to instabilities.
g. Increasing inlet loss coefficients may lead to the elimination of instability due to these multiple steady state solutions.
h. Increases in exit loss coefficients do not significantly affect the threshold power for the initiation of two phase flow or the slope with which the flow increases during heater power increases.

Oosthuizen (2003) simulated an annular and rectangular NCL (Figure 2-10, a and b). The homogenous model was used with programming code written in EES. The two concepts were modelled within the context of cooling the reactor cavity of a high temperature gas-cooled reactor design. The rectangular design had a downcomer (Figure 2-10, c) and a horizontal section (Figure 2-10, e), which fed water into the hot leg (Figure 2-10, d). Water vapour was vented to the atmosphere (Figure 2-10, h). The annular design had the downcomer inside the riser tube or hot leg (Figure 2-10, f). The reservoir was located on top of the entire loop (Figure 2-10, g).

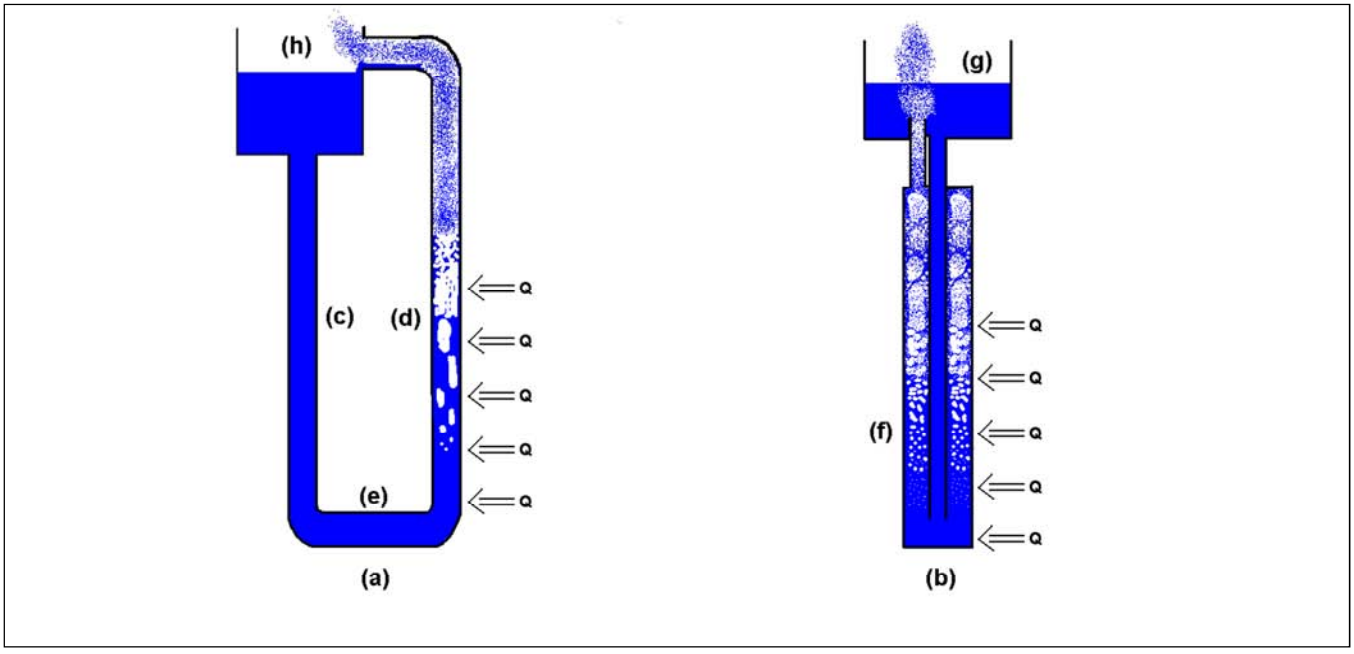


Figure 2-10. Rectangular and annular NCLs for gas reactor cavity cooling (Adapted from Oosthuizen, 2003:57-58).

The steady state characteristics were considered for both models. Single phase friction factors were determined by using the Moody Chart for the turbulent and laminar flow regions. For transition flow, a linear interpolation was made between the threshold friction values for laminar and turbulent flow (Figure 2-11). The result of this interpolation can be seen as a straight line with a positive slope. Pressure drops in the two phase region were computed using a single phase correlation combined with a two phase friction multiplier.

Oosthuizen (2003) found that many discrepancies existed when evaluating the frictional component of pressure drop experienced in the loop. After an extensive literature study, it was determined that a two phase multiplier was used frequently to determine the two phase frictional pressure drops. However, it was found that some discrepancies existed in the literature on the use of this method. Oosthuizen (2003) also found that many people used the homogenous model for investigative studies and that the homogenous model could not be applied to problems where periodic instabilities were present. Oosthuizen (2003) applied the model to an annular and rectangular NCL and it produced acceptable results. The comparison that was made between the results obtained for the two NCL designs showed that the rectangular NCL model had lower wall temperatures for an applied heat flux and the annulus model had higher mass flow rates.

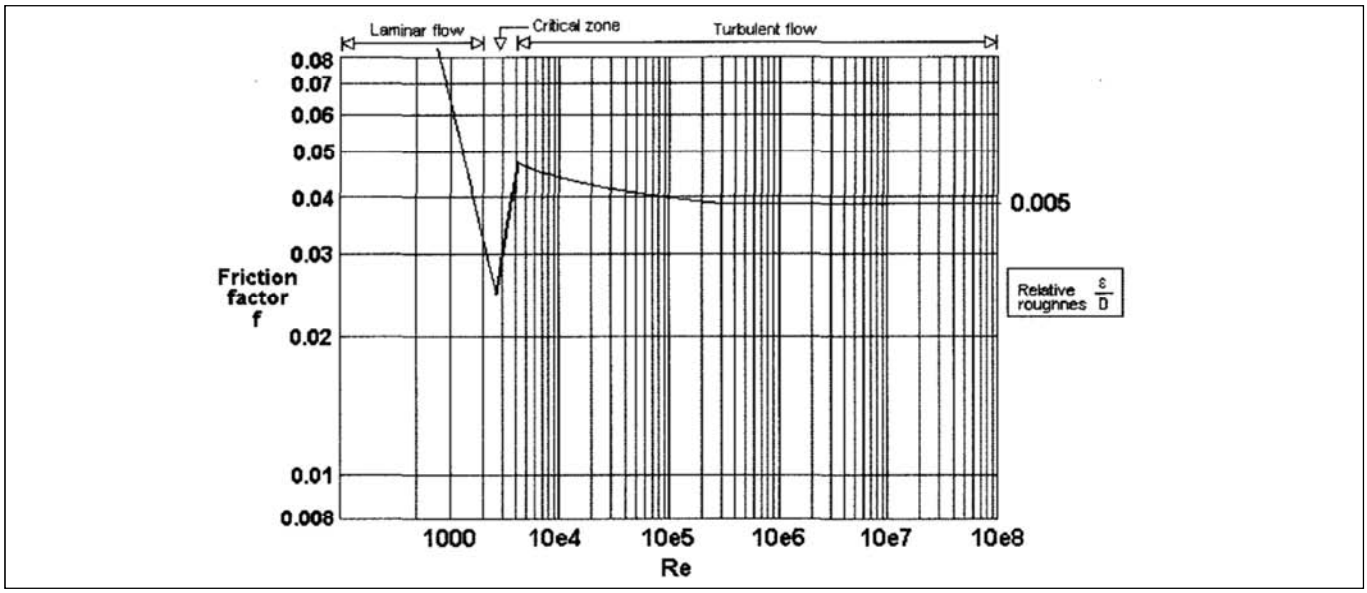


Figure 2-11. Friction factor determination (Oosthuizen, 2003:64).

Kim and Lee (2000) experimented with an NCL in VHVC configuration to observe the effect of an expansion tank on stability (simplified in Figure 2-12). Since two phase loops tend to be unstable due to the large volumetric changes that take place during phase changes between liquid and gas, it was thought than an expansion tank (Figure 2-12, b) may mitigate some of the instability. An expansion tank located at the same level as the top pipe sections was connected to the bottom horizontal section of the

loop. The liquid surface in the expansion tank was open to atmosphere. Special attention was given to the connecting pipe as pressure losses between the expansion tank and loop could have a large influence on loop stability.

Kim and Lee (2000) effectively described the onset of two phase flow from stable single phase flow in simple terms. Single phase circulation flow changes abruptly when boiling occurs in the heating section (Figure 2-12, a). The large void that forms in the heater causes liquid to be pushed upwards and downwards. This causes reverse flow at the heater inlet and increased flow at the heater outlet. The volume expansion is absorbed by the expansion tank, although the inertia in the expansion tank's connecting pipe causes the loop pressure to increase for a while. Two phase flow is established very quickly in the riser section that comes after the heater, while the cooling section condenses the vapour. The void collapses and single phase circulation is resumed again. This cycle is aptly called periodic circulation and is repeated until the heater power is raised to such an extent that two phase circulation is continuous.

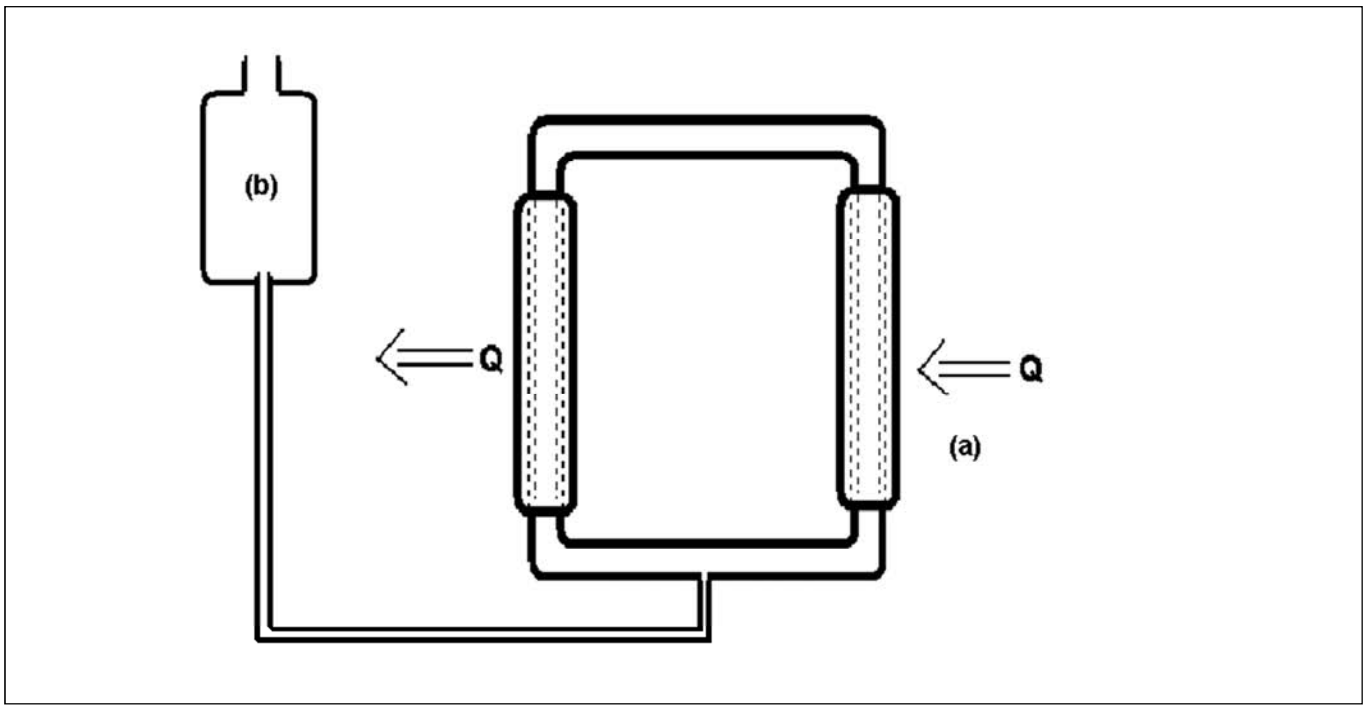


Figure 2-12. NCL with expansion tank connected by length of pipe (Adapted from Kim and Lee, 2000:361).

Before this power level was reached, a number of other instabilities were also observed. Density wave oscillations, which occur when the vapour void inside the heater section is maintained, but varies in size, result in this type of oscillations. As heater power is increased manometric oscillations also occur. These could be due to the boiling of liquid in the heating section with the void size being more stable. Many two

phase NCL systems tend to exhibit instabilities due to the large volumetric changes that the fluid undergoes during boiling and condensation.

It was found that by increasing the flow resistance or inertia of the fluid line to the expansion tank, the NCL's stability characteristics could be improved. The expansion tank was open to the atmosphere and thus the time average pressure in the loop was constant. Some oscillations modes still appeared due to the fluid inertia and pressure losses in the expansion tank. Overall, the concept was deemed to be a plausible method of increasing NCL stability.

Frankum *et al.* (1997) compared various methods of predicting two phase flow patterns. Empirical flow pattern maps and theoretical models were compared. The overall result was that an empirical flow pattern map was found to have the best performance. It was concluded that theoretical predictions that utilise an adiabatic approach, in general, gave satisfactory results. However, there are still some shortcomings in the methods used to predict flow patterns from thermal measurements. This implies that flow patterns cannot be reliably identified from thermal measurements alone.

A correlation for the frictional pressure drop of two phase flow in vertical and horizontal directions were given by Shannak (2008). The proposed correlation was an empirical correlation based on a large dataset of measured points.

The correlation was first evaluated against results obtained from a single experiment for a preliminary check. The predicted pressure drop was then calculated from the proposed correlation, as well as from other common correlations used. The correlation predicted the results with a standard deviation of 2%, a mean (or absolute) deviation of 1% and an average deviation of 0.5%. The second set of test data had more than 16 000 measurements over a diverse range of flow parameters and mixtures. The correlation calculated the pressure drops with a standard deviation of 35%, a mean deviation of 25% and an average deviation of -10%. The second dataset shows much larger deviations due to the wide range of fluids, flow conditions and other variations. Compared to other common methods using a friction multiplier the proposed correlation performed better. No explicit boundaries are given for the correlation, but the text recommends that it not be used outside the boundaries of the test data on which it was based.

Chen (1966) developed a correlation for two phase heat transfer. The article states that the case of fluid boiling, where there is a net generation of vapour, is a good example of how complex boiling heat transfer can be. This is due to the number of flow parameters, the presence of two phases and other parameters. The study was conducted within the following parameters which are typically found in the range of fluid quality from 1% to 70%:

a. Saturated two phase fluid in convective flow;
b. Vertical axial flow;
c. Stable flow;
d. No slug flow;
e. No liquid deficiency; and
f. Heat fluxes less than the critical heat flux.

It was theorised that there are two heat transfer mechanisms that come to the fore when boiling heat transfer is considered. It was theorised further that the effect of these two mechanisms can be summated. The mechanisms are:

a. Macro-convection mechanism: The same heat transfer method found in fluid flow and single phase heat transfer.
b. Micro-convection mechanism: The mechanism that considers the effect of bubble origin and growth in heat transfer.

When comparing the correlation with experimental data it was found that the new correlation predicted the experimental data well. The proposed correlation predicted heat transfer with an average deviation well within the 15% range for the datasets that were used. In conclusion it was found that this correlation appeared to give better accuracy than any of the other existing correlations.

The method of Gungor and Winterton can be used to adapt the Chen heat transfer correlation for use in determining the heat transfer of subcooled boiling (Thome, 2009:10–29).

Subcooled boiling takes place between single phase and fully boiling fluid flow. During subcooled boiling, the fluid is boiled at local volumes close to the heat transfer surface. However, since the bulk fluid temperature is still below the saturation temperature, the bubbles are condensed again. Thus, subcooled boiling can be termed as fluid boiling with no net generation of vapour. Kandlikar (1998) stated that the boiling process in subcooled flow improved the heat transfer rates significantly. He explained subcooled boiling in the case of liquid flow in a pipe with a constant heat flux boundary condition (Figure 2-13) as follows:

a. A subcooled liquid enters a pipe (Figure 2-13, a) with the tube wall temperature below the saturation temperature of the fluid.
b. The fluid temperature increases due to the steady heat flux condition imposed on the fluid. The wall temperature eventually reaches the saturation temperature of the fluid (Figure 2-13, b).

c. The forming of bubbles does not occur immediately, since the wall temperature needs to be above the fluid saturation temperature by a certain degree.
d. As the wall temperature exceeds the required temperature for subcooled boiling, the first bubbles appear (Figure 2-13, c). This point is termed the onset of nucleate boiling (ONB). As more bubbles begin to form, the wall temperature stabilises.
e. As the boiling continues the contribution of the single phase heat transfer diminishes, while the contribution from nucleate boiling increases. At a certain point the region becomes termed the partial boiling region. The region of fully developed boiling (FDB) (Figure 2-13, e) then follows. Another region is introduced in the study of Kandlikar (1998). This is called the significant void flow region.
f. As more heat is transferred to the fluid the bubbles eventually stop condensing due to the bulk fluid temperature reaching its saturation temperature (Figure 2-13, g). This is termed the region of net vapour generation (NVG). However, this region is not a pure two phase region since there are some unstable changes of the fluid properties in this region.
g. Heat being added to the fluid will then lead to the region being termed two phase flow (Figure 2-13, h) with stable net generation of vapour.

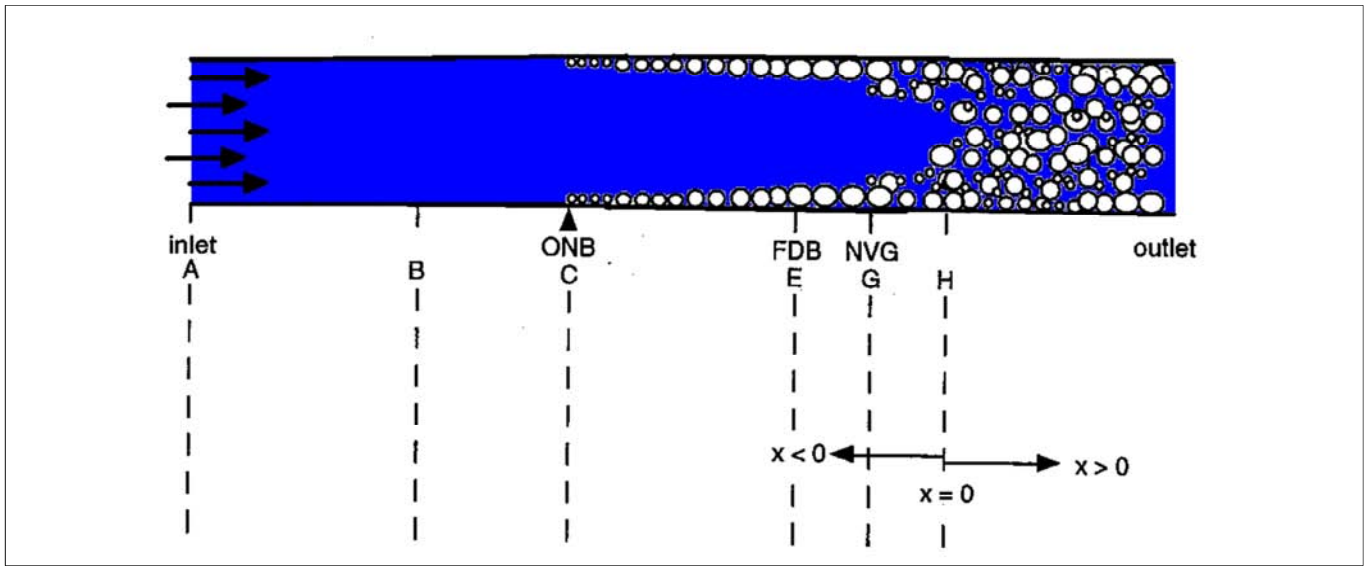


Figure 2-13. Schematic representation of subcooled flow boiling (Adapted from Kandlikar, 1998).

In this section of the literature study, work relevant to two phase NCLs was discussed. The following conclusions can be drawn:

a. Instability was found to be the subject of many investigations. Much information that is relevant to this study can be obtained from these studies.
b. Various two phase experiments and simulations were discussed.

c. Modelling two phase flow can become very complex.
d. The homogenous one-dimensional model can be used for investigative purposes.
e. The governing equations of the drift-flux and homogenous model were summarised. The drift-flux model is a suitable alternative to the homogenous model for a simple one-dimensional case, but uses many more equations.
f. The Chen heat transfer coefficient correlation was explored along with the saturated boiling method of Gungor and Winterton.
g. Friction coefficients for use in the determination of two phase flow pressure drop from different authors were summarised.

2.5 Stability of NCLs

Although the stability of NCLs was not the focus of this study, it occurs especially on single phase NCLs and was the subject of many research efforts. NCLs with a VHVC configuration are relatively stable when a single phase fluid is used. Yet, as soon as boiling occurs in the heating section and the NCL becomes a two phase loop, instabilities can be observed.

As the NCL used in this study was expected to undergo two phase flow it is to be expected that instabilities will occur. However, the aim of this conceptual study was to determine the potential value of such an NCL in removing heat. Thus fluctuations of flow or temperatures over short time periods were not taken into consideration.

Prasad *et al.* (2007) conducted a review of the research on boiling flow instabilities in boiling natural circulation systems, which is summarised in this section.

Consider a pipe heated along its length with a fluid entering at subcooled conditions. If the heating power is such that boiling takes place, it will have two flow regions. These are obviously the single and two phase regions. The two phase region will have a strongly coupled interaction between the fluid and heat transfer. Any heat transfer to or from the fluid will influence the quantity and distribution of the fluid phases present. This, in turn, will strongly influence the heat transfer in the area.

When a system is under natural circulation conditions it has a greater tendency to instability, mainly due to the low driving head and the heat transfer process being responsible for creating the said driving head. Consider a stable rectangular NCL in which a heater is creating the driving head by transferring heat to the fluid inside the hot leg of the NCL. The driving head is created due to the density difference between the heated fluid in the hot leg and the cold fluid in the cold leg. The heat applied to the NCL

results in a steady state velocity, where the pressure loss and driving head are balanced. Should the heater power be increased to above a certain threshold, the fluid inside the heater will be heated rather quickly, causing the flow to accelerate due to the increased driving head. Due to the higher velocity, cold water enters the hot leg faster and is heated less than the previous plug of water, thus reducing the driving head and velocity. The resultant lower velocity causes a plug of water to be heated to a higher temperature, again causing the velocity to increase. This instability may eventually die out, persist or even amplify itself, depending on the loop geometry and heater power. This is a very simple form of NCL instability. In the next section, various stability modes and other stability phenomena will be discussed to give the reader a short overview of the topic.

2.5.1 Types of instabilities

According to Prasad *et al.* (2007), three types of instabilities can be found on a boiling water reactor:

a. Control-system instabilities;
b. Thermal-hydraulic instabilities; and
c. Coupled neutronic thermal-hydraulic instabilities.

Of the three abovementioned instabilities, only the thermal-hydraulic instabilities are relevant for the NCL considered in this investigation. Thermal-hydraulic instabilities can be classified into static and dynamic instabilities.

2.5.1.1 Static instabilities

Static instabilities are associated with large and sudden flow parameter changes to a new stable point of operation. Static instability mechanisms and thresholds can be predicted using steady state characteristics. Factors that have an influence are the following:

a. Pressure drop characteristics of the flow channel;
b. Nucleation properties; and
c. Flow regime transitions.

There are different types of static instabilities, such as Ledinegg, geysering and flow pattern transition.

Ledinegg instability is when the flow quickly changes to a flow rate lower than the original value. The flow may even reverse. The cause of this type of instability is when the flow channel pressure drop characteristics are such that pressure drop decreases when the flow increases.
Geysering instability is when vapour voids form in the fluid when it moves through the heating section. On mixing with the liquid, perhaps when exiting the heating section, the vapour is condensed, causing the voids to collapse.

Flow pattern instability occurs when the flow is in a transition zone between two flow patterns with different pressure drop characteristics. A small disturbance in the flow can cause a change in void fraction or flow velocity, which can cause the flow conditions to change to another flow pattern. The change to another flow pattern causes the flow or heat transfer to change again, which leads to the flow pattern being altered back to the original pattern.

2.5.1.2 Dynamic instabilities

Dynamic instabilities relate to the propagation of pressure, void and density waves and are due to the interaction of flow rate, pressure drop and void fraction among others. An example of this would be that a system that is experiencing dynamic instability would have a fluctuating flow rate, resulting in a fluctuating pressure drop, which might affect the local pressure of the fluid. This fluctuating pressure could affect the void fraction of the fluid, which would again affect the flow rate. These fluctuations in an unstable system would persist and make stable heat transfer a challenge.

To predict the stability boundaries of a natural circulation system involves determining its transient or dynamic behaviour characteristics. The main types of dynamic instability are as follows:

a. Density wave oscillations (classified into Type I and Type II instabilities);
b. Parallel channel instability; and
c. Pressure drop oscillations.

Natural circulation systems are especially prone to a subdivision of density wave oscillations. These are known as Type I and Type II instabilities:

a. Type I instabilities typically occur at low pressures and when the quality of the fluid inside the heating section is very low. The flow in an NCL is driven by a density difference and is in a very sensitive stage when the void fraction inside the heater is small. Flow variations could lead to unstable void generation, which causes flow instability. Instability is observed as low frequency oscillations.

b. Type II instabilities are relevant in natural circulation and forced circulation reactors. They are caused mainly by the interaction of two phase frictional pressure drops, void formation and mass flow rate. Type II instabilities are manifested as high frequency oscillations.

Parallel channel instability refers to the interaction of channels that are parallel in orientation and fed from a common header. Changes of instability in one of the channels could affect the other channels and may cause the flow to oscillate between channels. This type of instability is only relevant to an NCL where there are parallel flow paths available to the fluid, but not in case of the NCL being investigated in the current study.

Pressure drop oscillations may be triggered by static instability or compounded dynamic instabilities. A system with a compressible volume upstream of the heater entrance may trigger this type of instability if the pressure drop curve with regard to flow velocity has a negative gradient.

2.5.1.3 Start-up transients

Systems that use natural circulation may go through thermal hydraulic instabilities during low-power and pressure conditions. At low pressures an NCL typically has three operation modes:

a. Stable single phase operation;
b. Unstable two phase operation; or
c. Stable two phase operation.

2.5.1.4 Stability maps

A stability map gives a graphic representation of stable and unstable regions for an NCL. It may even indicate a region where the NCL is neutrally stable. Nayak *et al.* (1995) showed an example of a stability map (Figure 2-14). In this case, the map was constructed from various points as a function of the dimensionless modified Stanton St_m and modified Grasshoff Gr_m numbers. Other researchers may choose different parameters to construct stability maps. A stability map is useful to determine the degree of stability of an NCL. In the case of a theoretically generated stability map, it is of course the theoretically predicted stability of the NCL. By computing the two dimensionless numbers that the stability map has on its axis, a point on the map can be plotted for a specific case of the NCL. Then, by noting whether the plotted point is in a stable or unstable area, the NCL can be predicted to be stable or unstable. If needed, the effect that adjusting loop parameters might have on the stability of the NCL can be calculated by plotting the new point of operation and noting in which region it is located.

Although stability analysis was not the goal of this investigation, it is certainly necessary to note that NCLs are very prone to instability. Detailed design of NCLs will have to consider their stability behaviour.

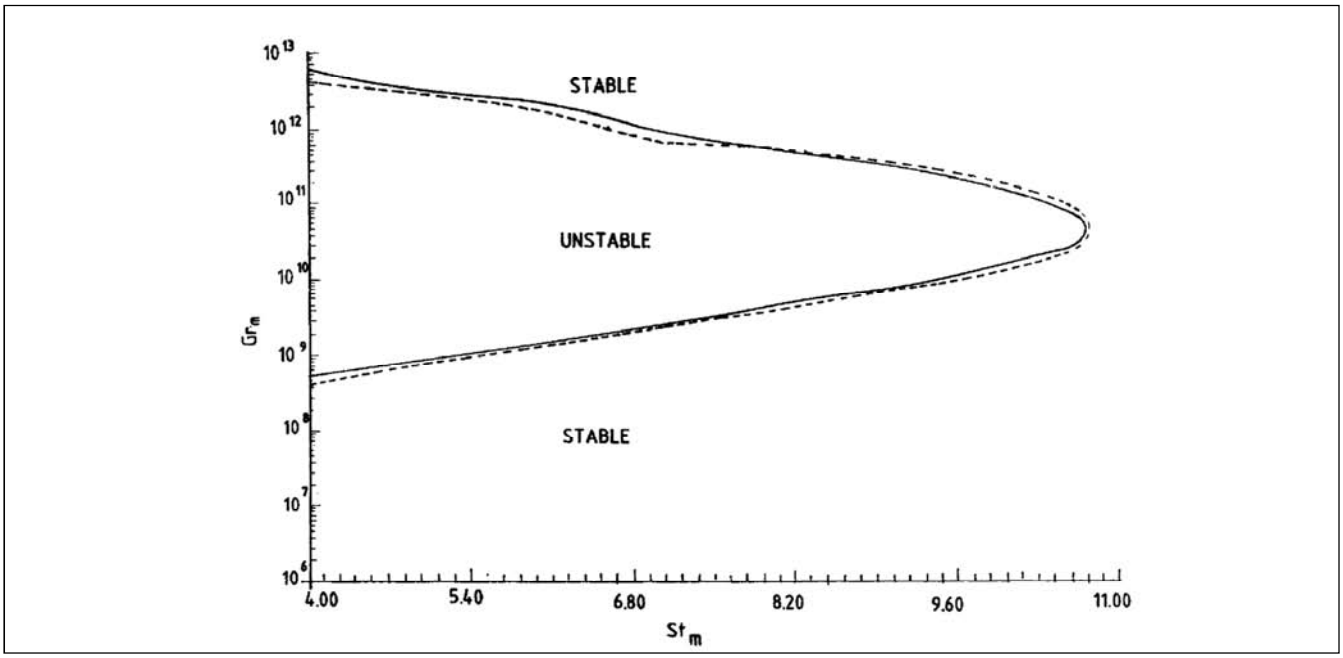


Figure 2-14. Example of an NCL stability map (Nayak *et al.*, 1995:85).

2.6 Conclusion of the literature study

This concludes the literature study. In this chapter, various sources of literature were referenced for use in the process of building a simulation program, as well as providing an introduction to the topic area. Passive containment cooling on PWRs, other applications of NCLs and the stability of NCLs were introduced. Single and two phase flow correlations and experiments were presented. These correlations will be used in the next chapter to build a base for the simulation program. The homogenous model's conservation equations were also presented. These will form the foundation on which the rest of the theoretical base of the simulation program will be built. A section on the stability of NCLs was presented to demonstrate the main types of stability phenomena that can be expected in an NCL. The next chapter will deal with the theoretical background of the simulation that was developed in this study.

Chapter 3 - Theoretical background

3.1 Introduction

The modelling of thermal phenomena such as conduction, convection and boiling can become very complex. It is therefore necessary to describe each mechanism sufficiently in a model in order for the model to yield the desired results. The effective modelling of these phenomena requires a model that is reasonably accurate for its intended purpose. For the purposes of this study, the model had to be as simple as possible as this is a conceptual study.

The main purpose of the NCL in the context of this investigation was to examine ways of transporting heat out of a containment building. This took place via two heat transfer processes:

a. Heat transfer to the fluid inside the NCL via convection heat transfer; and
b. Advective heat transfer.

Conduction, as a heat transfer mechanism through the pipe walls of the NCL, was not considered during the execution of this investigation. Even though advective heat transfer is not strictly a heat transfer mechanism in the same way as conduction is, within the context of the NCL as a whole, it can be seen as a means of transporting heat via mass flow.

An introduction to natural circulation systems and stability will be done. Each heat transfer process will be discussed, after which more detail will be provided in the appropriate sections of the chapter.

3.1.1 Natural circulation systems

The movement (or circulation) of a fluid in a system driven by a difference in densities (or buoyancy forces) is a natural circulation system. In the case of a heat removal concept the density difference is achieved by the heat transferred to the fluid, causing the expansion of the fluid and a decrease in density. These systems can use a fluid either in a single phase or two phase configuration depending on individual design and operating conditions.

A natural circulation system has no active components, pumps or compressors, nor does it have any driving force other than a difference in the densities of the fluid. It therefore becomes an attractive

concept to use in a cooling design as it is clear that fewer components mean a simpler and cheaper design.

However, systems that use natural circulation have some drawbacks. One of the largest is a lower achievable driving force (IAEA, 2002:9). A lower driving force implies a lower fluid velocity, translating into a lower heat removal capability. The circulation rates are restricted by differences in fluid densities. Thus, increasing or decreasing flow rates is possible within a narrow band which is limited by the available motive force for circulation.

The driving force can be increased by increasing the density of the fluid in the cold leg, by decreasing the density of the fluid in the hot leg, or by lowering system resistance. The density of the colder leg can be increased by removing more heat from the fluid. In other words, the temperature of the fluid can be lowered. This can be achieved with a longer length of pipe or by exposing it to a colder environment. The density of the hot leg can be decreased by transferring more heat to it which will lower the density of the fluid inside. This can be done by increasing the temperature to which the hot leg is exposed or by increasing its length so that more heat can be absorbed. The pressure inside the loop can also be manipulated to allow the fluid to boil in the hot leg. Due to the vapour present during boiling the fluid density in the hot leg will be reduced even further. Air bubbles can also be artificially introduced by bubbling air into the bottom of the hot leg. This will also have the effect of decreasing the density. Lowering the system resistance will reduce the friction that the moving fluid must overcome. The net result will be a higher flow rate.

3.1.2 Stability considerations

Some designs of NCLs may exhibit unstable behaviour under imposed conditions. This is due to a feedback effect that is strongly present in an NCL. A disturbance in the flow of a loop will affect the heat transfer and friction losses, since these are coupled to the flow. This will, in turn affect the fluid density. Thus, the driving force is again affected. This will give rise to an oscillatory mode in the flow, depending on the design and operating conditions.

Since the stability of flow in an NCL affects the heat transfer of the loop it is important to take this effect into consideration during the detailed design of NCLs. This topic was explored in slightly more detail in the previous chapter. However, since this is an investigative study the stability aspect of NCLs was not taken into consideration.

3.1.3 Advective heat transfer

Single phase flow of a fluid will have a fluid flowing in a single state of matter, meaning either a gas or a liquid.

The flow regime of single phase flow, which was explained in the previous section, is important to determine the basic properties of the flow. The velocity profiles for single phase laminar flow (Figure 3-1, a) and turbulent flow (Figure 3-1, b) differ substantially and give some indication of the differences between the two flow regimes (Incropera *et al.*, 2006:486).

Two phase fluids may refer to a fluid that consists of a combination of a gas and a liquid. This could also apply to substances with different chemical compositions. For the purposes of this investigation the phrase “two phase” will refer to a mixture of gas and liquid of the same chemical composition. In short, a two phase single component fluid. Two phase flow is a more complex type of flow to deal with.

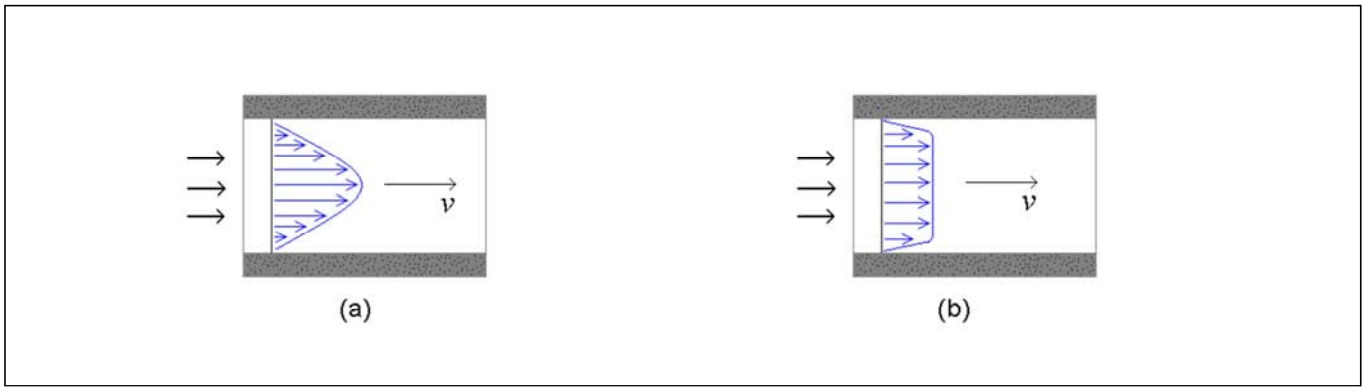


Figure 3-1. Fluid velocity profiles for laminar and turbulent flow through a tube (Adapted from Incropera *et al.*, 2006:486).

Consider a heated vertical tube (Figure 3-2) with subcooled liquid entering at the bottom. As the subcooled liquid enters the bottom of the pipe (Figure 3-2, a) it increases in temperature as heat is transferred to it. As the temperature reaches the saturation temperature of the liquid nucleate boiling takes place (Figure 3-2, b). These bubbles collapse again when they come into contact with still subcooled liquid. This phenomenon is called subcooled boiling. As the fluid progresses up the pipe, the boiling becomes more energetic (Figure 3-2, c to d) until it has completely boiled to a mist (Figure 3-2, e) and then to dry-out conditions (Figure 3-2, f).

Heat transfer to the fluid during boiling depends on the boiling and convection heat transfer mechanisms and these factors must be taken into account when the NCL is simulated.

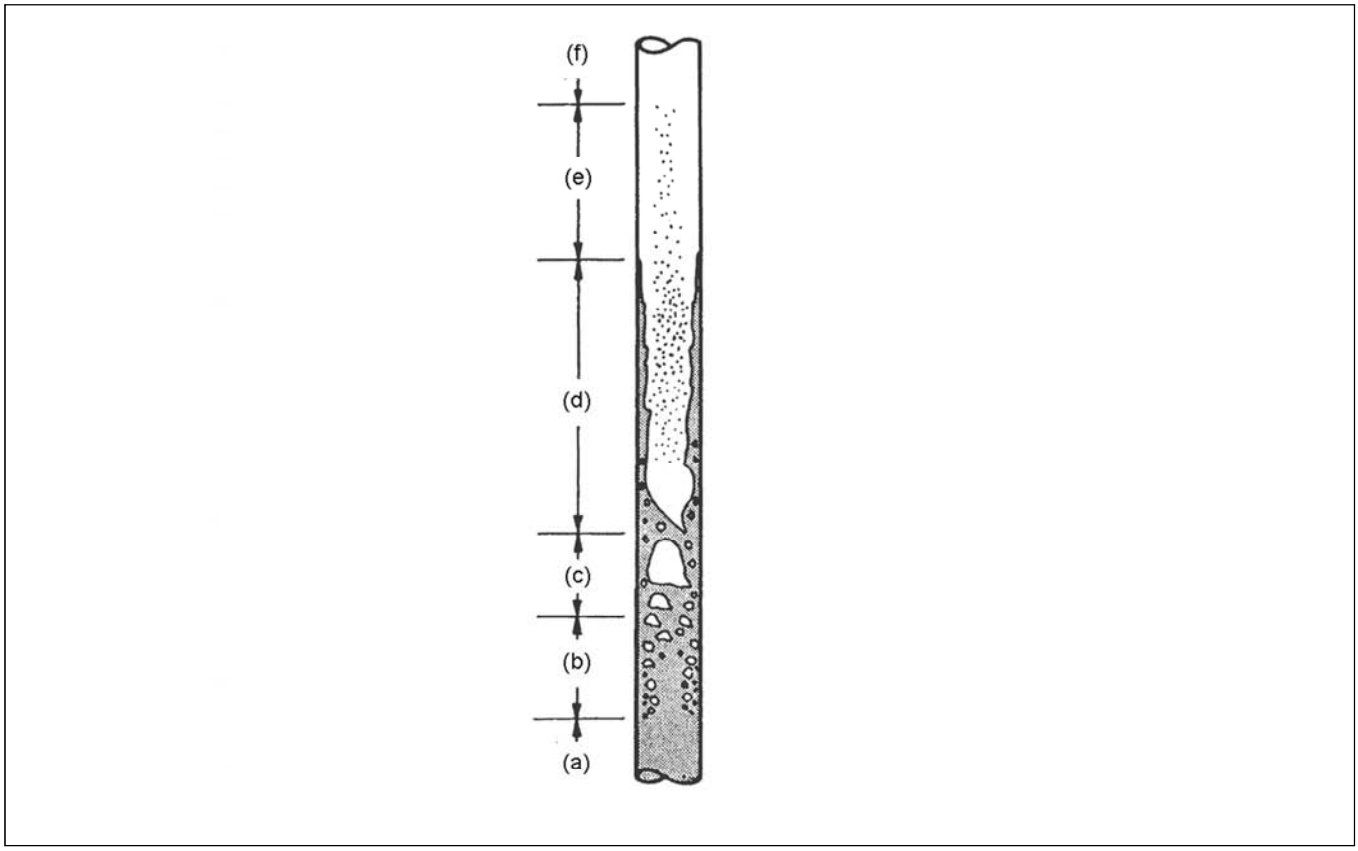


Figure 3-2 Boiling in a vertical pipe *(*Bejan & Kraus, 2003:671).

3.1.4 Convection heat transfer

When the fluid inside a pipe is moving and a temperature difference exists between the fluid and the wall surface, convection heat transfer will take place. Figure 3-3 illustrates heat transfer from a pipe wall at a fixed temperature (Figure 3-3, a) to a fluid at a certain temperature (Figure 3-3, b). When dealing with single phase flow the flow regime can be turbulent, laminar or in a transition zone between the two. Two phase flow is characterised by flow patterns which the liquid and vapour phases form as the flow parameters change. The single phase flow regime or two phase flow pattern is probably the most significant factor in determining the heat transfer achieved. In theory, heat transfer correlations can be quite accurate if they are derived for a single flow regime or pattern. The heat transfer is determined from a heat transfer coefficient, frequently calculated from an empirical correlation. Correlations for the heat transfer coefficient for single phase and two phase flow can be found in literature.

In the case of single phase flow the type of flow regime present will influence the potential heat transfer that can be achieved. Of these, turbulent flow is capable of more heat transfer for a given temperature difference, due to the more energetic movement of the fluid. The Reynolds number calculated from fluid flow and fluid property parameters, can be used to determine the flow type. Two phase flow patterns are

much more complicated. Where the Reynolds number can be used to determine the single phase flow regime, in the case of two phase flow many more parameters play a role. Given the simple model used in the simulation, it was decided that the consideration of two phase flow patterns would not contribute much to the investigation. Thus, individual two phase flow patterns were not taken into account in this investigation.

The inner pipe wall transfers heat to the fluid on the inside of the hot leg pipe (Figure 3-3). The heat may eventually cause the fluid to boil, creating a two phase mixture. A key variable that needs to be calculated is the heat transfer coefficient. This coefficient is used to determine the heat transfer rates and resultant fluid and wall temperatures. It depends on a number of flow variables, the most significant of which are perhaps the dimensionless Reynolds number and flow regimes. Various empirical correlations can be used to determine this coefficient. These correlations were obtained from the literature.

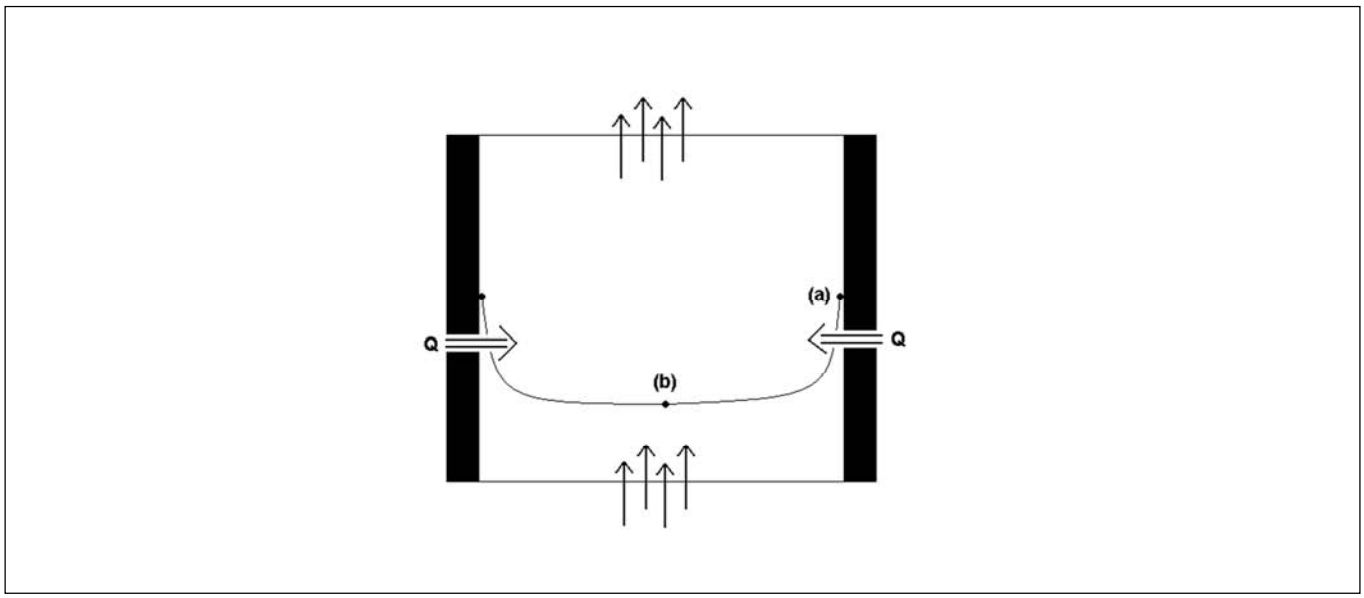


Figure 3-3. Convection heat transfer to a fluid flowing inside a pipe.

The NCL (Figure 3-4) transfers heat by using the driving head created by the density difference between the hot and cold legs of a pipe loop. The driving head is low compared to that used by forced convection systems. The NCL can be modelled by solving a set of conservation equations namely mass conservation, momentum conservation and energy conservation.

As was stated earlier, fluid flow can be divided into either single phase or two phase flow. Single phase flow is relatively simple to simulate and conservation equations can generally be solved with relative ease. Two phase flow is more complex. A number of different models can be used. These range from the simple homogenous approach to a complex two-fluid approach, which also takes mass transfer between the phases into consideration.

The natural circulation loop that is the subject of this study can be separated into two distinct components: The reservoir (Figure 3-4, a) and the pipe loop (Figure 3-4, b).

The reservoir stores water for the cold leg ensuring that it is always filled with liquid. It also serves as a point of entry for water from the hot leg and feedwater. If boiling takes place in the hot leg and vapour is formed, the reservoir acts as a vapour separator and the vapour is vented to the atmosphere. The feedwater supply ensures a constant level in the reservoir by replacing any fluid that is boiled off. The reservoir is a simple tank and its content is assumed to be well mixed and to have uniform fluid properties throughout.

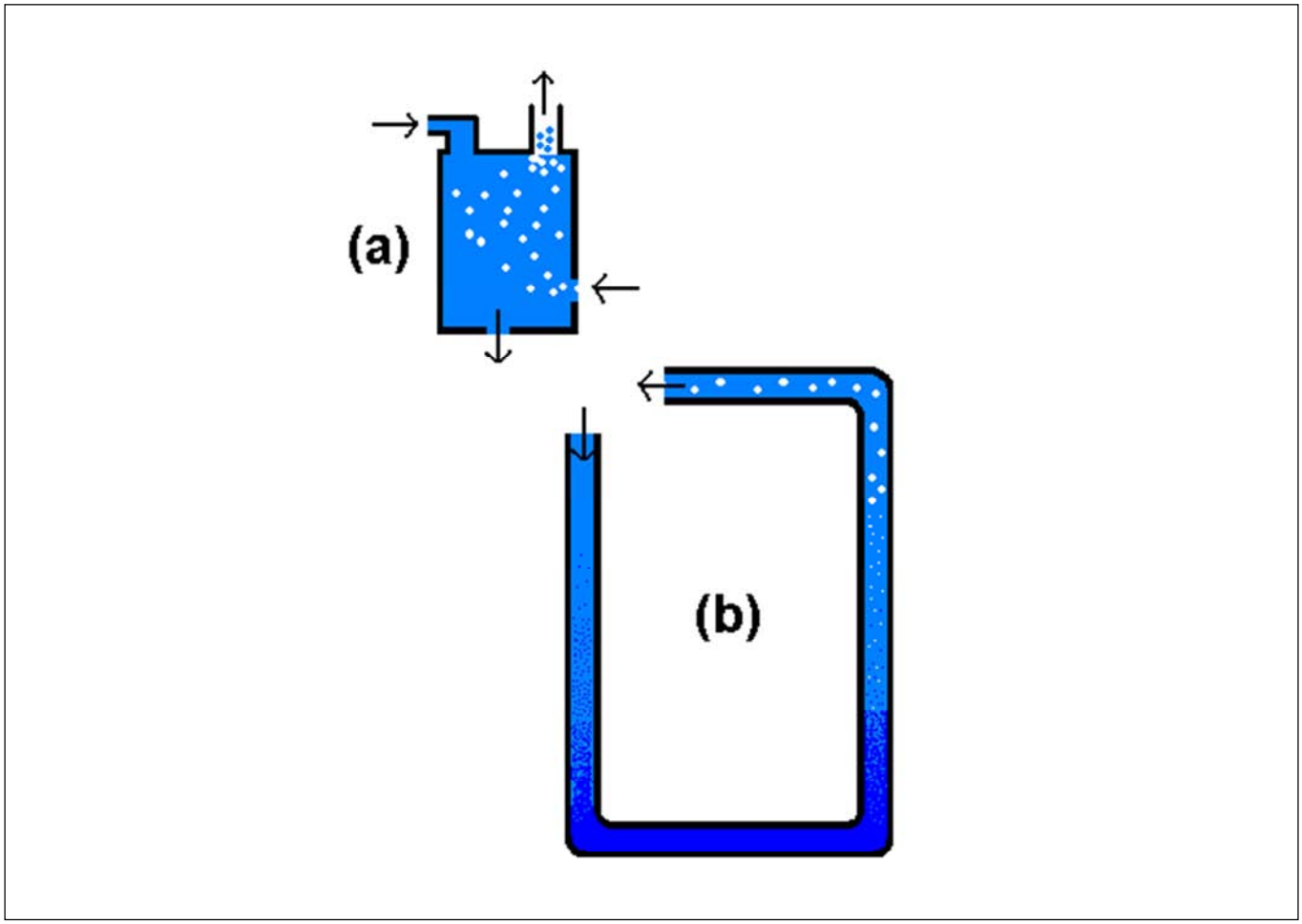


Figure 3-4. Natural circulation loop reservoir and pipes.

Two phase heat transfer introduces a number of difficulties in the modelling process. These difficulties include the following (Levy, 1999:87–88):

a. Some fluid properties are difficult or impossible to calculate when two phase conditions exist.

b. Two phase flow has a large number of interfaces between the vapour and liquid phases. Even more complexity is added when mass transfer over these interfaces is considered.
c. The two phases can be divided into certain flow patterns, depending on the conditions, each with some characteristic qualities.
d. The two phases can travel in a different or in the same direction.
e. Heat transfer can take place via condensation and evaporation.
f. Situations can develop where there may not be thermal equilibrium between the two phases. Bubbles may be generated in a stream of liquid, which is still subcooled.

As is the case with most computer simulations, a number of models are available for the simulation of two phase flow and heat transfer. In general, the models that can be used for one-dimensional two phase flow can be categorised as follows (Levy, 1999:89–143):

a. Homogeneous (or uniform) models;
b. Separated models with no interface exchange; and
c. Separated models with interface exchange.

It must be borne in mind that the one-dimensional approximation will only consider the variation of fluid properties and flow variables along the flow axis. These flow parameters are averaged across the flow cross-section for these models.

The homogeneous model is the simplest of the models. It assumes the following:

a. The vapour and liquid velocities and temperatures are equal over a given cross-section.
b. Fluid properties for both phases are averaged over the control volume cross-section.

The homogenous model treats the two phase fluid as a single phase one. The single-fluid properties are derived from averaged properties of the two phase fluid and are then used in the conservation equations. By not treating the two phases separately in the conservation equations, the model is simplified, but may also suffer from inaccuracies. The model requires closure laws for homogenous viscosity and thermal conductivity. It can also use single phase closure laws.

A separated model with no interface exchange addresses some of the limitations of the homogenous model. These models can take different vapour and liquid velocities into consideration. They provide adequate solutions for complex two phase systems, which are not subjected to severe transients. Single phase fluid properties can be used, but separate phase properties are preferred.

Separated models with interface exchange are the most complex of the models. Since these models take a lot of the physical mechanisms into consideration, they are also the most accurate of the one-dimensional models. Implementation in a computer code can be complex since flow patterns, interfacial areas, interfacial exchanges and other closure laws are required.

Since this study is a conceptual investigation, it was fitting that the simplest model be used. It was concluded from the literature study that the homogenous model provides results that may be inaccurate but still useful for this type of investigation.

In this chapter, the theory to support the modelling of the NCL and related phenomena is presented. The theory includes some of the correlations and information detailed in the literature study of the previous chapter.

3.1.5 Fluid properties and other flow related quantities

This section will cover miscellaneous variables that need to be calculated in order to solve the conservation equations.

The dimensionless Reynolds number for single phase flow can be calculated as follows (Cengel and Turner, 2005:608):

$$\mathrm{Re}_{sp} = \frac{\rho_{mix} v_{mix} D_H}{\mu_{mix}} \tag{3.1}$$

Where:

Re_{sp} is the single phase Reynolds number;

ρ_{mix} is the density of the fluid mixture;

v_{mix} is the velocity of the fluid mixture;

D_H is the hydraulic diameter of the pipe; and

μ_{mix} is the viscosity of the mixture.

Or alternatively:

$$\mathrm{Re}_{sp} = \frac{4\dot{m}_{mix}}{\pi D_H \mu_{mix}} \tag{3.2}$$

Where:

$\dot{m}_{mix}$ is the fluid mass flow; and

π is the value of Pi.

The Reynolds number of single phase flow can be used to determine in which flow regime the fluid is. Laminar and turbulent flow are separated by a transition region that is assumed to be present at the following Reynolds numbers based on the study by Vijayan (2002):

$$1000 < \mathrm{Re}_{sp} < 4000 \tag{3.3}$$

When two phase flow exists, there is sometimes a need to calculate the liquid phase Reynolds number, which can be calculated from the following equation (Thome 2009:10-7):

$$\mathrm{Re}_{liq} = \frac{\rho_{liq} v_{mix} D_H}{\mu_{liq}}(1-x) \tag{3.4}$$

Where:

Re_{liq} is the liquid phase Reynolds number;

ρ_{liq} is the density of the liquid in the two phase mixture;

μ_{liq} is the viscosity of the liquid phase of the mixture; and

x is the quality of the mixture.

The two phase Reynolds number can then be calculated as follows (Collier 1983:2.7.3-12):

$$\mathrm{Re}_{tp} = \mathrm{Re}_{liq} F^{1.25} \tag{3.5}$$

Where:

F is the ratio of the two phase mixture and liquid Reynolds numbers.

To determine the ratio between these two Reynolds numbers, the following formula can be used (Collier 1983:2.7.3-12):

$$F = \begin{cases} 1 & \text{for} \quad \dfrac{1}{X_{tt}} \le 0.1 \\ 2.35\left(\dfrac{1}{X_{tt}} + 0.213\right)^{0.736} & \text{for} \quad \dfrac{1}{X_{tt}} > 0.1 \end{cases} \tag{3.6}$$

Where:

X_{tt} is the Martinelli parameter.

The Martinelli parameter can then be obtained from the following (Collier 1983:2.7.3-12):

$$X_{tt} = \left(\frac{1-x}{x}\right)^{0.9} \left(\frac{\rho_{vap}}{\rho_{liq}}\right)^{0.5} \left(\frac{\mu_{liq}}{\mu_{vap}}\right)^{0.1} \tag{3.7}$$

Where:

ρ_{vap} is the density of the vapour in the two phase mixture; and

μ_{vap} is the viscosity of the vapour phase of the mixture.

The boiling suppression factor used during two phase heat transfer calculations is a function of the two phase Reynolds number (Collier 1983:2.7.3-12):

$$S = \frac{1}{1 + 2.53 \times 10^{-6}\, \mathrm{Re}_{tp}^{1.17}} \tag{3.8}$$

Where:

S is the boiling suppression factor; and

Re_{tp} is the two phase Reynolds number.

The quality of two phase flow can then be determined from the fluid enthalpies, using the following common equation:

$$x = \frac{\left(h_{mix} - h_{liq}\right)}{\left(h_{vap} - h_{liq}\right)} \tag{3.9}$$

Where:

h_{mix} is the enthalpy of the fluid mixture;

h_{liq} is the fluid liquid phase enthalpy at a quality of 0; and

h_{vap} is the fluid vapour phase enthalpy at a quality of 1.

Using the quality value, other fluid properties can be determined using a simple interpolation function:

$$\frac{1}{\phi_{mix}} = \frac{1-x}{\phi_{liq}} + \frac{x}{\phi_{vap}} \tag{3.10}$$

Where:

ϕ_{mix} is an arbitrary mixture property of a fluid mixture;

ϕ_{vap} is an arbitrary vapour phase property of a fluid mixture; and

ϕ_{liq} is an arbitrary liquid phase property of a fluid mixture.

The result of using this interpolation function is seen in Figure 3-5. The value of an arbitrary property is, as an example, taken as 100 and 1 at a fluid quality of 0 and 1 respectively. The result is plotted in the figure. It can be seen that the gradient of the values is steep when close to a quality value of 0.

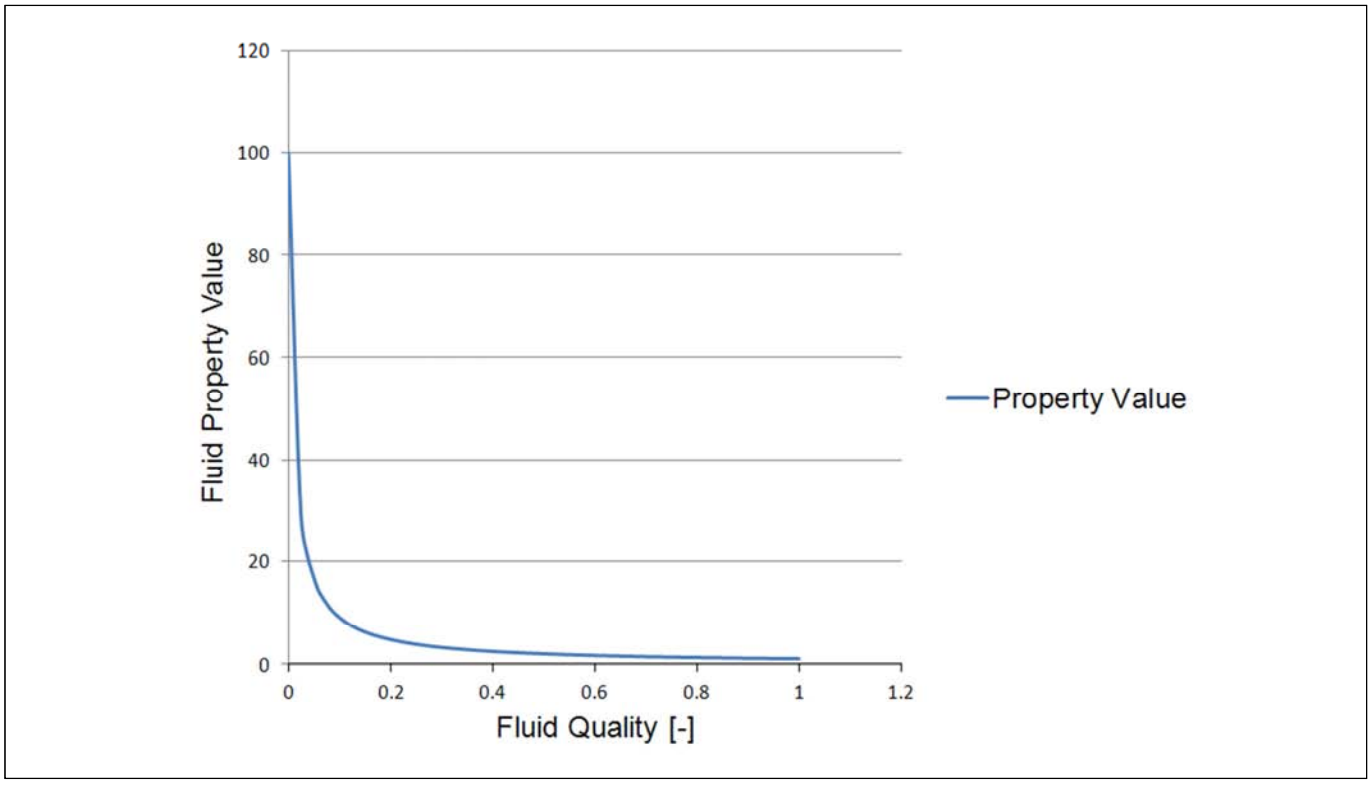


Figure 3-5. Fluid property interpolation function.

3.2 Introduction to conservation equations

The flow of the fluid (single and two phase) through the NCL was modelled using a one-dimensional model. The conservation equations will now be introduced. The following three conservation principles were applied:

a. The conservation of mass principle, which states that the control volume's change in mass is equal to the difference between the inflow and outflow of mass over the control volume's boundaries.
b. The conservation of momentum principle, which states that the change in the momentum of the contents of a control volume plus the net flux of momentum across the surface of the control volume is equal to the sum of the body forces and surface forces exerted on the control volume.
c. The conservation of energy principle, which states that the change in energy content of a control volume plus the net flux of energy across the surface of the control volume is equal to the heat added to the control volume and the work done on the control volume.

The next section will introduce each of the conservation equations and manipulate them into a suitable form for use in a simulation program. The NCL has the following two components when fluid flow is considered:

a. Pipe loop with the hot leg, cold leg and horizontal pipe sections; and
b. Reservoir with two inlets and two outlets.

Each component has a unique set of conservation equations, which will be considered in the following sections.

3.3 Conservation equations for the pipe loop

This section discusses the set of conservation equations for the pipes of the NCL. To modify the equations to a suitable form for discretisation, the integration method explained in Date (2005:23–24) is used. The spatial terms that are not dependant on time are integrated over the domain at a constant time parameter. Since this investigation covers only the steady state simulation, time-dependant terms are neglected.

The naming convention used in Figure 3-6 is chosen such that the equation is derived for a control volume. In the next chapter, the convention is adapted for ease of use in the simulation programming

process. Thus, the equations will be derived using subscripts of 1 and 2 relating to a single control volume in the current chapter. The next chapter will extend the numbering convention to i and $i+1$ for a number of control volumes.

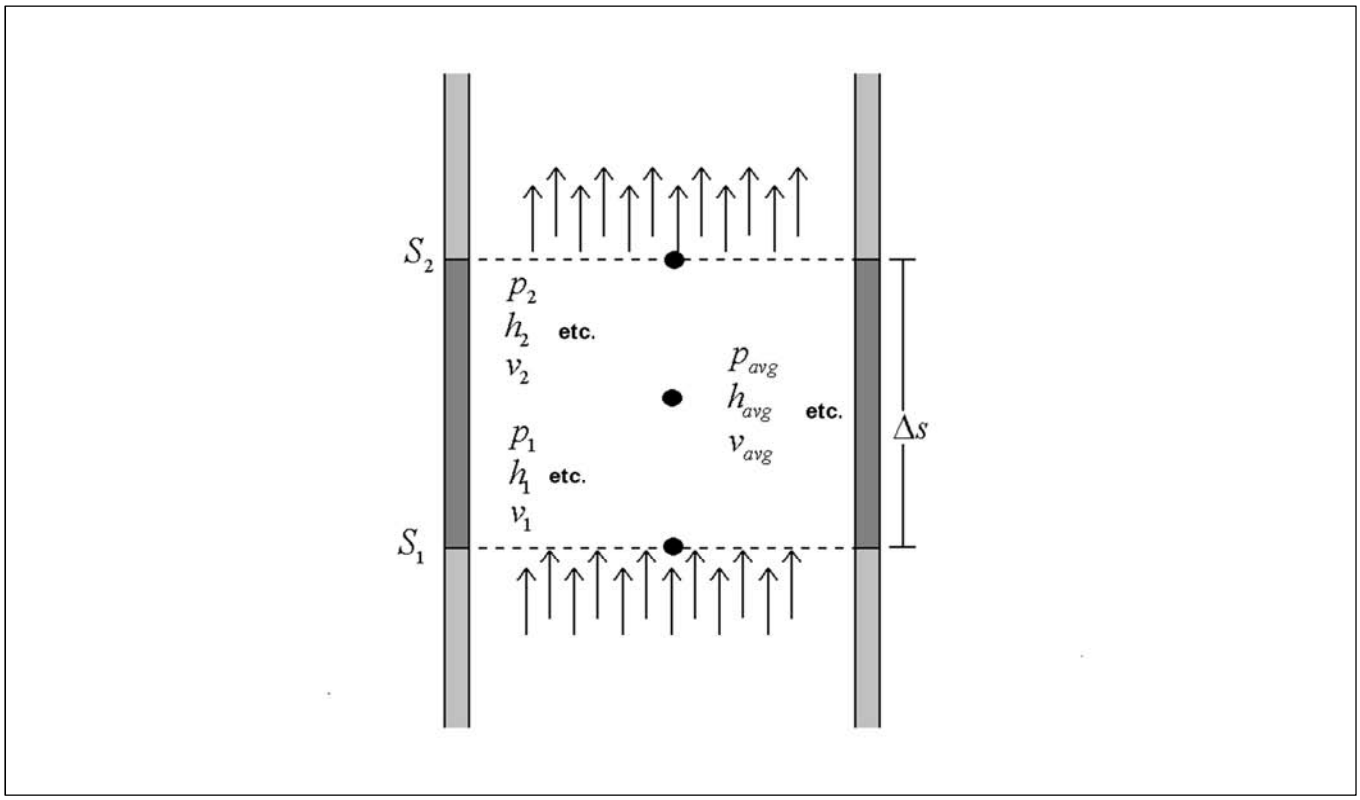


Figure 3-6. Naming convention for pipe loop conservation equation derivation.

3.3.1 Mass conservation for the pipe loop

The homogenous mass conservation equation for single and two phase flow is given by Levy (1999:99) as:

$$\frac{\partial}{\partial t}\left(\rho_{mix} A_{flow}\right) + \frac{\partial}{\partial s}\left(\rho_{mix} v_{mix} A_{flow}\right) = 0 \tag{3.11}$$

Where:

t is time;

A_{flow} is the fluid flow area; and

s is distance.

By integrating the equation and neglecting the time-dependant term, the following equation can be obtained:

$$0 + \int_{S_1}^{S_2} \frac{\partial}{\partial s}\left(\rho_{mix} v_{mix} A_{flow}\right) ds = 0 \tag{3.12}$$

Finally, the integration steps result in the following:

$$\left(\rho_{mix} v_{mix} A_{flow}\right)\Big|^{S_2} - \left(\rho_{mix} v_{mix} A_{flow}\right)\Big|^{S_1} = 0 \tag{3.13}$$

Where:
Term 1 deals with mass inflow and outflow across the domain boundary.

3.3.2 Momentum conservation for the pipe loop

The homogenous momentum conservation equation for single and two phase flow is taken from Levy (1999:99):

$$\frac{\partial}{\partial t}\left(\rho_{mix} v_{mix} A_{flow}\right) + \frac{\partial}{\partial s}\left(\rho_{mix} v_{mix}^2 A_{flow}\right) = -A_{flow}\frac{\partial p}{\partial s} - \tau_w \pi D_H - \rho_{mix} g A_{flow} \sin\left(\theta\right) \tag{3.14}$$

Where:

p is the pressure of the fluid;

τ_w is the shear force on fluid due to friction from the pipe wall per unit area;

g is the gravitational acceleration; and

θ is the angle of the flow direction from the horizontal.

Assuming that the entire loop has a constant diameter, dividing the whole equation by the constant flow area and deleting the time-dependant terms gives the following:

$$\frac{\partial p}{\partial s} = -\frac{\partial}{\partial s}\left(\rho_{mix} v_{mix}^2\right) - \frac{\tau_w \pi D_H}{A_{flow}} - \rho_{mix} g \sin\left(\theta\right) \tag{3.15}$$

Where:

Term 1 deals with the pressure change over the control volume;

Term 2 deals with the dynamic pressure change over the control volume;

Term 3 deals with the pressure change due to friction over the control volume; and

Term 4 deals with the pressure change due to elevation changes over the control volume.

The gradients of the frictional pressure losses are given by Levy (1999:94) as follows:

$$\frac{\partial p_{friction,loss}}{\partial s} = -\frac{\tau_w \pi D_H}{A_{flow}} \tag{3.16}$$

Where:

$p_{friction,loss}$ is the primary (or frictional) pressure losses.

The above conservation equation does not explicitly show another possible pressure loss which must be taken into consideration: Acceleration pressure losses. These secondary losses usually stem from a bend or pipe fitting that changes the fluid direction or upsets the normal fluid flow. These losses will be added to the conservation equation.

Using the abovementioned primary pressure loss equation and adding the secondary losses, the momentum conservation equation can be represented by the following equation:

$$\frac{\partial p}{\partial s} = -\frac{\partial}{\partial s}\left(\rho_{mix} v_{mix}^2\right) - \frac{\partial p_{friction,loss}}{\partial s} - \frac{\partial p_{acc,loss}}{\partial s} - \rho_{mix} g \sin(\theta) \tag{3.17}$$

Where:

$p_{acc,loss}$ is the accelerational (or secondary) pressure loss.

Again, by integrating the equation over the domain one can obtain the following equation. It will be difficult to do the integration, since two of the terms, the dynamic and frictional pressure change terms, are dependent on velocity. The velocity might change over the length of the control volume due to density changes. The integration can be made easier by assuming that the frictional pressure loss term is calculated using the average velocity of the control volume. Also, since this is a steady state equation, the mass flow over a control volume is constant. The integration equation can then be represented by the following equation:

$$\int_{S_1}^{S_2}\left(\frac{\partial p}{\partial s}\right)ds=\int_{S_1}^{S_2}\left(-\frac{\partial}{\partial s}\left(\rho_{mix}v_{mix}^2\right)\right)ds+\int_{S_1}^{S_2}\left(-\frac{\partial p_{friction,loss}}{\partial s}\right)ds+\int_{S_1}^{S_2}\left(-\frac{\partial p_{acc,loss}}{\partial s}\right)ds+\int_{S_1}^{S_2}\left(-\rho_{mix}g\sin(\theta)\right)ds \quad (3.18)$$

The integration yields the following (note the use of average fluid properties where applicable):

$$(p)\Big|_{S_1}^{S_2}=\left(\rho_{mix}v_{mix}^2\right)\Big|_{S_1}^{S_2}+\left(-p_{friction,loss}\right)+\left(-p_{acc,loss}\right)+\Delta s\left(-\rho_{avg}g\sin(\theta)\right) \quad (3.19)$$

Where:

ρ_{avg} is the average density over a domain;

Δs is the distance between two points;

Term 1 is the pressure difference between the inlet and outlet of the control volume;

Term 2 is the dynamic pressure change between the inlet and outlet of the control volume;

Term 3 is the primary (or frictional) pressure loss;

Term 4 is the secondary (or accelerational) pressure losses; and

Term 5 is the pressure changes due to elevation differences between the control volume inlet and outlet.

3.3.3 Energy conservation for the pipe loop

The homogenous energy conservation equation for single and two phase flow is given by Levy (1999:99):

$$\begin{aligned}&\frac{\partial}{\partial t}\left(\rho_{mix}h_{mix}A_{flow}\right)+\frac{\partial}{\partial s}\left(\rho_{mix}v_{mix}h_{mix}A_{flow}\right)+\frac{1}{2}\frac{\partial}{\partial t}\left(\rho_{mix}v_{mix}^2A_{flow}\right)+\\&\frac{1}{2}\frac{\partial}{\partial s}\left(\rho_{mix}v_{mix}^3A_{flow}\right)=\pi D_H q''+A_{flow}q'''+\frac{\partial}{\partial t}\left(pA_{flow}\right)-\rho_{mix}v_{mix}A_{flow}g\sin(\theta)\end{aligned} \quad (3.20)$$

Where:

q'' is the heat flux; and

q''' is the internal energy generation in the control volume.

If the time-dependant terms are set to zero for a steady state case, we obtain the following:

$$\frac{\partial}{\partial s}\left(\rho_{mix}v_{mix}h_{mix}A_{flow}\right)+\frac{1}{2}\frac{\partial}{\partial s}\left(\rho_{mix}v_{mix}^3A_{flow}\right)=\pi D_H q''+A_{flow}q'''-\rho_{mix}v_{mix}A_{flow}g\sin(\theta) \quad (3.21)$$

If internal heat generation is assumed to be zero, we obtain the following:

$$\frac{\partial}{\partial s}\left(\rho_{mix} v_{mix} h_{mix} A_{flow}\right) + \frac{1}{2}\frac{\partial}{\partial s}\left(\rho_{mix} v_{mix}^3 A_{flow}\right) = \pi D_H q'' - \rho_{mix} v_{mix} A_{flow} g \sin(\theta) \tag{3.22}$$

Setting up the necessary integrals over a one-dimensional control volume yields the following:

$$\int_{S_1}^{S_2} \frac{\partial}{\partial s}\left(\rho_{mix} v_{mix} h_{mix} A_{flow}\right) ds + \int_{S_1}^{S_2} \frac{1}{2}\frac{\partial}{\partial s}\left(\rho_{mix} v_{mix}^3 A_{flow}\right) ds = \int_{S_1}^{S_2} \left(\pi D_H q''\right) ds - \int_{S_1}^{S_2} \rho_{mix} v_{mix} A_{flow} g \sin(\theta)\, ds \tag{3.23}$$

Integrating over the domain results in the following (note the use of average fluid properties where applicable):

$$\left(\rho_{mix} v_{mix} h_{mix} A_{flow}\right)\Big|_{S_1}^{S_2} + \frac{1}{2}\left(\rho_{mix} v_{mix}^3 A_{flow}\right)\Big|_{S_1}^{S_2} = \pi D_H q'' \Delta s - \rho_{avg} v_{avg} A_{flow} g \sin(\theta) \Delta s \tag{3.24}$$

Where:
Term 1 is the energy inflow and outflow through domain boundaries;
Term 2 is the kinetic energy inflow and outflow through the domain boundaries;
Term 3 is the heat transfer from adjacent structures through the surfaces of the control volume to the fluid; and
Term 4 is the change in the potential energy of the fluid due to the elevation changes.

In this section, the main set of equations used to program the simulation model have been discussed and manipulated into a form suitable for use in a simulation program. The next section will discuss other equations that aid the solution of the conservation equations.

3.3.4 Boundary conditions for the pipe loop

The pipe loop has only two interfaces through which there is fluid flow: An inlet and an outlet. By using the conservation equations the flow parameters and fluid conditions can be determined if the following boundary conditions are known: Inlet enthalpy, inlet pressure and outlet pressure.

In addition, the heat fluxes (or heat transfer values) and pressure losses must be known for the relevant pipe sections. This was done by imposing a prescribed temperature value for the heat exchanging

surfaces and setting the heat flux to zero on insulated surfaces. The imposed temperature was then used to calculate the heat flux to or from the fluid to the control volume surface.

3.4 Conservation equations of the reservoir

Since the reservoir is not a pipe and has two inlet and two outlet flows, it will have a slightly different set of conservation equations. The reservoir has no heat transfer associated with it and will also not have any vapour content. Any vapour that may form in the pipe loop is directly vented to the atmosphere before interacting with the fluid in the mixture. With these basic assumptions fixed, the conservation equations can now be derived.

3.4.1 Mass conservation in the reservoir

According to the principle of mass conservation interpreted from Cengel and Turner (2005:567–568):

$$\begin{bmatrix}\text{Change in}\\ \text{Control Volume}\\ \text{Mass}\end{bmatrix}+\left[\text{Nett outflow of mass}\right]=0 \tag{3.25}$$

The mass conservation equation can then be written as follows:

$$\frac{\partial}{\partial t}\int_{CV}\rho dV+\int_{CS}\rho\left(\bar{v}\cdot\bar{n}\right)dA=0 \tag{3.26}$$

Where:

ρ is the density of the fluid in the control volume;

V is the volume of the control volume;

$\bar{v}$ is the velocity vector of the fluid relative to the coordinate system;

A is the area;

CV indicates a control volume;

CS indicates a control surface; and

$\bar{n}$ is the normal vector to the control surface.

The equation can then be manipulated to consider only a uniform density throughout the constant volume reservoir. By recognising that all mass flows through the surface are perpendicular to it and that this is for a steady state case, the following equation is the result:

$$\int_{CS} \rho v dA = 0 \tag{3.27}$$

Where:

v is the fluid velocity.

By evaluating the integral the following equation is produced:

$$-\sum_i \left(\rho_i v_i A_{flow,i}\right)\Big|_{in} + \sum_i \left(\rho_i v_i A_{flow,i}\right)\Big|_{ex} = 0 \tag{3.28}$$

Where:

i as a subscript indicates a position;

in as a subscript indicate inflow into a control volume; and

ex as a subscript indicate outflow from a control volume.

3.4.2 Momentum conservation in the reservoir

Momentum conservation in this case deals specifically with conserving linear momentum. Angular momentum is assumed not to have any effect in this investigation. Cengel and Turner (2005:569–572) state that momentum conservation can be written as follows:

$$\begin{bmatrix}\text{Rate of change of}\\ \text{a Control Volume's}\\ \text{linear momentum}\end{bmatrix} = \begin{bmatrix}\text{The sum of all external}\\ \text{forces acting on the}\\ \text{control volume}\end{bmatrix} \tag{3.29}$$

This can be expanded to a more detailed explanation:

$$\begin{bmatrix}\text{Rate of change of}\\ \text{a Control Volume's}\\ \text{linear momentum}\end{bmatrix} = \begin{bmatrix}\text{The sum of all external}\\ \text{forces acting on the surface}\\ \text{of the control volume}\end{bmatrix} + \begin{bmatrix}\text{The sum of all external}\\ \text{forces acting on the contents}\\ \text{of the control volume}\end{bmatrix} \tag{3.30}$$

or in the case of a mathematical equation for linear momentum:

$$\frac{\partial}{\partial t}\int_{CV}\bar{v}\rho dV+\int_{CS}\bar{v}\rho\left(\bar{v}_{rel}\cdot\bar{n}\right)dA=\sum\bar{F}_{res} \tag{3.31}$$

Where:

$\bar{v}_{rel}$ is the velocity vector of the fluid relative to the control volume surface; and

$\bar{F}_{res}$ is the resultant force on the control volume.

However, one cannot use the momentum equation because the resultant force also contains the unknown forces exerted by the reservoir on the fluid. Thus, in the case of the reservoir, it is appropriate to only consider the conservation of mass and energy.

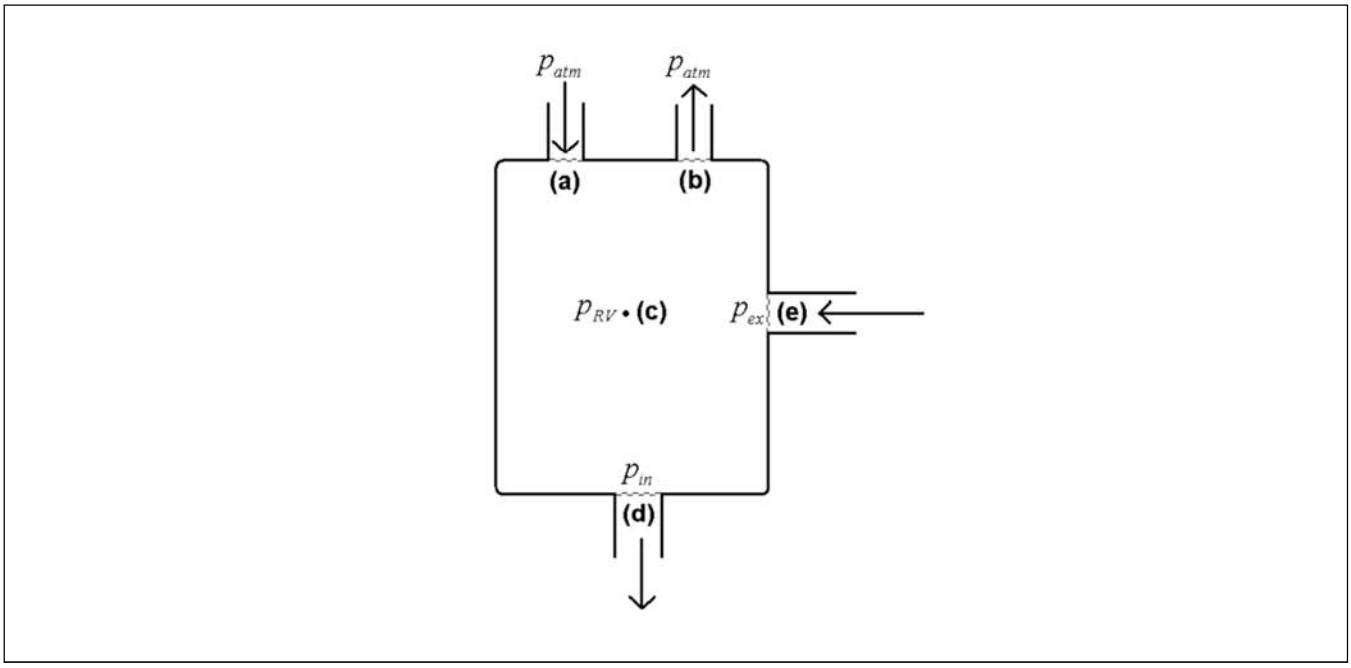


Figure 3-7. Pressure interfaces for the reservoir.

Thus the pressure in the reservoir is assumed to be hydrostatic (Figure 3-7, c). It is simple to implement if it is recalled that the fluid surface is at atmospheric pressure. The following formula will be used to calculate the pressures at the hot leg inlet and cold leg outlet in order to determine the absolute pressures at these two interfaces (Figure 3-7, d and e):

$$p_{RV,i}=p_{atm}+\rho_{RV}gz_i \tag{3.32}$$

Where:

p_{RV} is the pressure at various positions in the reservoir;

p_{atm} is the atmospheric pressure;

ρ_{RV} is the density of the fluid in the reservoir; and

z is the elevation of various positions in the reservoir.

The pressures of the pipe loop control volumes directly next to the reservoir can then be calculated by considering minor pressure losses (Figure 3-7, d and e). The reservoir has atmospheric pressures that act on its liquid surface (Figure 3-7, a and b)

3.4.3 Energy conservation in the reservoir

Energy conservation inside the reservoir will determine the temperature of the water that is being fed into the cold leg.

The conservation of energy can be stated as follows, according to Munson *et al.* (2006:229–232):

$$\begin{bmatrix}\text{Rate of increase}\\ \text{of total energy}\\ \text{stored in the}\\ \text{control volume}\end{bmatrix}+\begin{bmatrix}\text{Rate of energy}\\ \text{addition by flow}\\ \text{through control}\\ \text{volume boundaries}\end{bmatrix}=\begin{bmatrix}\text{Rate of energy}\\ \text{addition by heat}\\ \text{transfer to the}\\ \text{control volume}\end{bmatrix}+\begin{bmatrix}\text{Rate of energy}\\ \text{addition by work}\\ \text{transfer into the}\\ \text{control volume}\end{bmatrix} \tag{3.33}$$

or, in symbolic form, it can be written as:

$$\frac{\partial}{\partial t}\int_{CV} e\rho dV + \int_{CS} e\rho \bar{v}\cdot\bar{n}dA = q_{net} + W \tag{3.34}$$

Where:

e is the energy content of the fluid;

q_{net} is the rate of heat being added to the fluid; and

W is the rate of work being done on the fluid.

Since no work is being performed on the control volume or heat being transferred to the control volume and assuming a steady state condition, the equation can be simplified to the following:

$$\int_{CS} e\rho\bar{v}\cdot\bar{n}dA = 0 \tag{3.35}$$

By evaluating the integral and remembering that the reservoir simulation model is a one-dimensional point, in the case of energy conservation:

$$-\sum_i \left(e_i \rho_{mix,i} v_{mix,i} A_{flow,i}\right)\Big|_{in} + \sum_i \left(e_i \rho_{mix,i} v_{mix,i} A_{flow,i}\right)\Big|_{ex} = 0 \tag{3.36}$$

The energy content and mass flow terms are given by the following equations:

$$e_i = u_{mix,i} + \frac{v_{mix,i}^2}{2} + gz_i \tag{3.37}$$

Where:

u_{mix} is the internal energy content of the mixture.

$$\dot{m}_{mix,i} = \rho_{mix,i} v_{mix,i} A_{flow,i} \tag{3.38}$$

Thus, by replacing the energy content variable, the following equation is obtained:

$$-\sum_i \left(\left(u_{mix,i} + \frac{v_{mix,i}^2}{2} + gz_i\right)\rho_{mix,i} v_{mix,i} A_{flow,i}\right)\Big|_{in} + \sum_i \left(\left(u_{mix,i} + \frac{v_{mix,i}^2}{2} + gz_i\right)\rho_{mix,i} v_{mix,i} A_{flow,i}\right)\Big|_{ex} = 0 \tag{3.39}$$

Since enthalpy is defined as follows:

$$h = u + \frac{p}{\rho} \tag{3.40}$$

Where:

h is the internal energy of the fluid.

u is the internal energy of the fluid.

Equation (3.39) can be rewritten as follows:

$$-\sum_i \left(\left(h_{mix,i} - \frac{p_{mix,i}}{\rho_{mix,i}} + \frac{v_{mix,i}^2}{2} + gz_i\right)m_{mix,i}\right)\Big|_{in} + \sum_i \left(\left(h_{mix,i} - \frac{p_{mix,i}}{\rho_{mix,i}} + \frac{v_{mix,i}^2}{2} + gz_i\right)m_{mix,i}\right)\Big|_{ex} = 0 \tag{3.41}$$

3.4.4 Boundary conditions for the reservoir

The reservoir has four interfaces with other systems. Due to the assumption of steady state simulation, the reservoir model is very simple. Boundary conditions are limited to mass flows, pressures at the interfaces, inlet enthalpy from the hot leg and vapour fraction inlet from the hot leg.

3.5 Stability and convergence

Stability of the program was ensured by discretising the loop as finely as possible. Convergence of the solver was not a problem since the computer software that had been used had its own iterative solver routine.

3.6 Constitutive equations

The constitutive or closure equations provide inputs to the conservation equations for certain unknown quantities. This section also discusses how fluid properties were determined, as well as other relevant quantities that needed to be calculated to solve the set of conservation and closure equations.

3.6.1 Convection heat transfer

Convection heat transfer is a complex heat transfer phenomenon. The flow may be laminar or turbulent, single or two phase and flow in a vertical or horizontal direction. Convection heat transfer calculations focus on determining a heat transfer coefficient. Through the use of the coefficient, heat transfer rates can be determined. Typically, it is calculated through the use of a correlation. In this case convection heat transfer takes place in both the cold and the hot leg. The cold leg will always have a single phase liquid flowing through it, while the hot leg may have a liquid, two phase fluid or a superheated vapour.

3.6.1.1 Single phase heat transfer

Single phase heat transfer is the simplest of the convection mechanisms to be considered. Incropera *et al.* (2006:353) explains that the total heat transfer from a surface area due to convection can be determined by the following formula:

$$q = h_{coef,sp} A_{heat,trans} \left(T_{wall} - T_{fluid} \right) \tag{3.42}$$

Where:

q is the rate of heat transfer;

$h_{coef,sp}$ is the single phase heat transfer coefficient;

$A_{heat,trans}$ is the heat transfer area;

T_{wall} is the wall temperature of the tube; and

T_{fluid} is the temperature of the fluid.

For single phase flow the convection heat transfer coefficient can be determined from the dimensionless Nusselt number:

$$Nu_D = \frac{h_{coef,sp} D_H}{k_{sp}} \tag{3.43}$$

Where:

Nu_D is the dimensionless Nusselt number; and

k_{sp} is conductivity of the single phase fluid.

If fully developed laminar conditions exist, the Nusselt number is a constant value, depending only on the type of boundary condition. For a fixed heat transfer rate, it is calculated as follows for a flow in a circular cross-section:

$$Nu_D = 4.36 \quad \text{if} \quad q'' = \text{constant} \tag{3.44}$$

Otherwise if a surface temperature is specified then for flow in a circular cross section:

$$Nu_D = 3.66 \quad \text{if} \quad T_{wall} = \text{constant} \tag{3.45}$$

For fully developed, turbulent flow in a circular smooth pipe a range of correlations can be applied. The Dittus-Boelter equation states that (Incropera *et al.,* 2006:514):

$$Nu_D = 0.023 \, \mathrm{Re}_{sp}^{4/5} \, \mathrm{Pr}_{sp}^{n} \tag{3.46}$$

Where:

Pr_{sp} is the single phase Prandtl number and:

$n = 0.4$ for when the fluid is heated; or

$n = 0.3$ for when the fluid is cooled.

This correlation is valid over the following fluid parameters:

$$\begin{aligned} 0.6 <\approx \mathrm{Pr}_{sp} <\approx 160 \\ \mathrm{Re}_{sp} >\approx 10000 \\ \frac{L}{D_H} >\approx 10 \end{aligned} \tag{3.47}$$

Where:

L is the length of the pipe.

The Gnielinski correlation is more accurate, but it is also more complex to implement in a simulation since it employs the friction factor as well (Incropera *et al.,* 2006:515):

$$Nu_D = \frac{\left(\frac{f_{DW}}{8}\right)\left(\mathrm{Re}_{sp} - 1000\right)\mathrm{Pr}_{sp}}{1 + 12.7\left(\frac{f_{DW}}{8}\right)^{0.5}\left(\mathrm{Pr}_{sp}^{2/3} - 1\right)} \tag{3.48}$$

Where:

f_{DW} is the Darcy-Weisbach friction coefficient.

The correlation is valid for the following fluid parameters:

$$\begin{aligned} 0.5 <\approx \mathrm{Pr}_{sp} <\approx 2000 \\ 3000 <\approx \mathrm{Re}_{sp} <\approx 5\times 10^6 \end{aligned} \tag{3.49}$$

Since the Gnielinski correlation is more accurate and not much more complex to implement, it was used in the simulation program.

3.6.1.2 Two phase saturated and subcooled boiling heat transfer

The determination of the convection heat transfer coefficient can be done using a correlation from Chen (1966). The calculation has some resemblance to the single phase case as it also incorporates the single phase heat transfer coefficient. The Chen correlation computes two heat transfer coefficients, each of which separately considers a heat transfer mechanism. The overall effect can then be obtained by summation (Chen, 1966):

$$h_{coef,tp} = h_{coef,mic} + h_{coef,mac} \tag{3.50}$$

Where:

$h_{coef,tp}$ is the overall heat transfer coefficient;

$h_{coef,mic}$ is the micro heat transfer coefficient; and

$h_{coef,mac}$ is the macro heat transfer coefficient.

The overall heat transfer coefficient for boiling is calculated from this correlation by summation of two heat transfer phenomena. The first term in the equation represents the normal convection heat transfer, although slightly modified from single phase theory based on the Dittus-Boelter equation. The other contribution is heat transfer due to the effect of nucleate boiling. This refers to the additional heat transfer obtained due to the bubble movement.

The familiar Dittus-Boelter equation is presented in a slightly modified form where it gives the convection heat transfer contribution (Chen, 1966):

$$h_{coef,mac} = 0.023\left(\mathrm{Re}_{liq}^{0.8}\right)\left(\mathrm{Pr}_{liq}^{0.4}\right)\left(\frac{k_{liq}}{D_H}\right)F \tag{3.51}$$

Where:

Pr_{liq} is the Prandtl number of the liquid phase of the fluid; and

k_{liq} is the conductivity of the liquid phase of the fluid.

The nucleate boiling effect is taken into consideration by using the following equation from Chen (1966):

$$h_{coef,mic} = 0.00122\left(\frac{\left(k_{liq}^{0.79}\right)\left(C_{p,liq}^{0.45}\right)\left(\rho_{liq}^{0.49}\right)\left(g^{0.25}\right)}{\left(\sigma^{0.5}\right)\left(\mu_{liq}^{0.29}\right)\left(\rho_{vap}^{0.24}\right)\left(h_{fg}^{0.24}\right)}\right)\left(\left|T_{wall}-T_{fluid}\right|\right)^{0.24}\left(\left|P_{sat,T_{wall}}-P_{sat,T_{fluid}}\right|\right)^{0.75}S \quad (3.52)$$

Where:

$C_{p,liq}$ is the liquid phase specific heat value of the fluid;

σ is the surface tension of the fluid;

h_{fg} is the latent heat of vaporisation of the fluid;

$p_{sat,T_{wall}}$ is the saturated pressure of the fluid at the wall temperature; and

$p_{sat,T_{fluid}}$ is the saturated pressure of the fluid at the fluid temperature.

It can be seen from the abovementioned equations that the two heat transfer coefficients are dependent on quite a number of physical properties.

The method of Gungor and Winterton can be used to adapt the Chen heat transfer correlation for use in determining the heat transfer of subcooled boiling (Thome 2009:10-7). The method modifies the summation equation (equation (3.50)) of heat transfer coefficients in the boiling regime to the following:

$$q'' = \frac{h_{coef,mac}}{F}\left(T_{wall}-T_{fluid}\right)+h_{coef,mic}\left(T_{wall}-T_{sat}\right) \quad (3.53)$$

The heat transfer coefficients can then be determined in accordance with the Chen correlation (Thome 2009:10-7). Note that the Reynolds number ratio F is cancelled in the equation, for clarity refer to equation (3.51).

In the literature study it was found that the presence of subcooled boiling can be determined by computing the following two parameters, the required degree of wall superheat and heat flux as given by Kandlikar (1998):

$$\Delta T_{\sup,ONB} = \frac{4\sigma T_{sat}h_{coef,sp}}{\rho_{mix}k_{liq}h_{fg}}\left(1+\left(1+\frac{\rho_{mix}k_{liq}h_{fg}\Delta T_{sub}}{2\sigma T_{sat}h_{coef,sp}}\right)^{0.5}\right) \quad (3.54)$$

Where:

$\Delta T_{\sup,ONB}$ is the required degree of wall superheating for the ONB;

T_{sat} is the saturation temperature of the fluid at a particular pressure; and

ΔT_{sub} is the degree of subcooling of the liquid fluid.

$$q''_{ONB} = \left(\frac{\rho_{mix} k_{liq} h_{fg}}{8\sigma T_{sat}} \right) \left(\Delta T_{\text{sup},ONB} \right)^2 \tag{3.55}$$

Where:

q''_{ONB} is the required heat flux for the ONB.

According to Kandlikar (1998) the following equations are used in conjunction with the above equations to compute the fluid subcooling and wall superheating:

$$\Delta T_{sub} = T_{sat} - T_{fluid} \tag{3.56}$$

$$\Delta T_{\text{sup}} = T_{wall} - T_{sat} \tag{3.57}$$

This method will make the detection of subcooled boiling and the prediction of the associated heat transfer possible.

3.6.2 Pressure drop

Any fluid that flows through a pipe or conduit is subject to pressure losses. These losses are typically due to frictional losses and form losses.

It must be noted that pressure loss or gain due to changes in elevation are not discussed here as the conservation equations take this into account naturally.

According to Cengel and Turner (2005:613–614), frictional pressure drop can be calculated by using the following equation:

$$p_{loss,\,friction} = f_{DW} \frac{L}{D_H} \frac{\rho_{mix} v_{mix}^2}{2} \tag{3.58}$$

Form (or secondary) losses can be found in Cengel and Turner (2005:632–635):

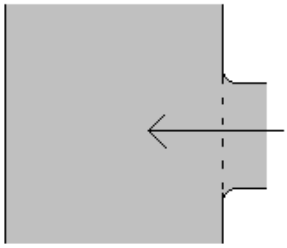
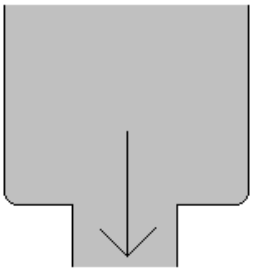
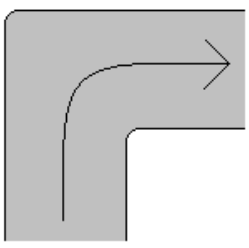
$$p_{loss,acc} = K_{loss} \frac{\rho_{mix} v_{mix}^2}{2} \tag{3.59}$$

Where:

K_{loss} is the secondary loss coefficient.

The minor loss coefficient was obtained from the literature (Cengel and Turner, 2005:634–635). The coefficients assumed in this investigation are listed in Table 2:

Table 2. Form loss coefficients for piping.

Form loss type	Form loss coefficient
 Slightly rounded pipe entrance	$K_{loss} = 1.0$
 Slightly rounded pipe exit	$K_{loss} = 0.12$
 Flanged smooth pipe bend	$K_{loss} = 0.3$

The Darcy-Weisbach friction factor was used throughout this report, unless otherwise stated. To determine the friction pressure loss the friction factor can be calculated from an appropriate empirical correlation. For single phase flow the flow regime must also be considered. This will influence which

correlation is used for the friction factor. For single phase the correlations for the friction factor were obtained from literature for the laminar flow region (Cengel & Turner, 2005:614) and for the turbulent flow region (Cengel & Turner, 2005:625):

$$f_{DW,lam} = \frac{64}{\mathrm{Re}_{sp}} \tag{3.60}$$

Where:

$f_{DW,lam}$ is the laminar Darcy-Weisbach friction factor.

$$f_{turb,DW} = \left[-1.8 \log \left(\frac{6.9}{\mathrm{Re}_{sp}} + \left(\frac{\frac{\varepsilon}{D_H}}{3.7} \right)^{1.11} \right) \right]^{-2} \tag{3.61}$$

Where:

$f_{DW,turb}$ is the turbulent Darcy-Weisbach friction factor; and

ε is the roughness of the pipe wall.

The correlation represents the familiar Moody diagram. Another correlation that can possibly be used for turbulent flow from Vijayan *et al.* (1995) is:

$$\left(f_{turb,\,fan} \right)^{-0.5} = 3.48 - 4 \log_{10} \left(\frac{2\varepsilon}{D_H} + \frac{9.35}{\left| \mathrm{Re}_{sp} \right| \left(f_{turb,\,fan} \right)^{0.5}} \right) \tag{3.62}$$

Where:

$f_{fan,turb}$ is the turbulent Fanning friction factor.

In the above equation, the friction factor used is the Fanning friction factor. It is related to the Darcy-Weisbach friction factor by the following:

$$f_{DW} = 4 f_{fan} \tag{3.63}$$

Where:

f_{fan} is the Fanning friction factor.

The friction factor in the transition zone between the turbulent and laminar flow regimes can be calculated from:

$$f_{DW,trans} = \begin{cases} f_{DW,lam} & \text{if } f_{DW,turb} \leq f_{DW,lam} \\ f_{DW,turb} & \text{if } f_{DW,lam} < f_{DW,turb} \end{cases} \tag{3.64}$$

Where:

$f_{DW,trans}$ is the Darcy-Weisbach friction factor in the transition zone.

In essence this method, from Vijayan *et al.* (1995), calculates the friction factor in the transition zone by taking the maximum of the friction factor values from the turbulent and laminar correlations.

The friction factor in the transition zone between the laminar and turbulent flow regions was taken as the maximum value between the laminar and turbulent correlation. By doing this, a smooth friction factor curve is obtained. Interpolation or use of the minimum correlation value would lead to the friction factor curve having a positive gradient in the transition zone, thus leading to instabilities in the solution of the NCL. The results of a quick calculation are shown in Figure 3-8.

The friction factor over the range of Reynolds numbers and with a fixed roughness and pipe diameter was calculated. The first set of values (Figure 3-8, a) was determined from equation (3.60) for the laminar zone, equation (3.61) for the turbulent zone and equation (3.64) for the transition zone. The second set of results (Figure 3-8, b) was determined from the same set of equations, except for the turbulent zone, where equation (3.62) was used. From the results, it can be seen that they are reasonably close. Thus, the simpler explicit correlation from equation (3.61) was chosen for use in the simulation model since its results can be calculated directly. If a simple switch from laminar to turbulent correlations took place at a Reynolds number of 4 000, the friction factor would no longer be smooth (Figure 3-8, c). The smooth behaviour of the friction factor in the transition zone, when it is calculated by taking the maximum of the values of the laminar and turbulent correlations into account, is preferred due to the aforementioned smooth slope of the friction factor value curve.

There are many correlations and methods to use when determining the two phase frictional pressure. The correlations that can be used include, but are not limited to the following:

a. Single phase correlations;
b. Single phase correlations modified by two phase factors;
c. Two phase correlations not specific to two phase flow patterns; and
d. Two phase correlations deduced for use in a certain two phase flow patterns.

Of course, a flow regime-dependant correlation should not be used if conservation laws have been derived for a homogenous model. On the other hand, single phase correlations should not be used for a more complex model, since significant additional loss of accuracy should be avoided. This leaves two possibilities for the simulation model: A two phase correlation or a modified single phase correlation. The ideal would be a simple explicit two phase flow correlation with reasonable accuracy, since a modified single phase correlation will be much more involved.

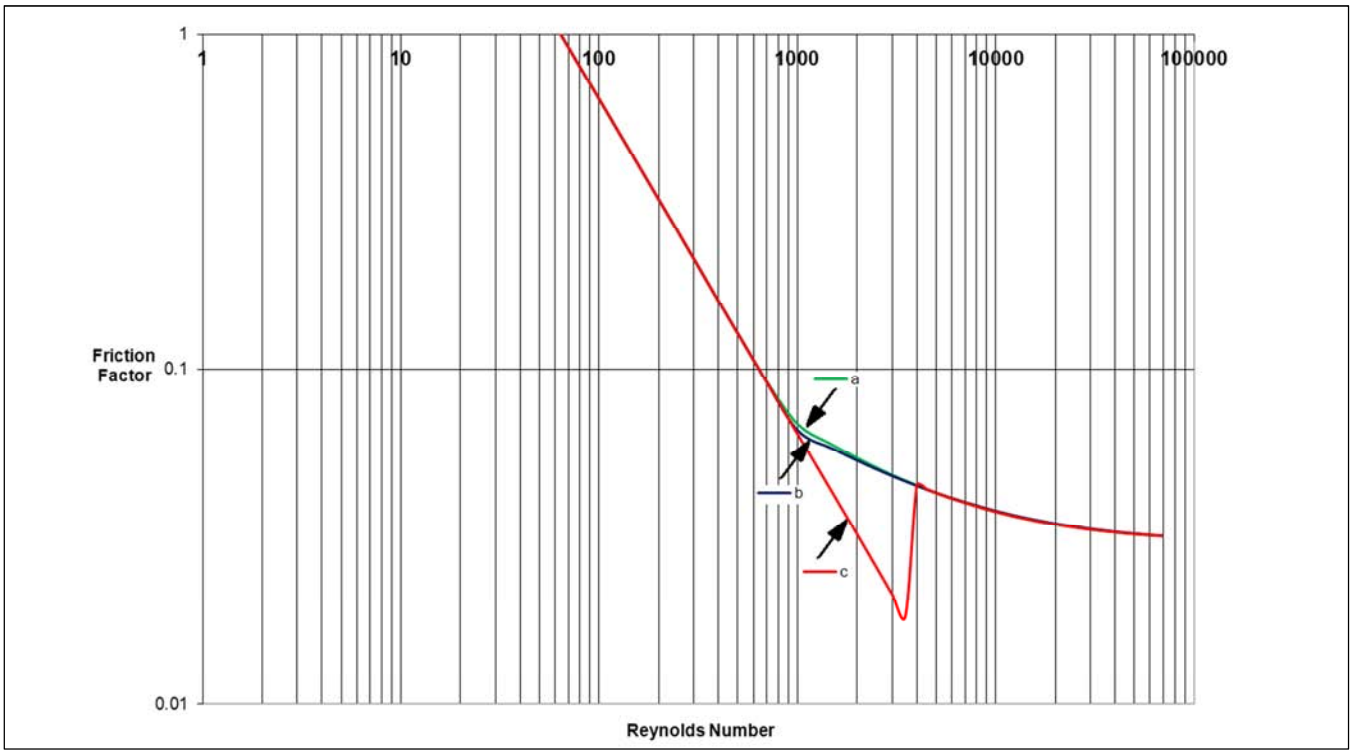


Figure 3-8. Comparison of different friction factor correlations and transition zone switching.

An explicit formulation for a two phase friction factor that is very simple to use was taken from the study by Shannak (2008):

$$f_{DW,tp} = \left[-2\log\left[\frac{1}{3.7065}\frac{\varepsilon}{D_H} - \frac{5.0452}{\mathrm{Re}_{tp}}\log\left(\frac{1}{2.8257}\left(\frac{\varepsilon}{D_H}\right)^{1.1098} + \frac{5.8506}{\mathrm{Re}_{tp}^{0.8981}} \right) \right] \right]^{-2} \tag{3.65}$$

Where:

$f_{DW,tp}$ is the Darcy-Weisbach friction factor for two phase flow.

The Reynolds numbers at which this equation is valid are as follows:

$$11 < \mathrm{Re}_{tp} \tag{3.66}$$

The two phase Reynolds number in the above equations was defined by Shannak (2008) as:

$$\mathrm{Re}_{tp} = \frac{\dot{m}_{mix} D_H \left(x^2 + (1-x)^2 \left(\frac{\rho_{vap}}{\rho_{mix}} \right) \right)}{\mu_{vap} x + \mu_{mix} (1-x) \left(\frac{\rho_{vap}}{\rho_{mix}} \right)} \tag{3.67}$$

3.7 Conclusion of the theoretical background

In this chapter, the theoretical background for the simulation program was discussed. The conservation equations for the homogenous model were rewritten in a discretised form. Heat transfer correlations for single and two phase flow were discussed and those to be used in the simulation program chosen. Pressure drop formulas were discussed and identified for use in the simulation program. The next chapter will build the simulation program upon the theoretical foundation that was given in this chapter.

Chapter 4 - Simulation

In this chapter, the simulation model and other details of the simulation methodology will be discussed. The programming approach will be explained and discretisation will be illustrated. The simulation model was based on the theory introduced in the previous chapter.

4.1 Software

The programming of the simulation program was done using the software package EES. EES has many functions and features, which can aid the researcher in the field of thermo-fluid calculations. The features of EES that were of particular importance to this investigation were (Klein, 2008:1–3, 26):

a. EES is able to solve a large set of equations simultaneously;
b. Solution times are generally fast;
c. A large database of thermo-physical data, including that of water, is provided; and
d. User-written functions and modules are supported.

One of the constraints of the academic version of EES, which was used in this investigation, was that it had a variable limit of 6 000 variables. This implied that models could not be discretised too finely as the number of variables would easily exceed the limit set by EES. The variable limit is a hindrance, especially if large simulations are attempted, but the ease of program implementation and speed of execution outweigh the negatives in a conceptual study such as the present one. During the grid independence study, which is explained in the next chapter, it was found that the total number of equations could be kept below the 6 000 limit without significantly affecting the accuracy of the solution.

Oosthuizen (2003) used EES in a very similar investigation and proved that it could be used in a conceptual study on NCLs, despite the variable limit. The abovementioned capabilities, in addition to the author's previous experience with this software, made EES a natural choice for this investigation, even if the difficulty with the variable limit is taken into consideration.

4.2 Simulation model philosophy

In this section, the background to the simulation philosophy will be discussed. This will explain the reasoning behind the simulation method that was followed.

The NCL was divided into the following two large parts for the purpose of the simulation model:

a. Pipe loop (Figure 4-1, a); and
b. Reservoir (Figure 4-1, b - h).

The division of the NCL into two was necessary since the philosophy behind the development of the conservation equation sets were different for the pipe loop and the reservoir. The pipe loop was discretised into a number of control volumes, each with one inlet and outlet. The reservoir was modelled as a single control volume with two inlets and two outlets. The pipe loop was divided into several subcomponents. Each subcomponent was implemented slightly differently according to its function in the pipe loop, while still using the same conservation equation set. The subcomponents are explained in greater detail later on in this chapter.

To simplify the handling of control volume lengths, positions and results, the pipe loop was represented in the simulation program as a single distance along the loop. Thus the position of a control volume could be represented by a single distance, with the origin at the start of the cold leg at the reservoir. The end of the loop, or maximum distance from the start of the loop, was at the end of the horizontal hot pipe, again at the reservoir. The distance values are only used in the presentation of the simulation results where the change of variables along the loop is illustrated in the form of a graph.

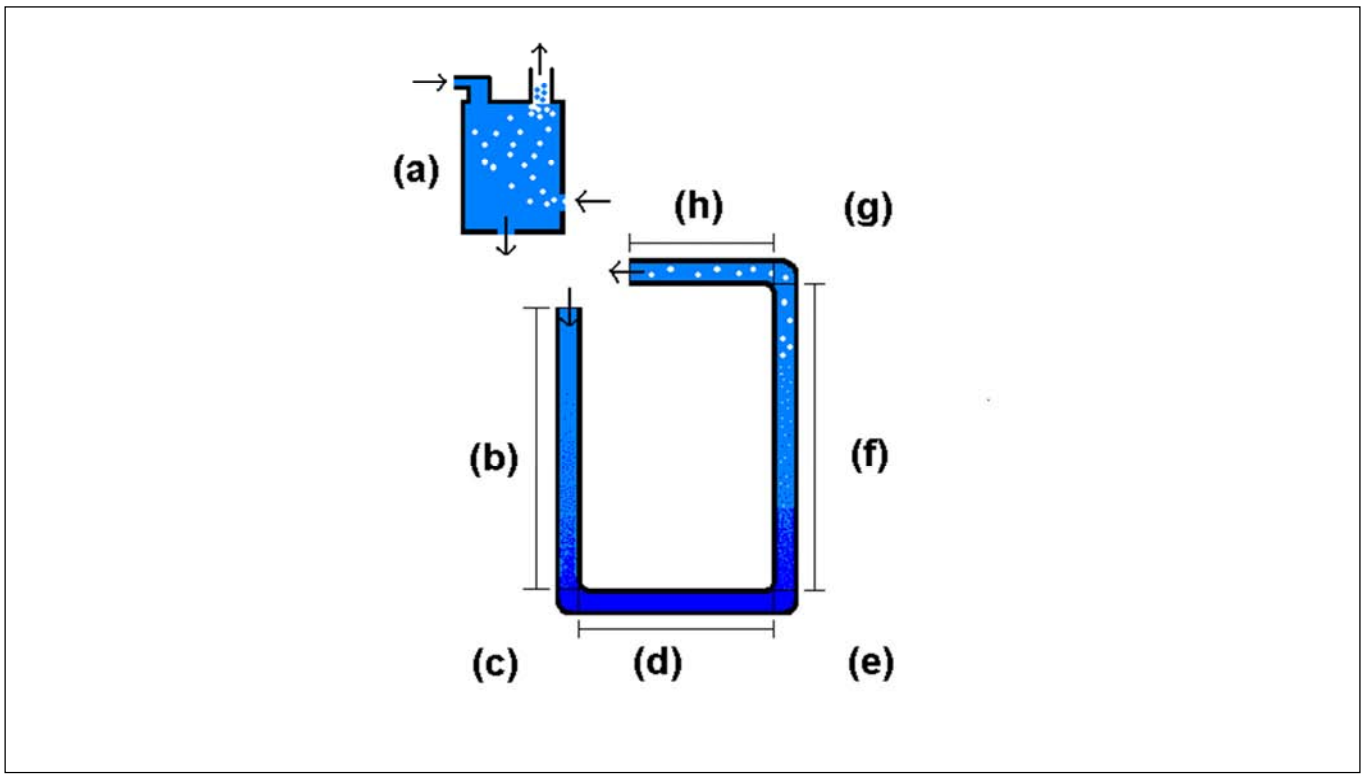


Figure 4-1. Natural circulation loop subcomponent breakdown.

4.3 Assumptions used in the simulation program

In this section, the assumptions made in the simulation program will be discussed. These assumptions where made for various reasons: Either simplicity of programming or adequate representation of reality.

Of the two sets of conservation equations, the set used for the reservoir was considered to be the simplest. There are no pressure losses within the reservoir and it was not discretised. It was, however, an important part of the model, since it was set up to provide the pipe loop with inlet pressures and enthalpies. It also determined the outlet pressure of the loop and was used as a water vapour separator. The pipe loop was where the bulk of calculations for the model took place. The loop was divided into a number of subcomponents, as indicated in Table 3. Each subcomponent was divided into control volumes, each control volume as classified in the table. The table also lists the assumptions that are specifically applicable to a pipe loop subcomponent. The assumptions are considered realistic in terms of that which can be expected of a typical pipe loop. The set of conservation equations for the pipe loop has been derived for a two phase mixture and considered gravity effects, heat transfer, pressure losses and others. By neglecting terms that were not applicable to the specific subcomponent and by considering the assumptions in Table 3, a simpler set of conservation equations could be obtained for some of the pipe loop subcomponents. An example of this is the absence of heat transfer on the horizontal and elbow sections of the pipe loop.

Assumptions for the simulation of the reservoir were as follows:

a. The reservoir was open to the atmosphere, thus it was at atmospheric pressure which was assumed to be 100 kPa.
b. The reservoir was an ideal water-steam separator. Thus, all the steam entering from the inlet pipe was released to the atmosphere.
c. Steam coming from the outlet of the pipe loop did not mix with or transfer energy to the liquid in reservoir.
d. The tank level was assumed to be constant due to a supply of feedwater continually being fed into it.
e. Feedwater was at a fixed temperature of 20˚C or 293 K (degrees Kelvin).
f. Feedwater, the water in the reservoir and the water from the pipe loop outlet mixed uniformly.
g. Water being fed from the reservoir into the cold leg water was taken from the uniformly mixed reservoir. Thus, the water entering the cold leg had properties equal to that of the fluid in the reservoir.
h. The reservoir was shaped like a cube, its sides having an arbitrarily chosen length of 0.50 m.

i. The inlet pipe to the cold leg was positioned in the middle of the bottom of the reservoir. The outlet pipe from the hot leg was positioned at the top of the reservoir. Thus, the cold leg was 0.5 m shorter than the hot leg. The top horizontal leg was 0.25 m shorter than the bottom one.
j. The outlet pressure of the hot leg was equal to the pressure at the top of the reservoir minus the secondary loss associated with it.
k. There were no heat or friction losses in the reservoir.
l. The pressures at the different pipe connections were calculated using a static pressure calculation.
m. The feedwater inlet and vapour outlet had no secondary pressure losses, while the connections to the loop had secondary losses.
n. The flow areas of the reservoir inlets and outlets are equal to those of the pipe loop.

The following additional assumption was made with regard to the pipe loop control volumes and the reservoir connections: Pipe elbows extend one and a half times the diameter of the pipe in both flow directions from the point where the two flow axes of the elbows cross.

Table 3. Subcomponent classification groups.

No.	Group	Discretised	Special considerations for conservation equations
1.	Reservoir (Figure 4-1, a)	No	Unique set of conservation equations. Singe phase liquid with static pressure balance and uniform fluid properties and conditions throughout.
2.	Cold leg (Figure 4-1, b)	Yes	Single phase - $x \leq 0$ with heat transfer, gravity effects and frictional pressure losses included.
3.	Cold leg elbow (Figure 4-1, c)	No	Single phase - $x \leq 0$ with no heat transfer effects included. Gravity effects, frictional pressure loss and accelerational pressure losses considered.
4.	Bottom horizontal leg (Figure 4-1, d)	Yes	Single phase - $x \leq 0$ with no heat transfer or gravity effects included. Friction pressure losses considered.
5.	Bottom leg elbow (Figure 4-1, e)	No	Single phase - $x \leq 0$ with no heat transfer effects included. Gravity effects, frictional pressure loss and accelerational pressure losses considered.

6.	Hot leg (Figure 4-1, f)	Yes	Single or two phase with heat transfer, gravity effects and friction pressure losses included.
7.	Hot leg elbow (Figure 4-1, g)	No	Single or two phase with no heat transfer effects included. Gravity effects, frictional pressure loss and accelerational pressure losses considered.
8.	Top horizontal leg (Figure 4-1, h)	Yes	Single or two phase with no heat transfer or gravity effects included. Friction pressure losses considered.

4.4 Structure of the simulation program

4.4.1 Simulation method

The numerical study of the NCL was divided into two phases. In the first phase, a base case of the NCL model was simulated. This was done to see how variables change along the length of the loop. The second phase consisted of a parametric study with variations on the base case of the loop to obtain a set of results that showed how the loop performance was affected by a change in its parameters.

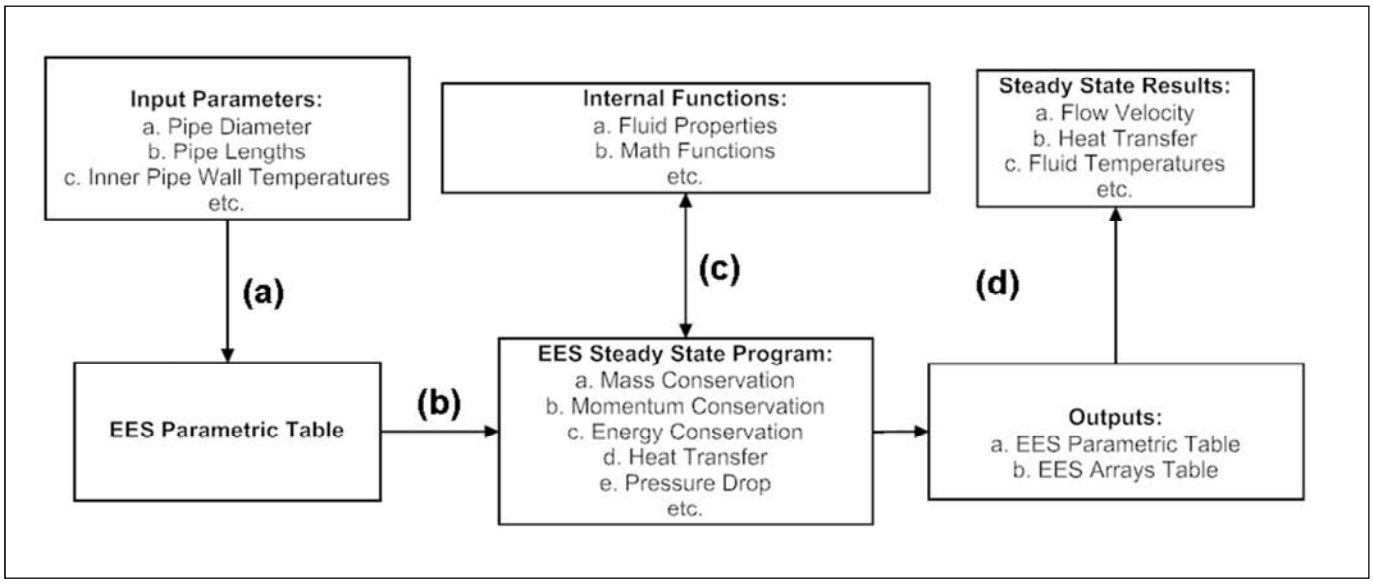


Figure 4-2. Steady state simulation program execution flow.

The simulation runs were executed in the EES software in the following manner (Figure 4-2):

a. First, a table of input values for the program was specified by the user (Figure 4-2, a).
b. The model used a parametric table of input values. These values were used as inputs in the simulation program solving process (Figure 4-2, b).
c. In the process, some internal EES functions, for example, fluid properties, were used as required (Figure 4-2, c).
d. Upon completion, results were provided as outputs (Figure 4-2, d).

4.4.2 Simulation program structure

The EES simulation program was divided into several blocks of code. To make sure that the program code was logically positioned, the code blocks were positioned, where applicable, in the same chronological order as the simulation loop. If the start of the loop was chosen to be the reservoir, the end would be the hot horizontal outlet.

The blocks of code, from the top of the code to the bottom, were as follows:

a. Global constants: This block of code contained the globally declared constants for the simulation program.
b. Functions: This section contained all the user-written functions used by the main program.
c. System parameters: In this block, all the variables that specify the physical size of the loop were set.
d. Boundary values and other coefficients: In this section, the boundary values of the loop were specified. This included wall temperatures and reservoir pressures. The secondary loss coefficients were also specified here.
e. Discretising parameters: This block of code specified the discretising sizes, number of control volumes and other related parameters.
f. Reservoir and loop inlet and outlet conditions: In this section, the reservoir fluid conditions at its inlets and outlets were set or calculated.
g. Cold vertical leg: This section contained the conservation and other calculations for this part of the loop.
h. Cold vertical leg exit elbow: This section contained the conservation and other calculations for this part of the loop.
i. Cold horizontal leg: This section contained the conservation and other calculations for this part of the loop.
j. Cold horizontal leg exit elbow: This section contained the conservation and other calculations for this part of the loop.

k. Hot vertical leg: This section contained the conservation and other calculations for this part of the loop.
l. Hot vertical leg exit elbow: This section contained the conservation and other calculations for this part of the loop.
m. Hot horizontal leg: This section contained the conservation and other calculations for this part of the loop.
n. Global loop parameters and calculations: In this part of the program, some global loop performance figures were calculated.

The main body of the program consisted of blocks (c) to (n), as numbered above.

4.4.3 Simulation discretisation

This section explains how the control volumes were set up in the simulation program. The generic form of coding used in the program is explained later on in this chapter.

Figure 4-3 (a) shows a single control volume with flow through it. It has a set of known fluid input parameters as shown, in the case of this study, pressure and enthalpy. It also has another known parameter at the outlet: Pressure. Based on the solution of the conservation equations the change in fluid parameters and thus other unknown fluid parameters are calculated. Thus, all the parameters of the control volume can be obtained. If another control volume, such as in Figure 4-3 (b), is added to the previous one and the outlet pressure boundary condition is moved to the outlet of the second control volume the same applies. The inlet fluid parameters of the second control volume can be set equal to that of the first control volume. Then again, the change in fluid parameters can be calculated based on the conservation equations. In this way, a whole simulation model of the pipe loop could be built up by stringing a number of these control volumes together as is shown in Figure 4-4.

For the purposes of the simulation program equations presented in this report, the naming convention is applied throughout. The actual simulation program used slightly different variable names, but in essence the convention remained the same.

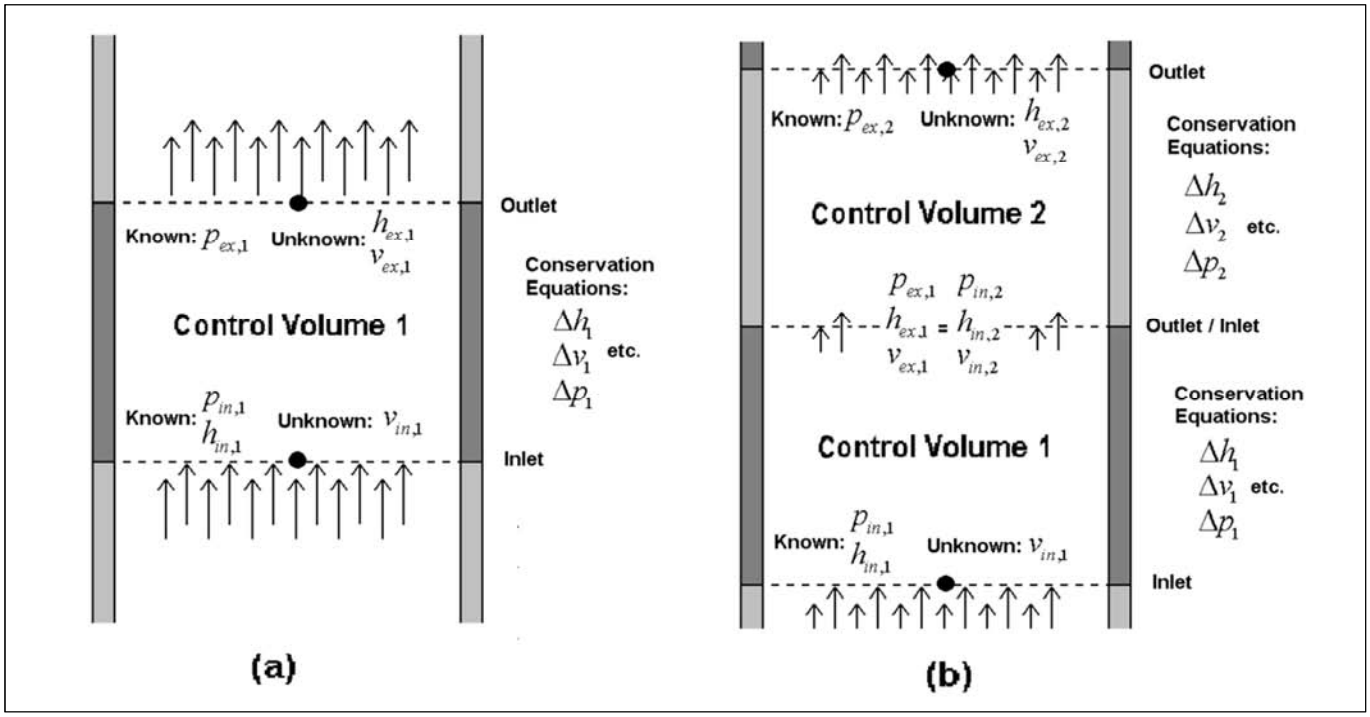


Figure 4-3. Single and two control volume stringing in the simulation program.

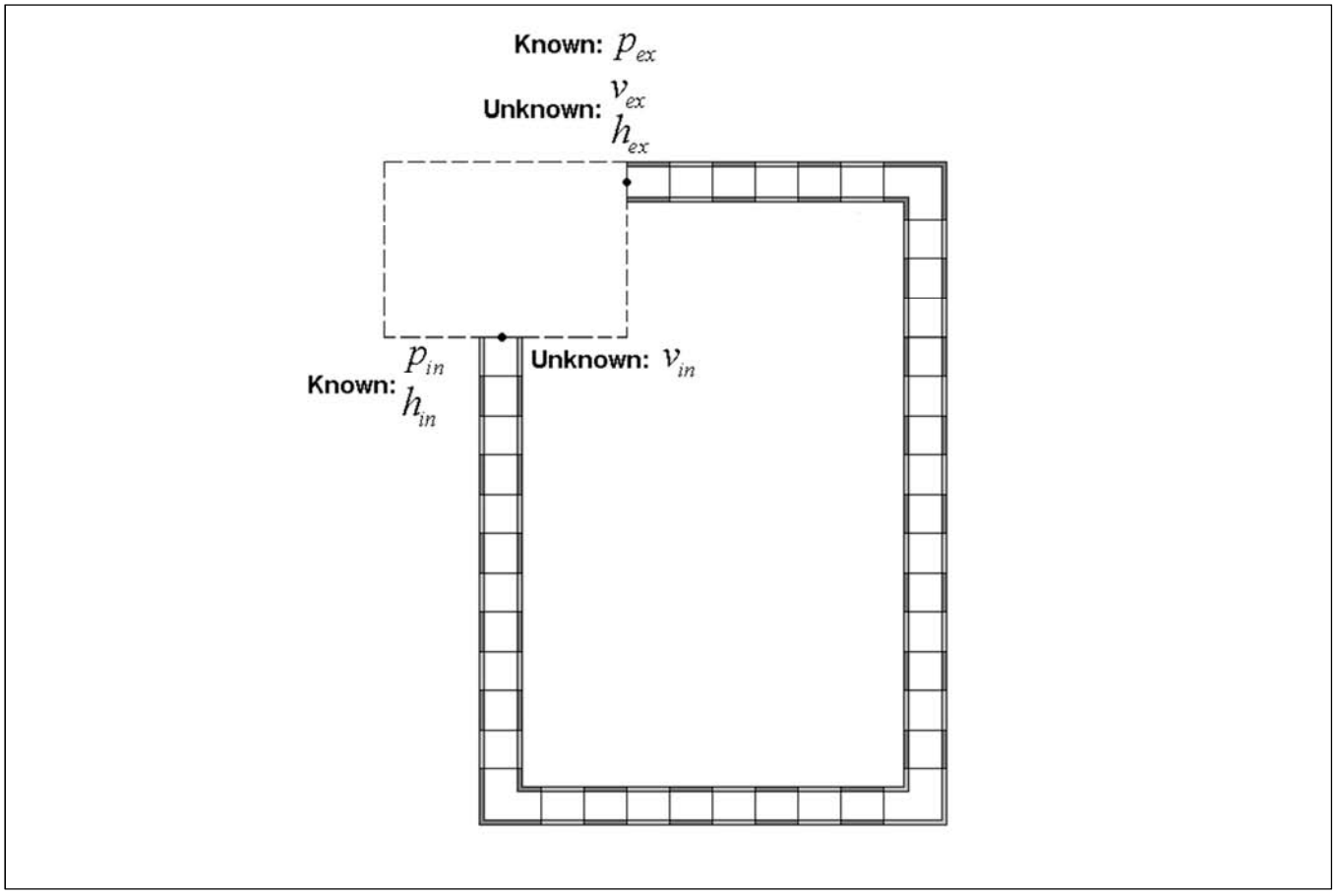


Figure 4-4. Control volume stringing in the NCL.

4.5 Component-specific conservation equations discretisation – Pipe loop

In this section, the conservation equations of the pipe loop are transformed into a suitable form for use in the simulation model by rewriting it for a specific naming convention.

4.5.1 Naming convention

Figure 4-5 demonstrates how the discretisation and numbering of control volumes was done. The conservation equations use the same naming conventions as in the figure.

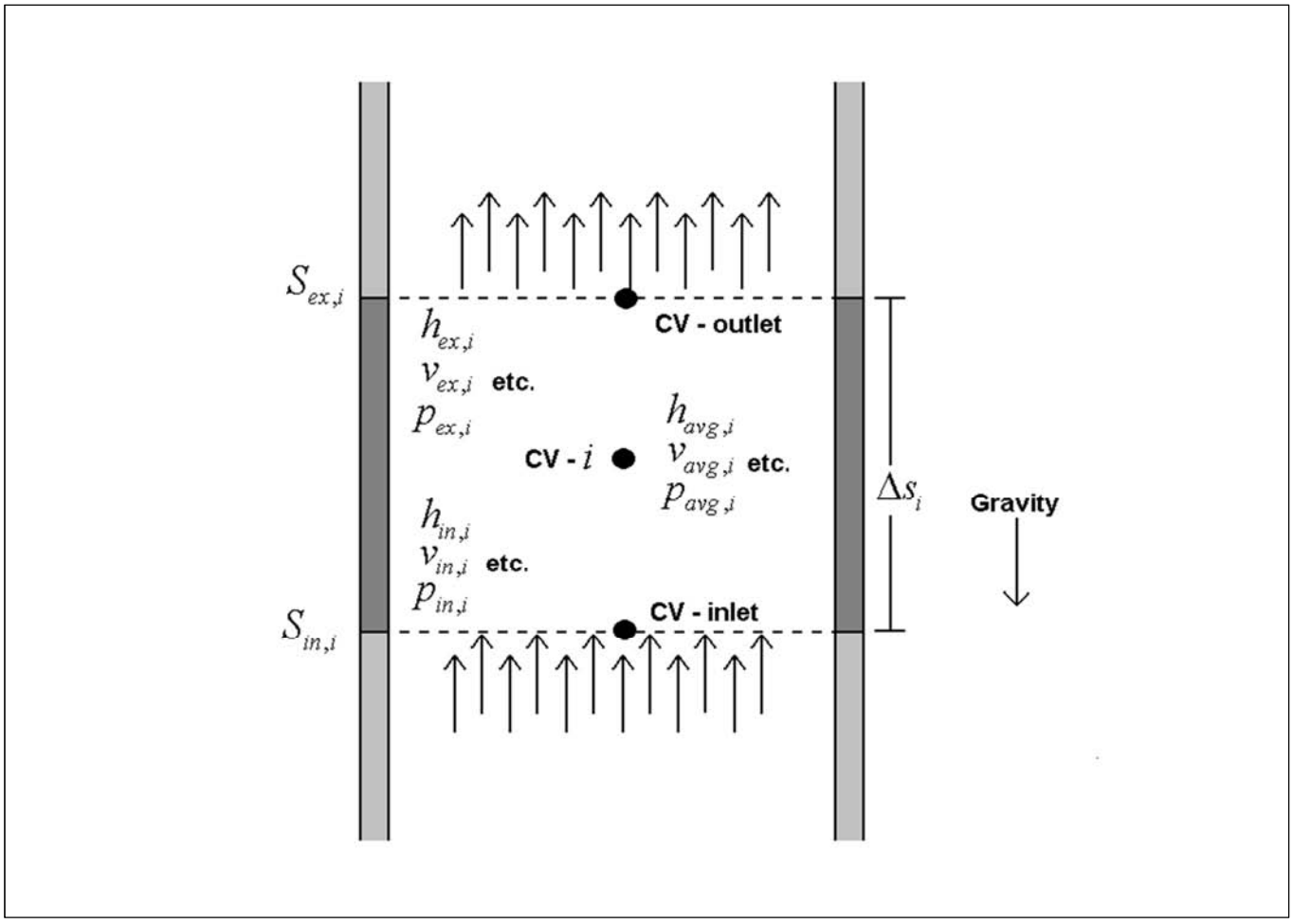


Figure 4-5. Naming convention for pipe control volumes in the simulation program.

The figure shows a generic pipe control volume with an inlet, an outlet and a centre denoted by CV – inlet, CV – outlet and CV – i respectively. Inlet properties of the fluid are distinguished by the in subscript, while the outlet properties are denoted by the ex subscript. Properties calculated at the centre

of the control volume use the avg subscript. The subscript in refers to "inlet", ex to "exit" or "outlet" and avg to "average". Later on in this chapter, it will be illustrated that the simulation program used the average fluid properties to calculate heat transfer, pressure drop and other related quantities. Also note that the convention for the flow direction was upward, while the convention for the direction of gravity was downward. Lastly, since there are multiple control volumes, each quantity will have the subscript i added to the subscripts described above, denoting the reference control volume. In short, each quantity calculated in a control volume has a subscript denoting the position of the quantity in the control volume and the control volume number.

In the next section, the pipe loop conservation equations derived in the previous chapter will be modified for use in the simulation program, using the naming convention presented in the current section.

4.5.2 Discretised conservation of mass – Pipe loop

The mass conservation that was derived for a pipe loop control volume (equation (3.13)) can be simplified to the following by remembering that the NCL is a constant diameter pipe loop:

$$\left(\rho_{mix} v_{mix}\right)\Big|^{i+1} - \left(\rho_{mix} v_{mix}\right)\Big|^{i-1} = 0 \tag{4.1}$$

Introducing the naming convention leads to the mass conservation equation that was implemented in the simulation program:

$$\left(\rho_{ex,i} v_{ex,i}\right) - \left(\rho_{in,i} v_{in,i}\right) = 0 \tag{4.2}$$

4.5.3 Discretised conservation of momentum – Pipe loop

The momentum conservation equation (equation (3.19)) can be rearranged into the form used in the simulation program and the naming convention added to give the following:

$$p_{ex,i} - p_{in,i} = -1\left(\left(\rho_{ex,i} v_{ex,i}^2 - \rho_{in,i} v_{in,i}^2\right) + p_{friction,loss,i} + \Delta s_i \rho_{avg,i} g \sin\left(\theta_i\right)\right) \tag{4.3}$$

Note that for the conservation of momentum and energy equations, some of the quantities, such as the frictional pressure loss, are calculated in functions, which is why it is presented as a single quantity in the conservation equations. The functions are explained later on in this chapter.

4.5.4 Discretised conservation of energy – Pipe loop

The conservation of energy equation (equation (3.24)) can be rewritten as follows:

$$\left(h_{ex,i} - h_{in,i}\right) = \left[q_i - \frac{1}{2} A_{flow} \left(\rho_{ex,i} v_{ex,i}^3 - \rho_{in,i} v_{in,i}^3 \right) - \Delta s_i \rho_{avg,i} v_{avg,i} A_{flow} g \sin\left(\theta_i\right) \right] \left(\dot{m}_{avg,i} \right) \tag{4.4}$$

Where:

v_{avg} is the average velocity of the fluid through the control volume; and

$\dot{m}_{avg}$ is the average mass flow of the fluid through the control volume.

4.6 Component-specific model – Reservoir

4.6.1 Naming convention

Figure 4-6 illustrates the naming convention that was used.

Figure 4-6 shows a reservoir with two inlets, two outlets and a point in the centre of the reservoir. There are four boundaries over which flow takes place. Subscript 1 denotes the cold feedwater flow into the reservoir, which replaces fluid mass lost to vapour. Subscript 2 denotes water vapour flow to the atmosphere. Subscript 3 denotes flow from the reservoir into the cold leg of the NCL. Subscript 4 denotes flow coming from the NCL's top horizontal leg into the reservoir. The average fluid properties inside the reservoir did not have a specific subscript. Each of these quantities also had a common subscript, RV, which signifies a reservoir-related quantity.

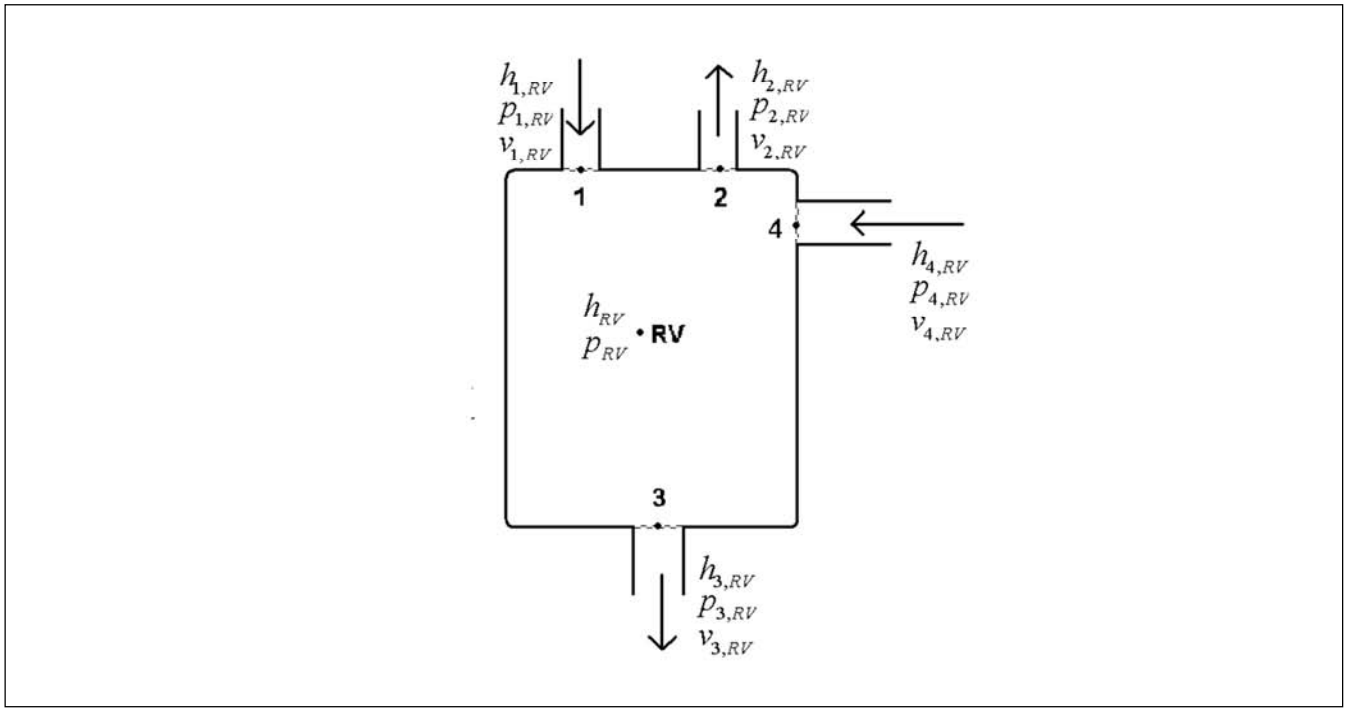


Figure 4-6. Reservoir naming convention for simulation program.

4.6.2 Discretised conservation of mass – Reservoir

Taking the naming convention into consideration, the reservoir mass conservation equation from equation (3.28) should then read as follows:

$$\sum_{i=2,3}\left(\rho_{i,RV}v_{i,RV}A_{flow}\right)-\sum_{i=1,4}\left(\rho_{i,RV}v_{i,RV}A_{flow}\right)=0 \tag{4.5}$$

Although the mass conservation equations for the reservoir are derived here, they were not used to simulate the actual flow conditions of the pipe loop. This was not necessary, as the pipe loop already had a mass conservation equation governing its mass flows. The solution of the reservoir mass conservation equation was used to test how successfully the pipe loop mass conservation was being applied by comparing it with the calculated results.

4.6.3 Discretised conservation of energy – Reservoir

By implementing the naming convention on the conservation of energy equation (equation (3.41)) and assuming that the only energy flows over the reservoir boundaries happen through the enthalpy of the fluid, the result is as follows:

$$\sum_{i=2,3}\left(h_{i,RV}\dot{m}_{i,RV}\right)-\sum_{i=1,4}\left(h_{i,RV}\dot{m}_{i,RV}\right)=0 \tag{4.6}$$

The only purpose of the reservoir in the simulation program was to provide a mixing tank for the various flows entering it and exiting from it. The reservoir equations provide three parameters that directly influence the pipe loop. Through the mass and energy conservation equations, the reservoir provides an inlet enthalpy (and thus temperature) to the water being fed into the cold leg of the loop, an inlet pressure to the cold leg and an outlet pressure to the pipe loop. As with the conservation of mass equations, the reservoir energy balance, together with the heat transferred at the cold and hot legs, was used to check the overall error in the calculated heat conservation of the simulation program.

4.7 Program code, heat transfer and other functions

This section provides a summary of all the other functions, such as heat transfer and pressure drop, that were used in the calculation of quantities used in the conservation equations. The overall structure of the simulation code is presented.

Several functions have been used in the simulation program. These include functions to calculate fluid properties, Reynolds numbers, friction factors, heat transfer, etc. These functions are summarised in the following sections, giving the reader an overview of other parts of the simulation program that supported the program code for the simulation of the conservation equations. Note that the actual program code has been rewritten for clarity here and not according to EES coding principles. The program code is attached in Appendix A.

4.7.1 Function used for fluid quality calculations

The quality of the fluid was determined using a simple straight-line interpolation equation (equation (3.10)).

Function declaration FUNCTION NAME (input parameters: fluid pressure, fluid enthalpy)

> *Determine the fluid enthalpy at the current pressure at saturated liquid conditions.*
> *Determine the fluid enthalpy at the current pressure at saturated vapour conditions.*
> *Test the function input enthalpy against the calculated fluid enthalpy of the saturated liquid and vapour phases as was calculated above.*

If the function input enthalpy is below the saturated liquid enthalpy, the function result (fluid quality) is = 0.
If the function input enthalpy is above the saturated vapour enthalpy, the function result (fluid quality) is = 1.
If the function input enthalpy is between the saturated liquid and vapour enthalpies the fluid quality is calculated according to equation (3.10).

End of function

The function name of the fluid quality function in the EES program was: FLUIDQUAL.

4.7.2 Functions used for the calculation of dimensionless numbers and two phase quantities

The dimensionless numbers play an important role in any thermal fluid related simulations or calculations. Dimensionless numbers are relatively simple to calculate, as they are mostly dependent on fluid or flow related quantities. Calculating them was simple using the appropriate correlations from equations (3.1) and (3.4) – (3.8).

Function declaration FUNCTION NAME (input parameters: as needed)

Determine the fluid properties relevant to the dimensionless number correlation.
Determine the dimensionless numbers or two phase quantity using equations (3.1) and (3.4) to (3.8).

End of function

The dimensionless numbers and two phase quantities that were used in the EES simulation program code are listed below. Function names used in the EES code are given in brackets:

a. Reynolds number (NREY);
b. Liquid Reynolds number (NREYLIQ);
c. Reynolds number ratio (FACTORF);
d. Martenelli factor (MARTENELLIF); and
e. Boiling suppression factor (SUPPF).

Note that the Prandtl number, although it is a dimensionless number, was calculated using another function, thus it is not listed here.

4.7.3 Functions used for fluid property calculations

The fluid property calculations used a simple interpolation function (equation (3.10)) to determine the value of any fluid property between the saturated liquid and vapour points. The generic way of writing a property function was as follows:

Function declaration FUNCTION NAME (input parameters: fluid pressure, fluid enthalpy)

> *Determine the fluid quality using the fluid quality function with the current function's input parameters.*
>
> *Use the fluid quality to determine if the fluid is in a liquid, saturated or vapour phase.*
>
> > *If the fluid's quality is equal to 0, it is a liquid, thus determine the fluid property using EES internal functions with the current function's input values of enthalpy and pressure.*
> > *If the fluid's quality is equal to 1, it is a vapour, thus determine the fluid property using EES internal functions with the current function's input values of enthalpy and pressure.*
> > *If the fluid's quality is between 0 and 1, it is a two phase mixture, thus determine the fluid property using the calculated fluid properties at qualities of 0 and 1, and interpolating between these points using equation (3.10).*

End of function

The above form was used as a generic framework for functions calculating fluid properties. The following fluid property functions were used. The actual function names used in the program code are shown in brackets:

a. Fluid density (FLUIDDENS);
b. Fluid viscosity (FLVISCO);
c. Fluid conductivity (FLCOND);
d. Fluid heat capacity or specific heat (FLHCAP); and
e. Fluid Prandtl Number (NPRND).

4.7.4 Functions used for reservoir-related quantities

The NCL was set up so that the reservoir could provide water to the cold leg and receive water from the hot leg. It also acted as a liquid-vapour separator and a receiver for cold feedwater. To determine the enthalpy of the water to the cold leg, the following function was used (from equation (4.6)):

Function declaration FUNCTION NAME (input parameters: fluid pressure, fluid enthalpy)

> *Determine the fluid quality using the fluid quality function with the current function's input parameters.*
>
> *Use the fluid quality to determine if the fluid is in a liquid, saturated or vapour phase.*
>
> > *If the fluid quality entering the reservoir from the hot leg is equal to 0, the fluid entering the reservoir is a liquid, thus no vapour is vented to the atmosphere and no feedwater is added, thus the reservoir enthalpy is equal to the enthalpy of the fluid entering the reservoir from the hot leg.*
> >
> > *If the fluid quality entering the reservoir from the hot leg is equal to 1, the fluid entering the reservoir is a vapour and all vapour is vented to the atmosphere, thus the reservoir enthalpy is equal to the enthalpy of the feedwater entering the reservoir.*
> >
> > *If the fluid quality entering the reservoir from the hot leg is between 0 and 1, the fluid entering the reservoir is a two phase mixture, thus some feedwater is added to compensate for the mass loss through vapour being vented to the atmosphere, thus the reservoir enthalpy is calculated from an energy balance from equation (4.6).*

End of function

The name of the function used to calculate the enthalpy of the water leaving the reservoir to the cold leg of the pipe loop in the EES program code was RVENTHALPY.

4.7.5 Functions used for frictional pressure drop calculations

Pressure drop was calculated both in the main program and in the functions. Static pressure drop and secondary pressure losses were calculated in the main program. The simplicity of these functions made them easy to implement and adding functions for these pressure drop quantities would have been unnecessary (see equation (3.59) and the last term of equation (4.3)). For frictional pressure drop, two functions were used. One function determined the friction factor, while the other determined the frictional

pressure drop using the friction factor. The friction factor was calculated in a separate function, since it was used in some of the heat transfer calculations as well. Equations (3.58) to (3.61) and equations (3.64) to (3.66) were used in the implementation of the friction factor.

The frictional pressure drop was calculated with the following function, using equation (3.58):

Function declaration FUNCTION NAME (input parameters: fluid pressure, fluid enthalpy, fluid velocity, pipe diameter, pipe wall roughness, pipe control volume length)

> *Determine the fluid density using fluid density function.*
> *Determine the friction factor using friction factor function.*
> *Determine the frictional pressure drop across the given pipe increment length using equation (3.58).*

End of function

The friction factor was determined by the following function:

Function declaration FUNCTION NAME (input parameters: fluid pressure, fluid enthalpy, fluid velocity, pipe diameter, pipe roughness)

> *Determine the fluid quality using the fluid quality function with the current function's input parameters.*
> *Determine the Reynolds number using the Reynolds number function.*
>
> *Use the fluid quality to determine if the fluid is in liquid, saturated or vapour phase.*
>
> > *If the fluid quality was equal to 0 or 1 and the calculated Reynolds number was below 64, flow was laminar single phase flow and equation (3.60) was used.*
> > *If the fluid quality was equal to 0 or 1 and the calculated Reynolds number was above 4 000, flow was turbulent single phase flow and equation (3.61) was used.*
> > *If the fluid quality was equal to 0 or 1 and the calculated Reynolds number was between 64 and 4 000, flow was in a transition regime and equations (3.60), (3.61) and (3.64) were used.*
> > *If the fluid quality was between 0 and 1 and the calculated Reynolds number was below 11, equation (3.60) was used.*
> > *If the fluid quality was between 0 and 1 and the calculated Reynolds number was above 11, equation (3.65) was used.*

End of function

The functions used for determining the friction factor and frictional pressure drop were named FRICFAC and DELTAPFRIC respectively in the EES program code.

4.7.6 Functions used in the calculation of heat transfer

The calculation of heat transfer was one of the major objectives of this simulation. The heat transfer function had to accommodate different heat transfer modes. These modes were laminar, transition zone and turbulent single phase heat transfer as well as subcooled boiling and two phase heat transfer. Due to the number of heat transfer modes the calculation of heat transfer was divided across several functions. A main function was used to determine the heat transfer mode. Depending on the mode of heat transfer this function calls another function to calculate the heat transfer of that particular mode. A separate, but almost identical function was used to determine the particular mode of heat transfer, either single phase, subcooled boiling or two phase heat transfer for the purpose of showing it in the program results.

The following function was called from the main program to determine the heat transfer value. The function that determined the heat transfer mode is almost identical to the main function and will therefore not be repeated here. Equations (3.42), (3.43), (3.45), (3.48) and (3.50) to (3.57) were used in the implementation of the heat transfer calculations.

Procedure declaration FUNCTION NAME (input parameters: fluid pressure, fluid enthalpy, fluid velocity, pipe wall temperature, pipe control volume length, pipe diameter, pipe wall roughness)

Determine the various required fluid properties.

Determine if the fluid quality is between 0 and 1

If the fluid quality is equal to 0, the next step of calculations is implemented.
If the fluid quality is equal to 1, the single phase heat transfer function is called, as it is superheated vapour heat transfer.
If the fluid quality is between 0 and 1, the two phase heat transfer function is called.

Further calculation steps are carried out when fluid quality is equal to 0. This is done to distinguish between normal subcooled and subcooled boiling heat transfer:

Determine the two factors for testing of the presence of subcooled boiling, based on the criteria from equations (3.54) to (3.57).

If the criterion for the presence of subcooled boiling is met, the subcooled boiling heat transfer function is called.
If the criterion for the presence of subcooled boiling is not met, the normal subcooled heat transfer function is called.

Based on the function that was called, the calculated heat transfer value is returned to the main program from the procedure.

End of function

The heat transfer functions have many fluid properties and quantities to eventually calculate the required heat transfer value. Generically, they are quite simple to implement if the required heat transfer correlation is known:

Function declaration FUNCTION NAME (input parameters: fluid pressure, fluid enthalpy, fluid velocity, pipe wall temperature, pipe control volume length, pipe diameter, pipe wall roughness)

Determine the fluid properties and quantities.
Based on the appropriate correlation (equations (3.45), (3.48) and (3.50) to (3.53)), determine the heat transfer coefficient.
(Single phase heat transfer implemented a laminar and turbulent correlation with linear interpolation between Reynolds numbers of 1 000 and 3 000).
Calculate the heat transfer rate.

End of function

The above function form was used as a generic framework for the functions that were used to calculate the heat transfer, which was dependant on the mode of heat transfer. The following procedure and functions were used in the EES program code. Actual names are shown in brackets:

a. Main heat transfer function (HEATTRANS);
b. Heat transfer mode (HEATMODE);
c. Single phase heat transfer (ONEPHASEHEAT);
d. Subcooled boiling heat transfer (SUBCOOLHEAT); and
e. Two phase heat transfer (TWOPHASEHEAT).

4.7.7 Calculated parameters used to calculate overall loop performance

Several parameters are calculated to serve as an indication of the performance of the loop's efficiency in removing heat from a containment building. As previously stated, a global mass and energy balance was also done to check the degree of mass and energy conservation. These could be called "error values". A small error would indicate that the conservation of mass or energy is good and vice versa.

The total heat transfer along the cold or hot legs was calculated by adding up the heat transfer of each increment to a sum total. In the EES program code, these variables were named *Heat_absorbed* and *Heat_removed* for the hot and cold leg respectively.

At the reservoir, the heat lost from the NCL due to the vapour being vented to the atmosphere and the heat being added through the feedwater were named *Heat_vap* and *Heat_feedwater* respectively in the EES program code.

The degree to which mass was conserved, was tested by taking the total of the fluid mass flows from the reservoir and subtracting the total of the fluid mass flows into the reservoir. The result of this calculation was used as a value to indicate the error in the conservation of mass for the loop. Another mass balance was done on the feedwater inflow and vapour outflow. The conservation of energy error was calculated in a similar way. Ideally the error value should be zero, but the acceptable values for errors were deemed to be orders of magnitudes less than the relevant calculated results. Variables used in the EES program for the calculated error quantities were *Mass_Error* and *Mass_Error2* for conservation of mass. For the conservation of energy, the variables *Heat_Error* and *Heat_Error2* were used for error calculations.

4.7.8 Simulation program input parameters and boundary values

The simulation program had several input parameters and boundary values. There were quite a large number of these. They are listed in Table 4 and Table 5, together with a short description and the variable name that was used in the actual simulation program. Table 4 shows variables that had fixed values throughout the various simulation runs, while Table 5 shows variables that were modified using a parametric table during the various simulation runs. Each table has a column showing the value of a fixed variable or the range in which it was varied where applicable. Otherwise, when the variable is the result of some calculation, its value is omitted. Where applicable the units of the variables are shown in the last column of Tables 4 and 5.

Where applicable, the symbols ### are used when the variables indicate a similar quantity, except for identifiers at the end of the variable name. For example, counters n_cum1 and n_cum2 were denoted as n_cum###.

Table 4. Description of the fixed variables used in the simulation program code.

Variable name	Variable description	Value
rad_pipe	Radius of the NCL loop pipes	- [m]
area_pipe	Area of the NCL loop pipes	- [m]
circum_pipe	Circumference of the NCL loop pipes	- [m]
epsilon_pipe	Pipe wall roughness	$4.5x10^{-5}$ [m]
height_RV	Height of the reservoir	0.5 [m]
width_RV	Width of the reservoir	0.5 [m]
depth_RV	Depth of the reservoir	0.5 [m]
Vol_RV	Volume of the reservoir	- [m^3]
P_atm	Atmospheric pressure	$100x10^3$ [Pa]
T_RV_FW	Feedwater temperature	293 [K] or 20 [ºC]
K_loss_ELB	Secondary loss coefficient, pipe bends	0.3 [-]
K_loss_ex	Secondary loss coefficient, inlet from pipe loop to reservoir	1 [-]
K_loss_in	Secondary loss coefficient, outlet from reservoir to pipe loop	0.12 [-]
n_###	Number of control volumes in the cold leg, bottom horizontal, hot leg, top horizontal leg, elbows and in total	Cold leg: 20 Bottom horizontal: 5 Hot leg: 190 Top horizontal: 10 Elbows: 1
n_size_###	Size of control volumes in the cold leg, bottom horizontal, hot leg, top horizontal and elbows	- [m]
num_elbows	Number of elbows in the NCL	3
n_cum###	The accumulative number of control volumes working from the reservoir through to the cold leg and around the loop	-
grav	A global constant, the gravitational acceleration	9.80665 [$m.s^{-2}$]
P###	Fluid pressure	- [Pa]
he###	Fluid enthalpy	- [$J.kg^{-1}$]
rho###	Fluid density	- [$kg.m^{-3}$]
vel###	Fluid velocity	- [$kg.m^{-3}$]
m_dot###	Mass flow	- [$kg.s^{-1}$]
mass_q###	Fluid quality	-
s_cvbound	The length along the flattened pipe loop	- [m]
s_cvcentre	The centre of each control volume along the flattened loop	- [m]

Variable name	Variable description	Value
DELTA_P_fric	Primary pressure losses between control volume boundaries	- [Pa]
DELTA_P_acc	Secondary pressure losses between control volume boundaries	- [Pa]
DELTA_P_static	Static pressure losses between control volume boundaries	- [Pa]
DELTA_H_KIN	Change in kinetic energy between control volume boundaries	- [W]
DELTA_H_HEAT	Heat transfer to control volume between control volume boundaries	- [W]
DELTA_H_POT	Change in potential energy between control volume boundaries	- [W]
Heat_Transmode	Mode of heat transfer in the control volume.	-
T_fluid	Fluid temperature	- [K]
T_wall	Pipe wall temperature	- [K]

Table 5. Description of the variables used in the simulation program code that will be varied parametrically.

Variable name	Variable description	Range of values
height_NCL	Height of the NCL loop	5-30 [m]
Width_NCL	Width of the NCL loop	1-5 [m]
diam_pipe	Diameter of the NCL loop pipes	0.0125 – 0.075 [m]
T_enviro	Cold leg pipe wall temperature	278 – 313 [K] or 5 - 40 [ºC]
T_contain	Hot leg pipe wall temperature	328 - 413 [K] or 55 - 140 [ºC]

4.7.9 Loop pipes simulation code

As was stated earlier in this chapter, each section of the pipe loop had a block of code in which it was modelled. The section was discretised according to the input parameters specified in the program. This divided each section into a number of control volumes, which were strung together. The conservation and other equations for each section are written for each control volume in each section. The EES software then solves the equation set simultaneously. The generic form of the code was implemented as shown below. It used the conservation equations (equations (4.2) to (4.4)). Note that this is a generic form of the program code. Small differences exist between individual blocks of code for each pipe section:

Start of the program loop for the current NCL subcomponent.

Spatial parameters

Set the inlet boundary position of the current control volume equal to the previous control volume's outlet boundary position.
Set the outlet boundary position of the current control volume equal to the inlet boundary position plus the size (or length) of the current control volume.

Coupling of fluid parameters to previous control volume

Set the inlet velocity of the current control volume equal to the outlet velocity of the previous control volume.
Set the inlet pressure of the current control volume equal to the outlet velocity of the previous control volume.
Set the inlet enthalpy of the current control volume equal to the outlet velocity of the previous control volume.

Mass conservation

Implement conservation of mass from equation (4.2) for the current control volume.

Momentum conservation

Call frictional pressure drop function for the current control volume.
Use equation (3.59) to determine the secondary pressure drop of the control volume.
Determine the change in dynamic pressure over the control volume using the third term from equation (4.3).
Determine the static pressure loss using the last term of the conservation of momentum (equation (4.3)).
Implement the conservation of momentum from equation (4.3) using the four quantities calculated above.

Energy conservation

Calculate the change in kinetic energy over the control volume using the appropriate term from equation (4.4).

Calculate the change in potential energy over the control volume using the appropriate term from equation (4.4).
Call the function for the calculation of heat transfer and the determination of heat transfer mode.
Implement the conservation of energy from equation (4.4) using the three calculated quantities above.

Determine the required fluid properties.
Determine the required average properties over control volume.
Determine other fluid parameters not used in the conservation equations, but which are used for information purposes: Fluid quality, fluid temperature, mass flow and the mode of heat transfer taking place.
Set the wall temperature equal to either the containment or environmental temperature.

End of the program loop, repeat for entire the NCL subcomponent

4.8 Conclusion of simulation program description

In this chapter, the simulation program was explained, as was the way in which the simulation process was executed. The naming convention that was used and the variables of the simulation program were listed and explained and the various functions and blocks of code in the simulation program were generically described.

In the next chapter the simulation program results are validated against published experimental results. The heat transfer and pressure drop functions are verified against their original sources in literature. A grid independence study to ensure that the solution was independent of the grid size is also discussed.

Chapter 5 - Simulation model validation and verification

This chapter presents the validation, verification and grid independence study of the simulation code.

Firstly, a grid independence study is discussed. This is followed by a presentation of the validation of the simulation program. Finally, the heat transfer and pressure drop functions used in the simulation program are verified against their respective sources in the published literature to ensure that no errors could have crept in during their implementation in the EES simulation program.

5.1 Grid-size independence check

Any discretised or grid-based simulation model must be checked for grid-independence. This ensures that the solution of the program is independent of the size of the grid. In other words, the grid or size of control volumes must be small enough for the solution results not to be affected significantly if the grid size is reduced.

For this investigation, the NCL was divided into seven different regions, which were discretised separately. Of these seven, there were three elbow components, which had only one control volume. Of the remaining four, each discretised component was simulated a number of times with different grid sizes. The change in key variables was then compared for each case. The chosen key variables for this grid independence study were pressure drop across the component, velocities and where applicable, heat transfer. Due to the dependence of the variables on each other, a typical grid test had a specified pressure drop and the velocities and heat transfer values were then noted and compared. Each component was modelled separately, in other words, in isolation so that the input and output parameters could be fixed to obtain a consistent result. If the components were simulated while being part of the loop, the solution might change due to other factors that affect the flow parameters in other areas of the pipe loop.

Table 6 lists the four components, the range of the control volume numbers per component that were tested and the number of control volumes that were used in the final simulation program. It was sometimes necessary to optimise the number of control volumes per component due to the limitation on the number of variables in the EES software program that was used. Thus, the fourth column contains a percentage value, which indicates the difference between the results calculated with the highest number of control volumes, in comparison to the number of control volumes that were chosen. Thus, a figure of 80% would indicate that while the specific component was tested with a number of different control

volume sizes, the one that was chosen returned a key variable value that was 80% of that obtained with the smallest grid size. If two variables were tested the largest deviation of the two was given in the table. This table gives the reader an idea of the degree of grid independence of the simulation program.

Table 6. Grid independence: Range of tested control volume counts, choice and deviations from the smallest control volume size that was tested.

Component	Number of control volumes tested	Chosen number of control values for the simulation program	Chosen number of control volume results: Percentage of value from the value of the finest discretisation [%]
Cold leg	5–30	20	99.96
Bottom horizontal leg	3–30	5	100.00
Hot leg	20–300	190	99.71
Top horizontal leg	5–50	10	100.00

During the grid independence study, the simulation program input parameters were set so that a reasonably difficult scenario could be simulated. This ensured that the grid independence study was not only valid for a single easy case. Then, the grid sizes were decreased until the total number of variables were close to the limit set by the EES software. This provided additional confidence in the grid independence of the simulation program. The final simulation program that was used to generate the results discussed in the next chapter used 5 963 variables.

In the next section, the validation process of the simulation program results is presented against published results in a source of literature.

5.2 Kyung and Lee study – Experimental facility

According to Oosthuizen (2003), many researchers used the experimental data of Kyun and Lee (1996) to validate their models. Thus it was decided that the current investigation's simulation program would also be validated against their study.

Kyung and Lee (1996) studied flow excursion instability in a closed two phase NCL. They first predicted experimental results using a simulation model. They then used an experimental setup to generate results for comparison.

The experimental facility of Kyung and Lee (1996) is shown in Figure 5-1. The figure shows dimensions, pipe diameter, condenser diameter and other geometry features. The facility consisted mainly of a condenser reservoir, a heater and connecting pipes. The whole experimental setup was filled with Freon-113. The condenser used a cooling coil inside a larger shell. The Freon level of the condenser shell was kept constant during the experiments. The condenser pressure was maintained at atmospheric pressure, even though it was a closed system. The heater was a pipe section which was uniformly heated by a coiled wire powered from an electric source. The maximum heating input that could be achieved by the heater was 50 $kW.m^{-2}$.

Two valves, one before the heater and one after the heater, were used to provide some restriction to the fluid flow, as was required. The valves were tested beforehand to correlate the degree of valve closure with a certain loss coefficient. The loss coefficients were defined in a similar equality to that of equation (3.60). Thus these secondary loss coefficients could be used directly in the equations of the current simulation program. The circulation rates were measured using a sharp-edged orifice with a 0.009 m hole. By measuring the pressure drop across the orifice the flow rate could be determined. Void fractions in the riser section were determined by measuring the hydrostatic pressure difference and comparing it to that expected of the fluid in liquid form. For the void fraction determination, the tube wall friction was assumed to be negligible. The working fluid temperature at the condenser outlet was controlled at a specific value by adjusting the coolant flow through the coiled cooling pipe inside the condenser volume.

The experimental loop had five main points of interest as far as the fluid conditions were concerned:

a. Subcooled coolant, in other words, liquid, flowed from the condenser into the downcomer of the NCL (Figure 5-1, a). The fluid then flowed through two bends in the pipe and then through an inlet valve with pressure loss coefficient K_{in}. It then flowed through a T-piece in the pipe, one end of which was closed. From there the fluid flowed through the orifice flow meter with loss coefficient K_{orf} and from there the fluid flowed to the inlet of the heating section.
b. The heating of the fluid started while the fluid was still a single phase liquid (Figure 5-1, b) and continued until the fluid boiled (Figure 5-1, c).
c. At a certain point the fluid was not heated anymore (Figure 5-1, d) and the flow continued through a riser section, where the void fraction measurements were done.
d. The fluid then flowed through a horizontal section with an exit valve with loss coefficient K_{ex}. It was then routed to the free surface of the condenser which was maintained at atmospheric pressure (Figure 5-1, e). However, it must be noted that since the working fluid was Freon-113, the condenser was not open to the atmosphere to prevent evaporation of the fluid.

The loop pipe diameter was 0.0166 m. Heights were measured from the centreline of the top horizontal pipe of the experimental setup. The tubes and fittings were made of copper and brass respectively. The condenser and riser sections were made of Pyrex tubes. During the experiments the sum of the pressure loss coefficients across the entire loop, including the orifice flow meter, valves and pipe bends, were measured to have a total value of 40.0. The total loss coefficient due to all the bends in the loop was measured to be 4.0. The orifice flow meter alone had a measured loss coefficient of 30.0. These values were measured from the experimental setup during initial trial runs.

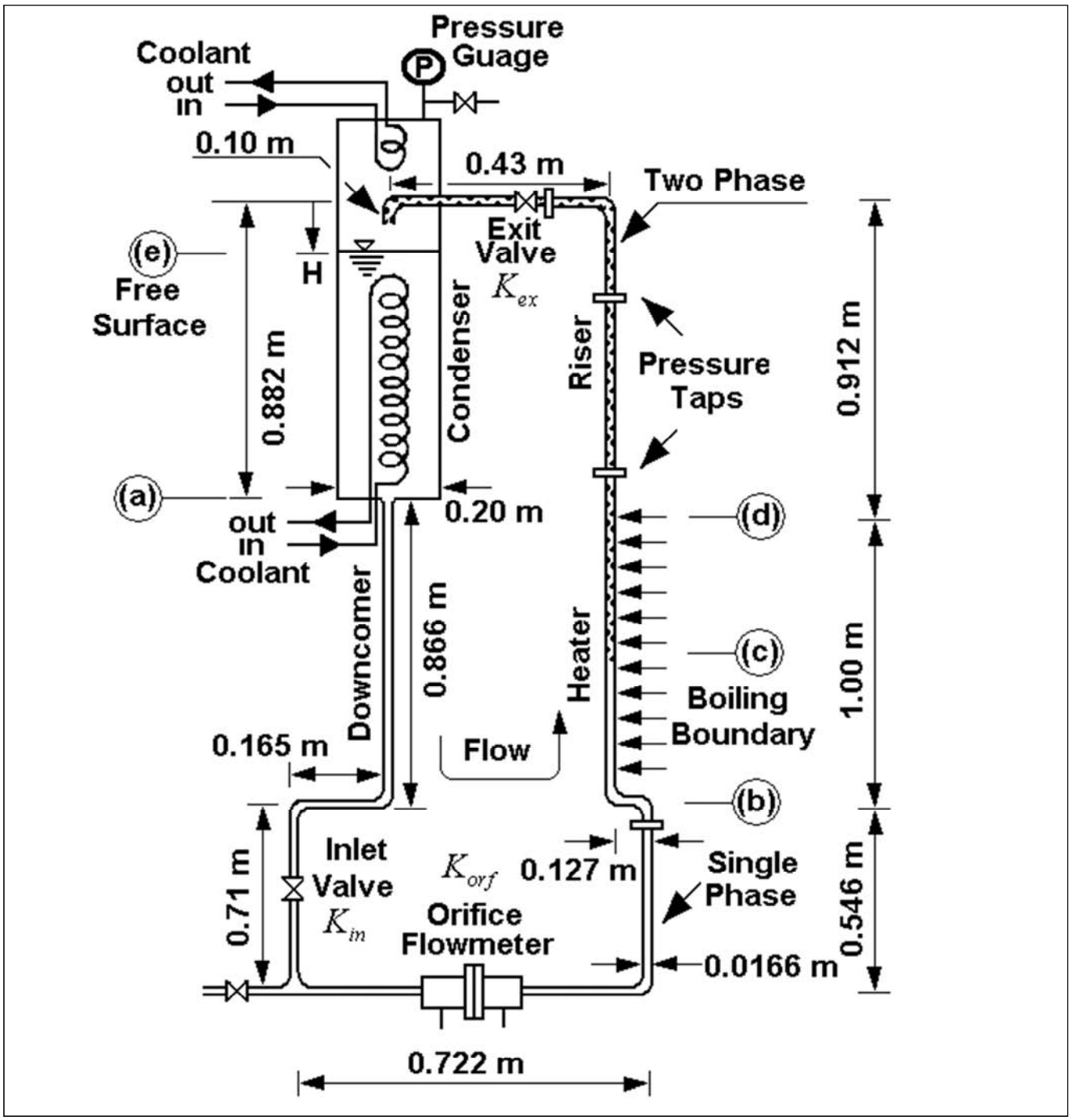


Figure 5-1. Experimental setup of Kyung and Lee.

The experimental results obtained were compared with the results of a calculation study done previously by Kyung and Lee (1996). These experimental and calculation results were then plotted on a graph, comparing the variation of heater inlet velocity against the heater flux value. The current investigation's simulation program was adapted for the experimental setup and used to predict results. The results obtained from the adapted simulation program were then compared to those of Kyung and Lee (1996).

5.3 Validation program preparation and adaption

In order to produce results that can be compared to those of Kyung and Lee (1996) the current investigation's simulation program had to be adapted to suit the experimental setup. The adaption was done without any modification to the correlations, functions or simulation methodology. Since the experimental setup of Kyung and Lee (1996) and the current study's NCL had similar geometry, the validation will provide confidence in the results obtained from the simulation program for the NCL loop in the context of the current investigation.

In order to adapt the simulation program, the differences between the experimental setup and the NCL, which was the subject of the current study, were identified. The differences between the current study's simulation model and the same model, which was adapted for use in the validation process, were as follows:

a. A heat flux value was specified at the heated pipe section, instead of being calculated as a result of an imposed temperature.
b. There were additional loss-inducing components in the loop: Extra pipe bends, valves and a flow meter.
c. There was no cooling section in the downcomer and a condenser was used instead of the cooling section in the cold leg, which had an imposed temperature on its pipe walls.
d. Freon-113 was used instead of water as a working fluid.

The simulation program was adapted with the minimum of changes. Table 7 lists all the relevant inputs to the adapted simulation model, which could be obtained from the description in the published article. Some of the inputs were assumed to be based on the indirect description of Kyung and Lee (1996), while others were taken directly from the published article. The Kyung and Lee study (1996) did not indicate what value for the pipe wall friction factor was assumed to be or used for the calculation results. Tabled values from Cengel and Turner (2005:625) were used to choose the said roughness factor based on the pipe material used in the experimental setup. Note that the smooth wall roughness values for the

Pyrex glass was zero, Kyung and Lee (1996) assumed that there was no frictional pressure drop in the riser section.

Figure 5-2 gives a graphic representation of the loop that was simulated to obtain the results used in the validation. A constant level reservoir that was open to the atmosphere was used and the outlet from the loop was dumped. This arrangement was so that the reservoir and pipe exit could have individual boundary conditions specified. It would not have been feasible to try and implement the closed reservoir system of the experimental setup. This setup was acceptable since there was no need to prevent the Freon from evaporating in the simulation program, as was required for the experimental setup.

Table 7. Experimental setup and other input parameters to the validation model.

Variables	Value(s) in study
Pipe loop diameter	0.0166 [m]
Flow meter orifice loss coefficient K_{orf}	30.0 [-]
Secondary losses of pipe bends	0.3 [-] per bend with eight in total
Inlet valve loss coefficient K_{in}	7.7, 134 [-]
Outlet valve loss coefficient K_{ex}	41 [-]
Loop inlet (or condenser outlet) degree of subcooling	5, 20, 35 [-]
Heat Flux on the heated section	0 - 45000 [$W.m^{-2}$]
Pipe wall roughness for tubes and riser sections	Copper tubes: 1.5 x 10^{-6} [m] Pyrex riser section (smooth): 0.0 x 10^{-6} [m]
Reference height of condenser water level	0.150 [m]
Height of water level from bottom of condenser section	0.782 [m]
Height of downcomer down to the bottom-most horizontal section	1.576 [m]
Total length of the lower horizontal sections before heater section	1.014 [m]
Total length of the vertical sections before the heater inlet where the flow is upward	0.546 [m]
Total length of heated section	1.000 [m]
Total vertical length of the riser section after the heater outlet to the top horizontal section	0.912 [m]
Total length of the top horizontal section	0.430 [m]
Total length of the downward pipe in the condenser	0.100 [m]

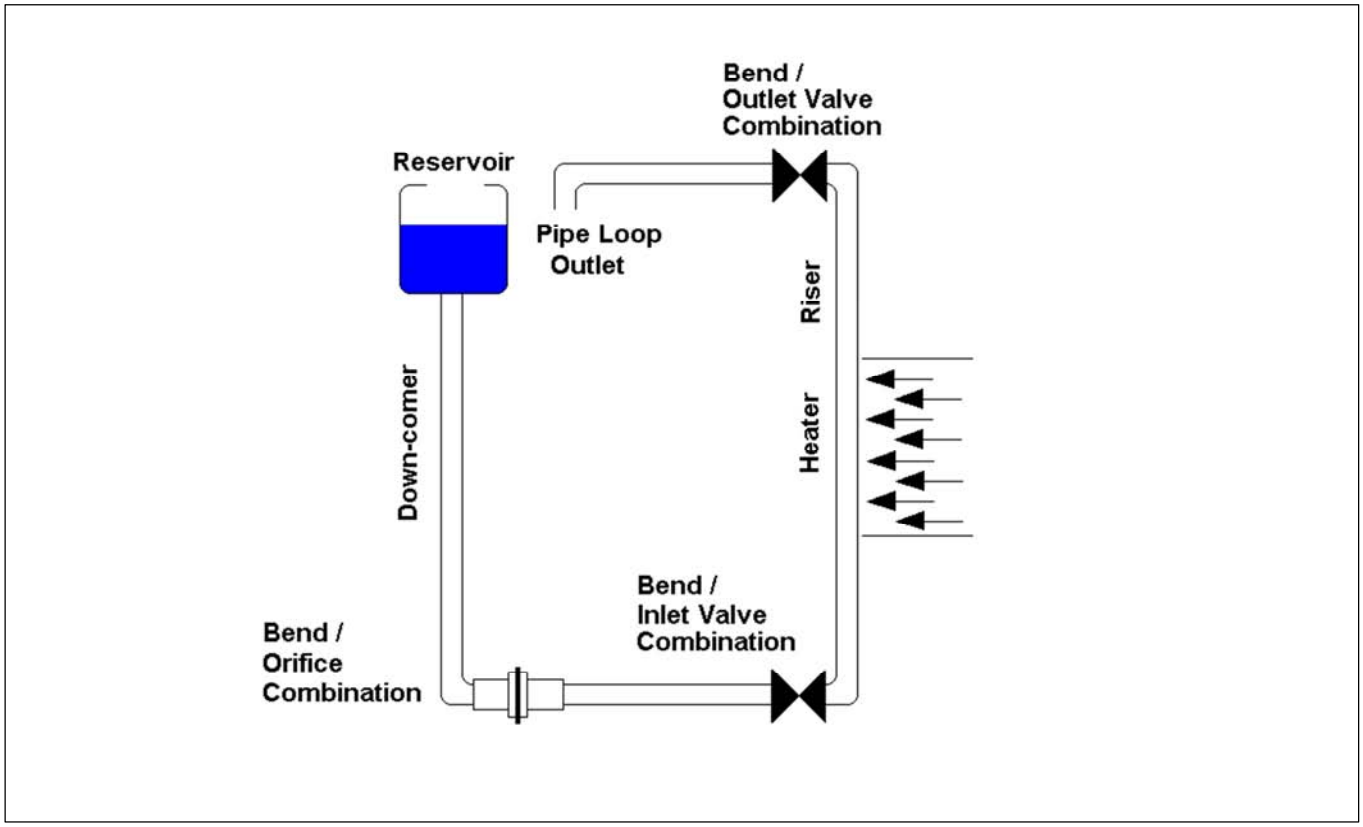


Figure 5-2. Representation of the adapted simulation model.

The inlet and outlet valve loss coefficients were combined with their closest bend fitting. The orifice was combined with the other remaining bottom pipe elbow. This had to be done as the current investigation's simulation program did not allow the use of secondary loss coefficients in straight discretised pipe sections. The secondary loss coefficients listed in Table 7 were used. Lengths and other input values were combined where necessary and used in the specification of the physical size loop parameters. Overall, the simulation was deemed to be a good representation of the experimental setup.

In the next section, the calculated and experimental results of Kyung and Lee (1996) and the adapted simulation program results will be discussed.

5.4 Comparison between Kyung and Lee results and adapted simulation program results

Kyung and Lee (1996) reported different sets of results. Of relevance here are only the steady state results. The steady state results were presented in a graph as the variation of heater inlet velocity as a function of heat flux. This was done at various levels of subcooling at the condenser outlet to the downcomer.

The adapted simulation model was used to simulate the experimental setup. Graphs were drawn up for three sets of results. These are shown in Figure 5-3, Figure 5-4 and Figure 5-5. The three graphs each contain three sets of data:

a. Experimental results from the Kyung and Lee (1996) study;
b. Calculation results from the Kyung and Lee (1996) study; and
c. Calculation results of the adapted simulation model (these results were added to the graphs obtained from Kyung and Lee (1996)).

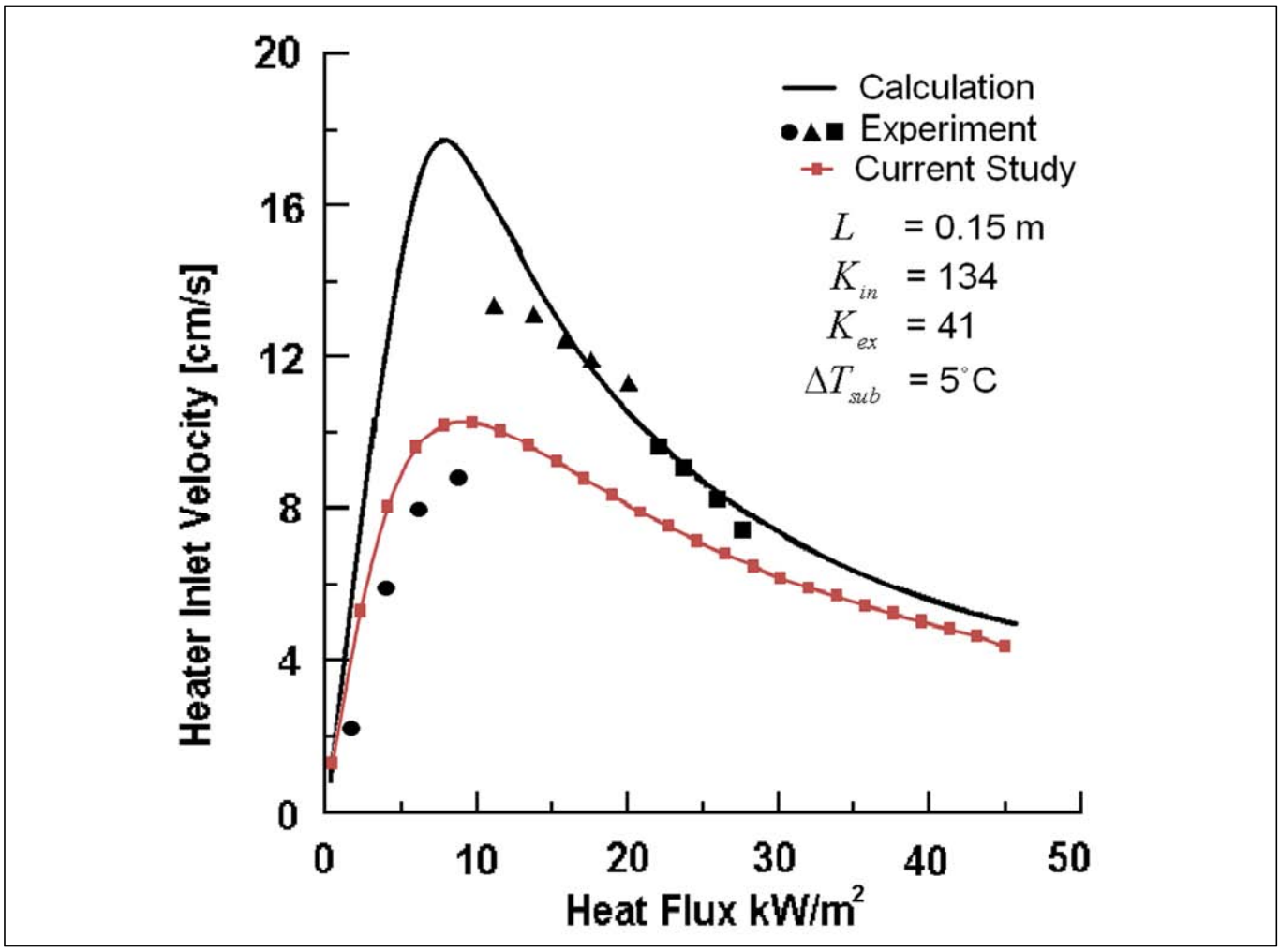


Figure 5-3. Graph of the change of heater inlet velocity as a result of the variation in heating flux (The first set of results from the current study overlaid on the graph of Kyung and Lee (1996)).

Figure 5-3 shows that the adapted simulation model predicted the experimental results quite well. From the lowest value of the heat flux on the graph, it tends to slightly overpredict the experimental results. From roughly 10 kW.m^{-2} the balance shifts and the adapted simulation model predicted a lower value than the experimental values. The calculation results from Kyung and Lee (1996) predicted the experimental results well, but at higher heat fluxes a much larger jump in the heater inlet velocity was

predicted than actually happened in the experimental setup. In general, the adapted simulation model followed the trend of the experimental results quite well. When compared with the experimental and calculation results of the reference study, the current adapted simulation model provided a good approximation. The calculated results fell within 34 % of the experimental results over the measured range of heat fluxes.

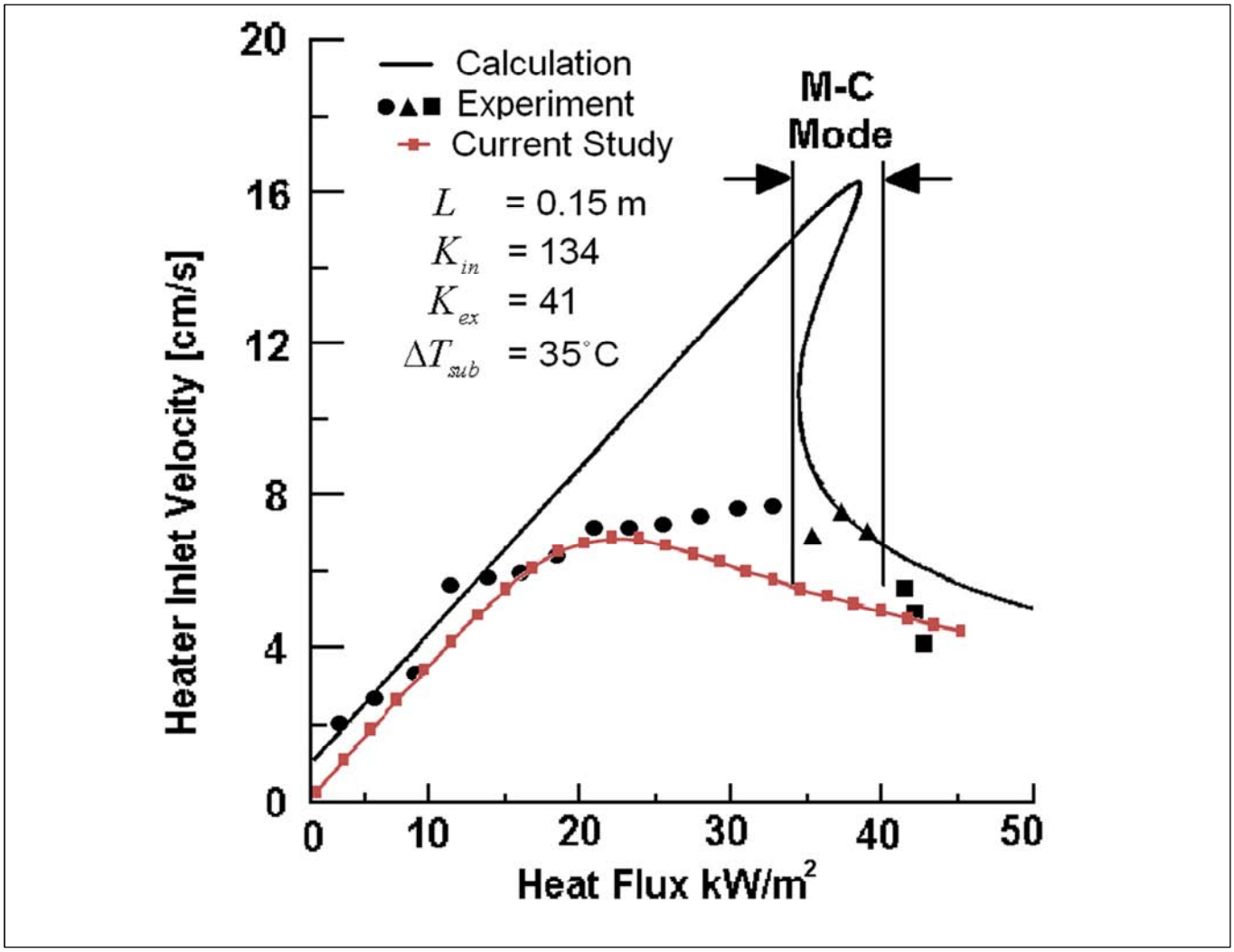


Figure 5-4. Graph of the change of heater inlet velocity as a result of the variation in heating flux (The second set of results from the current study overlaid on the graph of Kyung and Lee (1996)).

The same can be said of the results plotted on the next graph (Figure 5-4). Due to the higher degree of subcooling at the condenser outlet to the loop, the sudden jump in heater inlet velocity is not as large. The current study's results predict this high subcooling case well up to a heater power of 25 kW.m^{-2}. The results started to deviate from that point onward, but still fell within an acceptable range of 30 % from the experimental results. The current study's calculation model provides a better trending of the experimental results compared to those of Kyung and Lee (1996) at certain heat flux values. The

reference study calculation predicted an unstable zone of multiple modes of circulation (indicated as M-C mode in the figures) with multiple circulation modes, which the adapted simulation model did not show.

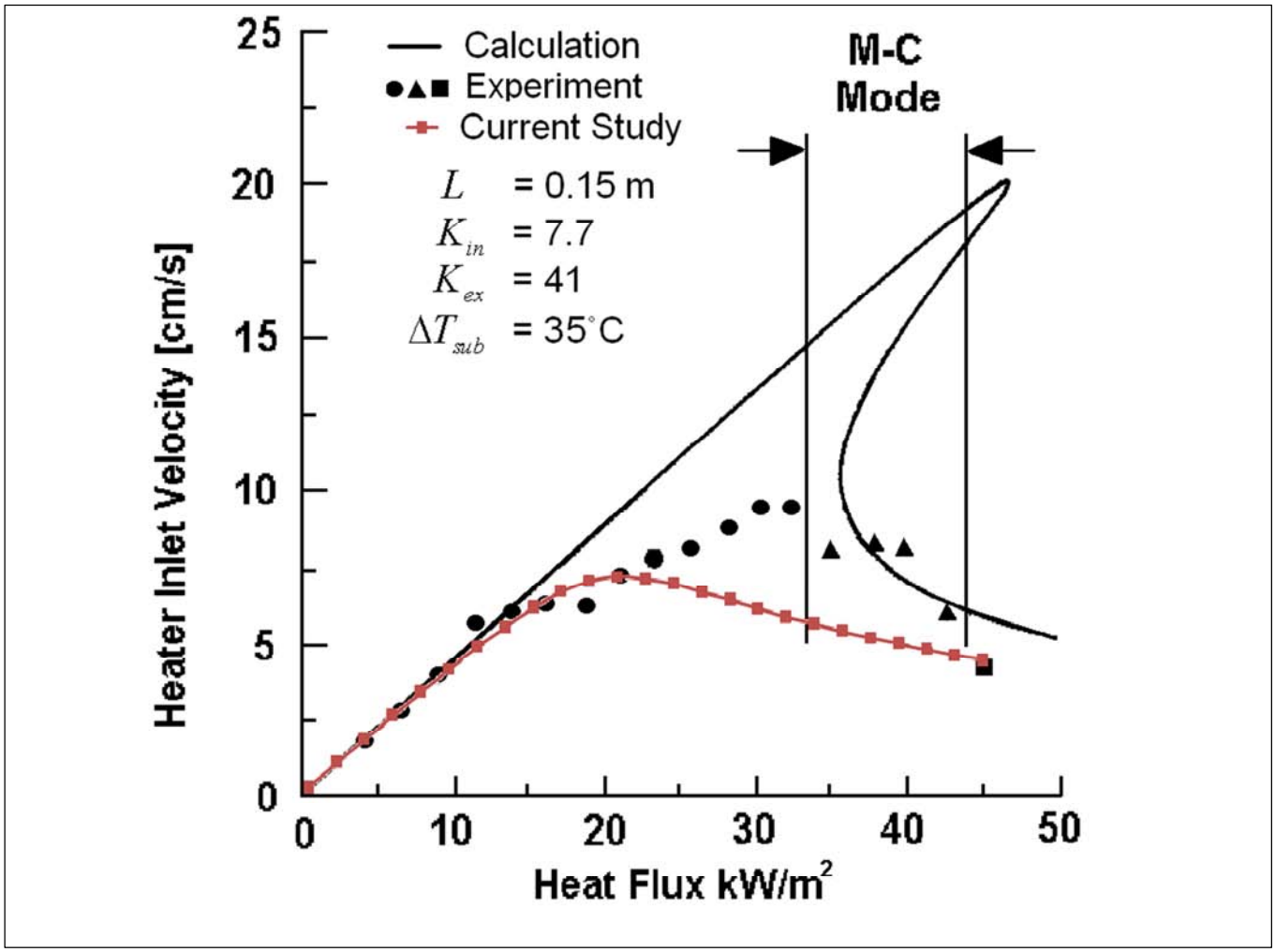


Figure 5-5. Graph of the change of heater inlet velocity as a result of the variation in heating flux (The third set of results from the current study overlaid on the graph of Kyung and Lee (1996)).

Figure 5-5 shows the experimental setup with a smaller inlet valve loss. Again, the same comments made on the graph of the previous results apply. The current study's calculated results fell within 38 % of the experimental results which, again, is acceptable.

The deviation of the current study's results compared to the experimental results of Kyung and Lee (1996) at higher heat fluxes may be due to the simple homogenous model that was used in the simulation program. The difference between the current study's results and the calculated results of Kyung and Lee (1996) might be due to some theoretical assumptions or detail differences. The calculated results of Kyung and Lee (1996) were based on a homogenous model, the same as the current study, but using a two phase friction modifier for pressure drop calculations. This could be one of the many factors that may influence a simulation model's results.

Despite the deviation in the adapted simulation model's calculated results at higher heater powers the calculated results are conservative, follow the right trend and were obtained using a simple homogenous modelling approach. This is in keeping with the purpose of this study, which does not attempt to replicate exact experimental results or use complicated models, but to provide a simple model for the evaluation of the NCL as a containment cooling mechanism. The simulation model that was part of the current investigation was deemed acceptable for use.

In the above comparison, the specified heat flux parameter allowed the variation of heat input to the loop to be set, instead of being calculated by correlations. Thus, the loop conservation equations and overall accuracy was validated. It was quite difficult to validate the complete model due to the difficulty of obtaining suitable published results. In particular, steady state experiments on NCLs are difficult to find, as many studies concentrate on the instability phenomena associated with these NCLs. Due to the use of a fixed heat flux in the study, the validation excluded the heat transfer correlations. The next section will focus on the verification of the friction factor and heat transfer functions used in the simulation program, since these functions and their individual results have a large influence on the model's results.

5.5 Heat transfer and frictional pressure drop function verification

The heat transfer and frictional pressure drop function of the simulation program are arguably the most influential functions used in the simulation program. In the previous section, the current investigation's simulation program was validated, with the exception of the heat transfer function. The heat transfer function was not used due to the heat flux on the heater sections of the pipe loop being specified. Thus, it was decided that the programmed friction factor and the heat transfer function should be verified against a manual calculation and their original literature source. These functions were based on correlations. Their results are therefore not as dependent on the rest of the simulation program as, for example, the conservation equations.

Each correlation and condition based implementation was checked against the original literature source, thus ensuring that the correlation was implemented correctly without dropped digits, missing multiplication signs or any other easily made mistakes. Each function and supporting programming was also run as a stand-alone simulation program. The results of these functions were checked for glaring errors or obviously wrong values and incorrect orders of magnitude. After this verification process, the heat transfer and friction factor correlations were deemed to be correctly implemented.

5.6 Conclusion of the simulation model validation and verification

In this chapter, the simulation model results were verified to be independent of grid size. They were also validated against published experimental results and the simulation program results were seen to compare well with the experimental results, which was referenced. The heat transfer and pressure drop functions used in the simulation program were verified against their original sources in literature.

Based on the results contained in this chapter, the simulation model was deemed acceptable for use in the calculation of the results for this conceptual study.

Chapter 6 - Results and analysis

The different simulation phases, cases and results generated by the simulation program will be discussed in this chapter.

The simulation phase of this study was divided into two phases:

a. The base NCL simulation cases; and
b. A parametric study.

The first phase of simulations was done to determine the baseline results for the typical NCL. In other words, the NCL was simulated with two separate sets of input parameters. The first set of input variables was chosen so that the NCL could operate in a single phase mode, while the second set was chosen so that the NCL could operate in two phase mode. The analysis of the results from these base simulation cases helps to gain an understanding of how certain key variables change and vary along the length of the loop as the fluid flows along the NCL and is heated or cooled.

After the base simulation case, a parametric study was performed with sets of different input variables. This was the main purpose of the investigation. The loop performance, in other words the heat absorbed from the containment building, is evaluated as a function of other key loop variables. The variation of loop performance with its physical size, temperature conditions and other factors gives the researcher a good indication of the loop's reaction to these changes.

In the following section, the two base simulation cases and their results will be discussed.

6.1 Base case simulations

6.1.1 Whole-loop results from the base case simulations

During the initial phase of this investigation it was planned that there would be five input parameters for the simulation program that would be varied to perform a parametric study. For the two base cases these parameters were not varied as was done in the parametric simulations. For the single and two phase base case simulations the input parameters were fixed values. The values to which the input parameters were set are listed in Table 8.

Table 8. Input parameters set for the single and two phase base case simulations.

Input variable	Value for single phase base case	Value for two phase base case
Hot leg or containment temperature [˚C]	90	110
Cold leg or environmental temperature [˚C]	10	20
NCL pipe diameter [m]	0.025	0.025
NCL height [m]	10	10
NCL sidth [m]	2	2

The results generated from these base case simulations can be classified according to two groups:

a. Global results indicating the performance of the loop as a whole; and
b. Control volume specific results that indicate the values of each variable in each control volume.

The most important global results were the heat transfer values for the loop, specifically the “Heat absorbed” results. This variable indicated the ability of the NCL to remove heat from the containment building. The heat absorbed from the containment building by the loop and other key global variable results are listed in Table 9.

Table 9. Global results for the single and two phase simulation cases of the NCL.

Global variable	Results for single phase case	Results for two phase Case
Heat absorbed	39.47 kW	83.30 kW
Heat rejected	39.47 kW	63.56 kW
Heat lost	0.00 kW	18.90 kW
Heat gained	0.00 kW	0.59 kW
Heat unaccounted for	0.54 and 0.93 W	57.36 and 1433 W
Mass unaccounted for	0.00 and 0.00 $kg.s^{-1}$	0.00 and 0.00 $kg.s^{-1}$
Mass flow	0.13 $kg.s^{-1}$	0.20 $kg.s^{-1}$
Outlet fluid quality	0.00	0.04
Hot leg inlet velocity	0.27 $m.s^{-1}$	0.41 $m.s^{-1}$
Hot leg outlet velocity	0.28 $m.s^{-1}$	23.66 $m.s^{-1}$
Hot leg inlet temperature	15.70˚C	20.40˚C
Hot leg outlet temperature	90˚C	103.90˚C

The results of the single phase case showed that roughly 40 kW is absorbed from the containment building. Since this specific base case was a single phase loop, it was expected that all the heat would be rejected into the atmosphere with no heat being lost in the atmosphere through vapour venting. The value of the “Heat rejected” parameter confirmed this expectation. Roughly 40 kW of the heat was rejected to the environment; the same as that absorbed from the containment building.

As was explained in the previous chapters, two mass balances and two energy balances were performed on the loop to check the degree to which these quantities were conserved. As can be seen from the results, the error values were very low for the single phase case, zero in the case of the mass flows. These low error values led to increased confidence in the results generated by the simulation program.

Other results applicable to the single phase case are also shown in Table 9. The mass flows and velocities were quite small. This is to be expected for fluid flow that is the result of only a small density difference between the vertical pipes of the NCL. As expected, the fluid quality of the hot leg outlet was zero.

Table 9 also lists the results that were obtained from a simulation run on a two phase NCL. The heat absorbed from the containment building in this case was roughly 83 kW. This was almost double the heat absorbed by the single phase loop. Since the vapour generated in the hot leg was released to the atmosphere at the reservoir and replaced by feedwater, the cold leg only rejected 64 kW to the environment. The vapour being released to the atmosphere removed 19 kW of heat from the NCL, while the feedwater, which replaced the mass of vapour being vented, added less than 1 kW of heat to the NCL. Again, the error values were calculated for the loop. The mass conservation was very good, but the heat error values were much higher. These values were still deemed acceptable, since the biggest error value was still below 2% of the heat being absorbed from the containment building. It is interesting to note that throughout the whole simulation phase of this investigation, the heat error was consistently higher for the two phase cases. This could indicate some shortcomings of the homogenous model that was used as a foundation for the simulation program.

The outlet fluid quality was 4% in the case of the two phase loop, but the effect on the hot leg outlet velocity was substantial. The velocity was in excess of 23 $m.s^{-1}$ (meters per second), compared to an inlet velocity of 0.41 $m.s^{-1}$ and a mass flow of 0.20 $kg.s^{-1}$ (kilograms per second).

In the following section the two base case loop results will be examined in more detail. This will help the reader understand the behaviour of the loop and the variation of fluid parameters as it flows through the loop. It must be noted that the pipe wall temperatures of the loop were also higher, as could be

expected, to enable the NCL fluid to boil. Thus, the results that were obtained for the base single phase and two phase cases are not directly comparable. However, comparing the results leads to a greater understanding of the NCL operation in single phase and two phase modes.

6.1.2 Examination of base case results – Enthalpy and temperatures

As was explained in the previous section, two base cases of the NCL were simulated. In this section, the variation of key variables along the length of the loop is discussed.

The variation of fluid enthalpy, pipe wall temperature and fluid temperature along the length of the NCL are shown in Figure 6-1 and Figure 6-2. Figure 6-1 shows the variation of these parameters for the single phase base case loop with input parameters, as explained in the previous section. Figure 6-2 shows the two phase base case NCL parameters.

The horizontal axis of Figure 6-1 details the distance from the loop inlet at the cold leg to the exit at the top horizontal pipe. The three vertical lines, as indicated by the legend on the figure, is the distance along the loop where the cold exit, hot leg inlet and hot leg outlet is located. These three positions, including the start of the cold leg located at zero, show the limits of the three heat transfer zones in the figures contained in this section. Figure 6-1 also contains two vertical axes. The left-hand or primary axis shows the enthalpy of the fluid. The right-hand or secondary axis shows the fluid temperature. Two horizontal lines are plotted on the graph. These lines indicate the pipe wall temperatures, the environmental and containment temperature. Although these values are not fluid parameters, they are shown on the graph as the lower and upper limits for the fluid temperature.

The fluid enthalpy, as indicated by the legend on the graph, started off at a relatively high value. As it entered the cold leg at distance zero, the fluid enthalpy decreased as heat was removed from the fluid by the cold leg pipe walls. At first the rate of heat removal was high, as can be seen by the slope of the graph. As the fluid temperature, indicated on the graph, approached the cold leg pipe wall temperature, the rate of heat removal decreased. When the fluid left the cold leg and entered the horizontal pipe section, the fluid enthalpy and temperature remained constant as no heat transfer took place. After the horizontal section, the fluid entered the vertical hot leg. Heat transfer to the fluid raised the enthalpy and temperature. Again, as with the cold leg, the rate of enthalpy and temperature increase varied along the length of the pipe section. The enthalpy and fluid temperature increased quickly, while the difference in fluid temperature and hot leg pipe wall temperature was large. The rate of increase in fluid enthalpy and temperature decreased as the fluid temperature approached the hot leg wall temperature. As the fluid

left the vertical hot leg, the fluid enthalpy and temperature remained constant as no heat transfer took place in the horizontal sections of the loop.

Figure 6-2 is identical in axes and plotted parameters. However, as was stated earlier, it shows the two phase base simulation case. The variation of fluid enthalpy and temperature in the cold leg and bottom horizontal section of the loop, as well as the first part of the vertical hot leg, resembles that of the single phase case explained above. However, roughly two thirds up the length of the vertical hot leg, the fluid boiled due to the enthalpy increasing above the saturated liquid threshold value. The enthalpy curve followed a strange, but expected, shape thereafter. When boiling of the fluid started at a distance of roughly 18 metres, the rate at which the enthalpy was changing was increased. This was due to the fluid boiling, which increased the heat transfer coefficients and resulted in greater heat transfer.

The temperature curve, curiously, started to decrease after the onset of boiling. This is quite strange as the fluid temperature is decreased while heat is added. This phenomenon can be better explained if it is remembered that the hot leg is a vertical section of pipe. As the fluid flows, upward the pressure decreases due to the frictional and static pressure losses. Since the fluid is in a saturated state, the decreased pressure leads to the fluid temperature decreasing to match the saturated pressure and temperature relation. The void fraction, which is not shown in the graph, increased in the process as the higher enthalpy at lower pressure thermodynamically dictated. The temperature decrease continued at a lower rate in the horizontal section of the pipe loop. This was due to the frictional pressure losses that were still present, while static pressure changes were absent.

6.1.3 Examination of base case results – Heat transfer, quality, densities and velocities

Figure 6-3 is a combination of the results of the single phase and two phase loop results. The horizontal axis of the graph again shows the distance from the loop inlet. On the primary axis, the calculated heat transfer is shown per metre. The secondary axis contains the fluid quality. As in the case of the two previous graphs, the vertical lines show various major positions along the loop. The single phase and two phase loop heat transfer curves started off at a negative value. The values were negative due to the heat transfer from the fluid to the environment. As the fluid left the cold leg, the heat transfer stopped. In the case of the single phase case, the fluid entered the hot leg and heat was transferred at a high rate, which decreased as the temperature approached the wall temperature. In the case of the two phase fluid, the heat transfer started at a higher value once it entered the hot leg. This is due to the slightly higher mass flow of the two phase loop and higher wall temperature in the hot leg. It must be noted that

the cold leg heat transfer curves were similar for the single and two phase cases, since much of the two phase loop's heat is vented to the environment as vapour.

The heat transfer in the hot leg followed the same trend as the single phase curve until the onset of boiling at a distance of roughly 18 metres from the loop inlet. The heat transfer rates increased again and kept on increasing until the fluid left the hot leg and heat transfer dropped to zero. This was caused by the increased heat transfer coefficient due to the boiling that took place. The fluid quality curve, which is shown from the hot leg inlet, is a confirmation that boiling has started. The fluid quality increased steadily until the fluid left the hot leg, at which point the quality increased at a lower rate. This can be ascribed to the frictional pressure losses in the pipe, which lowered the saturation pressure of the mixture, while the enthalpy stayed the same, leading to an increased fluid quality.

Figure 6-4 shows the variation of the fluid density and velocity along the single and two phase loops. Again, it is a combined graph for the single and two phase simulation base case results.

The single phase density variation along the loop was minimal. As the fluid was cooled in the cold leg, the density increased slightly. Again, as it was heated in the hot leg, the density decreased slightly. As a result, the velocities in the single phase loop did not vary much and can be seen on the graph as an almost constant value.

The two phase case was different. In the cold leg, the fluid density varied in much the same manner as the single phase loop. Once the fluid entered the hot leg and started to boil, however, the density decreased quite rapidly. As a result, the fluid velocity increased dramatically. The rate at which the velocity increased after the hot leg changed to a lower rate due to the frictional pressure losses in the following pipe section.

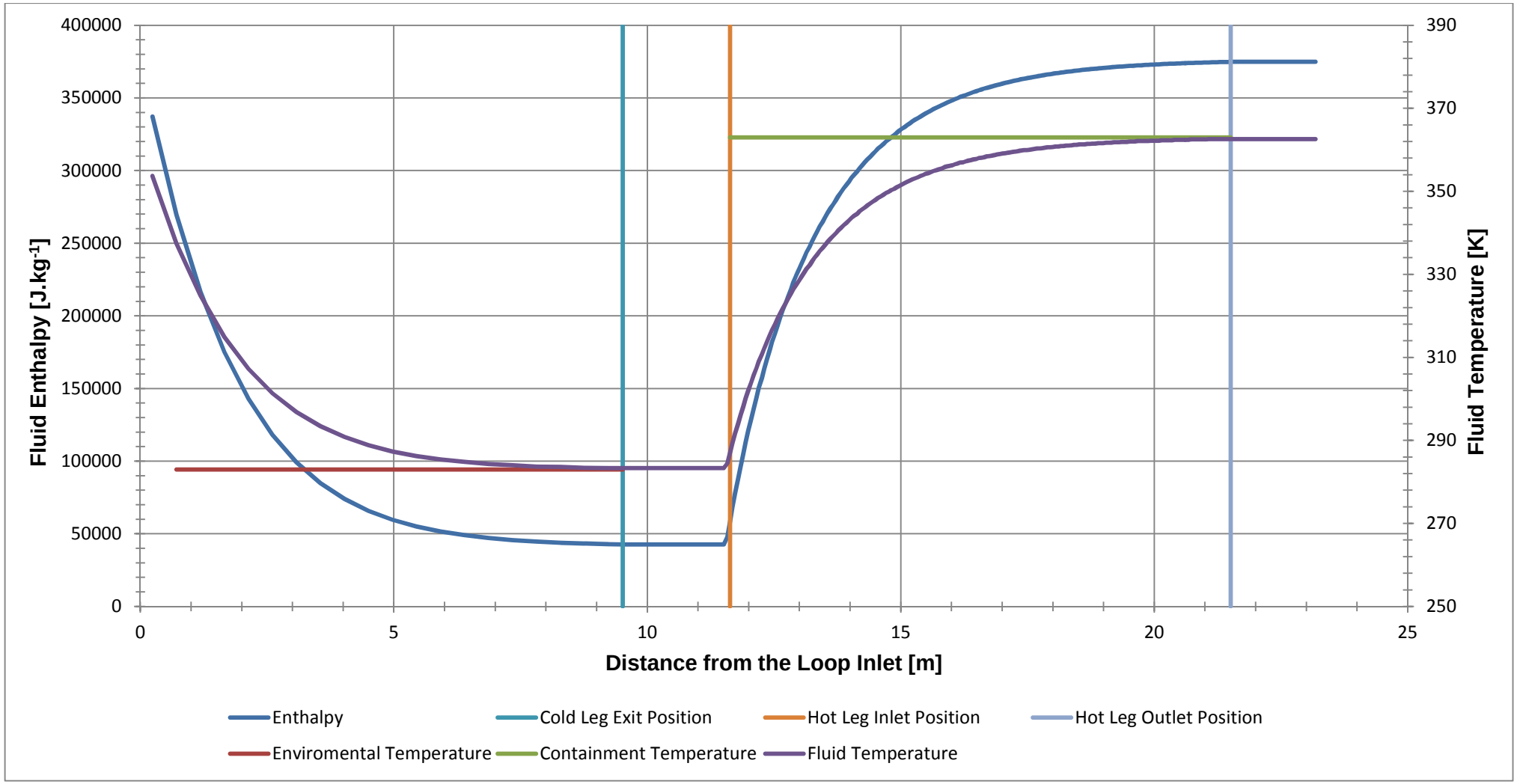


Figure 6-1. The variation of enthalpy, pipe wall temperature and fluid temperature along the length of the base single phase simulation case.

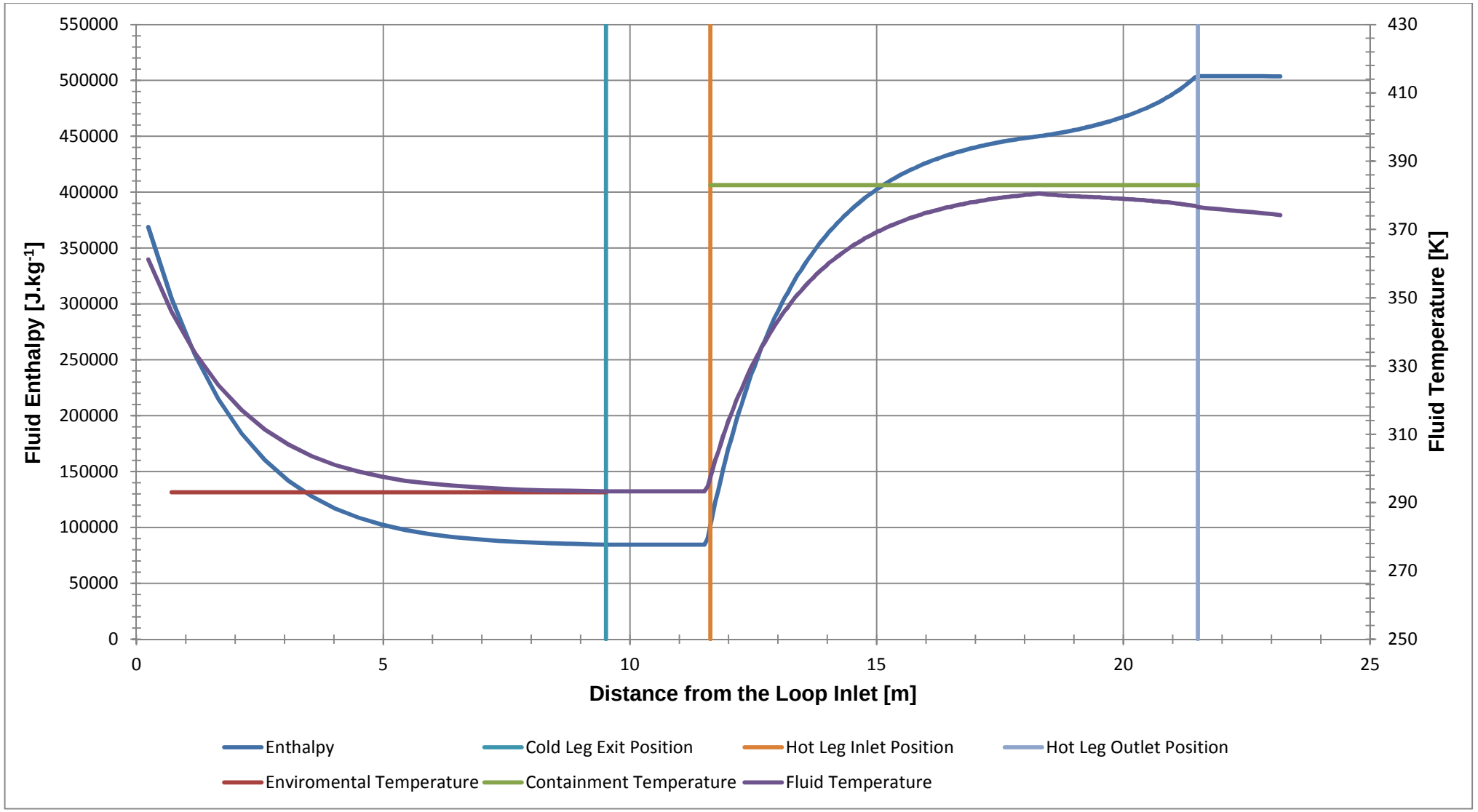


Figure 6-2. The variation of enthalpy, pipe wall temperature and fluid temperature along the length of the base two phase loop.

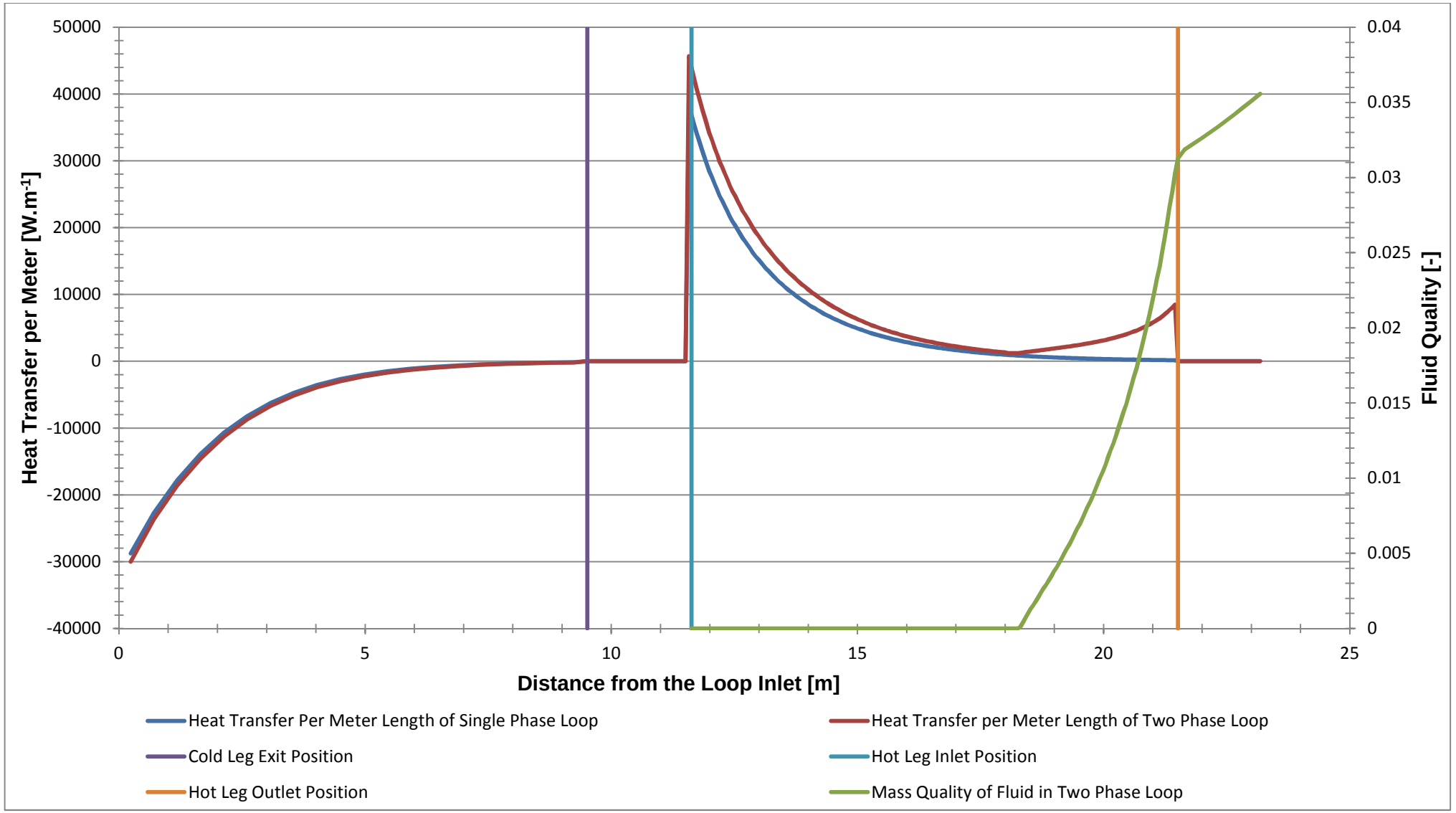


Figure 6-3. The variation of heat transfer per metre and fluid quality along the length of the single and two phase base loops.

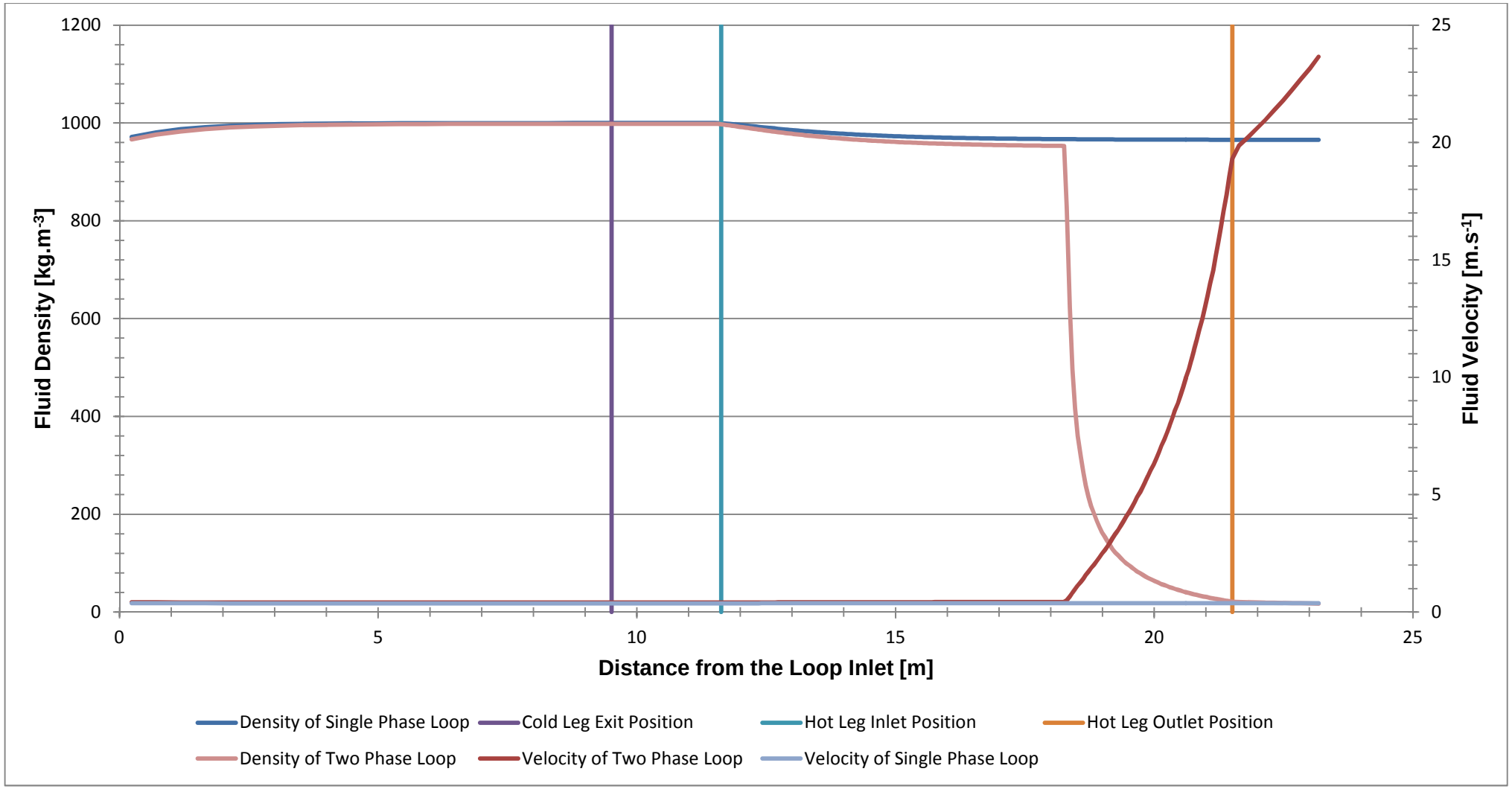


Figure 6-4. The variation of density and velocity along the length of the single and two phase loops.

6.2 Results from the parametric simulations

As part of the loop investigation using the simulation program, the loop was simulated with a number of input variables to determine the effect of these parameters on the heat that could be absorbed from a containment building. The results from these simulations will be explained in the following three sections.

6.2.1 Variation of pipe diameter

The diameter of the loop pipes were varied over a range of values to determine their effect on the heat that could be absorbed in the NCL. Table 10 shows the four cases that were simulated. The four cases used the same width and height parameters for the NCL. There were two single phase cases and the same number of two phase cases, each having a slightly different set of imposed temperature values. The pipe diameter was varied over the same range of values for all the cases, except for the last case. For the last case, D-2-2, a solution could not be obtained at the lower diameter values, possibly due to the instability of the loop with small diameters and high heat transfer values. For the four cases, the total number of simulation runs amounted to 26, 26, 126 and 116 runs respectively for each of the cases. The two phase runs had a much higher number of runs due to the need for smaller diameter increases at a time to ensure that convergence was obtained when solving the simulation program using EES. This helped to keep the guess values of the numerical routines used by EES close to the solution that was obtained. The pipe diameters were varied over the stated range with 0.0125 m intervals for the single phase cases and 0.0005 m intervals for the two phase cases.

After the 294 simulation runs, which translated into 294 data points of interest, the graph shown in Figure 6-5 was drawn. The figure shows a graph with four curves generated from the results of the simulation cases. A range of pipe diameters are shown on the horizontal axis of the graph. The vertical axis shows the heat absorbed from the containment building.

Table 10. Pipe loop diameter variation simulations and cases.

Simulation case	Input parameter values				
	Pipe diameter [m]	NCL height [m]	NCL width [m]	Cold leg wall temperature [˚C]	Hot leg wall temperature [˚C]
D-1-1	0.0125 – 0.075	10	2	20	80
D-1-2	0.0125 – 0.075	10	2	15	90
D-2-1	0.0125 – 0.075	10	2	10	105
D-2-2	0.0175 – 0.075	10	2	20	115

Each line of the graph represents a simulation curve. The four lines seem to be grouped into two groups with two lines each. The two bottom curves are the single phase loop results and the top two lines are the two phase loop results. This means that the two phase loops in general remove more heat than a NCL of the same geometry. This can possibly be attributed to the higher mass flows experienced in a two phase loop and the higher temperatures that enable the fluid to absorb more heat. However, to truly compare single and two phase loop performance a separate study would have to be performed, as this was outside the scope of the current investigation.

The second observation that can be made from the graphs is that for the single phase group, the loop with the highest temperature difference between the hot and cold leg transmitted the most heat.

The most obvious observation from the graph is that more heat is absorbed by larger pipe diameters. This is attributed to the larger heat transfer area, smaller friction losses and thus higher flow rates that the loop achieves when the diameter of the pipe loops are increased. It is not clear from the results why the results of case D-2-1 display such a dip in the heat transfer. It could be attributed to the loop bordering on some instability mode that is specific to the loop geometry and imposed temperatures.

As a result of this parametric study, it is clear that larger pipe diameters are beneficial to heat transfer in NCLs with imposed pipe wall temperatures.

6.2.2 Variation of loop height and width

The height and width of the NCL was varied over a range of values to determine its effect on the heat that could be absorbed by the NCL from a containment building. Table 11 shows the six cases that were simulated. Of these six cases, three cases used a single phase loop setup and three cases used a two phase loop setup. For each case, the loop height was varied over the same range using 1 m intervals. The loop width was changed between three values with an interval of 2 m. Thus, each single and two phase loop was simulated three times with a different width and each had a varying loop height. For the six cases, this amounted to 31 runs in each case, equating to 186 runs.

After the 186 simulation runs, which translated into 186 data points, the graph shown in Figure 6-6 was drawn. The graph contains six curves, which were generated from the above-stated simulation cases. On the horizontal axis of the graph, the range of pipe loop heights is shown. On the vertical axis, the heat absorbed from the containment building is shown.

The six curves can be grouped into two groups, each group representing the single phase or two phase case results. Also, since the loop width was varied as well, each of the lines in the different groups represents a different loop width.

Table 11. Pipe loop height and width variation simulations and cases.

Simulation case	Input parameter values				
	NCL height [m]	NCL width [m]	Pipe diameter [m]	Cold leg wall temperature [˚C]	Hot leg wall temperature [˚C]
G-1-1	5–35	1	0.05	20	80
G-1-2	5–35	3	0.05	20	80
G-1-3	5–35	5	0.05	20	80
G-2-1	5–35	1	0.05	20	115
G-2-2	5–35	3	0.05	20	115
G-2-3	5–35	5	0.05	20	115

After the 186 simulation runs, which translated into 186 data points, the graph shown in Figure 6-6 was drawn. The graph contains six curves, which were generated from the above-stated simulation cases. On the horizontal axis of the graph, the range of pipe loop heights is shown. On the vertical axis, the heat absorbed from the containment building is shown.

The six curves can be grouped into two groups, each group representing the single phase or two phase case results. Also, since the loop width was varied as well, each of the lines in the different groups represents a different loop width.

Again, as with the previous simulation run, where the NCL pipe diameters were varied, it is clear that the two phase loops absorbed a lot more heat from the containment building.

The next observation that can be made is that an increase in loop width leads to a decrease in the heat being absorbed in the hot leg of the loop for both the single and two phase loops. This is due to the added frictional pressure losses to which the extra width of the pipe loop contributes. It is notable that in the case of the two phase loop the impact of the extra loop width is much more than in the case of the single phase loop. In the case of the two phase loop the top horizontal pipe section contains a two phase mixture that increases the frictional losses to a greater extent compared to that of a single phase mixture.

The last observation made was that an increase in the NCL height led to an increase in the heat being absorbed. The gain achieved, however, decreased with an increase in the pipe length. This can be

attributed to the fluid temperature approaching the temperature of the pipe wall over the length of the hot leg. A further extension of the loop height would not transfer much more heat to the fluid. On the other hand, a higher loop would have a higher mass flow rate, due to the longer water columns in the hot and cold legs, which would also contribute to a higher mass flow rate and consequently higher heat absorption rates from the containment building.

From this parametric study, it is clear that larger NCL widths are detrimental to the heat transfer achieved with NCLs. An increase in the height of an NCL pipe loop led to an increase in the heat absorbed by the NCL from a containment building, but the gain achieved decreased the higher the NCL became.

6.2.3 Variation of pipe wall temperatures

The temperatures imposed on the pipe walls were varied over a range of values to determine the effect that it may have on the heat that the NCL can absorb from a containment building. Table 12 shows the six cases that were simulated with the simulation program. Each of the six cases used the same NCL geometry and two different NCL pipe diameters. The cold leg wall temperatures were varied over three values, while the hot leg wall temperatures were varied over a large range of values with intervals of 1˚C. For the first four cases, the simulation runs attempted with hot leg wall temperatures of 125˚C could not be solved due to problems with numerical convergence. With larger pipe diameters, a solution could be found. The inability of the simulation program to converge was attributed to vigorous boiling in the hot leg, which led to instability and periodic flow reversals. The six simulation runs equated to 52, 42, 42, 53, 44 and 44 runs respectively for each of the cases.

Table 12. Pipe loop hot and cold leg wall temperature variation simulations and cases.

Simulation case	**Input Parameter Values**				
	Cold leg wall temperature [˚C]	**Hot leg wall temperature [˚C]**	**Pipe diameter [m]**	**NCL height [m]**	**NCL width [m]**
T-1	5	45–123	0.05	10	2
T-2	25	65–123	0.05	10	2
T-3	45	65–123	0.05	10	2
T-4	5	45–124	0.075	10	2
T-5	25	65–125	0.075	10	2
T-6	45	65–125	0.075	10	2

After the 277 simulation runs, which translated into 277 data points of interest, the graph shown in Figure 6-7 was drawn. The figure shows a graph with six curves, each representing one of the simulation cases. On the horizontal axis, the variation of the hot leg wall temperature is shown. The vertical axis shows the heat absorbed from the containment building.

Of the three parametric simulation graphs the current one is the most confusing. Case T-4 had a smooth result. There were no dips in the results in its curve on the graph. T-4 is the simulation case with the lowest temperature on the cold leg pipe wall and also has a large pipe diameter. It also absorbed the most heat throughout the whole parametric evaluation. It is interesting to note that the detailed results (which are not shown here) indicated that the loop did not boil at all, even though a temperature of 125˚C was imposed on the tube. The tube diameter and sheer mass flow prevented the fluid from boiling.

Cases T-5 and T-6 were the same as T-4, except for the higher temperatures imposed on the cold leg wall. The heat absorbed by these NCLs was lower. A dip in the case of T-5 and a jump in the case of T-6 can also be seen towards the higher temperatures. It appears as though the results of the two cases are converging.

Cases T-1, T-2 and T-3 have heat removal rates in the lower range of the graph. Curiously, the three curves seem to converge to the same result towards the higher temperatures, the same phenomenon as with T-5 and T-6 mentioned above. It can be deduced from this tendency of the heat removal rates to converge that the quantity of absorbed heat becomes independent of the cold leg temperature. This can be attributed to the fluid temperatures becoming roughly equal in the hot legs, thus the heat transfer becomes similar as well. However, the true cause of these phenomena can only be speculated at this stage.

As a result of this parametric study, it is clear that higher temperatures at the cold leg results in lower absorbed heat values, although at very high hot leg temperatures the cold leg temperature becomes less of an influence. Higher hot leg wall temperatures generally also lead to higher levels of heat being absorbed.

6.3 Analysis of results

During the literature study, it was found that Gavrilas *et al*. (1998) had investigated various passive containment cooling designs. According to Figure 2-2, taken from their study, the required rate of heat removal from a generic containment building, housing a nuclear reactor of a typical power rating, can be deduced. By taking a rounded up value from Figure 2-2, it was found that the cooling system must

remove $1.0x10^7$ MJ (Megajoules) from the containment space over a time period of 100 hours. This equates to an average required heat removal rate of 28 MW (Megawatt). Table 13 shows the results of two possible NCL heat removal rates obtained from the simulation program. These rates correspond to the steady state results obtained from cases T-2 and T-5 as explained earlier in this chapter. Using the results of the simulation runs, it can be calculated that roughly 120 or 75 of these NCLs are needed to maintain an acceptable rate of cooling to keep the containment building safe. This is quite a large number of devices to have installed in a containment building, with an accompanying large number of holes in the containment wall.

To put this into perspective, the containment building's inner steel shell of the design which Gavrilas *et al*. (1998) investigated had a diameter of 42 m. If a 100 NCLs were used with an outer diameter of 0.075 m, 5.7 % of the circumference would be occupied by an NCL pipe protrusion through the containment shell. This however may be reduced by staggering the protrusion holes or by other creative measures.

Table 13. Analysis of the NCL as a suitable containment cooling device.

Description	**Analysis**	
Heat release Into containment [kW]	28 000	28 000
NCL pipe diameter [m]	0.05	0.075
NCL height [m]	10	10
NCL width [m]	2	2
Cold leg wall temperature [˚C]	25	25
Hot leg wall temperature [˚C]	105	105
Calculated heat absorption rate [kW]	232.48	375.48
Number of NCLs needed	120	75

Initially, the results look promising. However, a number of additional factors, which could change the picture, have to be considered.

a. The actual temperature of the NCL pipe wall when an accident happens and heat is released into the containment.
b. The effect of steam and other gases in the containment atmosphere.
c. The effect of the condensation of steam on the NCL pipes inside the containment building.
d. The effect that the NCLs themselves might have on the containment integrity.
e. The effect of heat transfer enhancing devices on the performance of the NCL.
f. The effect of instability on the performance of the NCL.
g. The response rate of an NCL, in other words, the time it takes to respond to changes in the containment conditions.

The NCL concept initially looks quite promising, if not as a primary heat removal device, but definitely as a secondary or passive backup heat removal device. If the heat removal rate requirement, as stated in Table 13, can be relaxed, either through the use of storage pools or through other passive devices, the degree of containment building integrity may be improved by the use of an NCL for cooling. This concept might be a viable option for the removal of usable quantities of heat from the containment building.

6.4 Closing comments and conclusion of results

The simulation results of the NCL concept were presented in this chapter. Utilising the simulation program that was compiled using the EES software the results of a large number of cases could be generated and explained. To generate the results took roughly two weeks in man hours and five days in computer time. Each iteration took roughly 40 seconds and a single simulation run took about three to seven minutes, depending on how good the guess values were. It was found that the EES simulation program was very sensitive to guess values. Guess values, which were used in the EES solution routine, had to be updated regularly. Especially two phase simulations could not obtain convergence without very good guess values. Incorrect guess values were at the root of most of the problems experienced during the simulation phase of this investigation.

During the parametric simulations, it was seen that increasing the pipe diameter of the NCL led to an increase in the heat being absorbed in the hot leg. An increase in the pipe height also led to an increase in absorbed heat. However, an increase in the NCL width led to a decrease in the heat that was absorbed from the containment building.

During the temperature variation parametric study, it was found that as the hot leg pipe wall or containment temperature was increased, the heat absorption rate from the containment building also increased. An increase in the cold leg pipe wall or environmental temperature led to a decrease in the heat that could be absorbed from the containment building. It was also seen that at very high hot leg pipe wall temperatures, the cold leg wall temperatures tended to have a smaller influence on the rate of heat absorption from the containment building.

The various parametric cases that were simulated were explained and the loop was evaluated against information obtained from the literature study. It was seen during the analysis of the results that the NCL concept could be used to remove usable quantities of heat from the containment building, but further studies are necessary to obtain the detailed result.

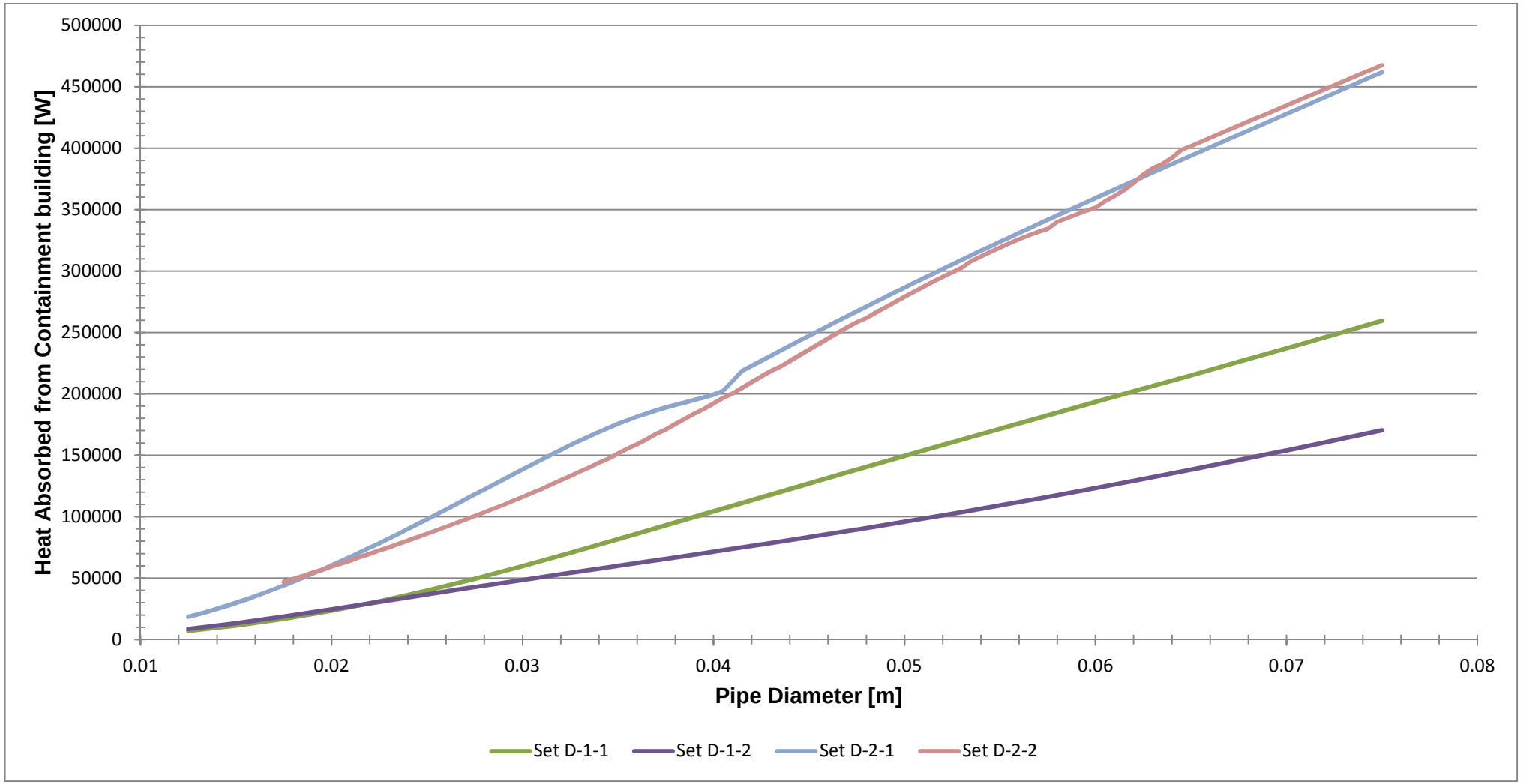


Figure 6-5. The variation of heat absorbed from the containment building by the hot leg as a result of change in the loop pipe diameter.

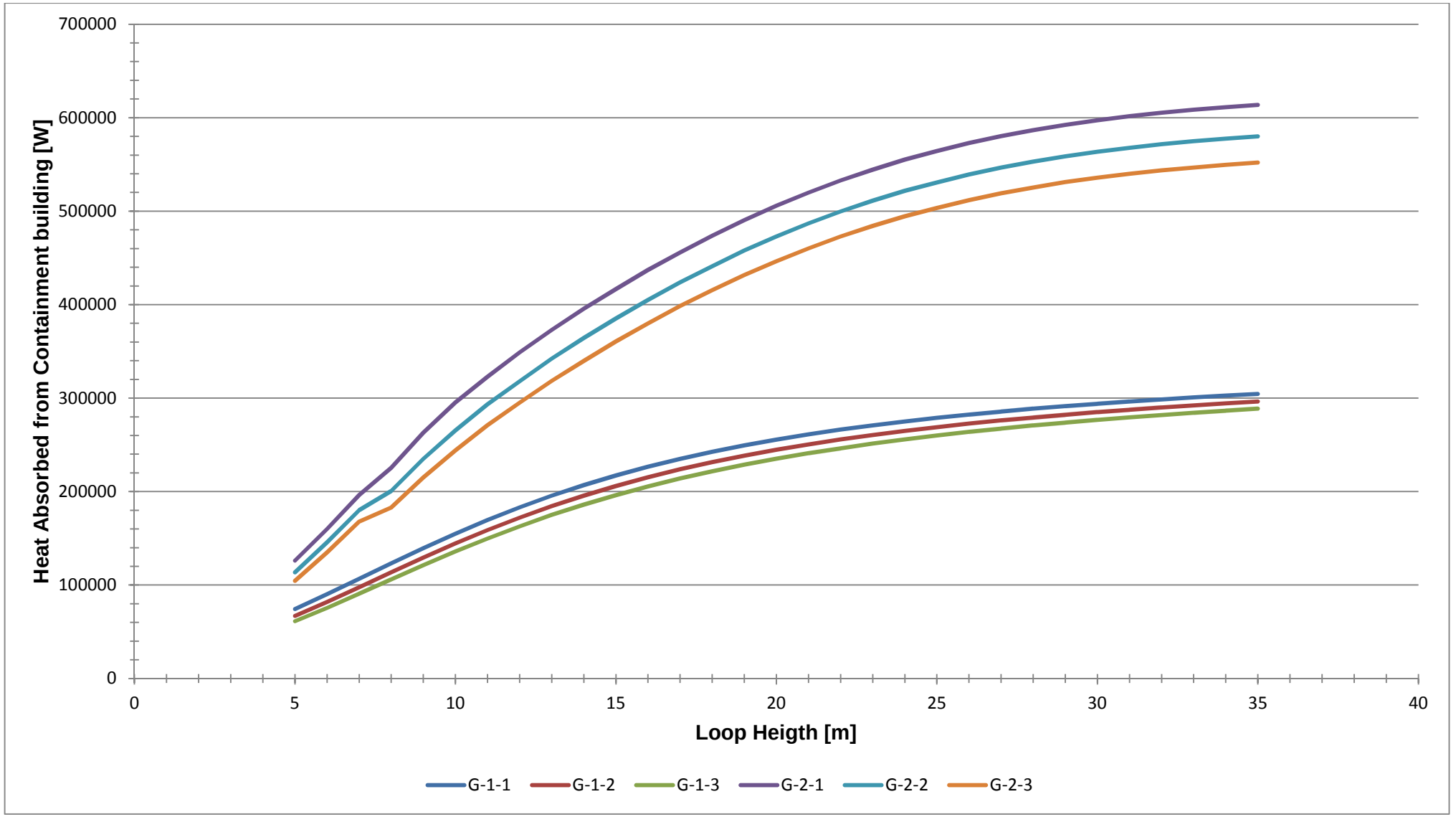


Figure 6-6. The variation of heat absorbed from the containment building by the hot leg as a result of a change in the loop pipe height and width.

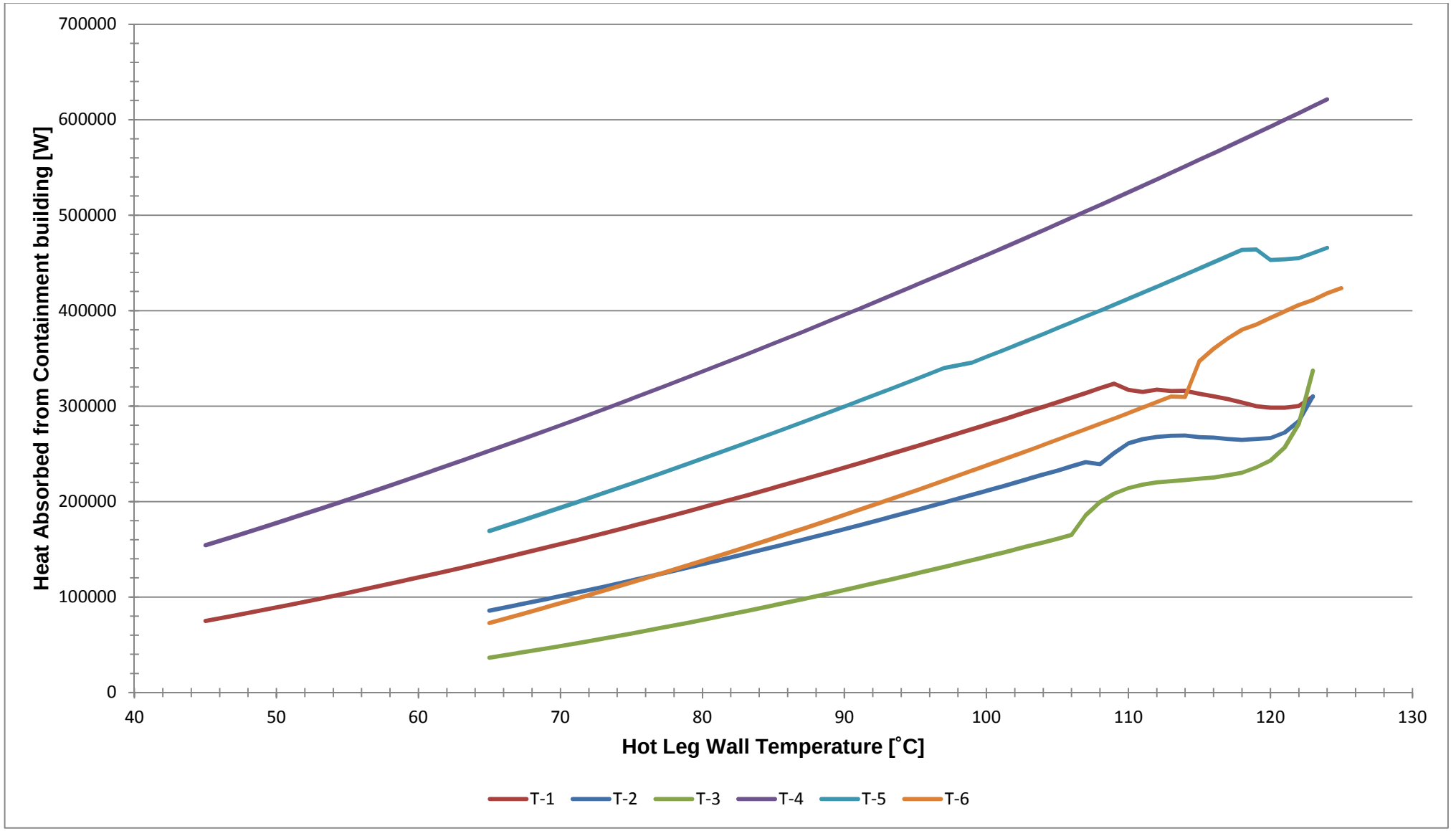


Figure 6-7. The variation of heat absorbed from the containment building by the hot leg as a result of a change in the imposed pipe wall temperatures.

Chapter 7 - Conclusion and recommendations

This chapter summarises the conceptual investigation. The investigation is concluded and recommendations for further studies are made.

7.1 Summary of the investigation

In Chapter 1 the conceptual investigation was introduced and the project purpose was stated. Background information on PWRs, containment buildings and containment building cooling concepts were discussed. The concept NCL was introduced and the working principle of an NCL was explained. The project definition, which included the problem statement, project scope and simulation methodology, was discussed. The project deliverables were listed. Some of the main project topics were discussed.

In Chapter 2, the literature study that was conducted was presented. The literature study covered background topics to NCLs, such as passive containment cooling and other applications of NCLs. In the following section, various articles on single phase natural circulation loops were discussed. This included studies on their instability and the calculation of friction factors for use in frictional pressure drop calculations. In the next section two phase natural circulation loops were discussed. The homogenous model's conservation equations, which were used in the simulation program, were presented. Two phase friction factors were explained and it was found that a simple explicit correlation existed for the two phase friction factor. Heat transfer correlations for boiling and subcooled flow were discussed. The chapter was concluded with a section to explain the instability phenomena associated with NCLs.

In Chapter 3, the theoretical background to the simulation program was derived and explained. The theory was based on the homogenous conservation equations for the NCL pipes and another set of conservation equations for the reservoir. Various other supporting equations for heat transfer, pressure drop and other flow related quantities were presented.

In Chapter 4, the theory presented in the previous chapter was used to build the equations used to compile the simulation program. The software, simulation methodology and basic assumptions were explained. The discretisation and naming convention that was used was discussed. The program code, functions and other variables that were used in the simulation program were explained.

In Chapter 5, the simulation program was checked for grid independence and its results were validated against experimental results obtained from literature. The heat transfer and pressure drop functions were also verified against their original sources in literature.

In Chapter 6, the results of the base single phase and two phase simulation cases were examined in detail. The parametric simulations were explained and their results were discussed. It was seen that the NCL concept could be a viable concept for the removal of usable quantities of heat from a containment building, especially when used in conjunction with other devices. However, some concerns were noted on the number of NCLs that would be required and the effect they might have on the integrity of the containment building.

In Chapter 7 (the current chapter), the investigation is summarised. The project purpose are revisited to gauge whether it was addressed. Some recommendations are made for further studies if the concept is deemed a feasible option.

7.2 Recommendations

The following recommendations can be made for further pursuing the subject:

a. During the literature study, it was determined that natural circulation loops are a lot more complex than originally thought. Transient and three-dimensional phenomena must be investigated using an appropriate computer code.
b. A detailed transient one-dimensional computer code must be developed to determine the stability behaviour of NCLs. This computer code should use a more complex model to describe the relation between the vapour and liquid phases of the fluid flow.
c. The response time of NCLs needs to be determined to see if their response is quick enough to deal with large energy release events inside the containment building.
d. This investigation assumed a fixed temperature value on the pipe walls to simulate containment and environmental temperatures. The relation between the pipe wall temperatures and the temperature of the surrounding atmosphere must be determined. Inside the containment, for example, the effects from water vapour, hydrogen, radiative heat transfer and non-condensable gases need to be considered. In the case of the environmental side of the loop, the effects of the wind, the sun and other elements have to be considered.
e. Additional heat transfer enhancement techniques to improve the heat removal rate of the NCL must be explored. This could lower the required number of NCLs.
f. A more detailed analysis needs to be done of the required heat removal rate for containment buildings in conjunction with other passive heat absorption measures.

7.3 Concluding remarks

In this section, some remarks are made on the project in retrospect of its execution.

The writing of a simulation code from scratch sometimes seems like a waste of time due to the availability of good simulation computer codes. However, writing a code from scratch for a specific situation allows specific tailoring of correlations and other details specific to NCLs. It also enables the investigator to understand the topic being investigated in detail, instead of taking a “black box” approach.

The EES code is a very useful platform for simulation, since it has a fast solver and comprehensive thermodynamic relations. However, to find the source of an error in the program code of complex simulations is very difficult.

NCLs are very simple to operate, yet very tricky to design; a fact that was emphasised during the execution of this project.

7.4 Conclusion

The aim of this conceptual investigation was to determine what value an NCL, running along the height of a PWR containment building, could have in terms of removing usable quantities of heat from the building. A literature study was conducted to provide background information, correlations, conservation equations and other supporting information, which was used to develop a theoretical background for the simulation program. The simulation program was validated and verified and deemed acceptable for use. The simulation program was used to simulate a set of two base case NCLs and also to do a number of parametric studies on the effect of loop geometry and temperatures that were imposed on the pipe walls. The effect of the variation of certain parameters on the heat transfer achieved by the loop was shown and discussed. It was estimated that the number of NCLs needed to remove sufficient heat from the containment ranged between 75 and 120, depending on the situation and specific loop design. This investigation was considered a success based on the simulation results, which addressed the original aim of this conceptual study.

References

ABU-MULAWEH, H.I. 2006. Design and performance of a thermosiphon heat recovery system. *Applied Thermal Engineering,* Vol. 26: 471–477.

AKYURT, M., LAMFON, N.J., NAJJAR, Y.S.H., HABEEBULLAH, M.H. & ALP, T.Y. 1995. Modeling of waste heat recovery by looped water-in-steel heat pipes. *International Journal of Heat and Fluid flow*, Vol. 16(4): 263–271.

AMBROSINI, W. & FERRERI, J.C. 2000. Stability analysis of single-phase thermosyphon loops by finite-difference numerical methods. *Nuclear Engineering and Design*, Vol. 201: 11–23.

AMBROSINI, W. & FERRERI, J.C. 2003. Prediction of one-dimensional natural circulation with a low diffusion numerical scheme. *Annals of Nuclear Energy*, Vol. 30: 1505–1537.

AMBROSINI, W., FORGIONE, N., FERRERI, J.C. & BUCCI, M. 2004. The effect of wall friction in single-phase natural circulation stability at the transition between laminar and turbulent flow. *Annals of Nuclear Energy*, Vol. 31: 1833–1865.

BABUSKA, I. & ODEN, J.T. 2004. Verification and validation in computational engineering and science: basic concepts. *Computer Methods in Applied Mechanics and Engineering*, Vol 193: 4057–4066.

BEJAN, A. & KRAUS, R.D. 2003. *Heat transfer handbook*. New Jersey, Hoboken: John Wiley & Sons Inc. 1399 p.

BELESSIOTIS, V. & MATHIOULAKIS, E. 2002. Analytical approach of thermosyphon solar domestic hot water system performance. *Solar Energy,* Vol. 72(4): 307–315.

BYUN, C.S., JERNG, D.W., TODREAS, N.E. & DRISCOLL, M.J. 2000. Conceptual design and analysis of a semi-passive containment cooling system for a large concrete containment. *Nuclear Engineering and Design*, Vol. 199: 227–242.

CENGEL, Y.A. & TURNER, R.H. 2005. *Fundamentals of thermal-fluid sciences*. 2nd ed. Singapore. Mcgraw-Hill Education. 1206 p.

CHEN, J.C. 1966. Correlation for boiling heat transfer to saturated fluids in convective flow. *Industrial and Engineering Chemistry Process Design and Development*, Vol. 5(3): 322–329.

CHUNG, Y.J., KIM, H.C., CHUNG, B.D., CHUNG, M.K. & ZEE, S.Q. 2006. Two phase natural circulation and the heat transfer in the passive residual heat removal system of an integral type reactor. *Annals of Nuclear Energy*, Vol. 33: 262–270.

COLLIER, J.G. 1983. Boiling Within Vertical Tubes. (*In* International Centre for Heat and Mass Transfer, *ed.* Heat Exchanger Design Handbook. Hemisphere Publishing Corporation. Washington, D.C. Vol. 2.7.3: 1–37)

DATE, A.W. 2005. Introduction to computational fluid dynamics. USA: Cambridge University Press. 398 p.

ESEN, M. & ESEN, H. 2005. Experimental investigation of a two-phase closed thermosyphon solar water heater. *Solar Energy,* Vol. 79: 459–468.

FORSBERG, C.W. & CONKLIN, J.C. 1994. Temperature-initiated passive cooling system. (*In* Proceedings of 29th Intersociety Energy Conversion Engineering Conference held on 7–12 August 1994. Monterey, California. 17p.). Oak Ridge National Laboratory, Tennessee.

FRANKUM, D.P., WADEKAR, V.V. & AZZOPARDI, B.J. 1997. Two-phase flow patterns for evaporating flow. *Experimental Thermal and Fluid Science*, Vol. 15: 183–192.

GAVRILAS, M., TODREAS, N.E. & DRISCOLL, M.J. 1998. Containment passive-cooling design concepts. *Progress in Nuclear Energy*, Vol. 32(3): 647–655.

HIBIKI, T. & ISHII, M. 2002. Distribution parameter and drift flux velocity of drift-flux model in bubbly flow. *International Journal of Heat and Mass Transfer,* Vol. 45: 707–721.

HIBIKI, T. & ISHII, M. 2003a. One-dimensional drift-flux model and constitutive equations for relative motion between phases in various two-phase flow regimes. *International Journal of Heat and Mass Transfer*, Vol. 46: 4935–4948.

HIBIKI, T. & ISHII, M. 2003b. One-dimensional drift-flux model for two-phase flow in a large diameter pipe. *International Journal of Heat and Mass Transfer*, Vol. 46: 1773–1790.

HUSSEIN, H.M.S. 2002. Transient investigation of a two phase closed thermosyphon flat plate solar water heater. *Energy Conversion and Management*, Vol. 43: 2479–2492.

INCROPERA, F.P., DEWITT, D.P., BERGMAN, T.L. & LAVINE, A.S. 2006. *Fundamentals of heat and mass transfer*. 6th ed. USA: John Wiley & Sons Inc. 995 p.

IAEA (International Atomic Energy Agency). 1994. *Status of advanced containment systems for next generation water reactors*. Vienna, Austria. 82 p.

IAEA (International Atomic Energy Agency). 2001. *Thermohydraulic relationships for advanced water cooled reactors*. Vienna, Austria. 343 p.

IAEA (International Atomic Energy Agency). 2002. *Natural Circulation data and methods for advanced water cooled nuclear power plant designs*. Vienna, Austria. 246 p.

IAEA (International Atomic Energy Agency). 2005. *Natural circulation in water cooled nuclear power plants: Phenomena, models, and methodology for system reliability assessment*s. Vienna, Austria. 649 p.

JENG, H.R. & PAN, C. 1999. Analysis of two-phase flow characteristics in a natural circulation loop using the drift-flux model taking flow pattern change and subcooled boiling into consideration. *Annals of Nuclear Energy*, Vol. 26: 1227–1251.

JOUDI, K.A. & AL-TABBAKH, A.A. 1999. Computer simulation of a two phase thermosyphon solar domestic hot water heating system. *Energy Conversions and Management,* Vol. 40: 775–793.

KAMIL, M., ALAM, S.S. & ALI, H. 1995a. Technical notes, Prediction of circulation rates in vertical thermosiphon reboiler. *International Journal of Heat and Mass Transfer*, Vol. 38(4): 745–748.

KAMIL, M., ALI, S.S. & ALAM, S.S. 1995b. Heat transfer to boiling liquids in a single vertical tube thermosiphon reboiler. *Experimental Thermal and Fluid Science*, Vol. 10: 44–53.

KANDLIKAR, S.G. 1998. Heat transfer characteristics in partial boiling, fully developed boiling, and significant void flow regions of subcooled flow boiling. *Journal of Heat Transfer*, Vol. 120: 395–410.

KHODABANDEH, R. 2004. Thermal performance of a closed advanced two-phase thermosyphon loop for cooling of radio base stations at different operating conditions. *Applied Thermal Engineering*, Vol. 24: 2643–2655.

KIM, J.M. & LEE, S.Y. 2000. Technical note: Experimental observation of flow instability in a semi-closed two-phase natural circulation loop. *Nuclear Engineering and Design*, Vol. 196: 359–367.

KLEIN, S.A. 2008. EES: Engineering Equation Solver for Microsoft Windows operating systems. F-Chart Software. 321 p.

KUMAR, S., JAIN, A., MOHANTY, B. & GUPTA, S.C. 2003. Recirculation model of a kettle reboiler. *International Journal of Heat and Mass Transfer*, Vol. 46: 2899–2909.

KYUNG, I.S. & LEE, S.Y. 1996. Periodic flow excursion in an open two-phase natural circulation loop. *Nuclear Engineering and Design,* Vol. 162: 233–244.

LEE, S.W., BAEK, W.P. & CHANG, S.H. 1997. Assessment of passive containment cooling concepts for advanced pressurised water reactors. *Annals of Nuclear Energy*, Vol. 24(6): 467–475.

LEVY, S. 1999. *Two phase flow in complex systems*. USA: John Wiley & Sons Inc. 448 p.

LIU, D., TANG, G.F., ZHAO, F.Y. & WANG, H.Q. 2006. Modelling and experimental investigation of looped separate heat pipe as waste heat recovery facility. *Applied Thermal Engineering*, Vol. 26: 2433–2441.

LIU, H., TODREAS, N.E. & DRISCOLL, M.J. 2000. An experimental investigation of a passive cooling unit for a nuclear plant containment. *Nuclear Engineering and Design*, Vol. 199: 243–255.

MISALE, M. & FROGHERI, M. 2001. Stabilization of a single-phase natural circulation loop by pressure drops. *Experimental Thermal and Fluid Science*, Vol. 25: 277–282.

MOUSAVIAN, S.K., MISALE, M., D'AURIA, F.D. & SALEHI, M.A. 2004. Transient and stability analysis in single-phase natural circulation. *Annals of Nuclear Energy*, Vol. 31: 1177–1198.

MUNSON, B.R., YOUNG, D.F. & OKIISHI, T.H. 2006. *Fundamentals of Fluid Mechanics*. 5th ed. USA: John Wiley & Sons.

NAYAK, A.K., VIJAYAN, P.K., SAHA, D. & RAJ, V.V. 1995. Mathematical modelling of the stability characteristics of a natural circulation loop. *Mathematical and Computer Modelling*, Vol. 22(9): 77–87.

OOSTHUIZEN, P.R. 2003. Thermal-Fluid simulation investigation of the reactor cavity cooling system standpipes design for the PBMR. Potchefstroom: PU of CHO. Dissertation – M.Eng. 172 p.

PILKHWAL, D.S., AMBROSINI, W., FORGIONE, N., VIJAYAN, P.K., SAHA, D. & FERRERI, J.C. 2007. Analysis of the unstable behaviour of a single-phase natural circulation loop with one-dimensional and computational fluid-dynamic models. *Annals of Nuclear Energy*, Vol. 34: 339–355.

PRASAD, G.V.D., PANDEY, M. & KALRA, M.S. 2007. Review of research on flow instability in natural circulation boiling systems. *Progress in Nuclear Energy*, Vol. 49: 429–451.

RAO, N.M., SEKHAR, C.C., MAITI, B. & DAS, P.K. 2006. Steady state performance of a two-phase natural circulation loop. *International Communications in Heat and Mass Transfer*, Vol. 33: 1042–1052.

REYES, J.N. 2005. Governing equations in two-phase fluid natural circulation flows. (International Atomic Energy Agency, *ed*. *Natural circulation in water cooled nuclear power plants*. Vienna, Austria: 155–172 p.)

SABHARWALL, P. & GUNNERSON, F. 2009. Engineering design elements of a two-phase thermosyphon for the purpose of transferring NGNP thermal energy to a hydrogen plant. *Nuclear Engineering and Design*, Vol. 239: 2293–2301.

SHANNAK, B.A. 2008. Frictional pressure drop of gas liquid two-phase flow in pipes. *Nuclear Engineering and Design*, Vol. 238: 3277–3284.

THOME, J.R. 2009. Engineering Data Book III. Wolverine Tube Incorporated. http://www.wlv.com/products/thermal-management-databooks.html. Date of access: 30 November 2009.

VIJAYAN, P.K. 2002. Experimental observations on the general trends of the steady state and stability behaviour of single-phase natural circulation loops. *Nuclear Engineering and Design*, Vol. 215: 139–152.

VIJAYAN, P.K., AUSTREGESILO, H. & TESCHENDORFF, V. 1995. Simulation of the unstable oscillatory behaviour of single-phase natural circulation with repetitive flow reversals in a rectangular loop using the computer code ATHLET. *Nuclear Engineering and Design,* Vol. 155: 623–641.

VIJAYAN, P.K., SHARMA, M. & SAHA, D. 2007. Steady state and stability characteristics of single-phase natural circulation in a rectangular loop with different heater and cooler orientations. *Experimental Thermal and Fluid Science*, Vol. 31: 925–945.

Appendix A – EES program code

This appendix contains the EES program code that was used to do the simulations. The code configuration reproduced here is for the base two phase case of the NCL, as described in Chapter 6.

```
"########################################"
"EES Simulation Program"
"Natural Circulation in a Pipe Loop using water"
"########################################"

"########################################"
"Global Constants"
"########################################"
$Constant grav# = 9.80665

"########################################"
"Functions"
"########################################"
"Calculates the fluid quality based on an ees functions"
"It modifies the standard EEs function to return a 0 for subcooled and 1 for superheat
conditions instead of -100 and 100"
FUNCTION FLUIDQUAL(Press, he_mix)
    "Determine saturated liquid and vapour enthalpies at the given pressure"
    he_liq = ENTHALPY(WATER, P = Press, x = 0)
    he_vap = ENTHALPY(WATER, P = Press, x = 1)

    "Test the given enthalpy to see if the fluid is subcooled, saturated or superheated"
    "Then asign the value as explained above"
    IF he_mix <= he_liq THEN
        "Fluid is subcooled"
        FLUIDQUAL = 0
    ELSE
        IF he_mix >= he_vap THEN
            "Fluid is superheated,"
            FLUIDQUAL = 1
        ELSE
            "Fluid is two phase, EES Function used"
            FLUIDQUAL = (he_mix - he_liq) / (he_vap - he_liq)
        ENDIF
    ENDIF

END

"Calculates the fluid density for a single or two phase fluid based on EES functions"
FUNCTION FLUIDDENS(Press,he_mix)
    "first determine mass quality using the appropiate function"
    mass_q = FLUIDQUAL(Press, he_mix)

    "test for liquid, gas or two phase"
    IF mass_q <= 0 THEN
        "Fluid is subcooled, EES function used"
        FLUIDDENS = DENSITY(WATER, P = Press, h = he_mix)
    ELSE
        IF mass_q >= 1 THEN
            "Fluid is superheated, EES function used"
            FLUIDDENS = DENSITY(WATER, P = Press, h = he_mix)
        ELSE
            "Fluid is two phase, use an interpolation function to determine density"
            "First determine saturated liquid density using EES function"
            rho_liq = DENSITY(WATER, P = Press, x = 0)
            "Then determine saturated vapour density using EEs function"
            rho_vap = DENSITY(WATER, P = Press, x = 1)
            "Then interpolate to find two phase density"
            FLUIDDENS = 1 / (((1 - mass_q) / rho_liq) + (mass_q / rho_vap))
        ENDIF
    ENDIF
END
```

```
"This function calculates the viscosity of the fluid based on an EES function"
"Subcooled and superheated properties are calculated using the EES functions
but at saturated conditions the properties are the result of an interpolation function
between the saturated liquid and vapour densities"
FUNCTION FLVISCO(Press, he_mix)
    "determine mass quality"
    mass_q = FLUIDQUAL(Press, he_mix)

    "test if the conditions supplied to the function is subcooled, saturated or superheated"
    IF mass_q <= 0 THEN
        "Fluid is subcooled, EES function used"
        FLVISCO = VISCOSITY(WATER, P = Press, h =he_mix)
    ELSE
        IF mass_q >= 1 THEN
            "Fluid is superheated, EES function used"
            FLVISCO = VISCOSITY(WATER, P = Press, h = he_mix)
        ELSE
            "Fluid is two phase, use an interpolation function to determine viscosity"
            "First determine saturated liquid viscosity using EES function"
            mu_liq = VISCOSITY(WATER, P = Press, x = 0)
            "Then determine saturated vapour viscosity using EEs function"
            mu_vap = VISCOSITY(WATER, P = Press, x = 1)
            "Then interpolate to find the two phase viscosity"
            FLVISCO = 1 / (((1 - mass_q ) / mu_liq )  + (mass_q / mu_vap))
        ENDIF
    ENDIF

END

"This function determines the conductivity of the fluid based on an EES function"
"Subcooled and superheated properties are calculated using the EES functions
but at saturated conditions the properties are the result of an interpolation function
between the saturated liquid and vapour densities"
FUNCTION FLCOND(Press, he_mix)
    "determine mass quality"
    mass_q = FLUIDQUAL(Press, he_mix)

    "test if the conditions supplied to the function is subcooled, saturated or superheated"
    IF mass_q <= 0 THEN
        "Fluid is subcooled, EES function used"
        FLCOND = CONDUCTIVITY(WATER, P = Press, h = he_mix)
    ELSE
        IF mass_q >= 1 THEN
            "Fluid is superheated, EES function used"
            FLCOND = CONDUCTIVITY(WATER, P = Press, h = he_mix)
        ELSE
            "Fluid is two phase, use an interpolation function to determine the conductivity"
            "First determine saturated liquid conductivity using EES function"
            cond_liq = CONDUCTIVITY(WATER, P = Press, x = 0)
            "Then determine saturated vapour conductivity using EEs function"
            cond_vap = CONDUCTIVITY(WATER, P = Press, x = 1)
            "Then interpolate to find the two phase conductivity"
            FLCOND = 1 / (((1 - mass_q ) / cond_liq )  + (mass_q / cond_vap))
        ENDIF
    ENDIF
END

"This function determines the heat capacity of the fluid based on an EES function"
"Subcooled and superheated properties are calculated using the EES functions
but at saturated conditions the properties are the result of an interpolation function
between the saturated liquid and vapour densities"
```

```
FUNCTION FLHCAP(Press, he_mix)
    "determine mass quality"
    mass_q = FLUIDQUAL(Press, he_mix)

    "test if the conditions supplied to the function is subcooled, saturated or superheated"
    IF mass_q <= 0 THEN
        "Fluid is subcooled, EES function used"
        FLHCAP = SPECHEAT(WATER, P = Press, h = he_mix)
    ELSE
        IF mass_q >= 1 THEN
            "Fluid is superheated, EES function used"
            FLHCAP = SPECHEAT(WATER, P = Press, h = he_mix)
        ELSE
            "Fluid is two phase, use an interpolation function to determine the heat capacity"
            "First determine saturated liquid heat capacity using EES function"
            cp_liq = SPECHEAT(WATER, P = Press, x = 0)
            "Then determine saturated vapour heat capacity using EEs function"
            cp_vap = SPECHEAT(WATER, P = Press, x = 1)
            "Then interpolate to find the two phase heat capacity"
            FLHCAP =1 / (((1 - mass_q ) / cp_liq )  + (mass_q / cp_vap))
        ENDIF
    ENDIF
END

"This function determines the Prandtl number of the fluid based on an EES function"
"Subcooled and superheated properties are calculated using the EES functions
but at saturated conditions the properties are the result of an interpolation function
between the saturated liquid and vapour densities"
FUNCTION NPRND(Press, he_mix)
    "determine mass quality"
    mass_q = FLUIDQUAL(Press, he_mix)

    "test if the conditions supplied to the function is subcooled, saturated or superheated"
    IF mass_q <= 0 THEN"Fluid is subcooled, EES function used"
        NPRND = PRANDTL(WATER, P = Press, h = he_mix)
    ELSE
        IF mass_q >= 1 THEN
            "Fluid is superheated, EES function used"
            NPRND = PRANDTL(WATER, P = Press, h = he_mix)
        ELSE
            "Fluid is two phase, use an interpolation function to determine the Prandtl number"
            "First determine saturated liquid Prandtl number using EES function"
            Pr_liq= PRANDTL(WATER, P = Press, x = 0)
            "Then determine saturated vapour Prandtl number using EEs function"
            Pr_vap = PRANDTL(WATER, P = Press, x = 1)
            "Then interpolate to find the two phase Prandtl number"
            NPRND =1 / (((1 - mass_q ) / Pr_liq )  + (mass_q / Pr_vap))
        ENDIF
    ENDIF
END

"This function determines the Renolds number of the fluid of subcooled, superheated and
two phase based on a simple calculation using the relevant parameters."

FUNCTION NREY(Press, he_mix, vel, diam_pipe)
    "Determine mass _quality"
    mass_q = FLUIDQUAL(Press, he_mix)
    IF mass_q <= 0 THEN
        "determine density"
        rho_mix = FLUIDDENS(Press, he_mix)
        "determine viscocity"
        mu_mix = FLVISCO(Press, he_mix)
```

```
        NREY = rho_mix * vel * diam_pipe / mu_mix
    ELSE
        IF mass_q >= 1 THEN
            "determine density"
            rho_mix = FLUIDDENS(Press, he_mix)
            "determine viscocity"
            mu_mix = FLVISCO(Press, he_mix)
            NREY = rho_mix * vel * diam_pipe / mu_mix
        ELSE
            "Determine liquid Reynolds number"
            N_Rey_liq = NREYLIQ(Press, he_mix, vel, diam_pipe)
            "Determine martenelli factor"
            Factor_Xtt = MARTENELLIF(Press, he_mix)
            "Determine factor F"
            Factor_F = FACTORF(Factor_Xtt)
            NREY = N_Rey_liq * (Factor_F ^ 1.25)
        ENDIF
    ENDIF
END

"This function determines the liquid Reynolds number"
FUNCTION NREYLIQ(Press, he_mix, vel, diam_pipe)
    "Determine mass quality"
    mass_q = FLUIDQUAL(Press, he_mix)
    "determine liquid density"
    rho_mix = FLUIDDENS( Press, he_mix)
    "Determine liquid viscosity"
    mu_mix = FLVISCO(Press, he_mix)
    "Then determine the liquid Reyolds number"
    NREYLIQ = (rho_mix * vel * diam_pipe / mu_mix ) * (1 - mass_q)
END

"This function determines the factor F"
FUNCTION FACTORF(Xtt)
    IF (1/Xtt) <= 0.1 THEN
        FACTORF = 1
    ELSE
        FACTORF = 2.35 * (((1 / Xtt) + 0.213) ^ 0.736)
    ENDIF

END

"This function determines the Martenelli factor"
FUNCTION MARTENELLIF(Press, he_mix)
    "Determine mass quality"
    mass_q = FLUIDQUAL(Press, he_mix)
    "determine liquid density"
    rho_liq = DENSITY(WATER, P = Press, x = 0)
    "determine vapour density"
    rho_vap = DENSITY(WATER, P = Press, x = 1)
    "Determine liquid viscosity"
    mu_liq = VISCOSITY(WATER, P = Press, x = 0)
    "Determine vapour viscosity"
    mu_vap = VISCOSITY(WATER, P = Press, x = 1)

    "Determine Martenelli factor"
    MARTENELLIF = (((1 - mass_q) / mass_q)^0.9)*((rho_vap / rho_liq)^0.5)*((mu_liq / mu_vap)^0.1)

END

"This function determines the boiling suppresion factor"
FUNCTION SUPPF(Press, he_mix, vel, diam_pipe)
```

```
    "Call function to determine liquid reynolds number"
    N_Rey_mix = NREY(Press, he_mix, vel, diam_pipe)
    "Determine suppresion factor"
    SUPPF = 1 / (1 + ((2.53e-6) * (N_Rey_mix ^ 1.17)))
END

"This function determines how much pressure drop happens over a pipe"
"it returns a positve value, thus it must be subtracted"
FUNCTION DELTAPFRIC(Press, he_mix, vel, diam_pipe, epsilon_pipe, n_size)
    "Determine the density of the fluid"
    rho_mix = FLUIDDENS(Press, he_mix)
    "determine friction factor from function"
    fric_fac = FRICFAC(Press, he_mix, vel, diam_pipe, epsilon_pipe)
    "After the friction factor has been determined, frictional pressure drop is calculated"
    DELTAPFRIC = fric_fac * n_size * rho_mix * vel * vel * 0.5 / diam_pipe

END

"This function determines the friction factor of the fluid in the pipes"
FUNCTION FRICFAC(Press, he_mix, vel, diam_pipe, epsilon_pipe)
    "determine mass quality"
    mass_q = FLUIDQUAL(Press, he_mix)
    "determine the reynolds number"
    N_Rey = NREY(Press, he_mix, vel, diam_pipe)

    "test if the conditions supplied to the function is subcooled, saturated or superheated"
    "then determine friction factor for the fluid using the appropiate correllation"
    IF mass_q <= 0 THEN
        "Fluid is subcooled, EES function used"
        "Determine flow regime"
        IF N_Rey < 1000 THEN
            "Subcooled Laminar Single phase Flow"
            FRICFAC = 64 / N_Rey
        ELSE
            IF N_Rey > 4000 THEN
                "Subcooled Turbulent Flow"
                FRICFAC = ((-1) * (1.8) * LOG10((6.9 / N_Rey) + ((epsilon_pipe / (diam_pipe * 3.7)) ^ 1.11))) ^ (-2)
            ELSE
                "Subcooled Transition zone flow"
                fric_fac_lam = 64 / N_Rey
                fric_fac_turb = ((-1) * (1.8) * LOG10((6.9 / N_Rey) + ((epsilon_pipe / (diam_pipe * 3.7)) ^ 1.11))) ^ (-
2)
                FRICFAC = MAX(fric_fac_lam, fric_fac_turb)
            ENDIF
        ENDIF

    ELSE
        IF mass_q >= 1 THEN
            "Fluid is superheated, EES function used"
            "Determine flow regime"
            IF N_Rey < 1000 THEN
                "Superheated Laminar Single phase Flow"
                FRICFAC = 64 / N_Rey
            ELSE
                IF N_Rey > 4000 THEN
                    "Superheated Turbulent Flow"
                    FRICFAC = ((-1) * (1.8) * LOG10((6.9 / N_Rey) + ((epsilon_pipe / (diam_pipe * 3.7)) ^ 1.11))) ^ (-
2)
                ELSE
                    "Superheated Transition zone flow"
                    fric_fac_lam = 64 / N_Rey
```

```
                fric_fac_turb = ((-1) * (1.8) * LOG10((6.9 / N_Rey) + ((epsilon_pipe / (diam_pipe * 3.7)) ^ 1.11)))
^ (-2)
                FRICFAC = MAX(fric_fac_lam, fric_fac_turb)
            ENDIF
        ENDIF
    ELSE
        "Two phase flow"
        "Test if within correllation bounds"
        IF N_Rey < 11 THEN
            "If reynolds number below 11 use laminar formula as per correlation instructions"
            FRICFAC = 64 / N_Rey
        ELSE
            "If reynolds number above 11 use two phase friction factor correlation"
            fric_fac_term1 = ((1 / 2.8257) * ((epsilon_pipe / diam_pipe)^1.1098)) + (5.8506 / (N_Rey ^ 0.8981))
            fric_fac_term2 = (epsilon_pipe / (diam_pipe * 3.7065)) - ((5.0452 / N_Rey) * LOG10(fric_fac_term1))
            FRICFAC = ((-1) * 2 * LOG10(fric_fac_term2)) ^ (-2)
        ENDIF
    ENDIF
ENDIF
END

"This function determines the two phase heat transfer in watts TO the fluid"
FUNCTION TWOPHASEHEAT(Press, he_mix, vel, T_wall, n_size, diam_pipe, epsilon_pipe)

    "Determine heat transfer area"
    area_heat = n_size * (PI * diam_pipe)
    "Determine the fluid temperature from the thermodynamic conditions"
    T_fluid = TEMPERATURE(WATER, P = Press, h = he_mix)

    "Fluid is two phase"
    "This heat transfer correlation is based on the CHEN correllation"
    "conductivity of liquid phase"
    cond_liq = CONDUCTIVITY(WATER, P = Press, x = 0)
    "heat capacity of liquid phase"
    Cp_liq = SPECHEAT(WATER, P = Press, x = 0)
    "Density of the liquid phase"
    rho_liq = DENSITY(WATER, P = Press, x = 0)
    "Density of the vapour phase"
    rho_vap = DENSITY(WATER, P = Press, x = 1)
    "fluid surface tension"
    sigma = SURFACETENSION(Water,T=T_fluid)
    "viscosity of the liquid phase"
    mu_liq = VISCOSITY(WATER, P = Press, x = 0)
    "Heat of vapourization of the mixture"
    he_liqvap = ENTHALPY(WATER, P = Press, x = 1) - ENTHALPY(WATER, P = Press, x = 0)
    "Saturation pressure of the fluid at the wall temperature"
    P_sat_walltemp = P_SAT(WATER, T = T_wall)
    "Saturation pressire of the fluid at the fluid tempeature"
    P_sat_fluidtemp = P_SAT(WATER,T = T_fluid)
    "Saturation temperature of fluid"
    T_sat_fluid_press = T_SAT(WATER, P = Press)
    "Liquid Reynolds number"
    N_Rey_liq = NREYLIQ(Press, he_mix, vel, diam_pipe)
    "Liquid Prandtl number"
    N_PR_liq = PRANDTL(WATER, P = Press, x = 0)
    "Determine the Martenilli factor"
    Factor_Xtt= MARTENELLIF(Press, he_mix)
    "Determine factor F"
    Factor_F = FACTORF(Factor_Xtt)
    "Determine the boiling suppresion factor"
    Factor_S = SUPPF(Press, he_mix, vel, diam_pipe)
```

```
    "Determine the macro heat transfer coefficient"
    h_coef_mac = 0.023 * (N_Rey_liq ^ 0.8) * (N_PR_liq ^ 0.4 ) * cond_liq * Factor_F / diam_pipe

    "Determine the nucleate boiling effect heat transfer coefficient"
    h_coef_mic_term1 = ((ABS(T_wall - T_sat_fluid_press)) ^ 0.24) * ((ABS(P_sat_walltemp - P_sat_fluidtemp)) ^
0.75) * Factor_S
    h_coef_mic_term2 = (sigma ^ 0.5) * (mu_liq ^ 0.29) * (rho_vap ^ 0.24) * (he_liqvap ^ 0.24)
    h_coef_mic_term3 = (cond_liq ^ 0.79) * (Cp_liq ^ 0.45) * (rho_liq ^ 0.49) * (grav# ^ 0.25)
    h_coef_mic = 0.00122 * h_coef_mic_term3 * h_coef_mic_term1 / h_coef_mic_term2

    "Determine the total heat transfer coefficient"
    h_coef = h_coef_mic + h_coef_mac
    "Determine heat transfer"
    TWOPHASEHEAT = h_coef * area_heat * (T_wall - T_fluid)
END

"This function determines the subooled boiling heat transfer in watts TO the fluid"
Function SUBCOOLHEAT(Press, he_mix, vel, T_wall, n_size, diam_pipe, epsilon_pipe)
    "Determine heat transfer area"
    area_heat = n_size * (PI * diam_pipe)
    "Determine the fluid temperature from the thermodynamic conditions"
    T_fluid = TEMPERATURE(WATER, P = Press, h = he_mix)

    "Fluid is two phase"
    "This heat transfer correlation is based on the CHEN correllation"
    "conductivity of liquid phase"
    cond_liq = CONDUCTIVITY(WATER, P = Press, x = 0)
    "heat capacity of liquid phase"
    Cp_liq = SPECHEAT(WATER, P = Press, x = 0)
    "Density of the liquid phase"
    rho_liq = DENSITY(WATER, P = Press, x = 0)
    "Density of the vapour phase"
    rho_vap = DENSITY(WATER, P = Press, x = 1)
    "fluid surface tension"
    sigma = SURFACETENSION(Water,T=T_fluid)
    "viscosity of the liquid phase"
    mu_liq = VISCOSITY(WATER, P = Press, x = 0)
    "Heat of vapourization of the mixture"
    he_liqvap = ENTHALPY(WATER, P = Press, x = 1) - ENTHALPY(WATER, P = Press, x = 0)
    "Saturation pressure of the fluid at the wall temperature"
    P_sat_walltemp = P_SAT(WATER, T = T_wall)
    "Saturation pressire of the fluid at the fluid tempeature"
    P_sat_fluidtemp = P_SAT(WATER,T = T_fluid)
    "Saturation Temperature of the fluid at the fluid pressure"
    T_sat_fluid_press = T_SAT(WATER, P = Press)
    "Liquid Reynolds number"
    N_Rey_liq = NREYLIQ(Press, he_mix, vel, diam_pipe)
    "Liquid Prandtl number"
    N_PR_liq = PRANDTL(WATER, P = Press, x = 0)
    "Determine the boiling suppresion factor"
    Factor_S = SUPPF(Press, he_mix, vel, diam_pipe)

    "Determine the macro heat transfer coefficient"
    h_coef_mac = 0.023 * (N_Rey_liq ^ 0.8) * (N_PR_liq ^ 0.4 ) * cond_liq / diam_pipe

    "Determine the nucleate boiling effect heat transfer coefficient"
    h_coef_mic_term1 = ((ABS(T_wall - T_sat_fluid_press)) ^ 0.24) * ((ABS(P_sat_walltemp - P_sat_fluidtemp)) ^
0.75) * Factor_S
    h_coef_mic_term2 = (sigma ^ 0.5) * (mu_liq ^ 0.29) * (rho_vap ^ 0.24) * (he_liqvap ^ 0.24)
    h_coef_mic_term3 = (cond_liq ^ 0.79) * (Cp_liq ^ 0.45) * (rho_liq ^ 0.49) * (grav# ^ 0.25)
    h_coef_mic = 0.00122 * h_coef_mic_term3 * h_coef_mic_term1 / h_coef_mic_term2
```

```
    "Determine heat transfer"
    SUBCOOLHEAT = (h_coef_mac * area_heat * (T_wall - T_fluid)) + (h_coef_mic * area_heat * (T_wall -
T_sat_fluid_press))
END

"This function determiens the single phase heat transfer in watts TO the fluid"
FUNCTION ONEPHASEHEAT(Press, he_mix, vel, T_wall, n_size, diam_pipe, epsilon_pipe)

    "Determine heat transfer area"
    area_heat = n_size * (PI * diam_pipe)
    "Determine reynolds number"
    N_Rey = NREY(Press, he_mix, vel, diam_pipe)
    "Determine Prandtl number"
    N_PR = NPRND(Press, he_mix)
    "Determine the fluid temperature from the thermodynamic conditions"
    T_fluid = TEMPERATURE(WATER, P = Press, h = he_mix)

    "Determine flow regime and then use appropiate heat transfer correllation"
    IF N_Rey < 1000 THEN
        "Laminar flow"
        "Set Nusselt number"
        N_NUS = 3.66
        "Determine conductivity of fluid"
        cond_mix = CONDUCTIVITY(WATER, P = Press, h = he_mix)
        "Determine heat transfer coefficient"
        h_coef = N_NUS * cond_mix / diam_pipe
        "Determine heat transfer in watts"
        ONEPHASEHEAT = h_coef * area_heat * (T_wall - T_fluid)
    ELSE
        IF N_Rey > 3000 THEN "Note that instead of 4000, the gnielinski correlation is valid as low as 3000"
            "Turbulent flow - Gnielinski correlation"
            "Determine conductivity of fluid"
            cond_mix = CONDUCTIVITY(WATER, P = Press, h = he_mix)
            "Determine friction factor from appropiate function"
            fric_fac = FRICFAC(Press, he_mix, vel, diam_pipe, epsilon_pipe)

            "Determine nusselt number from correllation"
            N_NUS_term1 = 1 + (12.7 * ((fric_fac/8)^0.5)*(((N_PR)^(2/3))-1))
            N_NUS = (fric_fac / 8) * (N_REY - 1000) * N_PR
            "Determine heat transfer coefficient"
            h_coef = N_NUS * cond_mix / diam_pipe
            "Determine heat transfer in watts"
            ONEPHASEHEAT = h_coef * area_heat * (T_wall - T_fluid)
        ELSE
            "Transitional flow regime heat transfer"
            "Determine the heat transfer in the transitional heat transfer using linear interpolation between the"
            "Heat transfer at Reynolds numbers of 1000 and 3000"
            "Laminar flow heat transfer"
            "Set Nusselt number"
            N_NUS_laminar = 3.66
            "Determine conductivity of fluid"
            cond_mix = CONDUCTIVITY(WATER, P = Press, h = he_mix)
            "Determine laminar heat transfer coefficient"
            h_coef_laminar = N_NUS_laminar * cond_mix / diam_pipe
            "Determine laminar heat transfer in watts"
            heat_laminar = h_coef_laminar * area_heat * (T_wall - T_fluid)

            "Turbulent flow - Gnielinski correlation"
            "Determine the velocity of the fluid at Re = 3000"
            rho_mix = FLUIDDENS(Press, he_mix)
            mu_mix = FLVISCO(Press, he_mix)
            vel_turb = 3000 * mu_mix / (rho_mix * diam_pipe)
```

```
            "Determine turbulent friction factor from appropiate function"
            fric_fac = FRICFAC(Press, he_mix, vel_turb, diam_pipe, epsilon_pipe)
            "Determine turbulent nusselt number from correllation, noting that Rey number = 3000"
            N_NUS_term1 = 1 + (12.7 * ((fric_fac/8)^0.5)*(((N_PR)^(2/3))-1))
            N_NUS_turb = (fric_fac / 8) * (3000 - 1000) * N_PR
            "Determine the turbulent heat transfer coefficient"
            h_coef_turb = N_NUS_turb * cond_mix / diam_pipe
            "Determine turbulent heat transfer in watts"
            heat_turb = h_coef_turb * area_heat * (T_wall - T_fluid)
            "Linearly interpolate between the Reynolds numbers of 1000 and 3000 to determine heat transfer"
            interpolate_x = (N_Rey - 1000) / 2000
            ONEPHASEHEAT = (heat_laminar * (1 - interpolate_x)) + (heat_turb * interpolate_x)
        ENDIF
    ENDIF

END

"This function determines the heat transfer in watts TO the fluid"
FUNCTION HEATTRANS(Press, he_mix, vel, T_wall, n_size, diam_pipe, epsilon_pipe)
    "Since the presence of subcooled boiling can not be detected by the mass quality function"
    "The first step is to determine the mass quality, if it is above 0 then two phase flow is taking place"
    "Then if it is above 1 superheated heat transfer is taking place"
    "If below or qual to 0 subcooled boiling criteria can be used to determine whether the heat transfer is normal
single "
    "phase heat transfer or subcooled boiling"
    "determine mass quality"
    mass_q = FLUIDQUAL(Press, he_mix)
    "Determine the fluid temperature from the thermodynamic conditions"
    T_fluid = TEMPERATURE(WATER, P = Press, h = he_mix)
    "Determine the fluid temperature from the thermodynamic conditions"
    T_fluid = TEMPERATURE(WATER, P = Press, h = he_mix)
    "Saturation Temperature of the fluid at the fluid pressure"
    T_sat = T_SAT(WATER, P = Press)

    "test if the conditions supplied to the function is subcooled single phase, subcooled boiling, saturated or
superheated heat transfer"
    IF mass_q <= 0 THEN
        "Heat transfer is either normal single phase or subcooled boiling"
        "fluid surface tension"
        "fluid surface tension"
        sigma = SURFACETENSION(Water,T=T_fluid)
        "Saturation Temperature of the fluid at the fluid pressure"
        T_sat_fluidpress = T_SAT(WATER, P = Press)
        "Determine heat transfer area"
        area_heat = n_size * (PI * diam_pipe)
        "Determine the fluid temperature from the thermodynamic conditions"
        T_fluid = TEMPERATURE(WATER, P = Press, h = he_mix)
        "Determine the single phase heat transfer, using the "
        "single phase heat transfer formula and working backwards"
        h_coef_singleph = ONEPHASEHEAT(Press, he_mix, vel, T_wall, n_size, diam_pipe, epsilon_pipe) /
(area_heat * (T_wall - T_fluid))
        "Determine the mixture density"
        rho_mix = FLUIDDENS(Press, he_mix)
        "Determine the fluid conductivity"
        cond_mix = CONDUCTIVITY(WATER, P = Press, h = he_mix)
        "Heat of vapourization of the mixture"
        he_liqvap = ENTHALPY(WATER, P = Press, x = 1) - ENTHALPY(WATER, P = Press, x = 0)
        "determine the current degree of wall superheat"
        T_wall_supheat = T_wall - T_sat
        "Determine the current degree of fluid subcooling"
        T_fluid_subcool = T_sat - T_fluid
```

```
        "Determine the required degree of wall superheating for subcooled boiling"
        T_wall_supheat_req_term1 = sigma * T_sat * h_coef_singleph / (rho_mix * cond_mix * he_liqvap)
        T_wall_supheat_req = (4 * T_wall_supheat_req_term1) * (1 + ((1 + (T_fluid_subcool * 0.5 /
T_wall_supheaT_req_term1)) ^ 0.5))

        "Determine the required heat transfer rate in watts for subcooled boiling"
        heat_trans_req = (area_heat * (T_wall - T_fluid)) * (rho_mix * cond_mix * he_liqvap / (8 * sigma * T_sat)) *
(T_wall_supheat_req^2)

        "Since the heat transfer (and thus indirectlty the heat flux) is calculated in these program functions"
        "There is no way to determine directly whteher the current heat transfer is in the subcooled boiling range"
        "Thus the single phase value, as calculated abaove as h_coef_singleph is used for comparison"
        heat_singleph = h_coef_singleph * (area_heat * (T_wall - T_fluid))

        "Determine whether single phase heat transfer or two phase heat transfer"
        "First use the wall superheat criteria"
        IF T_wall_supheat >T_wall_supheat_req THEN
            "If wall superheat criteria is met, check then for heat flux criteria"
            IF heat_singleph > heat_trans_req THEN
                "Subcooled boiling is taking place, use the correct function"
                HEATTRANS = SUBCOOLHEAT(Press, he_mix, vel, T_wall, n_size, diam_pipe, epsilon_pipe)
            ELSE
                "Normal single phase heat transfer"
                HEATTRANS = heat_singleph
            ENDIF
        ELSE
            "Normal single phase heat transfer"
            HEATTRANS = heat_singleph
        ENDIF
    ELSE
        IF mass_q >= 1 THEN
            "Fluid is superheated"
            HEATTRANS= ONEPHASEHEAT(Press, he_mix, vel, T_wall, n_size, diam_pipe, epsilon_pipe)
        ELSE
            "singe fluid is not singlephase, it is twophase"
            HEATTRANS = TWOPHASEHEAT(Press, he_mix, vel, T_wall, n_size, diam_pipe, epsilon_pipe)
        ENDIF
    ENDIF

END

"This function determines the  fluid heat transfer mode"
"It returns a number based in the type of heat transfer"
"1 = Subcooled heat transfer"
"2 = subcooled boiling heat transfer"
"3 = Two phase heat transfer"
"4 = Superheated single phase heat transfer"
FUNCTION HEATMODE(Press, he_mix, vel, T_wall, n_size, diam_pipe, epsilon_pipe)
    "Since the presence of subcooled boiling can not be detected by the mass quality function"
    "The first step is to determine the mass quality, if it is above 0 then two phase flow is taking place"
    "Then if it is above 1 superheated heat transfer is taking place"
    "If below or qual to 0 subcooled boiling criteria can be used to determine whether the heat transfer is normal
single "
    "phase heat transfer or subcooled boiling"
    "determine mass quality"
    mass_q = FLUIDQUAL(Press, he_mix)
    "Determine the fluid temperature from the thermodynamic conditions"
    T_fluid = TEMPERATURE(WATER, P = Press, h = he_mix)
    "Determine the fluid temperature from the thermodynamic conditions"
    T_fluid = TEMPERATURE(WATER, P = Press, h = he_mix)
    "Saturation Temperature of the fluid at the fluid pressure"
    T_sat = T_SAT(WATER, P = Press)
```

```
    "test if the conditions supplied to the function is subcooled single phase, subcooled boiling, saturated or
superheated heat transfer"
    IF mass_q <= 0 THEN
        "Heat transfer is either normal single phase or subcooled boiling"
        "fluid surface tension"
        "fluid surface tension"
        sigma = SURFACETENSION(Water,T=T_fluid)
        "Saturation Temperature of the fluid at the fluid pressure"
        T_sat_fluidpress = T_SAT(WATER, P = Press)
        "Determine heat transfer area"
        area_heat = n_size * (PI * diam_pipe)
        "Determine the fluid temperature from the thermodynamic conditions"
        T_fluid = TEMPERATURE(WATER, P = Press, h = he_mix)
        "Determine the single phase heat transfer, using the "
        "single phase heat transfer formula and working backwards"
        h_coef_singleph = ONEPHASEHEAT(Press, he_mix, vel, T_wall, n_size, diam_pipe, epsilon_pipe) /
(area_heat * (T_wall - T_fluid))
        "Determine the mixture density"
        rho_mix = FLUIDDENS(Press, he_mix)
        "Determine the fluid conductivity"
        cond_mix = CONDUCTIVITY(WATER, P = Press, h = he_mix)
        "Heat of vapourization of the mixture"
        he_liqvap = ENTHALPY(WATER, P = Press, x = 1) - ENTHALPY(WATER, P = Press, x = 0)
        "determine the current degree of wall superheat"
        T_wall_supheat = T_wall - T_sat
        "Determine the current degree of fluid subcooling"
        T_fluid_subcool = T_sat - T_fluid

        "Determine the required degree of wall superheating for subcooled boiling"
        T_wall_supheat_req_term1 = sigma * T_sat * h_coef_singleph / (rho_mix * cond_mix * he_liqvap)
        T_wall_supheat_req = (4 * T_wall_supheat_req_term1) * (1 + ((1 + (T_fluid_subcool * 0.5 /
T_wall_supheaT_req_term1)) ^ 0.5))

        "Determine the required heat transfer rate in watts for subcooled boiling"
        heat_trans_req = (area_heat * (T_wall - T_fluid)) * (rho_mix * cond_mix * he_liqvap / (8 * sigma * T_sat)) *
(T_wall_supheat_req^2)

        "Since the heat transfer (and thus indirectlty the heat flux) is calculated in these program functions"
        "There is no way to determine directly whetеher the current heat transfer is in the subcooled boiling range"
        "Thus the single phase value, as calculated abaove as h_coef_singleph is used for comparison"
        heat_singleph = h_coef_singleph * (area_heat * (T_wall - T_fluid))

        "Determine whether single phase heat transfer or two phase heat transfer"
        "First use the wall superheat criteria"
        IF T_wall_supheat >T_wall_supheat_req THEN
            "If wall superheat criteria is met, check then for heat flux criteria"
            IF heat_singleph > heat_trans_req THEN
                "Subcooled boiling is taking place, use the correct function"
                HEATMODE = 2
            ELSE
                "Normal single phase heat transfer"
                HEATMODE = 1
            ENDIF
        ELSE
            "Normal single phase heat transfer"
            HEATMODE = 1
        ENDIF
    ELSE
        IF mass_q >= 1 THEN
            "Fluid is superheated"
            HEATMODE = 4
```

```
        ELSE
            "singe fluid is not singlephase, it is twophase"
            HEATMODE = 3
        ENDIF
    ENDIF

END

"This function determines the average enthalpy of the reservoir"
FUNCTION  RVENTHALPY(Press, P_atm, he_mix, vel_mix, T_RV_FW, area_pipe)
    "Determine whether there is vapour present"
    "determine mass quality"
    mass_q = FLUIDQUAL(Press, he_mix)

    IF mass_q <= 0 THEN
        "if no vapour is present all fluid flows in to RV, thus in steady state this becomes the enthalpy"
        RVENTHALPY = he_mix
    ELSE
        IF mass_q >= 1 THEN
            "If only vapour is present, feedwater enthalpy is used"
            RVENTHALPY = ENTHALPY(WATER, P = P_atm, T = T_RV_FW)
        ELSE
            "if two pahse flow, only the liquid part is diverted into the RV and vapour mass replaced by feedwater"
            "determine enthalpy of liquid part coming from loop"
            he_liq = ENTHALPY(WATER, P = Press, x = 0)
            "determine enthalpy of the feedwater"
            he_FW = ENTHALPY(WATER, P = P_atm, T = T_RV_FW)
            "combine energies from both fluid flows, feedwater and liquid pipe loop flow to determine enthalpy by
using"
            "percentages of the mass quality and enthalpy of the feedwater and liquid pipe flow"
            RVENTHALPY = (he_FW * mass_q) + (he_liq * (1- mass_q))

        ENDIF
    ENDIF
END

"########################################"
"System Parameters"
"########################################"
"NCL Parameters"
"Height of NCL"
height_NCL = 10
"Width of NCL"
width_NCL = 2
"Inner diameter of NCL pipes"
diam_pipe = 0.025
"Inner radius of pipes"
rad_pipe = diam_pipe * 0.5
"Pipe area"
area_pipe = PI * (diam_pipe ^ 2) * 0.25
"Circumference of the pipe"
circum_pipe = PI * diam_pipe
"Surface roughness of pipe"
epsilon_pipe = 4.5e-5

"Reservoir Parameters"
"Height of reservoir"
height_RV = 0.5
"Width of reservoir"
width_RV = 0.5
"Depth of reservoir"
depth_RV = 0.5
```

```
"Volume of the reservoir"
Vol_RV = height_RV * width_RV * Depth_RV

"########################################"
"Boundary Values and other coefficients"
"########################################"
"Enviromental (cold leg) temperature"
T_enviro = 273 + T_enviro_C
T_enviro_C = 20
"Containment (hot leg) temperature"
T_contain = 273 + T_contain_C
T_contain_C = 110

"Atmosperic Pressure"
P_atm = 100e3
"Feedwater to reservoir temperature"
T_RV_FW = 273 + 20

"Pipe bend secondary loss coefficient"
K_loss_ELB = 0.3
"Pipe flow to reservoir secondary loss coefficient"
K_loss_ex = 1
"Pipe flow from reservoir secondary loss coefficient"
K_loss_in = 0.12

"########################################"
"Discretising parameters"
"########################################"
"Number of cold leg control volumes"
n_CL = 20
"Size of cold leg control volumes"
n_size_CL = (height_NCL + (2 * 0.5 * diam_pipe) - height_RV - (2 * diam_pipe)) / n_CL

"Number of bottom horizontal leg control volumes"
n_BHL = 5
"Size of bottom horizontal leg control volumes"
n_size_BHL = (width_NCL + (2 * 0.5 * diam_pipe) - (2 * 2 * diam_pipe)) / n_BHL

"Number of hot leg control volumes"
n_HL = 190
"Size of the hot leg control volumes"
n_size_HL = (height_NCL + (2 * 0.5 * diam_pipe) - (2 * 2 * diam_pipe)) / n_HL

"Number of top horizontal leg control volumes"
n_THL = 10
"Size of the top horizontal leg control volumes"
n_size_THL = (width_NCL + (0.5 * diam_pipe) - (2 * diam_pipe) - (0.5 * width_RV)) / n_THL

"number of control volumes in elbows"
n_ELB = 1
"Size lentghwise of elbow control volumes"
n_size_ELB = 2 * 1.5 * diam_pipe
"total number of elbow control volumes"
num_elbows = 3

"Total number of control volumes"
n_total = n_CL + n_BHL + n_HL + n_THL + (num_elbows * n_ELB)
"accumalitve number of control volumes"
n_cum1 = n_CL
n_cum2 = n_cum1 + n_ELB
n_cum3 = n_cum2 + n_BHL
n_cum4 = n_cum3 + n_ELB
```

```
n_cum5 = n_cum4 + n_HL
n_cum6 = n_cum5 + n_ELB
n_cum7 = n_cum6 + n_THL

"########################################"
"Reservoir and loop inlet and outlet conditions"
"########################################"

"Inlet properties for the loop from the reservoir"
"Pressures minus losses"
P_RV3 = P_atm + (rho_ex[0] * grav# * height_RV)
P_ex[0] = P_RV3 -  (K_loss_in * 0.5 * rho_ex[0] * vel_ex[0] * vel_ex[0])

"Enthalpies"
he_ex[0] =he_RV_avg
he_RV1 = ENTHALPY(WATER, P = P_atm, T = T_RV_FW)
he_RV2 = ENTHALPY(WATER, P = P_RV4, x = 1)
he_RV3 = he_RV_avg

"Density"
"use reservoir enthalpy and pressure at RV point 3"
rho_ex[0] = DENSITY(WATER, P = P_RV3, h = he_RV_avg)
rho_RV1 = DENSITY(WATER, P = P_atm, T = T_RV_FW)
rho_RV2 = DENSITY(WATER, P = P_atm, h = he_RV2)
rho_RV3 = DENSITY(WATER, P = P_RV3, h = he_RV_avg)
rho_RV4 = DENSITY(WATER, P = P_atm, h = he_RV4)

"Reservoir properties"
"equate the total enthalpy of the reservoir to that of the incoming total enthalpy"
"It is like the velocity component of the incoming fluid is dissapated into the reservoir contents"
he_RV_avg = RVENTHALPY(P_RV4, P_atm, he_RV4, vel_RV4, T_RV_FW, area_pipe)

"Exit properties for the pipe loop into the reservoir"
"Exit pressure minus losses"
P_ex[n_cum7] = P_RV4+ (K_loss_ex * 0.5 * rho_ex[n_cum7] * vel_ex[n_cum7] * vel_ex[n_cum7])
"Enthalpies"
he_RV4 = he_ex[n_cum7]

"velocities"
vel_RV1 = m_dot_RV1 / (area_pipe * rho_RV1)
vel_RV2 = m_dot_RV2 / (area_pipe * rho_RV2)
vel_RV3 = vel_ex[0]
vel_RV4 = vel_ex[n_cum7]

"Reservoir properties"
P_RV4 = P_atm

"mass flows"
m_dot_RV1 = m_dot_RV2
m_dot_RV2 = m_dot_RV4 * mass_q_avg[n_cum7]
m_dot_RV3 = m_dot_avg[1]
m_dot_RV4 = m_dot_avg[n_cum7]

"########################################"
"Cold Vertical Leg"
"########################################"
"Spatial Setting"
"Control Volume boundaries"
s_cvbound[0] = 0

DUPLICATE i = 1, n_cum1
    "Spatial Setting"
```

```
    "Control volume boundaries"
    s_cvbound[i] = s_cvbound[i - 1] + n_size_CL
    "Control volume centres"
    s_cvcentre[i - 1] = s_cvbound[i - 1] + ((s_cvbound[i] - s_cvbound[i - 1]) * 0.5)

    "Inlet coupling to the previous control volume"
    "Velocity"
    vel_in[i] = vel_ex[i - 1]
    "Pressure"
    P_in[i] = P_ex[i - 1]
    "Enthalpy"
    he_in[i] = he_ex[i - 1]

    "Mass conservation"
    0 = (rho_ex[i] * vel_ex[i]) - (rho_in[i] * vel_in[i])

    "Momentum conservation"
    P_ex[i]  - P_in[i] = (-1) * (DELTA_P_kin[i] + DELTA_P_fric[i] + DELTA_P_acc[i] + DELTA_P_static[i])
    "Determine change in dynamic pressure"
    DELTA_P_kin[i] = ((rho_ex[i] * vel_ex[i] * vel_ex[i]) - (rho_in[i] * vel_in[i] * vel_in[i]))
    "Determine frictional pressure loss using a function"
    DELTA_P_fric[i] = DELTAPFRIC(P_avg[i], he_avg[i], vel_avg[i], diam_pipe, epsilon_pipe, n_size_CL)
    "Determine secondary pressure losses using loss coefficients"
    DELTA_P_acc[i] = 0
    "Determine static pressure loss using simple formula"
    DELTA_P_static[i] = n_size_CL * rho_avg[i] * grav# * SIN(-90)

    "Energy Conservation"
    he_ex[i] - he_in[i] = (DELTA_H_HEAT[i] - DELTA_H_KIN[i] - DELTA_H_POT[i]) / m_dot_avg[i]
    DELTA_H_KIN[i] = 0.5 * ((rho_ex[i] * (vel_ex[i] ^ 3) * area_pipe) - (rho_in[i] * (vel_in[i] ^ 3) * area_pipe))
    DELTA_H_HEAT[i] = HEATTRANS(P_avg[i], he_avg[i], vel_avg[i], T_wall[i], n_size_CL, diam_pipe,
epsilon_pipe)
    DELTA_H_POT[i] = n_size_CL * rho_avg[i] * vel_avg[i] * area_pipe * grav# * SIN(-90)

    "Properties and Total Properties"
    "Fluid density at inlet"
    rho_in[i] = FLUIDDENS(P_in[i], he_in[i])
    "Fluid density at outlet"
    rho_ex[i] = FLUIDDENS(P_ex[i], he_ex[i])

    "averages"
    rho_avg[i] = 0.5 * (rho_in[i] + rho_ex[i])
    vel_avg[i] = 0.5 * (vel_in[i] + vel_ex[i])
    P_avg[i] = 0.5 * (P_in[i] + P_ex[i])
    he_avg[i] = 0.5 * (he_in[i] + he_ex[i])

    "Other fluid parameters"
    "Average mass quality"
    mass_q_avg[i] = FLUIDQUAL(P_avg[i], he_avg[i])
    "Average fluid temperature"
    T_fluid_avg[i] = TEMPERATURE(WATER, P = P_avg[i], h =he_avg[i])
    "Average mass flow"
    m_dot_avg[i] = rho_avg[i] * vel_avg[i] * area_pipe
    "Wall temperature"
    T_wall[i] = T_enviro
    "Heat transfer type"
    HeatTransMode[i] = HEATMODE(P_avg[i], he_avg[i], vel_avg[i], T_wall[i], n_size_CL, diam_pipe, epsilon_pipe)
END

"########################################"
"Cold Vertical Leg Exit Elbow"
"########################################"
```

```
    "Spatial Setting"
    "Control Volume boundaries"
    s_cvbound[n_cum2] = s_cvbound[n_cum2 - 1] + n_size_ELB
    "Control Volume Centres"
    s_cvcentre[n_cum2 - 1] = s_cvbound[n_cum2 - 1] + ((s_cvbound[n_cum2] - s_cvbound[n_cum2 - 1]) * 0.5)

    "Inlet coupling to the previous control volume"
    "Velocity"
    vel_in[n_cum2] = vel_ex[n_cum2 - 1]
    "Pressure"
    P_in[n_cum2] = P_ex[n_cum2 - 1]
    "Enthalpy"
    he_in[n_cum2] = he_ex[n_cum2 - 1]

    "Mass conservation"
    0 = (rho_ex[n_cum2] * vel_ex[n_cum2]) - (rho_in[n_cum2] * vel_in[n_cum2])

    "Momentum conservation"
    P_ex[n_cum2]  - P_in[n_cum2] = (-1) * (DELTA_P_kin[n_cum2] + DELTA_P_fric[n_cum2] +
DELTA_P_acc[n_cum2] + DELTA_P_static[n_cum2])
    "Determine change in dynamic pressure"
    DELTA_P_kin[n_cum2] = ((rho_ex[n_cum2] * vel_ex[n_cum2] * vel_ex[n_cum2]) - (rho_in[n_cum2] *
vel_in[n_cum2] * vel_in[n_cum2]))
    "Determine frictional pressure loss using a function"
    DELTA_P_fric[n_cum2] = DELTAPFRIC(P_avg[n_cum2], he_avg[n_cum2], vel_avg[n_cum2], diam_pipe,
epsilon_pipe, n_size_ELB)
    "Determine secondary pressure losses using loss coefficients"
    DELTA_P_acc[n_cum2] = K_loss_ELB * rho_avg[n_cum2] * vel_avg[n_cum2] * vel_avg[n_cum2] * 0.5
    "Determine static pressure loss using simple formula, half of the elbow size since the size is in the "
    DELTA_P_static[n_cum2] = 0.5 * n_size_ELB * rho_avg[n_cum2] * grav# * SIN(-90)

    "Energy Conservation"
    he_ex[n_cum2] - he_in[n_cum2] = (DELTA_H_HEAT[n_cum2] - DELTA_H_KIN[n_cum2] -
DELTA_H_POT[n_cum2]) / m_dot_avg[n_cum2]
    DELTA_H_KIN[n_cum2] = 0.5 * ((rho_ex[n_cum2] * (vel_ex[n_cum2] ^ 3) * area_pipe) - (rho_in[n_cum2] *
(vel_in[n_cum2] ^ 3) * area_pipe))
    DELTA_H_HEAT[n_cum2] = 0
    DELTA_H_POT[n_cum2] = 0.5 * n_size_ELB * rho_avg[n_cum2] * vel_avg[n_cum2] * area_pipe * grav# * SIN(-
90)

    "Properties"
    "Fluid density at inlet"
    rho_in[n_cum2] = FLUIDDENS(P_in[n_cum2], he_in[n_cum2])
    "Fluid density at outlet"
    rho_ex[n_cum2] = FLUIDDENS(P_ex[n_cum2], he_ex[n_cum2])

    "averages"
    rho_avg[n_cum2] = 0.5 * (rho_in[n_cum2] + rho_ex[n_cum2])
    vel_avg[n_cum2] = 0.5 * (vel_in[n_cum2] + vel_ex[n_cum2])
    P_avg[n_cum2] = 0.5 * (P_in[n_cum2] + P_ex[n_cum2])
    he_avg[n_cum2] = 0.5 * (he_in[n_cum2] + he_ex[n_cum2])

    "Other fluid parameters"
    "Average mass quality"
    mass_q_avg[n_cum2] = FLUIDQUAL(P_avg[n_cum2], he_avg[n_cum2])
    "Average fluid temperature"
    T_fluid_avg[n_cum2] = TEMPERATURE(WATER, P = P_avg[n_cum2], h =he_avg[n_cum2])
    "Average mass flow"
    m_dot_avg[n_cum2] = rho_avg[n_cum2] * vel_avg[n_cum2] * area_pipe

"########################################"
"Cold Horizontal Leg"
```

```
"########################################"
DUPLICATE i = n_cum2 + 1, n_cum3
    "Spatial Setting"
    "Control volume boundaries"
    s_cvbound[i] = s_cvbound[i - 1] + n_size_BHL
    "Control volume centres"
    s_cvcentre[i - 1] = s_cvbound[i - 1] + ((s_cvbound[i] - s_cvbound[i - 1]) * 0.5)

    "Inlet coupling to the previous control volume"
    "Velocity"
    vel_in[i] = vel_ex[i - 1]
    "Pressure"
    P_in[i] = P_ex[i - 1]
    "Enthalpy"
    he_in[i] = he_ex[i - 1]

    "Mass conservation"
    0 = (rho_ex[i] * vel_ex[i]) - (rho_in[i] * vel_in[i])

    "Momentum conservation"
    P_ex[i]  - P_in[i] = (-1) * (DELTA_P_kin[i] + DELTA_P_fric[i] + DELTA_P_acc[i] + DELTA_P_static[i])
    "Determine change in dynamic pressure"
    DELTA_P_kin[i] = ((rho_ex[i] * vel_ex[i] * vel_ex[i]) - (rho_in[i] * vel_in[i] * vel_in[i]))
    "Determine frictional pressure loss using a function"
    DELTA_P_fric[i] = DELTAPFRIC(P_avg[i], he_avg[i], vel_avg[i], diam_pipe, epsilon_pipe, n_size_BHL)
    "Determine secondary pressure losses using loss coefficients"
    DELTA_P_acc[i] = 0
    "Determine static pressure loss using simple formula"
    DELTA_P_static[i] = n_size_BHL * rho_avg[i] * grav# * SIN(0)

    "Energy Conservation"
    he_ex[i] - he_in[i] = (DELTA_H_HEAT[i] - DELTA_H_KIN[i] - DELTA_H_POT[i]) / m_dot_avg[i]
    DELTA_H_KIN[i] = 0.5 * ((rho_ex[i] * (vel_ex[i] ^ 3) * area_pipe) - (rho_in[i] * (vel_in[i] ^ 3) * area_pipe))
    DELTA_H_HEAT[i] = 0
    DELTA_H_POT[i] = n_size_BHL * rho_avg[i] * vel_avg[i] * area_pipe * grav# * SIN(0)

    "Properties"
    "Fluid density at inlet"
    rho_in[i] = FLUIDDENS(P_in[i], he_in[i])
    "Fluid density at outlet"
    rho_ex[i] = FLUIDDENS(P_ex[i], he_ex[i])

    "averages"
    rho_avg[i] = 0.5 * (rho_in[i] + rho_ex[i])
    vel_avg[i] = 0.5 * (vel_in[i] + vel_ex[i])
    P_avg[i] = 0.5 * (P_in[i] + P_ex[i])
    he_avg[i] = 0.5 * (he_in[i] + he_ex[i])

    "Other fluid parameters"
    "Average mass quality"
    mass_q_avg[i] = FLUIDQUAL(P_avg[i], he_avg[i])
    "Average fluid temperature"
    T_fluid_avg[i] = TEMPERATURE(WATER, P = P_avg[i], h =he_avg[i])
    "Average mass flow"
    m_dot_avg[i] = rho_avg[i] * vel_avg[i] * area_pipe
END

"########################################"
"Cold Horizontal Leg Exit Elbow"
"########################################"
    "Spatial Setting"
    "Control Volume boundaries"
```

```
    s_cvbound[n_cum4] = s_cvbound[n_cum4 - 1] + n_size_ELB
    "Control Volume Centres"
    s_cvcentre[n_cum4 - 1] = s_cvbound[n_cum4 - 1] + ((s_cvbound[n_cum4] - s_cvbound[n_cum4 - 1]) * 0.5)

    "Inlet coupling to the previous control volume"
    "Velocity"
    vel_in[n_cum4] = vel_ex[n_cum4 - 1]
    "Pressure"
    P_in[n_cum4] = P_ex[n_cum4 - 1]
    "Enthalpy"
    he_in[n_cum4] = he_ex[n_cum4 - 1]

    "Mass conservation"
    0 = (rho_ex[n_cum4] * vel_ex[n_cum4]) - (rho_in[n_cum4] * vel_in[n_cum4])

    "Momentum conservation"
    P_ex[n_cum4]  - P_in[n_cum4] = (-1) * (DELTA_P_kin[n_cum4] + DELTA_P_fric[n_cum4] +
DELTA_P_acc[n_cum4] + DELTA_P_static[n_cum4])
    "Determine change in dynamic pressure"
    DELTA_P_kin[n_cum4] = ((rho_ex[n_cum4] * vel_ex[n_cum4] * vel_ex[n_cum4]) - (rho_in[n_cum4] *
vel_in[n_cum4] * vel_in[n_cum4]))
    "Determine frictional pressure loss using a function"
    DELTA_P_fric[n_cum4] = DELTAPFRIC(P_avg[n_cum4], he_avg[n_cum4], vel_avg[n_cum4], diam_pipe,
epsilon_pipe, n_size_ELB)
    "Determine secondary pressure losses using loss coefficients"
    DELTA_P_acc[n_cum4] = K_loss_ELB * rho_avg[n_cum4] * vel_avg[n_cum4] * vel_avg[n_cum4] * 0.5
    "Determine static pressure loss using simple formula, half of the elbow size since the size is in the "
    DELTA_P_static[n_cum4] = 0.5 * n_size_ELB * rho_avg[n_cum4] * grav# * SIN(90)

    "Energy Conservation"
    he_ex[n_cum4] - he_in[n_cum4] = (DELTA_H_HEAT[n_cum4] - DELTA_H_KIN[n_cum4] -
DELTA_H_POT[n_cum4]) / m_dot_avg[n_cum4]
    DELTA_H_KIN[n_cum4] = 0.5 * ((rho_ex[n_cum4] * (vel_ex[n_cum4] ^ 3) * area_pipe) - (rho_in[n_cum4] *
(vel_in[n_cum4] ^ 3) * area_pipe))
    DELTA_H_HEAT[n_cum4] = 0
    DELTA_H_POT[n_cum4] = 0.5 * n_size_ELB * rho_avg[n_cum4] * vel_avg[n_cum4] * area_pipe * grav# *
SIN(90)

    "Properties"
    "Fluid density at inlet"
    rho_in[n_cum4] = FLUIDDENS(P_in[n_cum4], he_in[n_cum4])
    "Fluid density at outlet"
    rho_ex[n_cum4] = FLUIDDENS(P_ex[n_cum4], he_ex[n_cum4])

    "averages"
    rho_avg[n_cum4] = 0.5 * (rho_in[n_cum4] + rho_ex[n_cum4])
    vel_avg[n_cum4] = 0.5 * (vel_in[n_cum4] + vel_ex[n_cum4])
    P_avg[n_cum4] = 0.5 * (P_in[n_cum4] + P_ex[n_cum4])
    he_avg[n_cum4] = 0.5 * (he_in[n_cum4] + he_ex[n_cum4])

    "Other fluid parameters"
    "Average mass quality"
    mass_q_avg[n_cum4] = FLUIDQUAL(P_avg[n_cum4], he_avg[n_cum4])
    "Average fluid temperature"
    T_fluid_avg[n_cum4] = TEMPERATURE(WATER, P = P_avg[n_cum4], h =he_avg[n_cum4])
    "Average mass flow"
    m_dot_avg[n_cum4] = rho_avg[n_cum4] * vel_avg[n_cum4] * area_pipe

"########################################"
"Hot Vertical Leg"
"########################################"
```

```
DUPLICATE i = n_cum4 + 1, n_cum5
    "Spatial Setting"
    "Control volume boundaries"
    s_cvbound[i] = s_cvbound[i - 1] + n_size_HL
    "Control volume centres"
    s_cvcentre[i - 1] = s_cvbound[i - 1] + ((s_cvbound[i] - s_cvbound[i - 1]) * 0.5)

    "Inlet coupling to the previous control volume"
    "Velocity"
    vel_in[i] = vel_ex[i - 1]
    "Pressure"
    P_in[i] = P_ex[i - 1]
    "Enthalpy"
    he_in[i] = he_ex[i - 1]

    "Mass conservation"
    0 = (rho_ex[i] * vel_ex[i]) - (rho_in[i] * vel_in[i])

    "Momentum conservation"
    P_ex[i]  - P_in[i] = (-1) * (DELTA_P_kin[i] + DELTA_P_fric[i] + DELTA_P_acc[i] + DELTA_P_static[i])
    "Determine change in dynamic pressure"
    DELTA_P_kin[i] = ((rho_ex[i] * vel_ex[i] * vel_ex[i]) - (rho_in[i] * vel_in[i] * vel_in[i]))
    "Determine frictional pressure loss using a function"
    DELTA_P_fric[i] = DELTAPFRIC(P_avg[i], he_avg[i], vel_avg[i], diam_pipe, epsilon_pipe, n_size_HL)
    "Determine secondary pressure losses using loss coefficients"
    DELTA_P_acc[i] = 0
    "Determine static pressure loss using simple formula"
    DELTA_P_static[i] = n_size_HL * rho_avg[i] * grav# * SIN(90)

    "Energy Conservation"
    he_ex[i] - he_in[i] = (DELTA_H_HEAT[i] - DELTA_H_KIN[i] - DELTA_H_POT[i]) / m_dot_avg[i]
    DELTA_H_KIN[i] = 0.5 * ((rho_ex[i] * (vel_ex[i] ^ 3) * area_pipe) - (rho_in[i] * (vel_in[i] ^ 3) * area_pipe))
    DELTA_H_HEAT[i] = HEATTRANS(P_avg[i], he_avg[i], vel_avg[i], T_wall[i], n_size_HL, diam_pipe,
epsilon_pipe)
    DELTA_H_POT[i] = n_size_HL * rho_avg[i] * vel_avg[i] * area_pipe * grav# * SIN(90)

    "Properties"
    "Fluid density at inlet"
    rho_in[i] = FLUIDDENS(P_in[i], he_in[i])
    "Fluid density at outlet"
    rho_ex[i] = FLUIDDENS(P_ex[i], he_ex[i])

    "averages"
    rho_avg[i] = 0.5 * (rho_in[i] + rho_ex[i])
    vel_avg[i] = 0.5 * (vel_in[i] + vel_ex[i])
    P_avg[i] = 0.5 * (P_in[i] + P_ex[i])
    he_avg[i] = 0.5 * (he_in[i] + he_ex[i])

    "Other fluid parameters"
    "Average mass quality"
    mass_q_avg[i] = FLUIDQUAL(P_avg[i], he_avg[i])
    "Average fluid temperature"
    T_fluid_avg[i] = TEMPERATURE(WATER, P = P_avg[i], h =he_avg[i])
    "Average mass flow"
    m_dot_avg[i] = rho_avg[i] * vel_avg[i] * area_pipe
    "Wall temperature"
    T_wall[i] = T_contain
    "Heat transfer type"
    HeatTransMode[i] = HEATMODE(P_avg[i], he_avg[i], vel_avg[i], T_wall[i], n_size_HL, diam_pipe, epsilon_pipe)

END
```

```
"########################################"
"Hot Vertical Leg Exit Elbow"
"########################################"
    "Spatial Setting"
    "Control Volume boundaries"
    s_cvbound[n_cum6] = s_cvbound[n_cum6 - 1] + n_size_ELB
    "Control Volume Centres"
    s_cvcentre[n_cum6 - 1] = s_cvbound[n_cum6 - 1] + ((s_cvbound[n_cum6] - s_cvbound[n_cum6 - 1]) * 0.5)

    "Inlet coupling to the previous control volume"
    "Velocity"
    vel_in[n_cum6] = vel_ex[n_cum6 - 1]
    "Pressure"
    P_in[n_cum6] = P_ex[n_cum6 - 1]
    "Enthalpy"
    he_in[n_cum6] = he_ex[n_cum6 - 1]

    "Mass conservation"
    0 = (rho_ex[n_cum6] * vel_ex[n_cum6]) - (rho_in[n_cum6] * vel_in[n_cum6])

    "Momentum conservation"
    P_ex[n_cum6]  - P_in[n_cum6] = (-1) * (DELTA_P_kin[n_cum6] + DELTA_P_fric[n_cum6] +
DELTA_P_acc[n_cum6] + DELTA_P_static[n_cum6])
    "Determine change in dynamic pressure"
    DELTA_P_kin[n_cum6] = ((rho_ex[n_cum6] * vel_ex[n_cum6] * vel_ex[n_cum6]) - (rho_in[n_cum6] *
vel_in[n_cum6] * vel_in[n_cum6]))
    "Determine frictional pressure loss using a function"
    DELTA_P_fric[n_cum6] = DELTAPFRIC(P_avg[n_cum6], he_avg[n_cum6], vel_avg[n_cum6], diam_pipe,
epsilon_pipe, n_size_ELB)
    "Determine secondary pressure losses using loss coefficients"
    DELTA_P_acc[n_cum6] = K_loss_ELB * rho_avg[n_cum6] * vel_avg[n_cum6] * vel_avg[n_cum6] * 0.5
    "Determine static pressure loss using simple formula, half of the elbow size since the size is in the "
    DELTA_P_static[n_cum6] = 0.5 * n_size_ELB * rho_avg[n_cum6] * grav# * SIN(90)

    "Energy Conservation"
    he_ex[n_cum6] - he_in[n_cum6] = (DELTA_H_HEAT[n_cum6] - DELTA_H_KIN[n_cum6] -
DELTA_H_POT[n_cum6]) / m_dot_avg[n_cum6]
    DELTA_H_KIN[n_cum6] = 0.5 * ((rho_ex[n_cum6] * (vel_ex[n_cum6] ^ 3) * area_pipe) - (rho_in[n_cum6] *
(vel_in[n_cum6] ^ 3) * area_pipe))
    DELTA_H_HEAT[n_cum6] = 0
    DELTA_H_POT[n_cum6] = 0.5 * n_size_ELB * rho_avg[n_cum6] * vel_avg[n_cum6] * area_pipe * grav# *
SIN(90)

    "Properties"
    "Fluid density at inlet"
    rho_in[n_cum6] = FLUIDDENS(P_in[n_cum6], he_in[n_cum6])
    "Fluid density at outlet"
    rho_ex[n_cum6] = FLUIDDENS(P_ex[n_cum6], he_ex[n_cum6])

    "averages"
    rho_avg[n_cum6] = 0.5 * (rho_in[n_cum6] + rho_ex[n_cum6])
    vel_avg[n_cum6] = 0.5 * (vel_in[n_cum6] + vel_ex[n_cum6])
    P_avg[n_cum6] = 0.5 * (P_in[n_cum6] + P_ex[n_cum6])
    he_avg[n_cum6] = 0.5 * (he_in[n_cum6] + he_ex[n_cum6])

    "Other fluid parameters"
    "Average mass quality"
    mass_q_avg[n_cum6] = FLUIDQUAL(P_avg[n_cum6], he_avg[n_cum6])
    "Average fluid temperature"
    T_fluid_avg[n_cum6] = TEMPERATURE(WATER, P = P_avg[n_cum6], h =he_avg[n_cum6])
    "Average mass flow"
    m_dot_avg[n_cum6] = rho_avg[n_cum6] * vel_avg[n_cum6] * area_pipe
```

```
"########################################"
"Hot Horizontal Leg"
"########################################"
DUPLICATE i = n_cum6 + 1, n_cum7
    "Spatial Setting"
    "Control volume boundaries"
    s_cvbound[i] = s_cvbound[i - 1] + n_size_THL
    "Control volume centres"
    s_cvcentre[i - 1] = s_cvbound[i - 1] + ((s_cvbound[i] - s_cvbound[i - 1]) * 0.5)

    "Inlet coupling to the previous control volume"
    "Velocity"
    vel_in[i] = vel_ex[i - 1]
    "Pressure"
    P_in[i] = P_ex[i - 1]
    "Enthalpy"
    he_in[i] = he_ex[i - 1]

    "Mass conservation"
    0 = (rho_ex[i] * vel_ex[i]) - (rho_in[i] * vel_in[i])

    "Momentum conservation"
    P_ex[i]  - P_in[i] = (-1) * (DELTA_P_kin[i] + DELTA_P_fric[i] + DELTA_P_acc[i] + DELTA_P_static[i])
    "Determine change in dynamic pressure"
    DELTA_P_kin[i] = ((rho_ex[i] * vel_ex[i] * vel_ex[i]) - (rho_in[i] * vel_in[i] * vel_in[i]))
    "Determine frictional pressure loss using a function"
    DELTA_P_fric[i] = DELTAPFRIC(P_avg[i], he_avg[i], vel_avg[i], diam_pipe, epsilon_pipe, n_size_THL)
    "Determine secondary pressure losses using loss coefficients"
    DELTA_P_acc[i] = 0
    "Determine static pressure loss using simple formula"
    DELTA_P_static[i] = n_size_THL * rho_avg[i] * grav# * SIN(0)

    "Energy Conservation"
    he_ex[i] - he_in[i] = (DELTA_H_HEAT[i] - DELTA_H_KIN[i] - DELTA_H_POT[i]) / m_dot_avg[i]
    DELTA_H_KIN[i] = 0.5 * ((rho_ex[i] * (vel_ex[i] ^ 3) * area_pipe) - (rho_in[i] * (vel_in[i] ^ 3) * area_pipe))
    DELTA_H_HEAT[i] = 0
    DELTA_H_POT[i] = n_size_THL * rho_avg[i] * vel_avg[i] * area_pipe * grav# * SIN(0)

    "Properties"
    "Fluid density at inlet"
    rho_in[i] = FLUIDDENS(P_in[i], he_in[i])
    "Fluid density at outlet"
    rho_ex[i] = FLUIDDENS(P_ex[i], he_ex[i])

    "averages"
    rho_avg[i] = 0.5 * (rho_in[i] + rho_ex[i])
    vel_avg[i] = 0.5 * (vel_in[i] + vel_ex[i])
    P_avg[i] = 0.5 * (P_in[i] + P_ex[i])
    he_avg[i] = 0.5 * (he_in[i] + he_ex[i])

    "Other fluid parameters"
    "Average mass quality"
    mass_q_avg[i] = FLUIDQUAL(P_avg[i], he_avg[i])
    "Average fluid temperature"
    T_fluid_avg[i] = TEMPERATURE(WATER, P = P_avg[i], h =he_avg[i])
    "Average mass flow"
    m_dot_avg[i] = rho_avg[i] * vel_avg[i] * area_pipe

END
"########################################"
"Global Loop Parameters and Calculations"
```

```
"########################################"
"Heat lost through vapour"
Heat_vap = (m_dot_RV2 * he_RV2)
"Heat gained through feedwater"
Heat_feedwater = (m_dot_RV1 * he_RV1)
"Heat absorbed in hot leg"
Heat_absorbed = SUM(DELTA_H_HEAT[i], i = n_cum4 + 1, n_cum5)
"Heat removed in cold leg"
Heat_removed = SUM(DELTA_H_HEAT[i], i = 1, n_cum1)
"Heat flow from reservoir to loop"
Heat_loop_out = (m_dot_RV3 * he_RV3)
"Heat flow into reservoir from loop"
Heat_loop_in = (m_dot_RV4 * he_RV4)

"Testing of Conservation of Mass using Reservoir Equations"
Mass_Error = (m_dot_RV2 + m_dot_RV3) - (m_dot_RV1 + m_dot_RV4)
"Testing of Loop conservation of Mass"
Mass_Error2 =  m_dot_RV3 -  m_dot_RV4
"Testing of Conservation of Energy using reservoir Equations"
Heat_Error = (Heat_removed + Heat_absorbed ) + (Heat_feedwater - Heat_vap)
"Testing of loop conservation of energy"
Heat_Error2 = (Heat_removed + Heat_absorbed ) + (Heat_loop_out - Heat_loop_in)

"########################################"
"End of Program"
"########################################"
```